Author:
Creed, Eloise

Title:
The effects of monovalent and multivalent cations on phosphatidylcholine liposomes

A study of the Hofmeister series

The effects of monovalent and multivalent cations on phosphatidylcholine liposomes: A study of the Hofmeister series

Eloise Frances Alexandra Creed

A dissertation submitted to the University of Bristol in accordance with the requirements for award of the degree of Research Master of Science in the Faculty of Science, School of Chemistry

August 2018

Supervisor: Wuge H. Briscoe

Section: Physical and Theoretical Chemistry

Project Group: Soft Matter at Interfaces (Briscoe) Group

Word count: 53,484

Abstract

In this project, liposomes, self-assembled from lipids, have been used as a model system to study specific ion effects. Specific ion effects have been discussed for over a century since the pioneering work carried out by Franz Hofmeister and his group in Prague. A more comprehensive understanding of specific ion effects is vital in many branches of science and important for a wide variety of applications. A deeper understanding of specific ion effects would also shed light on the Hofmeister series, first proposed by Hofmeister himself in 1888 which ordered ions according to their ability to affect the solubilities of proteins in aqueous solutions. To investigate the Hofmeister series more comprehensively and gain a deeper insight into the interactions occurring, dynamic light scattering (DLS) and cryo-transmission electron microscopy (TEM) have been employed to determine the effects of a number of ions on liposomes. Three main aqueous systems have been investigated: the effect of multivalent inorganic cations on the size, polydispersity index and zeta potential of 1, 2-dioleoyl-sn-glycero-3-phosphocholine (DOPC) liposomes; the effect of hydrophobic, organic cations on the size, polydispersity index and zeta potential of DOPC liposomes; and the effect of temperature on liposomes comprised of DOPC and 1, 2-dipalmitoyl-sn-glycero-3-phosphocholine (DPPC) respectively. TEM was employed in order to study the effect of ions on the morphology and lamellarity of the liposomes.

The liposome suspensions were prepared via the hydration of lipid films with salt solution, followed by sonication and extrusion. Liposomes formed in the absence of salt were found to be spherical, monodisperse and unilamellar with a zeta potential value of -13.23 mV. Zeta potential measurements obtained for the liposomes in the presence of inorganic cations indicate there is an electrostatic interaction between the cations and the phosphate groups of the lipids which causes changes in the orientation of the lipid head groups as well as reduced repulsion between neighbouring lipids, resulting in changes in the size of the liposomes. Hydrophobic, organic ions were found to have a significant effect on the size and zeta potential of the liposomes and in some cases fusion or aggregation of the liposomes occurred. The effect of temperature on the liposome suspensions was also examined and the most important effect induced by cations on the liposomes was found to be the effect on the transition temperature of the lipids. The transition temperatures themselves and the breadth of the transition temperatures were affected by the ions in all three cases. The Hofmeister series has not been investigated previously with DLS and TEM using such a range of systems. The results have provided insights into the interactions between ions and liposomes, and will stimulate further research into the Hofmeister series.

To my mother,

Suzanne Keogh

And to my father,

Simon Creed

Acknowledgements

First of all I would like to thank my supervisor, Dr. Wuge H. Briscoe, for all the support and guidance he has given me throughout the course of this work. Without his help, advice and discussions, this work would not have been possible and I extend my deepest gratitude to him for allowing me to carry out this project in his research group.

I would also like to thank Prof. Jonathan Reid, my second assessor, for valuable discussions and useful suggestions given to me during my annual progress monitoring.

I am indebted to members of Prof. Stephen Mann's research group, University of Bristol, for allowing me to regularly use their DLS machine, and I would like to extend a special thanks to Laura Rodriguez Arco for her help and training on the machine throughout the course of this project. I would also like to thank the members of the Mann group for their friendliness and enthusiasm.

I would like to express my gratitude to Judith Mantell, University of Bristol, who gave up her time to help me with TEM. Preparing the samples and collecting the images would not have been possible without her help and it was a pleasure to work with someone so experienced in the area.

A special thanks goes to Manon Jannaud, University of Rennes, who I worked closely with for 3 months during her visit and who collected the data on the effect of trivalent cations on DPPC liposomes. I feel lucky to have been able to work alongside such an enthusiastic and hard-working student.

A huge thanks must also be extended to all the past and present members of the Briscoe group for their feedback and enthusiasm during this project and for making the experience so enjoyable and unforgettable. I feel very fortunate to have been able to work alongside such talented individuals and I am extremely grateful that their paths intertwined with mine. A special thanks goes to the E010 office, Nick Taylor, Michael Greaves, Dan Rose, DK Kim, Adam Fauzi and Abinash Tripathy, for the countless laughs and the fruitful discussions. Other members of the Briscoe group I would like to thank are Chris Redeker, Liangzhi Zhou, Anna Slastanova and Luisa Islas Flores for their help both in, and out of the lab.

Finally, I must extend my deepest thanks to my friends and family who have helped me and supported me throughout the course of this project.

Last but not least, I thank my mum, Suzanne, who has guided me through all the ups and downs and provided exceptional support and advice for me throughout all of my academic work. I simply could have not done it without you.

Author’s declaration

I declare that the work in this dissertation was carried out in accordance with the requirements of the University's *Regulations and Code of Practice for Research Degree Programmes* and that it has not been submitted for any other academic award. Except where indicated by specific reference in the text, the work is the candidate's own work. Work done in collaboration with, or with the assistance of, others, is indicated as such. Any views expressed in the dissertation are those of the author.

SIGNED: ..... DATE:.....

Contents

Chapter 6: The effect of temperature and trivalent cations on DOPC and DPPC liposomes

Chapter 7: TEM images

Chapter 8: Conclusions and future works

Appendices

List of figures

List of tables

Chapter 1: Introduction to the Hofmeister series

1.1 Project motivation

Specific ion effects are significant in numerous areas of science and technology. They have been studied by scientists since the pioneering work of Franz Hofmeister and his group at the University of Prague over 100 years ago. Throughout this time, many examples of specific ion effects in biological and colloidal systems have been published, a variety of explanations for the Hofmeister series have been proposed, and it remains an active research area. New ideas about the origins of the effects have been suggested and modern experimental techniques have allowed new parameters to be measured with increased accuracy, however, a general explanation of specific ion effects has not yet been achieved.

Since specific ion effects are fundamental in so many areas of chemistry and biology, research towards understanding them is very important, in particular, understanding the effects of ions on biological molecules is of great significance. Learning more about the specific molecular interactions and forces between ions and biological molecules is vital for fundamental knowledge and for applications in a wide variety of fields such as medicine (i.e. drug delivery and vaccinations) and in the food industry (i.e. dietary supplements and nutritional products).

This project aims to contribute to understanding specific ion effects, taking a comprehensive experimental approach by using lipids as probe systems. Amphiphilic molecules, both lipids and surfactants, have the tendency to aggregate in solution and form a range of self-assembled structures. In this work, lipids are used to form liposomes and the effects of a range of ions on these liposomes are studied with the hope of shedding light on the Hofmeister series, and the fundamental interactions involved in ion specific effects.

In order to investigate changes in the size, polydispersity index and zeta potential of the liposomes in the presence of ions, dynamic light scattering (DLS) was employed, as it is a widely used and well-established technique for the characterisation of colloidal nanoparticles in aqueous solutions. Additional information on the morphology of the liposomes was obtained using cryo-transmission electron microscopy (TEM) which allows high quality and well-defined images to be obtained.

The early chapters of this work aim to provide the background on the subjects discussed in this project to enable the interpretation of the experimental results and findings. Chapter 1 will provide an introduction to specific ion effects, with particular focus on the Hofmeister series, the mechanism of the series and the previous work which has aimed to explore the series in depth. Chapter 2 will provide

an introduction to self-assembly, concentrating on classification, applications and preparation of liposomes.

The third chapter of this thesis will describe and explain the theoretical considerations and execution of the experimental procedures implemented in this work. Chapters 4 to 7 of this work will present the results obtained. Included in these chapters are extensive analysis and discussion of the results in the context of current literature. The closing chapters of this work will provide conclusions and review the results in the framework of the Hofmeister series.

1.2 Specific ion effects in biology

Specific ion effects are ubiquitous in biology, biochemistry, chemistry and chemical engineering and are vital in a range of biological systems. In the human body, especially in the fluids, numerous ions take part in a variety of chemical processes.

Sodium (Na^+), calcium (Ca^{2+}), potassium (K^+) and magnesium (Mg^{2+}) ions are amongst the most abundant cations in the body. Calcium carries out many important functions and is extensively found in the bones and teeth. When combined with phosphate, calcium increases the rigidity and hardness of enamel in the tooth[1]. In addition, calcium ions and their movement in the cytoplasm are essential as signals in several cellular processes, making them vital in blood clotting, muscle contraction and nerve activity[2]. Sodium ions are the predominant cations in extracellular fluids and affect the transport of water through the cell membrane. Additionally, these ions are involved in the sodium-potassium pump, which describes the mechanism by which sodium ions move out of the cell and potassium ions move in across the cell membrane[3]. Furthermore, potassium is used in protein synthesis, to help regulate the heartbeat, reduce blood pressure, and in the contraction of muscles[4].

Chloride (Cl^-) is the most important anion in the body, controlling the flow of fluid in the blood vessels and tissues and helping maintain the correct acidity levels in the blood[5]. This anion is also key in the formation of hydrochloric acid (HCl) in the stomach which is necessary for healthy digestion[5].

Along with animals, plants also rely on a number of ions. Plants require nutrients in order to carry out photosynthesis and maintain healthy growth. One way ions required by plants can be obtained is from soil, where they are dissolved in water. Nitrate (NO_3^-), phosphate (PO_4^{3-}) and potassium ions are required in the greatest quantities in plants. Nitrate is a major component of chlorophyll, phosphate is required for membrane formation, and potassium ions are needed for enzymatic activity and osmoregulation[6].

Understanding how ions interact with other molecules can shed light on their role in numerous biological processes. As illustrated, ions are vital in nature and by studying specific ion effects on a range of physical phenomena scientists can gain a deeper understanding of the interactions occurring and what properties of the ions cause these specific effects. A more profound understanding of specific ion effects would also benefit research in all areas of science.

1.3 Franz Hofmeister

More than a century ago, Professor of pharmacology at the University of Prague, Franz Hofmeister, published a series of papers in German, entitled '*Zur Lehre von der Wirkung der Salze'*, in English, '*About the science of the effect of salts'*[7]. Hofmeister systematically studied the effects of anions and cations on proteins and in 1888 he observed a trend that classified ions on their ability to precipitate proteins from aqueous solutions[7]. In his original study on the influence of a range of ions on the precipitation of proteins found in egg whites[8], anions were found to have a larger effect than cations and therefore the series tend to be divided into two separate anionic and cationic series. An example of an anionic series is shown in Figure 1**.**

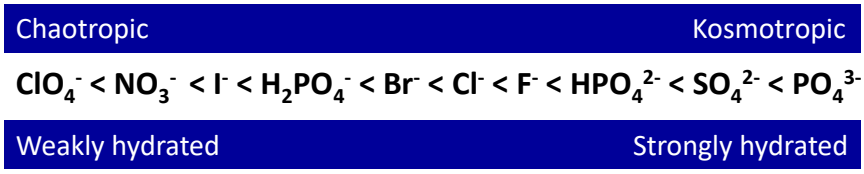

Figure 1: The anionic Hofmeister series, illustrating the weakly and strongly hydrated ions and also the chaotropic and kosmotropic ions.

Ions of the Hofmeister series can be broadly classified into two categories, the ions on the left hand side of the series are called 'chaotropes' and the ions on the right hand side are called 'kosmotropes'. Chaotropes[9] are referred to as '*structure breakers'*, these ions have weak interactions with water and increase protein solubility. Kosmotropes[9] are denoted as '*structure makers'*, these ions have strong interactions with water and decrease the solubility of proteins in aqueous solutions.

As previously mentioned, Hofmeister effects can be seen vastly in biology. Ions can be classified in accordance with their interactions with cell membranes, biopolymers[10], enzymes[11], and even their ability to cross the blood-brain barrier[12]. For this reason, within the last century the Hofmeister series and specific ion effects have been a prominent topic of research, yet the exact mechanism for the Hofmeister series and the position of ions within the series is still poorly understood.

1.4 Mechanisms of the Hofmeister series

It is widely acknowledged that liquid water has many properties which make it unique as a solvent. The anomalous properties of water can be attributed to the intermolecular, three dimensional hydrogen bonding network[13] which is formed due to the partial positive charges of the hydrogen atoms and the partial negative charges of the oxygen atoms. In this way, water molecules can act as both hydrogen bond donors and acceptors.

When ions are added to water the hydrogen bonding network of water molecules is disrupted as the ions become hydrated. The degree of hydration of ions in water is ion-specific in bulk solutions and at interfaces and has been an extensive topic of research for many years[14, 15]. Ions have a large influence on the structure and dynamics of water molecules, especially water molecules in their hydration shells and therefore can be classified according to their relative abilities to induce the ordering of water molecules. In general, kosmotropes have higher charge densities than chaotropes[8], and are hydrated to a greater degree, hence named '*structure makers*'. Chaotropes are generally less hydrated owing to their lower charge densities.

Consequently, it has been suggested that the ordering of ions in an aqueous solution within the Hofmeister series may be due to the influence of ions on the bulk structure of water. This is still an area of intensive research and there remain many unanswered questions.

In order to shed light on the ordering of ions in the Hofmeister series it is vital to understand how specific ion effects are studied and what interactions need to be considered. Specific ion effects can be studied in a vast array of ways and the viscosity, density, heat capacity and freeing point depressions of electrolytes[16] are some examples that occur widely in the literature. The intermolecular interactions between the solvent, solute molecules and the ions on the addition of salts to non-electrolytes, make ion effects very complex.

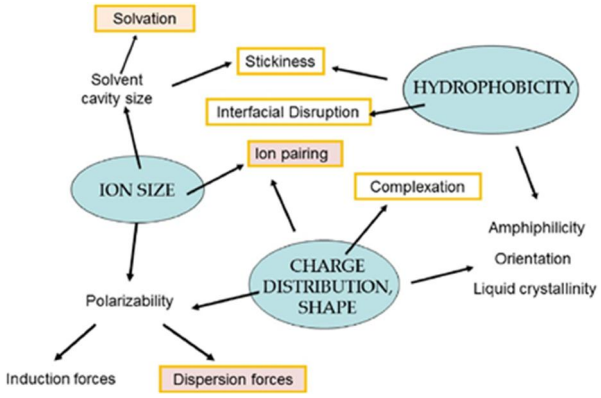

Figure 2: A chart of connections showing ionic parameters that are used to determine ion specific effects. Reprinted from Reference 10. Copyright © 2016, with permission from Elsevier.

1.5 Classical theories to explain the Hofmeister series

1.5.1 Debye–Hückel theory

In 1923 a quantitative theory was put forward by Peter Debye and Eric Hückel which advanced knowledge of electrolyte solutions[17]. The Debye–Hückel theory provides an explanation of non-ideal solutions of electrolytes. It is a linearized Poisson-Boltzmann model[18] which helps to predict the activity coefficients and behaviour of ions in dilute solutions. The model is based on the fact that in electrolytes, oppositely charged ions attract one another and therefore cations are more likely to be found near anions and vice versa.

Hence, in an ideal solution, there is a spherical haze around each ion, where there are a higher number of counter ions than ions of the same charge as the central ion. The energy and consequently the chemical potential of any given ion is lowered as a result of the interaction with the surrounding spherical haze[17] (Figure 3). These concepts were developed into a quantitative theory from which at very low concentrations the activity coefficient can be calculated.

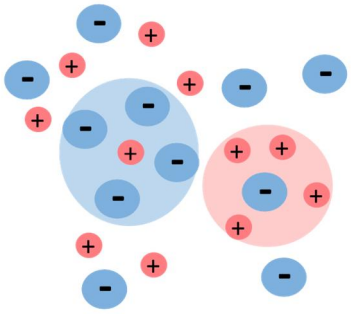

Figure 3: Schematic illustration of the ion distribution surrounding a cation.

However, the Debye–Hückel theory contains some underlying assumptions which render it unrealistic when attempting to predict specific ion effects. The first is the assumption that the solute is completely dissociated[19] (it is a strong electrolyte) which is not applicable to weak electrolytes. Secondly, the ions are assumed to be spherical in shape, which becomes a problem for non-spherical ions that solicit isotropic interactions[16]. In many cases, biological ions are non-spherical and therefore their interactions change depending on the direction of their approach. Finally, the model assumes that each ion is surrounded by an ionic atmosphere of counter ions[20], as described above.

This theory provides a useful insight into the interactions within electrolyte solutions; however, it is not extensive enough to explain the relative positions of ions in the Hofmeister series. In more recent literature, attempts have been made to extend the Debye–Hückel[17, 21-23] theory to better encompass all the interactions in electrolyte solutions.

1.5.2 The DLVO theory

In the 1940s, Derjaguin, Landau, Vervey, and Overbeek (DLVO)[24] developed a theory which helped to explain the stability of colloidal systems. This theory is now a cornerstone of colloid science. The DLVO theory describes the forces between two charged particles, considering a balance between the electrostatic double layer repulsion and the van der Waals attractions[25, 26], which are the attractions between fluctuating dipoles and induced dipoles caused by the movement of electrons (Figure 4). By considering these two forces it is possible to predict the stability of a colloid suspension and whether aggregation will occur in the system.

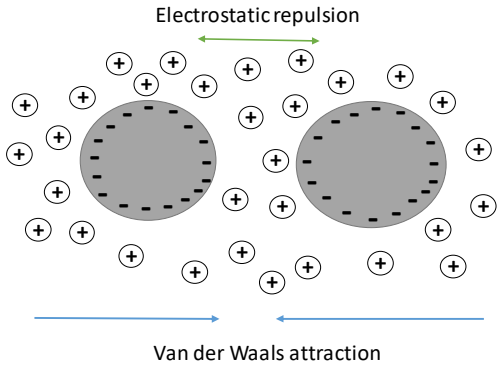

Figure 4: Schematic illustration of the electrostatic repulsion and Van der Waals attraction that exists between two charged particles in a colloidal system.

The Hofmeister effects of salt addition on a colloidal suspension can also be studied and explained by the DLVO theory. On addition of an electrolyte, the electrostatic Columbic repulsion is screened and therefore the particles are less strongly repulsive to each other. The colloid suspension becomes more unstable and aggregation of the particles can occur. The effects of different salts can be studied, and the stability of the colloidal particles is found to be salt dependant [27].

Although this theory can help to shed light on specific ion effects in colloids, it does not unravel the ordering of ions in the Hofmeister series. The problem lies with the assumptions made by the DLVO theory. Firstly, the DLVO theory makes a *dielectric continuum* solvent approximation[25, 28], which means that hydration of ions and solvent structure are ignored. Here lies one problem in using this theory to help understand the Hofmeister series, as ion interactions with the solvent water molecules are not evaluated. As the solvent molecules are hypothesised to play a role in the ordering of ions in the series, it is vital that these interactions are included. Secondly, the ions are treated as point charges[26] and therefore the shape of the ion is ignored when using the DLVO theory which is an important parameter when considering ion specific effects. Finally, the electrical double layer and van der Waals forces are assumed to be additive[26]. The electrostatic forces are treated in a non-linear form (Poisson-Boltzman equation[25], which describes the electrochemical potential of ions in the diffuse layer) and the opposing

van der Waals forces are treated in a linear (the Lifschitz theory[29]) form. This is indicative of a fundamental inconsistency built into the DLVO theory and the reason that it falls short in explaining the ordering of ions in the Hofmeister series.

Despite the fact that conventional electrostatic theories cannot explain the Hofmeister effect of ions, analysis of correlations between different experimental findings can help reveal properties that are specific for individual ions.

1.5.3 Ion specific parameters and water structure

In order to untangle the problem of the Hofmeister series, attempts were made to empirically classify ions as either chaotropes or kosmotropes. This would act as a starting point and help to advance the understanding of the hydration of ions in aqueous solutions, a seemingly crucial parameter to grasp for a comprehensive appreciation of specific ion effects.

Sephadex G-10 gel sieving chromatography on a number of anions and cations was carried out by Collins[30] in 1995. Sephadex G-10 is dextran highly crosslinked with epichlorohydrin, from which beads with a small pore size and a non-polar surface can be produced, which can separate solutes by gel sieving. Larger molecules are excluded by the small pores of the beads and therefore emerge from the column early. The smaller molecules are able to penetrate into the beads, and therefore their path through the column is longer and they emerge later.

The results of Collins' work are shown in Figures 5 and 6[30]. The Sephadex G-10 column separates the ions and, therefore, from the graphs we can classify the examined ions into chaotropes and kosmotropes. The chaotropic ions are above the calibration line, these ions were found to destabilise proteins whereas the kosmotropic ions, appearing below the calibration line, stabilise proteins.

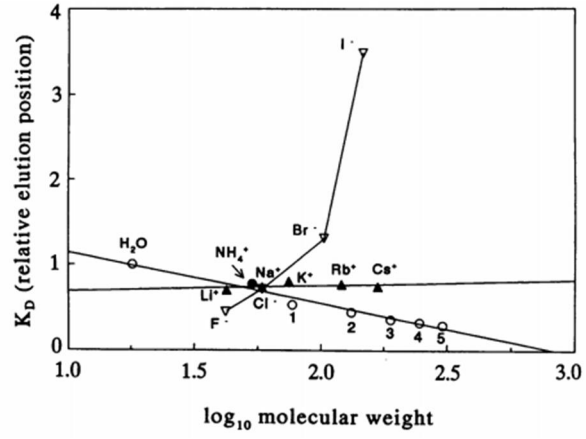

Figure 5: Results of work carried out by Collins. Aqueous gel sieving chromatography on Sephadex G-10 of cations (Li^+, Na^+, K^+, Rb^+, Cs^+ and NH_4^+ as the Cl^- salts as well as F^-, Cl^-, Br^- and I^- as the Na^+ salts.) Image taken from Reference 30.

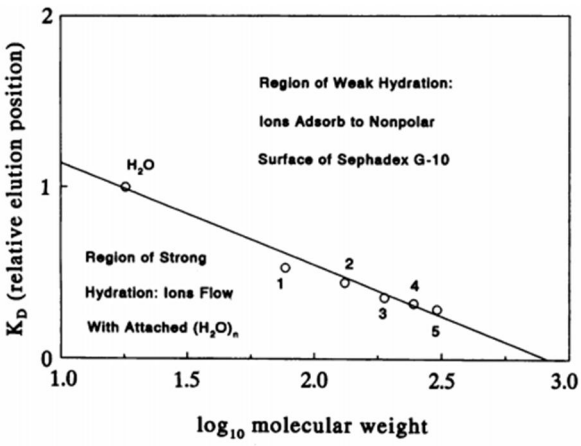

Figure 6: Results of work carried out by Collins. Calibration curve for the Sephadex G-10 column eluted with 0.1 M NaCl. Image taken from Reference 30.

From the results of the halide ions it can be hypothesised that the charge density of the ion is the controlling property[31] and therefore an important consideration when the Hofmeister series is considered. Collins also discovered from this work that the stabilizing anions (kosmotropes) had an apparent molecular weight greater than their anhydrous molecular weight which may be attributed to water molecules bound to the ion. It can therefore be confirmed from this work that the kosmotropic ions are more strongly hydrated than the chaotropic ions. Finally, the elution of the destabilizing (chaotropic) ions was found to be temperature and concentration dependent which is characteristic of ion adsorption to the nonpolar surface of the gel[31]. One hypothesis for the driving force of this adsorption is the release of weakly bound water molecules which are able to interact more strongly in the bulk solution than with the chaotropic anion[32, 33].

The Jones- Dole viscosity B coefficient systematically confirmed the results obtained by Collins from the Sephadex G-10 gel sieving chromatography and therefore provided a quantitative way to define kosmotropes and chaotropes. The viscosity of a salt solution can be simply measured and the viscosity B coefficient is defined by the expression in Equation 1 [34, 35].

$$\eta/\eta_0 = 1 + Ac^{1/2} + Bc \qquad (1)$$

where η is the viscosity of salt solution, η_0 is the viscosity of pure water, A is the electrostatic term, c is the concentration and B is a direct measure of the strength of ion water interactions normalized to the strength of water-water interactions[31]. The Jones-Dole B coefficient separates the ions into two groups according to their degree of water structuring. Positive B coefficients signify strongly hydrated

ions (kosmotropes), whilst negative B coefficients signify weakly hydrated ions (chaotropes). Some examples of B coefficient values are listed in Table 1[32].

Table 1: Jones Dole viscosity B coefficients. Reprinted from reference 32, Copyright © 1997, with permission from Elsevier.

Cations	B	Anions	B
Mg^{2+}	0.385	PO_4^{3-}	0.590
Ca^{2+}	0.285	$CH_3CO_2^-$	0.250
Ba^{2+}	0.22	SO_4^{2-}	0.208
Li^+	0.150	F^-	0.10
Na^+	0.086	HCO_2^-	0.052
K^+	−0.007	Cl^-	−0.007
NH_4^+	−0.007	Br^-	−0.032
Rb^+	−0.030	NO_3^-	−0.046
Cs^+	−0.045	ClO_4^-	−0.061
		I^-	−0.068
		SCN^-	−0.103

It is interesting to note that the ions are ordered according to their charge density, therefore as would be expected, the degree of hydration of an ion increases with increasing charge density, and this is in good agreement with the trend in the previously discussed literature.

Quantification of the Hofmeister effect of an ion has been widely obtained in the literature by means of a linear regression of the relative solubility of a solute (proteins[36], macromolecules[37, 38] *etc.*) against the concentration of the ion. The gradient of such a correlation plotted on a graph is termed the Setchenow constant[36, 38, 39], calculated by Equation 2[36].

$$log[C_i/C_i(0)] = -k_s C_s \qquad (2)$$

where C_i is the molar concentration of the solute, C_s is the concentration of the salt and k_s is the salting out constant. The Setchenow constants are available for a wide range of salts and provide a measure of 'salting in' and 'salting out' ability of individual ions. The more positive the Setchenow constant, the more the ion induces 'salting out'. Magnesium (Mg^{2+}) has a Setchenow constant value of +0.17[40] for example, compared sodium (Na^+) which has a constant value of +0.11[40], therefore Mg^{2+} decreases the aqueous solubility of hydrophobic molecules to a greater degree than Na^+. More diffuse ions such as $(CH_3CH_2)_4N^+$ have actually been found to increase solubility, with a Setchenow constant value of approximately -0.10[40].

Although these constants are helpful, they do not provide information about the mechanism by which ion specific effects on macromolecules occur. Indirect clues can, however, be obtained by studying ion specific effects on macroscopic solution properties and comparing the results to the constants for individual ions. In addition, the importance of hydration and charge density is conveyed in these constants which helps to begin to shed light on the Hofmeister series.

1.5.4 Recent approaches to Hofmeister phenomena

1.5.4. i. Collins law of matching water affinities

In 1997 Collins[32] presented a convincing, yet extremely simple concept which became known as the *law of matching water affinities* (LMWA). This concept helps shed light on the Hofmeister series by providing a method for predicating how electrolytes behave in aqueous systems. The LMWA is based on the observation that for monovalent ions, there is a much stronger attraction between ions of similar sizes than for ions of dissimilar sizes in water[16, 32]. This can clearly be seen from Table 2[41], where the solubility of very simple group one halide salts shows a remarkable pattern.

Table 2: Solubilities of Group 1 halides. Taken from Reference 41.

	Solubility (Molar value first, g/100 g H_2O given in brackets)			
	MF	MCl	MBr	MI
Li	0.1 (0.27)	19.6 (830)	20.4 (177)	8.8 (165)
Na	1.0 (4.22)	6.2 (36)	8.8 (91)	11.9 (179)
K	15.9 (92.3)	4.8 (34.7)	7.6 (67)	8.7 (144)
Rb	12.5 (130.6)	7.5 (91)	6.7 (110)	7.2 (152)
Cs	24.2 (367.0)	11.0 (186)	5.1 (108)	3.0 (79)

Large ions paired with small ions give very highly soluble salts, whereas salts made up of only small ions or only large ions are moderately soluble in comparison. In his work, Collins focussed on the tendency of ions to form inner sphere pairs in solution, according to the equation below, Equation 3[32].

$$M^{n+}(hydrate) + X^{n-}(hydrate) \leftrightarrow MX(hydrate) + mH_20 \qquad (3)$$

To explain theses interactions Collins considered ions as spheres with a point charge at the centre[27, 32]. Consequently, he also considered small (hard) ions to be strongly hydrated as there is a small distance between the point charge on the ion and the point charge of opposite sign on a water molecule and therefore a strong electrostatic attraction between the two. In contrast, larger (soft)

ions are considered to be more weakly hydrated owing to the larger distance between the point charge of the ion and the water molecules. It is energetically unfavourable to remove water molecules from a small ion. However, if the water molecules removed are replaced with a small ion of opposite charge, the unfavourable increase in energy is more than compensated for by the resulting strong electrostatic interaction between the ions in the newly formed salt as the point charges are close together. It can be concluded therefore that the formation of small- small inner sphere ion pairs is energetically favourable. Similarly, it is energetically favourable for large-large inner sphere ion pairs to form. The interaction of the point charges in a salt made of two large ions is weak due to the large distance between point charges. However, on the formation of salt, the liberation of weakly bound water molecules from an ion is able to compensate for this weak interaction as the water-water interactions in the bulk are much stronger than the large ion-water interactions.

In contrast, small ions do not tend to form ion pairs with large ions. The energy required to remove water molecules from a small hydrated ion is not regained by the replacement with a large ion. This is because the point charges are too far apart to interact strongly. Large-small ion pairs tend to remain in aqueous solution and hence, they are soluble. In general, strong interactions form at the expense of weaker ones in solution and any system will also aim to maximise the number of strong interactions. The figure below shows schematics of the LMWA.

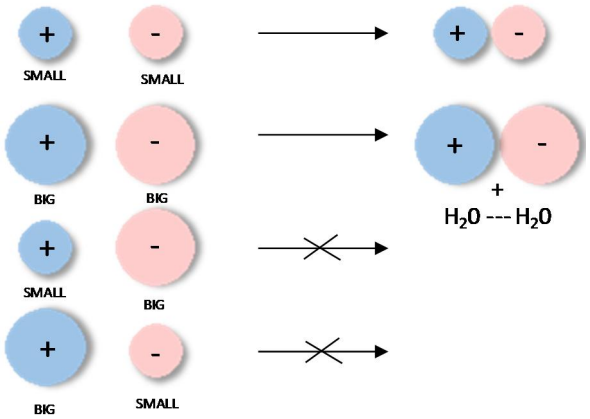

Figure 7: Schematic illustration of the Law of matching water affinities.

It can be stated that when two ions have similar free energies of hydration, the enthalpy of solubilisation, ΔH_{sol}, in water is an endothermic (positive) process. Conversely, when the electrolyte is made of ions which have large differences in their free energies of hydration, the enthalpy of solubilisation is exothermic (negative).

The tendency of ions to form ion pairs can be summarized using the 'volcano' graph[16, 31, 32]. Figure 8[32] shows that at the top of the volcano the inner sphere ion pairs are likely to form, and at the foot of the volcano the ion pairs are less likely to form.

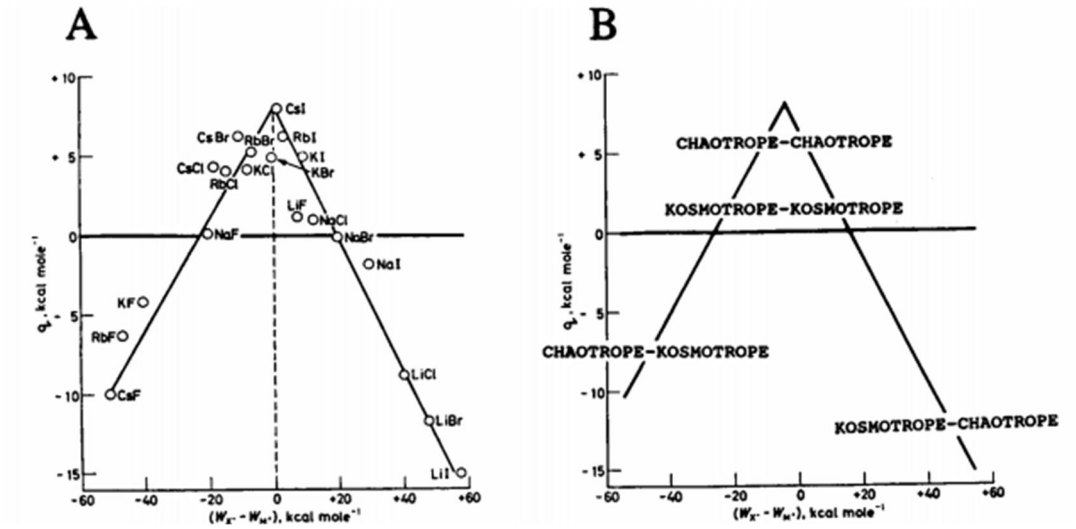

Figure 8: (A) The relationship between the standard heat of solution of a crystalline alkali halide and the difference between the absolute heats of hydration of the corresponding gaseous anion and cation. (B) Corresponding graph to identify ions as chaotropes (weakly hydrated) or kosmotropes (strongly hydrated). Reprinted, with permission, from Reference 32. Copyright ©1997, Elsevier.

Collins rule of matching water affinities has been found to be successful in qualitatively understanding specific ion effects in various systems. A neat example, which confirmed this rule, was a study carried out by Xie *et al*. in 2014[8]. Specifically, $M(H_20)_n$ (M= Li and Cs, n= 0-6,10 and 18) clusters[8] were studied by photoelectron spectroscopy (PES) and quantum mechanical (QM) calculations. The results are shown below in Figure 9[8].

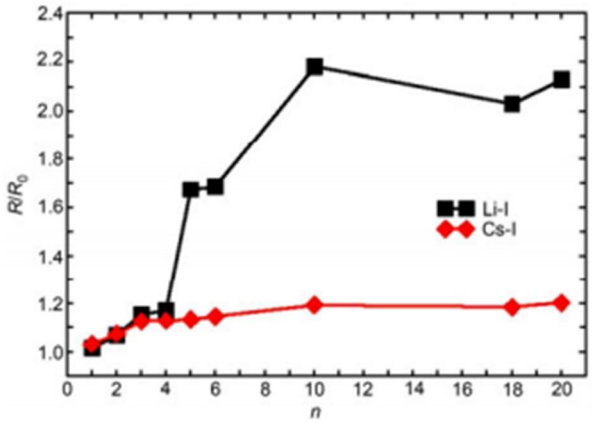

Figure 9: The change in ion pair distances (divided by the bare ion pair distance) in salt water clusters as a function of water molecule number. Reprinted by permission from Springer, reference 8, Copyright © 2013

At first glance, it can be seen from the obtained results that the structure of salt/water clusters alter in very different ways for Li^+ and Cs^+ as the number of bound water molecules increases. At n=5 there is a sharp increase in the Li-I distance in the $LiI(H_2O)_n$ cluster which does not appear at any value of n for the $CsI(H_2O)_n$ cluster. The ionic radii of Li^+ and Cs^+ are 0.074 nm[42] and 0.170 nm[42] respectively and the ionic radii of I^- is 0.22 nm[43], the Li^+ ion can therefore be considered comparatively 'small' and the Cs^+ and I^- ions can be deemed comparatively 'big'. Therefore, according to the LMWA, the two 'big' ions are more likely to form contact ion pairs (CIP) and remain close to one another whilst the 'big' I^- ion is unlikely to form a CIP with the 'small' Li^+ ion and hence the distance between the two is large, and solvent separated ion pairs (SSIP) form. These predictions are clearly confirmed by the results obtained from this literature and hence it is clear the LMWA is a valid rule which can be helpful in obtaining information about the behaviour of ions in solution and predicting specific ion effects.

1.5.4. ii. Binding to surfactant head groups

In order to gain a more comprehensive understanding of the Hofmeister series, Kunz and coworkers[44] proposed a Hofmeister-like ordering of charged head groups with the law of matching water affinities. By using the LMWA in this way, interactions of ions with head groups of phospholipids and surfactants can begin to be understood and the influence on a range of physical properties can start to be unravelled. The head groups are first classified as chaotropic (soft) or kosmotropic (hard). According to this classification, Kunz *et al.* proposed that the softness of the head groups studied, from kosmotropic to chaotropic, is carboxylate ($RCOO^-$) < phosphate ($R_2PO_4^-$) < sulfate (RSO_4^-) < sulfonate ($RSO3^-$) [44]. Figure 10[44] shows the ordering of the head groups and the respective counter ions according to their ability to form contact ion pairs.

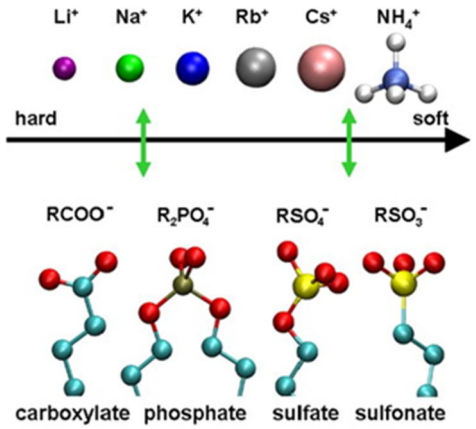

Figure 10: Ordering of anionic surfactant head groups and their respective counter ions in order of their capabilities to form close ion pairs. Strong interactions are represented by the green arrows. Reprinted from reference 44. Copyright © 2009, with permission from Elsevier

The above series together with Collins' LMWA can help to explain numerous experimental results and can also help to predict effects when one ion is substituted for another. For example, when studying the interactions of proteins and ions, classifying the groups and residues on the protein as 'hard' or 'soft' can help to predict as to where the ions would reside.

As with all simple concepts, the LMWA should be considered with care, and it should be noted that the complexity of specific ion effects cannot be described by one single, simple model. Nevertheless, this exceptional rule presented by Collins has helped scientists understand the results of studies on specific ion effects in a multitude of cases in biological and colloidal science.

1.6 The ongoing challenges of the Hofmeister series

Despite the recent advances in Hofmeister effects, there remains a number of grey areas in the research conducted. The first and foremost is the influence of the ions on the bulk water structure. As mentioned, it is hypothesised that the ordering of ions in the Hofmeister series may be due to their influence on the bulk structure of water molecules. The traditional explanation for the interactions of ions with proteins attributed Hofmeister effects to the salt induced withdrawal of water from protein surfaces[21, 45]. A protein 'salts out' if the ion in solution is strongly hydrated as the ion successfully competes for the water molecules in the electrolyte and therefore causes a decrease in the number of water molecules surrounding the protein. Experiments have in some cases, however, demonstrated that ions do not affect the hydrogen bonding network of water molecules beyond their first solvation shells[46, 47]. Bakker and co-workers[47] used femtosecond pump-probe spectroscopy to investigate the rotational dynamics of water molecules outside the first solvation shell of ions in electrolyte solutions. The results of the work, established that the presence of ions does *not* lead to the alteration of the hydrogen-bonded network of bulk liquid water. The conclusions regarding the Hofmeister series that were drawn from this work was that no long-range structure making or structure breaking effects for kosmotropes or chaotropes were taking place, therefore the observed effects were attributed to direct ion- protein interactions.

The second unanswered observation regarding the Hofmeister series manifests itself in the findings that in some cases the Hofmeister series is reversed in order (the Hofmeister series listed previously (Figure 1) will be taken as the direct Hofmeister series). The best known example is the interaction of ions with the enzyme, lysozyme[48-50]. These interactions behave according to the direct Hofmeister series at high pH or high ionic strength, and then according to the reverse, indirect series under acidic conditions or at neutral conditions[48], therefore there are two distinct Hofmeister series. These findings illustrate the importance of the specific surface hydration- ion hydration interactions, and it is seemingly impossible to provide a plausible explanation for the Hofmeister series by considering the ion-water interactions alone[48]. Additionally, the ionic volume and polarization are important parameters that should not be ignored. By considering the direct adsorption of ions onto surfaces and the alteration and screening of surface charge, the Hofmeister series can begin to be understood, and although reverse Hofmeister series have been observed, the idea that there is a universal Hofmeister series persists.

The third observation which has troubled physical chemists is the effect of cations. The water 'withdrawing power' approach appears to provide an explanation for the behaviour of anions witnessed by Hofmeister, however, it cannot explain why kosmotropic cations cause proteins to salt in and chaotropic cations can cause proteins to salt out[51]. This presents an asymmetry in the results for cations and anions, shown in Figure 11[51].

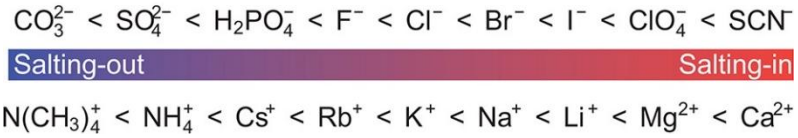

Figure 11: Ordering of anions and cations according to the Hofmeister series based on precipitation studies of solutions of proteins. Reprinted with permission from reference 51. Copyright © 2013, American Chemical Society.

Immediately, it is clear to see that the halide ions are ordered according to increasing size, and therefore decreasing charge density from left to right. Whilst for the cations, the series follows a pattern of increasing charge density from left to right. This asymmetry between the ion series, demonstrates that the ion specific behaviour is not trivially linked to size and charge density, and with these parameters alone the Hofmeister series cannot be explained.

Although there are still questions regarding the Hofmeister series, recent advances in science technology have allowed far more progressive and comprehensive research into ion specific effects to be carried out. This project was carried out with the hope of shedding light on the Hofmeister series and advancing current understanding of the positions of ions within the series.

1.7 Previous work on the Hofmeister series in different media

1.7.1 Aqueous media

For over a century, Franz Hofmeister's work on specific ion effects has inspired a large amount of research. Specific ion effects on a range of physical phenomena have allowed a deeper understanding of the Hofmeister series and has bought scientists closer to understanding this invaluable concept. A large number of studies on specific ion effects have been carried out in aqueous media. The unique structure of liquid water and the relevance of specific ion effects in biology have prompted scientists to investigate the behaviour of ions in water. Lund *et al*.[33] studied the binding of ions to non-polar surface patches of proteins. Molecular dynamics simulations were used to study Lysozyme in a mixed aqueous solution of potassium iodide (KI) and potassium chloride (KCl). It was found that the Cl^- ion resided in the basic residues, which are cationic, and in contrast, the I^- ion resided in the non-polar sites. Lund *et al.* proposed that the binding of anions to the protein was driven by direct ion-ion interactions and solvent assisted interactions with non-polar patches on the protein. This hypothesis is derived from considering the change of intermolecular interactions that come about when the ion is moved closer to the non-polar patch on the protein. These consist of the loss of dipole energy, the reduction in the unfavourable organised network of water molecules around both the ion and the interface, and the attractive induced dipole interactions which occur between the protein surface and a polarizable ion[33]. The smaller chloride ion, will have a smaller reduction in the unfavourable organised water network than the iodide ion as it moves towards the non-polar surface. In addition, and more importantly, the chloride ion is less polarizable and therefore the induced attractive dipoles are much weaker, hence the iodide ion is more likely to be found in the non-polar patches of the proteins. Owing to the important role played by water, the interaction between the ions and the protein surface is said to be *solvent assisted.*

1.7.2 Non-aqueous media

Although there has been an ongoing amount of research carried out on the Hofmeister series in aqueous media, research studying the series in non-aqueous media has become increasingly more profound. Considering the series in non-aqueous media allows a greater understanding as to whether specific ion effects are restricted to hydration in water as a solvent medium. Additionally, research of this type can allow the influence of hydrogen bonding on the position of ions in the series to be better

understood. As the hydration of ions in water is hypothesised to play a role in the ordering of ions in the Hofmeister series, as previously discussed, using non aqueous media can allow this theory to be further tested. Bilaničová et *al*.[52] studied the effect of anions on enzymatic activity in aqueous and non-aqueous media, using the activity of P. *cepacia* Lipase in water and also 2-methyl-2-butanol. The results show that the influence of anions, in both aqueous and non-aqueous media, follow the direct Hofmeister series. Therefore a conclusion is that the ordering of ions in the series is attributed to the direct interactions of the anions with the enzyme surface, as opposed to the ion-water interactions. The observation that the series remains the same in aqueous and non-aqueous media confirms that the effect of ions on the three dimensional hydrogen bonding network of water molecules is not the effect that is responsible for the ordering of ions in the series. This idea is reinforced in work carried out by Pinna et *al*.[11], where the influence of anions on the enzymatic activity of *Aspergillus niger* Lipase in water was studied. The results were found to follow a direct anionic Hofmeister series. Pinna *et al*. concluded that the results were due to a specific interaction (adsorption) of anions to the surface of the enzyme instead of salt induced water structure modification. Additionally Peruzzi *et al*.[53] found that Hofmeister effects were not restricted to aqueous media by studying the solubility of electrolytes in ethylene carbonate. Ethylene carbonate is an aprotic, polar solvent[54] which does not possess hydrogen bonding. Therefore by using this as a solvent, the importance of hydrogen bonding in specific ion effects can begin to be better understood. The results of this study produced a series of anions that followed the same Hofmeister series as that in water (the solubility increases according to the series $F^- < Cl^- < Br^- < NO_3^- < ClO_4^- < I^-$)[53]. The results of this work led to the conclusion that the behaviour of electrolytes depended on solvent-solute (solvent-ion) interactions, rather than the hydrogen bonding.

By altering the medium in which ion specific effects are studied, research can allow clues to be gained about the mechanism of the Hofmeister series. The outcome of work carried out in non-aqueous media suggests that the ordering of ions in the Hofmeister series is not due to the hydration of ions and the alteration of the bulk water structure, but instead, direct interactions between the ion and the macromolecule or solvent surface.

Chapter 2: Introduction to self-assembly and liposomes

2.1 Introduction and examples of self-assembly

Self-assembly occurs under defined conditions and refers to the spontaneous association of building units in a system into defined larger structures with precise geometry. Self-assembly is, therefore, thermodynamically favourable and can occur on a variety of different length scales ranging from atomic to colloidal [55].

Molecular self-assembly occurs widely in nature, and many biological systems and processes rely on this phenomenon. Protein folding from a polypeptide, for example, is a fundamental self-assembly process which involves a large number of complex interactions, including electrostatic interactions, dipole moments, hydrogen bonds and van der Waals interactions[55]. In addition, the formation of cell membranes via the molecular self-assembly of phospholipids is another crucial process, vital for all living cells[56]. Phospholipids in cell membranes will be discussed in more detail later in the introduction of this work. Another interesting biological example is DNA-lipid complexation via self-assembly, which has received significant attention in biology and biotechnology due to the potential applications in gene therapy [57]. In this example, the organisation of DNA and lipid self-assembly is controlled by the lipophilic properties of each component and the DNA packing constraints [57].

Self-assembly occurs due to the delicate balance between attractive and repulsive intermolecular forces [58]. For some solute in a solvent, its dissolution or phase separation from the solvent is driven by the minimisation of the free energy. This is given by the balance between the entropy gain due to the mixing and the free interaction energy increase.

2.2 Phospholipids: molecules that self-assemble

Phospholipids are a vital class of lipids that are of significant interest because they are a major component of the cell membrane. Phospholipids are made up of a hydrophilic head group attached to two hydrophobic fatty acid chains. The hydrophilic head group is comprised of a glycerol backbone, a phosphate group and a polar R group[59]. Phospholipids can be divided into groups based on their hydrophilic head groups, common examples are neutral phosphatidylcholine (PC), negatively charged phosphatidylethanolamine (PE) and phosphatidylserine (PS).

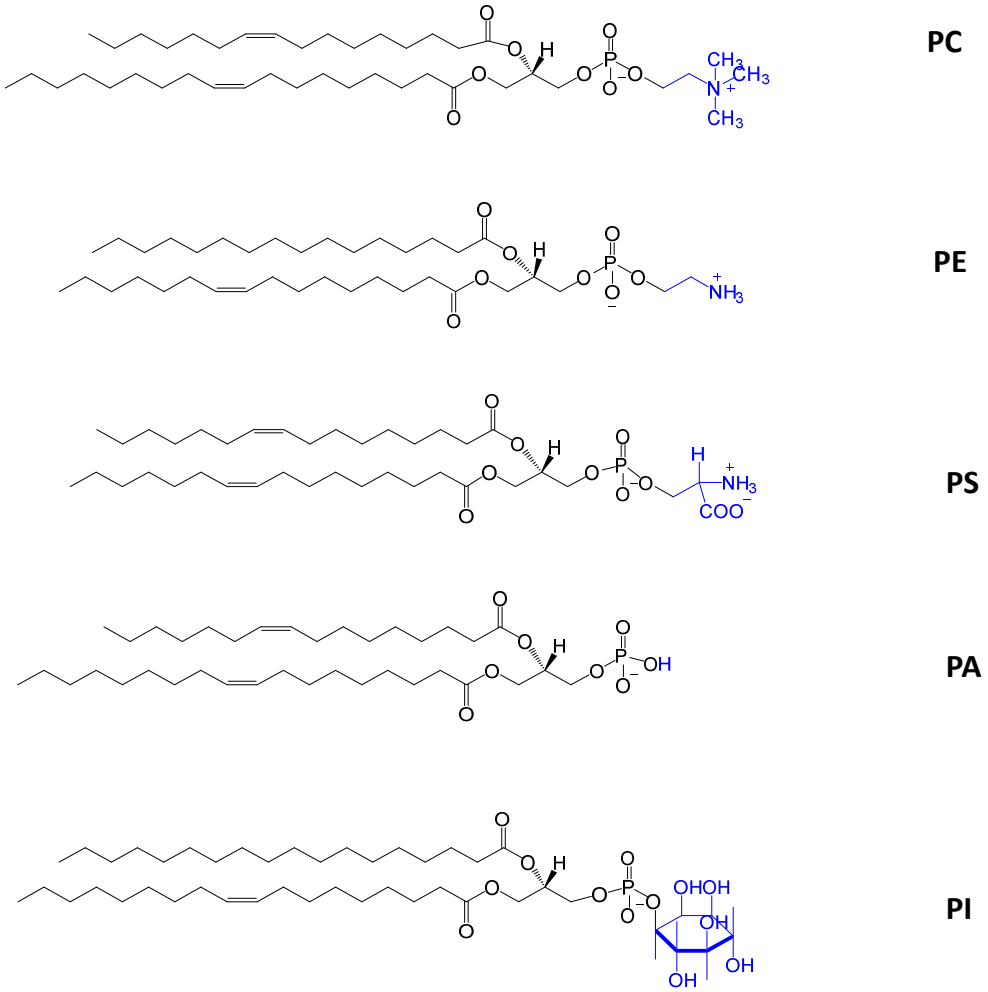

Figure 12: Examples of common phospholipids, neutral phosphatidylcholine (PC), negatively charged phosphatidylethanolamine (PE), phosphatidylserine (PS), phosphatidic acid (PA) and phosphoinositides (PI). The head group of the phospholipid is shown in blue.

The polar head groups of the phospholipids have a high affinity for water and are comprised of a negatively charged phosphate group. The solubility of lipid molecules in water is very low (10^{-6} – 10^{-8} M), and as a consequence, the fatty acid chains on the phospholipid are hydrophobic and aim to minimise their contact with water molecules. As a result of their amphiphilic nature, when dispersed in the aqueous phase, phospholipids spontaneously self-assemble into a variety of structures, a

process known as 'phospholipid polymorphism'[60]. The self-assembled structures formed are arranged with the hydrophilic head groups in contact with the aqueous medium, while the hydrophobic tails are on the inside of the structure, shielded from the unfavourable interactions with the aqueous phase [60, 61].

The self-assembly process occurs due to a balance between the attractive and repulsive forces. When the hydrophobic tails are brought into contact with water, the hydrogen bonding network of water molecules is disrupted as the water molecules re-orientate themselves around the hydrophobe, resulting in a significant loss of entropy [62]. As the phospholipids self-assemble, the hydrophobic tails aggregate, decreasing the number of water molecules in contact with the hydrophobe and hence, causing an increase in the entropy. This observation is known as the 'hydrophobic effect' [62, 63]. The fatty acid tails appear to 'attract' each other in order to minimise the hydrophobic interfacial energy and increase the entropy of the water molecules in the bulk.

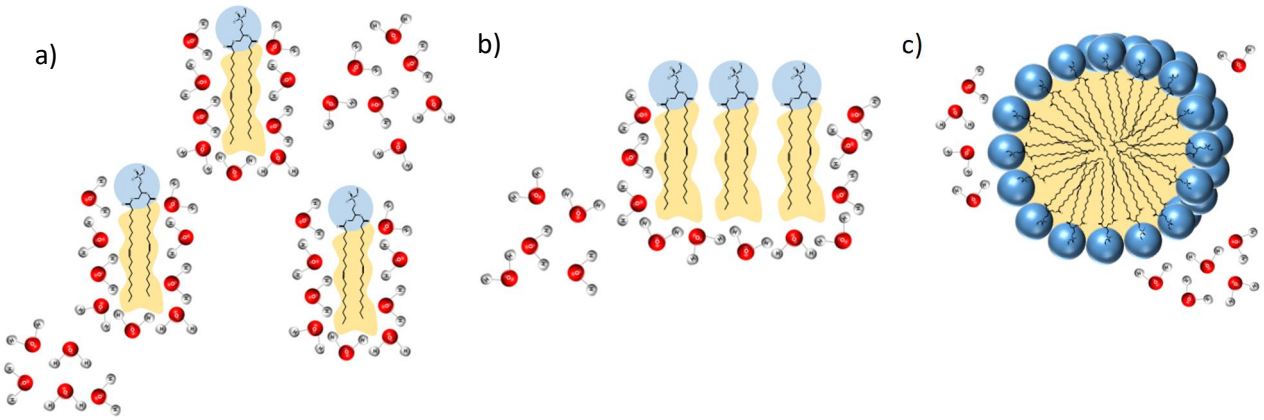

Figure 13: The hydrophobic effect. a) Water molecules form cages around the hydrophobic tails of phospholipids causing a decrease in entropy. b) As the hydrophobic tails come together, there are less ordered water molecules forming cages. c) On the formation on a vesicle, the hydrophobic tails are shielded from the water and therefore ordered water is minimal. On moving from a) to c) the entropy of the system increases.

As well as attractive forces, there are also repulsive forces which drive self-assembly. The hydrophilic head groups of phospholipids are hydrated, which means that they have water molecules strongly bound to them. The hydration layers around the head groups experience ionic, steric and hydrophilic repulsion between each other, and therefore allow the formation of stable self-assembled structures, an observation sometimes referred to as 'hydration repulsion' [64, 65].

When considering the thermodynamics of self-assembly, for phospholipids in water, the condition for thermodynamic equilibrium is that for individual lipids and aggregates, the chemical potential (total free energy) of each lipid molecule in different sized aggregates is the same,[66] thus:

$$\mu(N) = \mu_N^0 + \frac{k_B T}{N} ln(\frac{X_N}{N}) \quad (4)$$

where N is the number of lipid molecules present in aggregate, k_bT is the thermal energy, μ_N^0 is mean interaction free energy of the molecule in the aggregate of N molecules and X_N is the volume fraction (activity)[67]. The above equation therefore infers that:

$$X_N = N(X_1 e^{\left[\frac{(\mu_1^0 - \mu_N^0)}{k_b T}\right]}) \quad (5)$$

where X_1 is the activity of the monomer in solution[67 68]. Since the activity, X_N, must be less than 1 and aggregation occurs due to the differences in interaction free energy between lipid molecules of different size, from Equation 5 it can be seen that aggregates only form in solution if the interaction free energy decreases with increasing number of monomers in the aggregates (i.e. $\mu_1^0 - \mu_N^0 > 0$).

Therefore, the above equations can help explain why phospholipids aggregate and form self-assembled structures when submerged in an aqueous phase. The self-assembled structures formed are mesoscopic phases (vesicles, micelles, lamellae, hexagonal, inverted hexagonal etc). To describe the formation of these mesophases, it is necessary to consider how the interaction free energy differs with the size of aggregates.

The interaction free energy per molecule can be described as the sum of four terms, which describes the contributions from different intermolecular forces.

$$\mu_N^0 = \mu_N^0[HG] + \mu_N^0[HPh] + \mu_N^0[CP] + \mu_N^0[IA] \quad (6)$$

The first and second terms in the above equation describe the head group hydration repulsion and hydrophobic attraction respectively, as described previously. The third term in the equation describes the chain packing and the chain repulsive pressure. The chain repulsive pressure encompasses the configurational constraints of the chain (decrease in chain freedom) during the formation of the self-

assembled structures and gives rise to the curvature dependence of μ_N^0. The final term in the equation describes the inter-aggregate forces.

In order to incorporate a geometric parameter in the self-assembly phenomena, the concept of a 'packing parameter' was introduced and is part of the third term in the above equation [69].

$$P = \frac{v}{a_o l_c} \qquad (7)$$

The packing parameter, P, takes into account three different geometric parameters, v is the volume of the hydrocarbon tail in the core, l_c is the critical chain length of the tail and finally, a_0 is the optimal head group area[70].

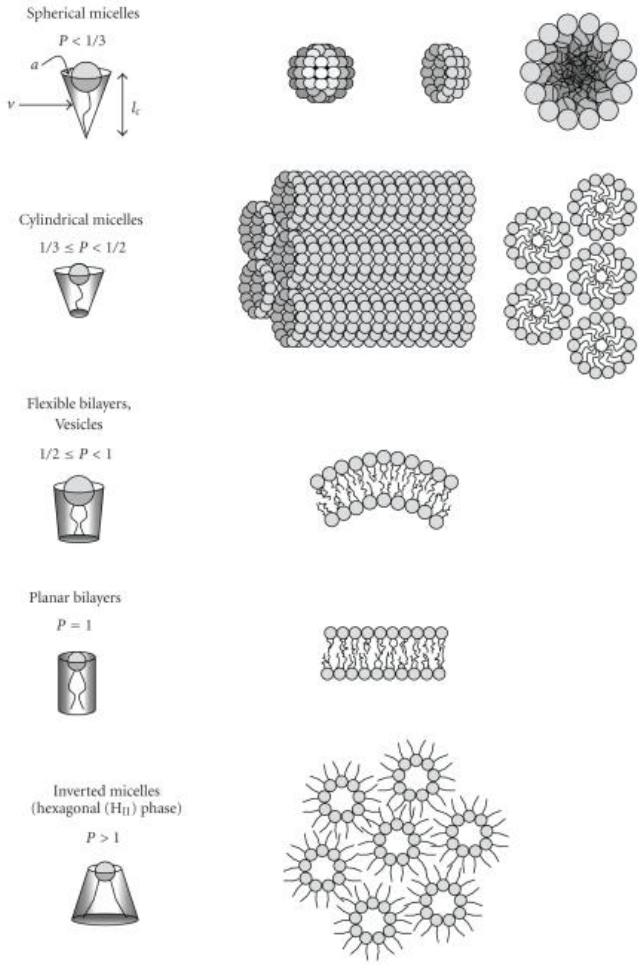

Figure 14: Schematic illustration of the structures formed corresponding to the value of the packing parameter. Taken from Reference 71.

In a practical sense, the packing parameter of a phospholipid terms the shape occupied by a molecule inside a self-assembled structure and therefore determines the equilibrium structure. The value obtained from the packing parameter defines five different cases, each case corresponding to a particular shape of an assembled structure. Figure 14 summarises the structures schematically [70].

For a value of P < 1/3 the packing shape is a cone and the assembled structure formed is a spherical micelle, for 1/3 < P < 1/2 the volume is a truncated cone and the resulting aggregates will be a cylindrical micelles. For 1/2 < P < 1 the packing shape is again a truncated cone, however vesicles form. For P ~ 1, planar bilayers form and the volume is a cylinder, finally, for P >1 the volume is a wedge and the aggregates formed will be inverse micelles[71 72, 73].

The interpretation of the formation of vesicles is more complex than micelles, owing to the fact that vesicles have an inner and outer layer. In order to understand it, additional parameters need to be considered. These are the radius of the vesicle outer layer (R_0), the thickness of the outer layer (t_0) and the outer surface area (S_0)[73].

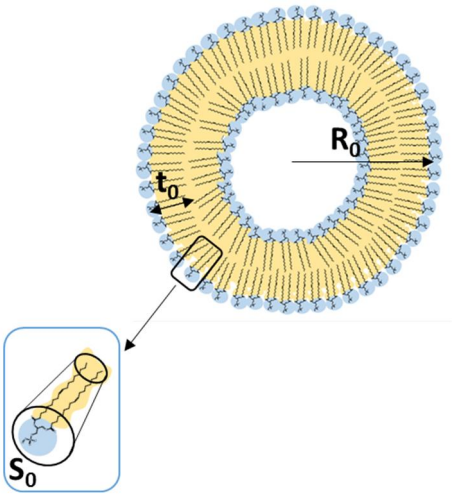

Figure 15: A diagram of a liposome, highlighting the radius of the vesicle outer layer (R_0), the thickness of the outer layer (t_0) and the outer surface area (S_0).

For a vesicle containing N_0 molecules, then the volume occupied by the outer layer (V_0) and the outer surface area (S_0) can be defined by the following expressions [73],

$$V_0 = N_0 v = \frac{4}{3}\pi[R_0^3 - (R_0 - t_0)^3] \quad (8)$$

and

$$S_0 = 4\pi R_0^2 \quad (9)$$

The actual area per head group *(a)* can therefore be given as the outer surface area divided by the number of molecules, as can be seen in Equation 10[73].

$$a = \frac{4\pi R_0^2}{N_o} = \frac{3vR_0^2}{[R_0^3 - (R_0 - t_0)^3]} \quad (10)$$

The ratio of the actual area to the optimal area, a/a_0, is therefore given by Equation 11[73].

$$\frac{a}{a_0} = 3\left(\frac{v}{a_0 l_c}\right) l_c \frac{R_0^2}{[R_0^3-(R_0-t_0)^3]} \qquad (11)$$

Equation 11 is a function of the packing parameter, the critical chain length, the outer radius of the vesicle and then thickness of the outer layer. When the packing parameter and the critical chain length are fixed, the ratio, a/a_0, increases with decreasing radius of the vesicle (R_0) and additionally, decreases with increasing outer layer thickness (t_0). In order for the formation of a vesicle to occur, the actual area (a) has to approach the optimal head group area (a_0) and consequently the ratio of the actual area to the optimal area needs to approach 1. This can be achieved by decreasing the outer radius (R_0), and the minimum value of R_0 is reached when the outer layer thickness (t_0) is equal to the critical chain length (l_c). Therefore, by setting the ratio of a/a_0 to 1 and setting $t_0 = l_c$, solving Equation 11 (above) for R_0 an expression for the minimum radius, R_{min} can be obtained.

$$R_{min} = \frac{3+\left[3\left(\frac{4v}{a_0 l_c}-1\right)\right]^{1/2}}{\frac{6\left(1-\frac{v}{a_0 l_c}\right)}{l_c}} \qquad (12)$$

Therefore from Equation 12 it can be seen that R_{min} is dependent on the packing parameter and therefore also on the critical chain length.

Through the interactions and equations discussed above one can understand, why and how self-assembled structures form, the attractive and repulsive forces at play, and the thermodynamics behind the self-assembly process.

2.3 Liposomes

2.3.1 History and classification

Liposomes (from the Greek '*lipos*' meaning fat and '*soma*' meaning body) are self-assembled, spherically shaped vesicles which were first discovered in 1961 by British biophysicist Dr A. D. Bangham [74]. Liposomes consist of one or more bilayers, most commonly made of phospholipids, encircling an aqueous core that is usually made of the same composition as the suspension medium.

Liposomes are typically classified according to their morphology (the liposome size and the number of bilayers). Uni-lamellar vesicles (ULVs) are formed of a single bilayer and can be further characterised according to their size, small (SUVs), large (LUVs) and giant (GUVs). Multi-lamellar vesicles (MLVs) consist of a number of concentric bilayers inside one another, each separated by a layer of water. Oligolamellar vesicles (OLVs) are vesicles made of a small number of concentric bilayers and multivesicular (MVVs) are giant vesicles that encapsulate smaller liposomes.[75] The classification of liposomes is outlined schematically in Figure 16 below which is adapted from Reference 76.

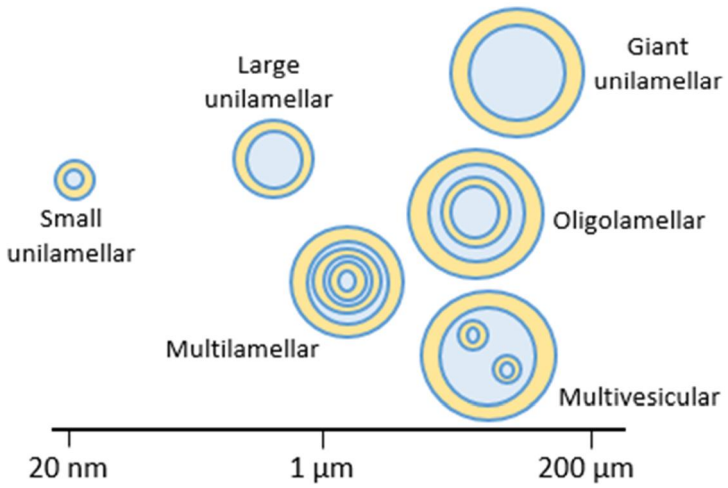

Figure 16: Schematic representation of the commonly applied classification of liposomes. Adapted from Reference 76. Copyright © 2008, Annual review of analytical chemistry.

2.3.2 Applications of liposomes

The method chosen to prepare liposomes can influence the composition, lamellarity, size and structure of the acquired liposomes which renders them very useful for a large number of applications. Since their discovery in the early 1960s, liposomes have been used in many fields.

In 1971, liposomes were first used to deliver bioactive substances by Gregoriadis et *al.*[76] and subsequently investigations into liposomes as drug delivery tools have flourished. Liposomes possess advantages as drug delivery systems because they can deliver both hydrophilic and lipophilic drugs[77], and they possess controlled release properties, cell affinity and tissue compatibility as well as the ability to improve drug stability [60, 74, 78]. Materials encapsulated by liposomes are protected from degradation as they move through the body and then are released to the target area via the opening of the bilayer. As well as drug delivery systems, liposomes have other medical applications and are used in anticancer and gene therapy [74, 79, 80], diagnostic imaging [81] and vaccinations [82, 83]. In all of the listed medical applications, liposomes are used in bulk solutions to carry biologically active molecules and release them in a specific environment (Figure 17).

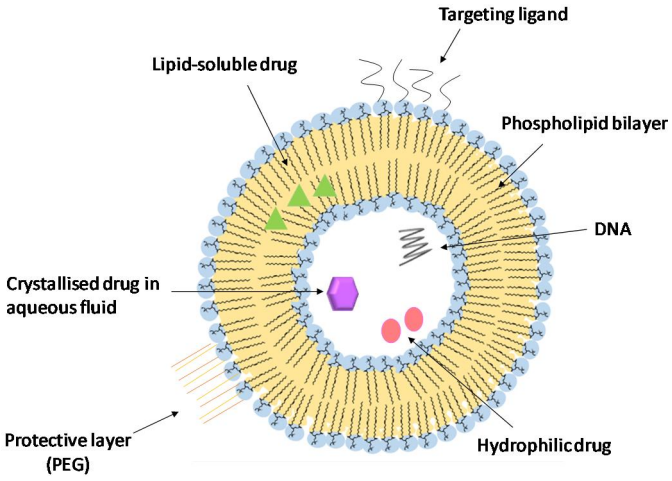

Figure 17: Schematic illustration of a liposome as a drug delivery vehicle.

Additionally, liposomes have proved to be good vehicles for applications in the cosmetic industry. Liposomes made of natural lipid extract were found to be effective in the prevention and treatment of skin diseases following topical application [84]. Dermal liposome products have been used since 1987 and there is an increasing market for products of this kind [85].

In the last decade, the dietary supplement industry has expanded rapidly and the use of nutritional supplements which have established health benefits is at an all-time high. Liposomes which contain vitamins, herbs and enzymes have become increasingly popular products since oral liposomes were formulated in the early 1970s[77]. Examples of liposomal nutrition products which are currently available on the market contain vitamin C[86], vitamin A, vitamin B_2, vitamin B_{12}, vitamin E, Echinacea and Melatonin[77]. Liposomal supplements are readily available to the be purchased by the public and seem to be increasingly well established and prevalent in the health industry today.

Liposomes are also key tools in research because they very closely resemble the cell membrane. Cell membranes consist of a phospholipid bilayer with embedded proteins and other components such as cholesterol and protein channels[56]. The current model for the cell membrane is called the 'fluid mosaic model', and was originally proposed by J. Singer and G. Nicolson in 1972[87]. The cell membrane performs vital functions in living cells, physically separating the intracellular constituents and the extracellular environment. It is partially permeable and only selectively allows molecules or ions to cross. Uncharged, small molecules such as oxygen (O_2) and carbon dioxide (CO_2) can readily cross the membrane via diffusion, however larger molecules such as sugars and amino acids are moved into the cell via protein channels[88]. In this way, the cell membrane can regulate what enters and leaves the cell and also enable transport across the bilayer.

By using liposomes as models for biological membranes, scientists can gain a deeper understanding of the properties, function and structure of the cell membrane. As well as closely resembling the structure of the membrane, liposomes can be modified to alter their composition, for example cholesterol can easily be incorporated into the bilayer[89].

Furthermore, using liposomes as models of cell membranes can be advantageous in pharmaceuticals and the study of drugs. The models can be used to predict the efficacy of drugs, mechanism of drug transport into cells and also to understand mechanisms of toxicity[90]. Maheswari et *al*.[91] measured changes in the electrical properties of model membranes after the addition of the anti-cancer agent, methotrexate, and it was found that the neurological side effects of the drug are caused by the interaction with the lipid bilayer. Liposomes can, therefore, be useful tools in medicinal fields and provide insight into how to improve new and existing drugs.

2.3.3 Thermodynamics of liposome formation

As previously discussed, when phospholipids are added to water self-assembled bilayer structures are formed. In the bilayer structure, there are a number of hydrophobic phospholipid tails that are in contact with the aqueous medium at the edge of the bilayer. This interaction has an energy associated with it, called the edge or disk energy[71, 83].

$$E_{disk} = 2\pi R_D \gamma \quad (13)$$

where R_D is the diameter of the bilayer disk and γ is the line tension. On the bending of the bilayer, this edge energy is minimised and as the bilayer closes to form a spherical vesicle the edge energy is eradicated completely[92]. There is, however, an energy penalty associated with the bending of the bilayer which is minimised when the two edges of the bilayers join together. This is called the bending energy.

$$E_{bend} = 8\pi\kappa \quad (14)$$

where κ is the bending modulus. The disk radius (R_D) is related to the vesicle radius (R_0) according to Equation 15.

$$R_0 = \frac{R_D}{2} \quad (15)$$

During the bending of the bilayer, additional phospholipid molecules of bilayer fragments may be incorporated which causes the size of the vesicle to increase. Liposomes form readily when the edge energy exceeds the bending energy.

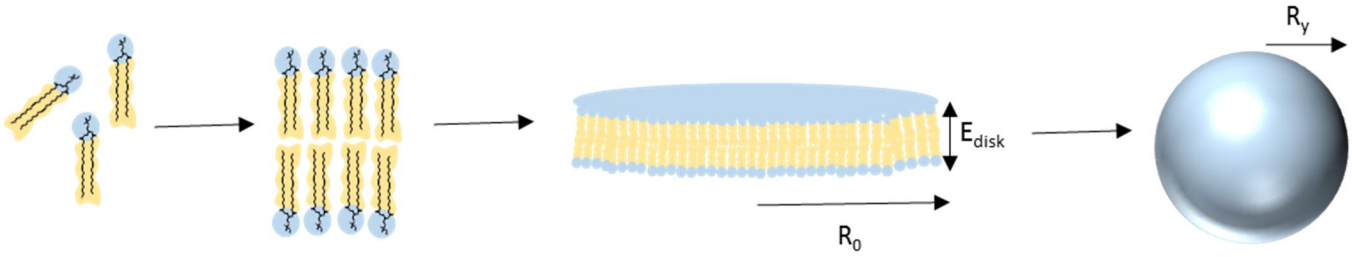

Figure 18: Schematic illustration of the formation of phospholipid bilayers and their self-closure to form vesicles. Adapted from Reference 73.

2.3.4 Methods of liposome formation

An assortment of different methods have been used in recent years for the formation of liposomes. As previously mentioned, the selected method determines the properties of the liposomes formed, such as size, polydispersity and lamellarity.

Liposomes can be formed from solutions of phospholipids in organic solvent. The phospholipids dissolve into the molecular form in the organic solvent and produce a film as the solvent is evaporated off [83]. The next step is to hydrate the lipid film which causes the bilayers to swell and begin to separate. As the hydrated sheets swell further, they become detached and the two ends of the removed bilayer then begin to merge and eventually self-close to form a large multi-lamellar vesicle. These large multilamellar vesicles (LMVs) can then be reduced in size and lamellarity to create small unilamellar vesicles (SUVs).

2.3.5 Sizing of liposome suspensions

2.3.5. i. Extrusion

Extrusion is one of the techniques used to create uni-lamellar liposomes in a monodisperse suspension, and it is likely to be the most common method used for liposome preparation. In this method, the multi-lamellar liposome suspension is forced though a polycarbonate membrane using high pressures[93]. The polycarbonate membranes have uniform, cylindrical pores which have a defined size and these allow vesicles to be produced which have a diameter comparable to the pore size of the membrane used. In most cases, the MLV suspension is passed through a membrane with larger pore size than the desired size, which pre-filters the suspension and initially disrupts the larger vesicles[94]. This initial process can help improve the homogeneity of the liposome system.

During the extrusion process, the number of extrusion cycles and the pressure used determines the size and size distribution of the vesicles formed. A profound advantage of using extrusion is that the need to remove organic solvent or detergents, a problem associated with other methods, is eliminated[95].

2.3.5. ii. Sonication

This preparation technique allows SUVs to be produced through the disruption of LMV suspensions using sonic energy. There are two types of sonication techniques, either the tip of a sonicator probe is immersed directly into a liposome suspension or the sample is placed into a bath sonicator. These

types of sonication are named probe tip and bath sonication respectively. The probe tip sonicator can cause an increase in the temperature of the liposome system, and often requires a water/ice bath to prevent overheating (and consequently, degradation)[96]. In addition, the mean liposome size and polydispersity of the solutions depend on the power of the sonicator, the temperature and the time undergoing sonication. In a bath sonicator the temperature and power can be carefully monitored and for these reasons the bath sonicator tends to be the more popular choice and more widely used.

A significant disadvantage of both sonication techniques is that they are limited in their ability to produce homogeneous liposome suspensions, containing liposomes of the same size[97]. Sonication is however, advantageous over extrusion as it is a lot less time consuming.

2.3.6 Direct preparation of SUVs

2.3.6. i. Detergent removal methods

In contrast to the two methods described above, small uni-lamellar vesicles can be prepared directly from the removal of detergent from phospholipid-detergent mixtures. Detergents are a subgroup of surfactants that are able to solubilize lipid membranes [98]. When the detergent is added, the lipid bilayers organise into smaller, detergent-lipid aggregates which are called mixed micelles (MM) [99]. As the detergent is removed the micelles become increasingly rich in phospholipids and they will combine to form vesicles. The detergent can be removed by controlled dialysis, and the rate of removal of the detergent influences the size of the vesicles formed [100]. Detergent removal methods can, however, lead to increasing impurities in the liposomes formed and the size of the resulting vesicles is largely dependent on the lipid composition of the vesicles [101].

2.3.6. ii. Ethanol injection

An alternative method for the direct preparation of SUVs which avoids the use of detergents is ethanol injection. This method, first described in 1973 by S. Batzri and E. Korn [102], involves injecting an ethanol solution containing lipids into an aqueous medium through a needle. The injection is sufficient to achieve complete mixing and the phospholipid molecules are evenly dispersed through the medium and then self-assemble to form SUVs [103]. This method is advantageous as it is simple, rapid and does not require the use of potentially harmful chemical and physical treatments [104]. The major drawback of this method is that the suspension formed contains a relatively dilute liposome system, which decreases the encapsulation efficiency of the aqueous phase [97 103].

In this project, the chosen preparation method was sonication using a bath sonicator followed by membrane extrusion. These methods were chosen because they have been widely used in the literature and produce a monodisperse suspension of uniformly sized liposomes.

2.3.7 Interactions of liposomes with salts

The desire to understand the effects of various ions on biological systems has prompted a vast amount of research to be carried out into the interactions of ions and phospholipid structures. The interactions of salts with monolayers [105-107], bilayers [108-110] and micelles[61] has been widely studied in order to better understand specific ion effects and in more recent literature, there has been an increasing amount of interest in studying specific ion effects using liposomes.

Specific salt effects on liposomes can be studied in a number of ways, most broadly reported is by examining the change in the size (diameter), size distribution and zeta potential of the liposomes on the addition of salt. The zeta potential is the electrostatic potential that exists at the shear plane and can provide information on the stability of the liposome suspension. The binding and adsorption of ions with liposomes has also been extensively investigated, as well as the influence of ions on the fusion of vesicles. In this section, a variety of the previous work conducted in this area and the results of the work will be discussed.

Ruso *et al* [111] perfromed a study on the interactions between phosphatidylcholine–cholesterol–phosphatidylinositol (PC–Chol–PI) liposomes and cations by examining the change in the zeta potential as ion concentration was altered. The zeta potential was found to become more positive on the addition, and increasing concentration, of the ions for all cations studied, which suggested that binding of the cations to the phospholipid head group occurred. As the concentration was increased further however, there was a decrease followed by a plateau for the value of the zeta potential, which may be indicative of anion association with the head group or saturation of the head group with ions. These results agree well with other reported literature [61, 112, 113] and it is thought that the ions penetrated into the bilayer and bound tightly with the carbonyl group of the lipid which subsequently affected the structure of the bilayer.[114, 115] The mechanism by which this association of cations with lipid head groups occurs still remains unclear; however, the charge density and hydration of the cations are alleged to play an important role[116, 117].

Klasczyk *et al*. [118] used isothermal titration calorimetry to understand the binding of ions to the POPC membrane and produced a Hofmeister series of ions according to the zeta potential measurements. The zeta potential increased on the addition, and increasing concentration of all cations studied (Li^+,

Na^+, K^+, Rb^+ and Cs^+). The zeta potential increased according to the Hofmeister like series, ζ (Li) > ζ (Na) > ζ (K) ≈ ζ (Rb)≈ ζ(Cs), and these results agree with the previously discussed literature. The following, Table 3 [118], shows further results from this work.

Table 3: Thermodynamic parameters characterising the association of Alkali metal cations to POPC lipid vesicles. Standard errors are also shown. Taken from Reference 119 with permission from ACS publications.

alkali cation	apparent binding constant, K [l/mol]	molar enthalpy, ΔH [kcal/mol]	Gibbs free energy, ΔG [kcal/mol]	entropic contribution, $T\Delta S$ [kcal/mol]
Li	1.37 ± 0.06	2.39 ± 0.09	-2.58 ± 0.03	4.97 ± 0.09
Na	1.25 ± 0.05	2.33 ± 0.09	-2.53 ± 0.02	4.86 ± 0.09
K	1.17 ± 0.13	2.13 ± 0.23	-2.49 ± 0.07	4.62 ± 0.24
Rb	1.14 ± 0.28	1.75 ± 0.40	-2.47 ± 0.15	4.22 ± 0.43
Cs	1.10 ± 0.14	1.67 ± 0.19	-2.45 ± 0.08	4.12 ± 0.20

As can be seen from Table 3, the enthalpies of binding of the metal cation to the vesicles is endothermic, hence the process must be entropically driven. The binding can be understood in terms of a gain of entropy. On the binding of the cations to the lipid, the hydration shell of the ion and lipid is disrupted, leading to the liberation of water molecules. Following calculations by the authors this hypothesis was confirmed, as can be seen from the entropy values in the table above. These calculations also allow insight into the Hofmeister series. The greatest gain in entropy is obtained by the smallest ions, and hence, hydration is an important parameter when studying the mechanism of the Hofmeister series.

The interactions of ions with lipid head groups can also affect the size and size distribution of the liposome suspensions. It is recognised in the literature that, in significant concentrations, the presence of some salts can cause an increase in the size of liposomes which can be attributed to the screening of the head groups of the lipids[117] or the fusion of vesicles[119, 120]. Sabín J *et al.*[113] studied closely the effect of calcium and lanthanum ions of the coilloidal stability of phosphatidylcholine (PC) liposomes and found that La^{3+} ions promoted the formation of vesicles of up to 600 nm (Figure 19). The authors then hypothesised that fusion of liposomes must be occurring and later confirmed this notion using transmission electron microscopy (TEM) and polydispersity measurements, carried out using photon correlation spectroscopy (PCS) (Figure 19).

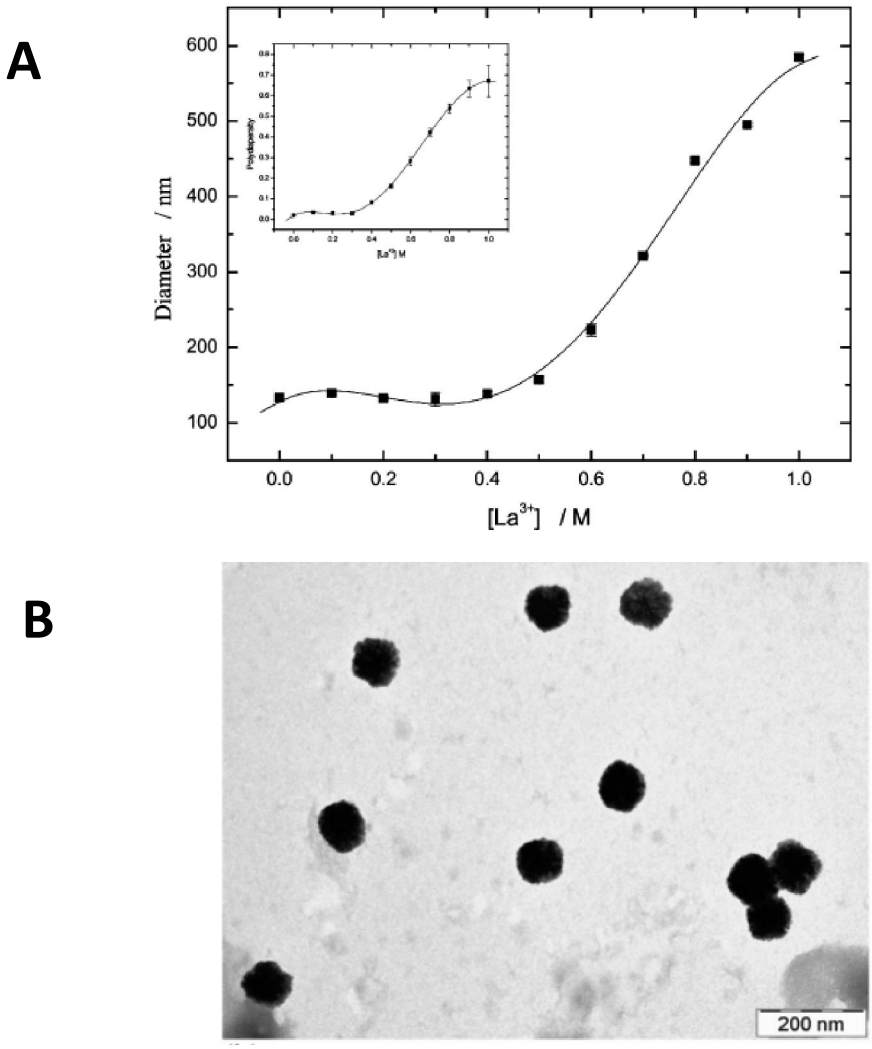

Figure 19: (A) Graph to show the size (nm) of PC liposomes as a function of La^{+} concentration (M). (B) Transmission electron microscopy image taken to show the influence of La^{3+} on PC liposomes. Reprinted with permission from reference 114, Copyright © 2005, American Chemical Society.

An observation recorded in this work, and extensively in the literature[117, 121], is that at low concentrations of ions there is a decrease in the size of liposomes (Figure 19). Sabin J *et al.*[112] suggested that osmotic forces, generated by a concetration gradient at both sides of the membrane, were responsible for this decrease in liposome size. Athough this theory has been reported in other work,[122] this fundemental mechanism is still the subject of research and remains largely unknown.

Liposomes have been found to be exceptional tools for studying the Hofmeister series. Work conducted using liposomes has allowed insight into the mechanism of the Hofmeister series and liposomes are increasingly used in physical chemistry to study specific ion effects. This project was carried out in the hope of better understanding specific ion effects, using liposomes as tools to gain insight into the Hofmeister series.

2.4 Justification for project

Phosphatidylcholines (PC) are a category of phospholipids, which are a major component of the eukaryotic cell membrane. The extracellular, outer leaflet of the membrane is comprised mainly of PCs, while the main component of the inner leaflet is phosphatidylethanolamines (PE)[114]. Zwitterionic, neutral lipid 1, 2-dioleoyl-sn-glycero-3-phosphocholine (DOPC) (Figure 20) was chosen as the use of synthetic lipids allows the project to be carried out using well characterized, pure materials. DOPC is practical to work with as it is unsaturated, and therefore, possesses an increased solubility in organic solvents and is able to hydrate more readily[123]. Additionally, size modification of liposomes after their initial formation is easier with unsaturated lipids.

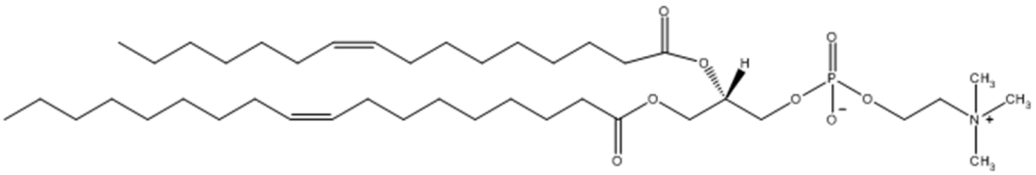

Figure 20: The skeletal formula of phospholipid, 1, 2-dioleoyl-sn-glycero-3-phosphocholine (DOPC).

1, 2-dipalmitoyl-sn-glycero-3-phosphocholine (DPPC) was also chosen to be used in this project. DPPC was selected as it has been widely studied previously in the literature and DPPC liposomes have well defined preparation. Additionally, it is interesting to compare and contrast liposomes made of DOPC and DPPC as the lipids have varying fluidity and vastly different transition temperatures.

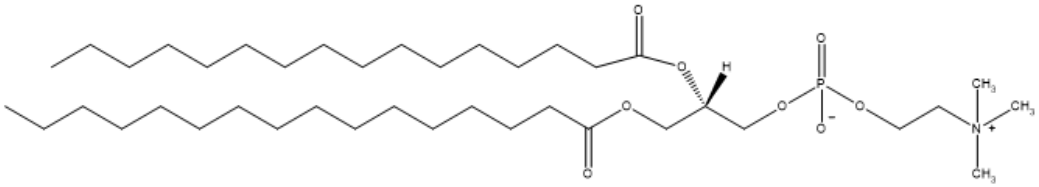

Figure 21: The skeletal formula of phospholipid 1, 2-dipalmitoyl-sn-glycero-3-phosphocholine (DPPC).

Table 4: Summary of properties of phospholipids studied [60, 124]. M_w: Molecular weight, T_m phase transition temperature

Name	Abbreviation	M_w	T_m
1,2-dioleoyl-sn-glycero-3-phosphocholine	DOPC	786.11 $gmol^{-1}$	-17 °C
1,2-dipalmitoyl-sn-glycero-3-phosphocholine	DPPC	734.04 $gmol^{-1}$	41 °C

Liposomes were chosen to be used as the tools in this project as they are excellent models of biological membranes. There has been a large amount of work in the academic literature which focuses on salt effects on bilayers[61, 108, 120], monolayers[61, 105, 106] and micelles[61], but significantly less on liposomes comprised of DOPC. Liposomes and bilayers comprised of other phospholipids have been more widely studied in the literature, especially 1,2-dipalmitoyl-sn-glycero-3-phosphocholine (DPPC)[116, 117] and 1-palmitoyl,2-oleoyl-sn-glycero-3-phosphocholine (POPC)[109, 118]. Liposomes are also excellent tools as the hydration of the liposome surface can be regulated by altering the phospholipid molecules used. The experimental method for preparation of uni-lamellar liposomes is well defined and has been reproduced vastly in the literature, hence liposomes were an appropriate choice for this project.

Lithium (Li^+) was chosen to be used in this project as it has been found to be anomalous in some cases in previous work in the literature. Li^+ has been found to behave more like the larger metal ions, and shows results which do not fit with the trend of the group 1 metal ions[125, 126]. It has been hypothesised that the higher degree of hydrogen bonding, owing to the very high charge density of the ion, is responsible for the ion being an exception to the rule. Lithium has not been as widely studied in research of this type and hence it is a thought-provoking prospect in this project. Sodium (Na^+), potassium (K^+), magnesium (Mg^{2+}) and calcium (Ca^{2+}) are interesting ions to study as they are biologically relevant, as discussed, and have been widely studied in the context of the Hofmeister series in previous literature. By better understanding the mechanism by which these cations bind to phospholipids, the role of cations in the cell membrane can begin to be better understood.

Furthermore, by using the alkali earth metals, which decrease in charge density down the series, the role of hydration in the ordering of ion in the Hofmeister series can more easily be established.

Lanthanum (La^{3+}) is of specific interest to this work as it has been found in previous literature to induce the fusion of phosphatidylcholine vesicles[113]. In addition, highly charged trivalent cations provide a thought-provoking comparison to larger monovalent, singly charged cations. To draw comparisons with lanthanum, chromium (Cr^{3+}), another trivalent cation, was chosen as it has been found to be kosmotropic in the literature[37], and has a strong hydration layer. Chromium has also not been as widely studied in the framework of the Hofmeister series, and therefore would be of specific interest

to this field of research. Similarly, iron (Fe^{3+}) was chosen as it is not widespread in the literature and is of great biological relevance.

In addition to inorganic cations, this project also examines the effect of a number of hydrophobic organic ions on DOPC liposomes. Sodium tetraphenylborate (Figure 23) and tetraphenylphosphonium chloride (Figure 22) have been previously studied in detail in the framework of the Hofmeister series by E. Leontidis[127], and it was found that the chaotropic tetraphenylborate anions altered the structure of soft-matter due to their very strong interfacial activity. The hydrophobic nature of these anions also allow them to readily permeate the lipid bilayers and this unique property makes organic, hydrophobic ions appealing in this project as they provide a contrast to the inorganic cations also used.

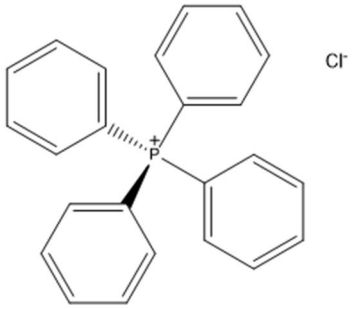

Figure 22: The structure of tetraphenylphosphonium chloride.

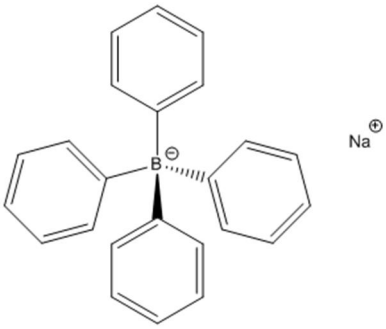

Figure 23: The structure of sodium tetraphenylborate.

Using specific salt effects and liposomes to gain insight into the mechanism of the Hofmeister series is vital in many branches of science. Understanding the specific ion effects of ions on macromolecules can help scientists unravel the mechanism to many biological processes, most profoundly, the interactions of ions with cell membranes. As well as understanding specific ion effects on macromolecule surfaces, the role of water and hydration on the position of ions in the series will begin to be understood. By understanding the role of hydration of ions, the ongoing problem of the Hofmeister series will begin to be resolved. In addition, gaining a deeper insight into the mechanism of hydration of ions and the structure and dynamics of water, will be beneficial to many branches of science.

Chapter 3: Experimental

3.1 Materials and methods

1, 2-dioleoyl-sn-glycero-3-phosphocholine (DOPC) and 1, 2-dipalmitoyl-sn-glycero-3-phosphocholine (DPPC) in chloroform (25 mg/ml) were purchased from Avanti Polar Lipids Inc. and stored at -30 ˚C until use. Sodium chloride (NaCl, ACS reagent, ≥ 99 %), lanthanum chloride ($LaCl_3 \cdot 7H_2O$, ACS reagent, 64.5-70%), chromium (III) chloride ($CrCl_3 \cdot 6H_20$, 96%) and iron chloride ($FeCl_3$, anhydrous, powder, ≥ 99.99%, trace metals) were purchased from Sigma Aldrich. Calcium chloride ($CaCl_2$, ACS reagent, ≥ 99 %) and cesium chloride (CsCl, 99+%, pure) were purchased from Agro Organics. Lithium chloride (LiCl, ACS reagent, 99+ %) and potassium chloride (KCl, ACS reagent, 99+ %) were purchased from Fisher Scientific and magnesium chloride hexahydrate ($MgCl_2$ $6H_2O$, ACS grade) was purchased from VWR international. Sodium tetraphenylborate ($(C_6H_5)_4BNa$, ACS reagent, ≥ 99.5%) and tetraphenylphosphonium chloride ($C_{24}H_{20}ClP$, 98%) were purchased from Sigma Aldrich. Water used for the preparation of salt solutions was purified by a MilliQ Advantage A10 purification system (Merck Millipore) with a resistivity of 18.2 MΩ cm^{-1} and a total organic content (ToC) ~ 3 ppb.

The liposome dispersions were prepared using a Lipex 10/1.5 mL thermobarrel extruder from Northern Lipids Inc. and the filter drain disks (25 mm diameter, polyester) which were used in the extruder were purchased from A.M.D. Manufacturing Inc. The membranes used in the extruder were Whatman nuclepore track-etched membranes (25 mm diameter, polycarbonate, 0.2 and 0.1 µm pore size), and they were purchased from Sigma Aldrich. The sonicator used was an Ultrawave bath sonicator.

The dynamic light scattering (DLS) measurements were performed using a Zetasizer Nano ZS from Malvern instruments running Zetasizer software 7.12. The DLS machine was operated with a detector positioned at the scattering angle of 173°, and a temperature control jacket for the cuvette. Three DLS measurements consisting of fourteen runs in total were performed for each sample for the size measurement. For the zeta potential measurements, three measurements consisting of up to one hundred runs were carried out for each sample. The U.V. cuvettes, used for the size measurements, were purchased from Fisher Scientific. Finally, the folded capillary cells (DTS1060) with gold plated electrodes, used for the zeta potential measurements, were purchased from Malvern instruments. It is important to note that at high salt concentrations it is possible to damage and degrade the electrodes or the sample being studied. Blackening of the gold electrodes, caused by Joule heating[128], gives inaccurate zeta potential readings and also causes irreversible damage to the folded capillary cells used. In order to avoid this problem and obtain accurate zeta potential values for liposomes in

high concentration salt solutions, a high concentration zeta potential cell (ZEN1010), purchased from Malvern Instruments, was used. It contains palladium electrodes which are more resistant to damage in high concentration of ions.

The temperature trend measurements, carried out by DLS, allowed the size and scattering intensity of the liposomes be measured as a function of temperature. The automated trend measurements were set to take 3 measurements at every 2.5 ˚C increment starting at a temperature of 25 ˚C and finishing at a temperature of 60 ˚C. After a size measurement was recorded at a certain temperature, the sample was allowed to equilibrate for 120 seconds at the next temperature before the size of the liposomes was recorded.

The TEM measurements were carried out on a Tecnai 20 - FEI 200kV twin lens scanning transmission electron microscope (STEM). The microscope is fitted with a LaB6 filament for high resolution results, a FEI Eagle 4k x4k CCD camera as well as a plate camera. The samples were prepared on carbon coated, copper grids, purchased from EM Resolutions. The machine used for glow discharging the grids was an Edwards 306 carbon coater. An FEI Vitrobot™ Mark IV was then used to plunge-freeze the sample and a Cryo holder was used in the transfer of grids. The preparation of samples for TEM will is described in more detail in Section 3.7.2.

3.2 Glassware

All glassware and lids used in the preparation of the samples were thoroughly cleaned with water followed by ethanol and then dried under a stream of nitrogen before use.

3.3 Preparation of salt solutions

Sodium chloride (NaCl), lithium chloride (LiCl), potassium chloride (KCl), cesium chloride (CsCl), calcium chloride ($CaCl_2$), magnesium chloride ($MgCl_2$), iron (III) chloride ($FeCl_3$), chromium (III) chloride ($CrCl_3$) and lanthanum chloride ($LaCl_3$) inorganic salt solutions (1 mM –40 mM) were obtained by dissolving appropriate masses of salt in volumetric flasks and making up to the correct mark with MilliQ water.

The solutions containing the organic ions (1 mM – 40 mM) were prepared by dissolving appropriate masses of tetraphenylphosphonium chloride ($(C_6H_5)_4PCl$) or sodium tetraphenylborate ($(C_6H_5)_4BNa$) in volumetric flasks and making up to the correct mark with MilliQ water.

3.4 DOPC liposome synthesis

1, 2-dioleoyl-*sn*-glycero-3-phosphocholine (DOPC) liposomes (2 mM) were prepared in either pure water or salt solution.

Lipids in chloroform were weighed into to an empty 7 mL vial and then dried by removing the solvent using a stream of nitrogen. The vial was then left in a vacuum oven (Heraeus Vacutherm under 1 mbar) for 1 hour at 25 °C to ensure that all the chloroform was removed. The lipid film was then hydrated using either MilliQ water or a salt solution of chosen concentration. Following hydration, the solution was placed in a sonicator bath at room temperature (above the DOPC phase transition temperature of -17 ˚C) for 30 minutes. A cloudy white suspension was obtained following sonication. This suspension was then passed through the extruder under pressurised nitrogen (10 bars) 6 times using two stacked membranes (0.2 µm pore size). Finally, the solution was then passed through the extruder a further 6 times using two stacked membranes (0.1 µm pore size), resulting in a transparent DOPC liposome dispersion.

3.5 DPPC liposome synthesis

1, 2-dipalmitoyl-sn-glycero-3-phosphocoline (DPPC) liposomes (2 mM) were prepared in either pure water or salt solution.

Firstly, lipids in chloroform were weighed into to an empty 7 mL vial and then dried by removing the solvent using a stream of nitrogen. Secondly, the vial was left in a vacuum oven (Heraeus Vacutherm under 1 mbar) for 20 minutes at 55 °C to ensure that all the chloroform was removed. After this step, a clear translucent film was obtained containing some small DPPC crystals. The lipid film was then hydrated with either MilliQ water or a salt solution of chosen concentration. The solution was placed in a sonicator bath at 60 °C (above the DPPC gel-liquid transition temperature of 41 °C) for 30 minutes resulting in a cloudy liposome suspension. The cloudy white suspension was then passed through an extruder, heated at 60°C by a circulating water bath (Optima TC 120, Gant), by pressurised nitrogen (10 bars) 6 times using two stacked membranes with 0.2 µm pore size and then further 6 times using membranes with 0.1 µm pore size. The resulting solution was a clear DPPC liposome suspension.

3.6 Dynamic light scattering (DLS)

3.6.1. Introduction to DLS

Dynamic light scattering, also referred to as photon correlation spectroscopy or quasi-elastic light scattering (QELS), is a popular, non-invasive and well established technique in physical chemistry, used to measure the size of particles and molecules usually in the submicron region. DLS can be widely used to study emulsions, polymers, colloids, nanoparticles and proteins and is therefore a valuable and broadly applicable sizing technique. It can provide accurate and reliable particle size analysis in a short amount of time, sample preparation is simple, and only a low volume of sample is required, making DLS a very beneficial technique in research.

Typical applications of DLS are the characterisation of particles dispersed in a liquid. The Brownian motion of particles in suspension refers to the random movement of the particles, caused by collisions with surrounding solvent molecules in the suspension[129]. The speed of the Brownian motion is influenced by the temperature of the sample, the particle size and the sample viscosity. For example, the smaller the particle or the higher the temperature, the more rapid the Brownian motion becomes, hence when conducting DLS it is necessary to know the exact temperature of the sample. During DLS, the Brownian motion of the particles in suspension causes laser light to be scattered in different directions and at different intensities[129]. Analysis of the recorded intensity fluctuations yields the Brownian motion of the particles and relates this to their size[130]. The velocity of the Brownian motion is defined by the translational diffusion coefficient (*D*), and the particle radius can be calculated from this parameter by using the Stokes-Einstein equation[130, 131] (Equation 16).

$$D = \frac{k_B T}{6 \pi \eta r} \qquad (16)$$

Where *D* is the diffusion coefficient, k_B is the Boltzmann's constant ($1.38064852 \times 10^{-23}$ JK^{-1}), T is the temperature in kelvin, η is the dynamic velocity of the solvent and *r* is the radius of the spherical particle.

Because the particles are moving, the scattered light undergoes a Doppler shift. The Doppler shift (or the Doppler effect) is the '*shift in the observed frequency of a wave as the result of relative motion of source and observer*'[132]. Larger particles move more slowly and exhibit a smaller Doppler shift, whereas smaller particles move more rapidly and, as a consequence, exhibit a larger Doppler shift. A photon counter is able to detect the light scattered towards it and measure the fluctuations in light

intensity that result from the Doppler shift. Over a period of time, the fluctuations are measured and the obtained data is processed into a correlation function, which allows a pattern to be identified in the data. Secondary mathematical analysis is then performed on the correlation function which allows the required information to be obtained. The experimental set up of DLS is depicted diagrammatically in Figure 24.

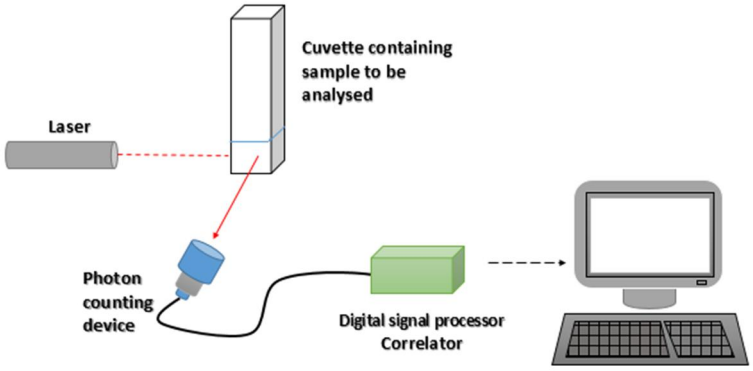

Figure 24: Diagram of the experimental set up of dynamic light scattering.

In this research, DLS was used to obtain the Z-average size of the liposomes, the polydispersity index (PdI) and the zeta potential (discussed in detail in the Section 3.6.3). The polydispersity index is a dimensionless number, ranging in value from 0 to 1, which is a measure of the broadness of the size distribution of a sample. In DLS, a PdI of less than 0.2 is indicative of a system that is relatively monodisperse, meaning all particles in the system are of fairly uniform size. A PdI value of higher than 0.7 for a system points to a very broad size distribution indicating the particles dispersed in the system have a wide range of sizes.

3.6.2. Sample preparation for DLS

To prepare the samples for DLS analysis, the DOPC liposome suspensions were diluted to give concentrations ranging from 0.001 $mgmL^{-1}$ to 0.1 $mgmL^{-1}$. The concentration of the sample was prepared in accordance with the concentration of salt solution in question. The samples were stored in the fridge following preparation and were all analysed within a few hours of being prepared. 1 mL of the solution was injected into a UV cuvette (Fisher, UV Grade Cuvettes) in order to carry out the size measurement, and folded capillary cells (Malvern Instruments, DTS1070) or a high concentration zeta potential cell (Malvern Instruments, ZEN1010) were used in order to obtain the zeta potential measurements. The samples were left to equilibrate for at least 1 minute at a particular temperature

prior to the measurement. All measurements were taken at room temperature (25 °) unless otherwise stated.

3.6.3. Introduction to zeta potential (ζ)

In physical chemistry, the electrical double layer model is used to explain the ionic environment around a charged colloid particle. The model is important in understanding how electrical repulsive and attractive forces occur and is vital to help explain the stability of colloidal systems. In order to describe the double layer, the counter-ions of the charge particle in question must be considered. Bound to the surface of a charged particle there exists an inner layer of tightly bound counter-ions, this region of ions is referred to as the s*tern layer.* Additional counter-ions are attracted by the charged particle but they are also repelled by the inner Stern layer and hence a *diffuse layer* exists, comprised of less firmly attached ions. Thus an electrical double layer exists around each charged particle. Within the diffuse layer, there is a boundary, inside which the surrounding ions are stable. When the particle in the system begins to move, the ions within the boundary will move with it, and conversely, the ions outside of the boundary remain in the bulk system. This boundary is referred to as the *slipping plane* and the potential that exists at the slipping plane is referred to as the *zeta potential* (ζ)[133]. The zeta potential is depicted schematically in Figure 25**,** which is adapted from reference 130.

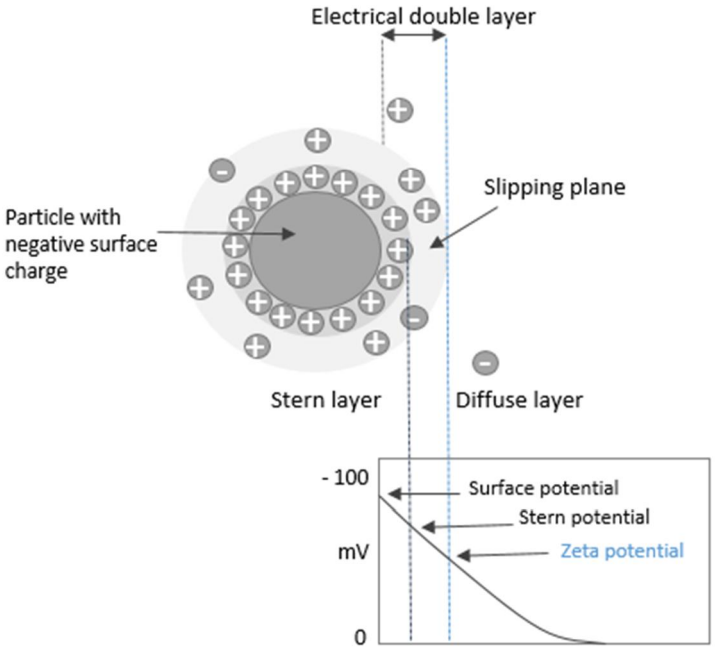

Figure 25: Schematic illustration of the zeta potential, showing the electrical double layer and the potentials that exist at the planes. Adapted from image in Zetasizer Nano Series manual in reference

3.6.4. Measuring the zeta potential

Electrophoresis is the term used to describe the movement of a charged particle in suspension under the influence of an electric field relative to the liquid it is suspended in. When an electric field is applied to an electrolyte, charged particles which are in suspension in the electrolyte experience an attractive force towards the electrode of opposite charge. The attractive force is opposed by viscous forces acting on the particle; however, when the forces reach an equilibrium, the particle will begin to move with a constant velocity. This velocity of the particle in the electric field is referred to as the *electrophoretic mobility*[134]. When DLS is carried out, the electrophoretic mobility is measured by laser doppler velocimetry (LDV)[133]. The zeta potential can then be calculated from the electrophoretic mobility by application of the Henry equation[135, 136] (Equation 17).

$$U_E = \frac{2\varepsilon_r \varepsilon_o \zeta f(\kappa a)}{3\eta} \qquad (17)$$

where U_E is the electrophoretic mobility, ε_r is the relative permittivity (dielectric constant), ε_0 is the permittivity of a vacuum, *f(κa)* is Henry's function (κ is the electrical double layer thickness, with the dimension κ^{-1} and a is the particle radius), η is the viscosity and ζ is the zeta potential.

When the thickness of the electrical double layer is much smaller than the particle radius in aqueous solutions, the value of *f*(*κa*) is taken as 1.5 and is referred to as the Smoluchowski approximation[135]. In contrast, when the particle radius is smaller than the electrical double layer thickness the value of *f*(*κa*) is taken as 1, and this is referred to as the Hückel approximation[135] (non-aqueous measurements also generally use the Hückel approximation).

In this project, in order to obtain accurate values of the zeta potential, the exact value of *f(κα)* was calculated for each cation and at each concentration using equations 18 and 19.

f(κα) can be expressed as:[137]

$$f(\kappa\alpha) = 1 + \frac{1}{2}\left[1 + \left(\frac{2.5}{\kappa\alpha\,[1+2e^{-\kappa\alpha}]}\right)\right]^{-3} \qquad (18)$$

known as the Ohshima relation, where α is the particle radius which is approximately equal to the hydrodynamic radius[138], r_h, and κ^{-1} is the Debye length of the medium[139].

The calculated values of κ^{-1} and *f(κα)* at various salt concentrations for each ion used in this project are listed in Appendix A. These *f(κα)* values were then used to calculate the zeta potential. It is important to note that the Ohshima expression must be treated with caution, and is only valid for relatively low zeta potentials ($\zeta \leq \pm 50$ mV) where concentration polarization is negligible[137]. For higher values of the zeta potential ($\zeta > \pm 50$ mV) then the above expression can no longer be used and a more elaborate model would need to be considered. In this project, the majority of the calculated zeta potential values were sufficiently low ($\zeta \leq \approx 35$ mV), therefore, the model can be regarded as accurate and the discussion will focus on the zeta potential rather than the electrophoretic mobility. However, the values of the zeta potential, which were obtained for DPPC liposomes in the presence of trivalent ions, were ≥ ±50 mV. Therefore for these ions, the electrophoretic mobility will be discussed instead of the zeta potential, and it is important to treat the calculated values for the zeta potential with caution.

The calculation of the magnitude of the zeta potential gives an indication of the stability of the system in question. If the particles in the system have a very large positive or negative zeta potential (more positive than 30 mV or more negative than -30 mV [129]) then the particles will tend to repel each other with sufficient magnitude, suggesting the absence of aggregation and flocculation. This is indicative of a stable colloidal system. On the other hand, if the particles have smaller zeta potential values, then the colloidal system is deemed unstable and flocculation or aggregation of particles may be observed.

In a colloidal suspension, the zeta position is influenced by three main factors. The first factor, and conceivably the most influential factor, is pH. As the pH becomes more acidic, the zeta potential will become more positive, while as the pH increases and becomes more basic, the zeta potential value will become more negative. The pH where the zeta potential becomes zero is known as the *isoelectric point*[140]. The pH can therefore, be considered a very important factor when conducting zeta potential measurements. The second factor which is vastly influential on the value of the zeta potential is the ionic strength. A change in ionic strength causes an alteration in the thickness of the electrical double layer and hence has a large impact on the zeta potential value. The electrical double layer thickness, κ^{-1}, is related to ionic strength, *I,* via Equation 19[141].

$$\kappa^{-1} = \left(\frac{\varepsilon_0 \, \varepsilon_r k_B T}{2000 \, e^2 I N}\right)^{0.5} \qquad (19)$$

where k_B is the Boltzmann's constant ($1.38064852 \times 10^{-23}$ JK^{-1}), T is the temperature, *I* is the ionic strength of the salt solution, and *N* is Avogadro's number (6.02×10^{23} mol^{-1}).

The final factor that the zeta potential is sensitive to, is the particle concentration. The relationship between the particle concentration and the zeta potential is complex and is generally determined by ion adsorption of the particle surface and how the electrical double layer interactions may be affected by the particle concentration.

3.6.5. Applications of the zeta potential

There are a wide range of practical applications of the zeta potential, and it is a useful measurement in a broad array of industries. An example of how zeta potential measurements can be exploited is the control of the composition of paints. The pigments in paint are required to be well dispersed in order for the paint to possess high colour quality and to appear glossy[142]. In order to obtain the optimum dispersion, the zeta potential can be measured so as to ascertain the dosage of additive required for the paint to perform successfully. As well as in paints, the zeta potential is also important in the preparation of clays. Clays are an essential component of rubber, adhesives, and paper. Knowledge of the zeta potential is helpful to understand the behaviour of dispersions of clay in water and tailor the characteristics of the suspension to fit the use it is required for. Additionally, the zeta potential is a vital parameter in the pharmaceutical industry. Pharmaceuticals can be prepared by suspending particles of a drug uniformly throughout a liquid carrier. The more physically stable the suspension, the longer shelf life it has, and hence the more successful and desirable they are. The stability of the drug in the liquid can be studied and altered by examining the value for the zeta potential, making this measurement valuable to the industry[143].

Zeta potential is often the key to understanding stability, dispersion and aggregation processes in suspensions and emulsions, and it is a beneficial measurement in numerous different industries, a small number of which are described above. Dynamic light scattering allows the value for the zeta potential of a system to be obtained accurately and reliably, making it a vital technique used widely in a range of scientific research.

3.7 Transmission electron microscopy (TEM)

3.7.1. Principles of TEM

Cryogenic transmission electron microscopy (Cryo TEM) is a modern technique which allows the analysis of biological specimens in three dimensions with nanometre resolution. Cryo TEM can reveal cellular morphology, the shape of membranous structures, and the internal macromolecular arrangements of larger molecules[144]. In this project this technique was very valuable as it enabled the direct visualisation of the vesicles and provided essential morphological information. The DOPC liposomes were characterised with transmission electron microscopy (TEM) to determine their lamellarity and to confirm their average shape, size and size distribution. .

In order to overcome the resolution limit imposed by the wavelength of visible light in traditional light microscopes and see smaller details, TEM uses a beam of electrons. Electrons possess a shorter de Broglie wavelength compared to the wavelength of visible light, enabling smaller materials to be observed. In TEM an electron beam from an electron source, such as a tungsten or lanthanum hexaboride (LaB_6) filament[145], releases electrons which are directed towards an anode and then further directed through an electromagnetic field. The electron beam is focused using an electromagnetic lenses and shone through the sample. The electrons then interact with the specimen and some electrons are scattered. The unscattered electrons are focused onto an imaging device at the bottom of the microscope, which is usually a fluorescent screen. The areas of different density in the sample result in a 'shadow image' and this image can help reveal the sample properties.

The sample environment is kept under vacuum in TEM, as electrons could interact with air molecules and become deflected which would cause the electron beam to distort. As suggested by its name, the electrons must transmit through the sample, therefore this technique is limited to thin samples (normally < 1 µm). For samples which are unstable under vacuum, it is possible to freeze the specimen before carrying out cryo-TEM. Freezing samples allows analysis to be carried out without destroying the delicate morphology of the sample.

3.7.2. Sample preparation for TEM

In order to obtain high resolution and high quality images from TEM a very precise method for sample preparation was followed in this project. The DOPC liposome suspensions were prepared 24 hours prior to sample preparation for TEM, in order to ensure they were fresh and stable and they were analysed by DLS to verify they were not contaminated. The four systems studied by TEM were DOPC liposomes in pure water, DOPC liposomes in NaCl, $CaCl_2$ and $LaCl_3$. The salt solutions were all of equal ionic strength (I= 5 mM) in order to allow the effect of mono-, di- and trivalent cations to be compared effectively.

The TEM work in this project was carried out on small copper discs which have a fine mesh and are referred to as *grids.* The grids used here were purchased from EM Resolutions and they have lacey carbon films. Carbon is chosen as it is a low absorption material, but it is usually a hydrophobic substance, therefore to make the surface accessible to the aqueous samples used in this project, the carbon needs to be made hydrophilic, which is accomplished by 'glow discharging'. In this project glow discharging was carried out using an Edwards 306 carbon coater. In this process, the grids are placed in a chamber which is connected to a power supply. A high voltage is then applied between the anode and cathode at opposite ends of the chamber and the electrical potential ionises gas within the chamber. The negatively charged ions are then deposited onto the carbon, giving the lacey carbon a slight negative charge and causing the carbon film to become hydrophilic.

The next stage in the preparation process is to load the sample to the grid and freeze it. The sample must be frozen very rapidly (at a rate of ≈10^6 ˚C/s) so that the water in and surrounding the specimen is held in a vitreous state[146]. If the sample is not frozen sufficiently quickly or the sample is warmed after freezing, poor quality, crystalline or hexagonal ice can form, which is referred to as '*ice contamination'*[147]. Ice contamination can cause degradation in image quality as ice is capable of diffracting electrons[147].

In the preparation of these samples, an FEI Vitrobot™ Mark IV was used to plunge-freeze the samples. The grids were held at the bottom of the plunger by fine tweezers and ≈5 µL of the sample was pipetted onto the grid. The grid was then blotted by being pressed against filter paper, in order to remove excess sample and allow a thin liquid film containing sample to be formed. After a preprogramed time, the plunger is rapidly dropped into a cryogen and frozen; in this incidence, the cryogen was liquid ethane. Following the plunge freezing, the grid was transferred into a cryo grid storage box and was stored in liquid nitrogen.

Cryo-TEM grids were then transported to the microscope in stainless steel flasks containing liquid nitrogen. The storage boxes for EM grids were held inside Greiner tubes in liquid nitrogen suspended

by a rope inside the flasks. A single tilt cryo-transfer holder then enabled the transfer of the frozen grids into the cryo holder at liquid nitrogen temperatures. The frozen samples were then ready to be inserted into the microscope and analysed. The microscope used in this work was a Tecnai 20 - FEI 200kV twin lens transmission electron microscope (TEM/STEM), the images were collected on an FEI Eagle 4k x 4k CCD camera using FEI TIA software.

Chapter 4: The effect of inorganic cations on DOPC liposomes

4.1 Effect of inorganic cations on the electrophoretic mobility and zeta potential of DOPC liposomes

4.1.1 Effect of monovalent cations: Li^+, Na^+, K^+, and Cs^+

In order to better understand the effect of inorganic cations on DOPC liposomes, zeta potential measurements were carried out in the cation-liposome suspensions. The zeta potential is a useful measure of colloidal stability and can provide insight as to where the cations are associating with the phospholipids. Moreover, even though the zeta potential does not directly represent the lipid membrane surface charge, it is believed to provide a good approximation for the surface potential, for low electrolyte concentrations (up to 0.1 M)[148]. The impact of a number of inorganic cations, at concentrations ranging from 0 mM - 40 mM, on the zeta potential of the DOPC liposomes at 25 ˚C was studied. A temperature of 25 ˚C was chosen because it is higher than the transition temperature (T_m) for DOPC (DOPC, T_m = -17 ˚C). Hence, by using temperatures higher than the T_m, it is possible to carry out a more focussed study on the interactions between the cations and the liposomes without having to take into account a change in the lipid physical state.

Despite the zwitterionic head group of the DOPC phospholipids, the zeta potential of the liposomes in water is negative, with a value of ξ = -13.23 mV. This value is consistent with that reported by Chibowski *et al.*[149] who found the zeta potential of DOPC liposomes in water to be -14.5 mV. The negative zeta potential of the liposomes in water has been interpreted in terms of the orientation of the head groups of the phospholipids, caused by the negatively charged phosphatidyl group pointing outwards from the liposome, whilst the choline group is orientated inwards[149-151]. Additionally, it is hypothesised that the orientation of the hydration layers formed around the surface of the liposomes contributes to the negative zeta potential value of liposomes in water[152].

The zeta potential values recoded for the monovalent alkali metal cations are shown in Figures 26- 29. For completeness, Appendix B shows all the graphs of the electrophoretic mobilities of liposomes in the presence of all the inorganic cations studied. The results show that the zeta potential of the DOPC liposomes is affected by the presence of cations.

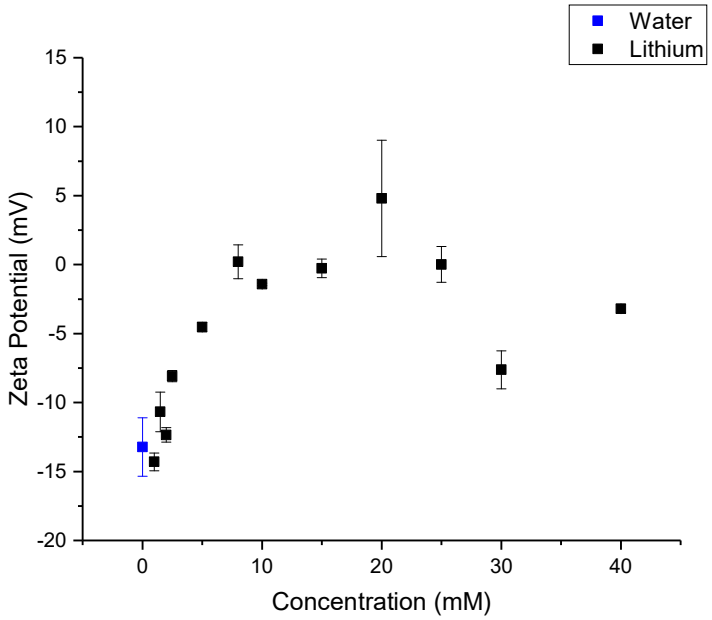

Figure 26: The effect of Li^+ cations on the zeta potential of DOPC liposomes at 25˚C.

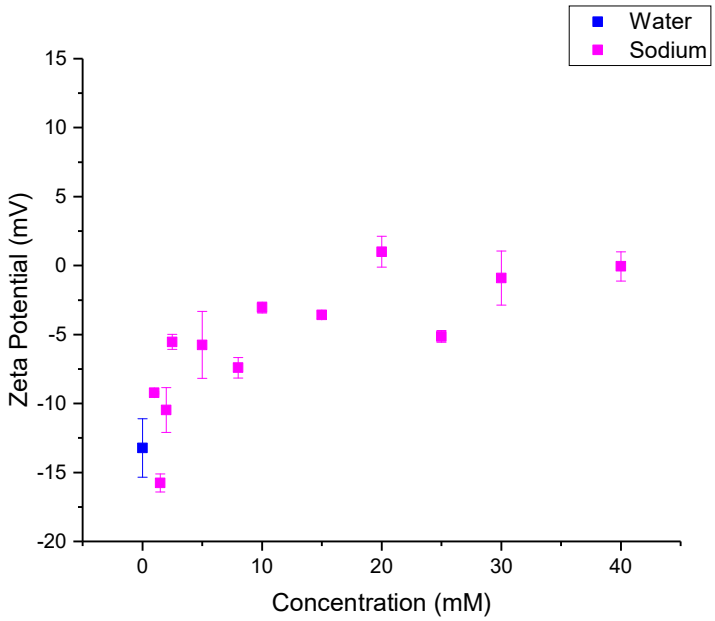

Figure 27: The effect of Na^+ cations on the zeta potential of DOPC liposomes at 25˚C.

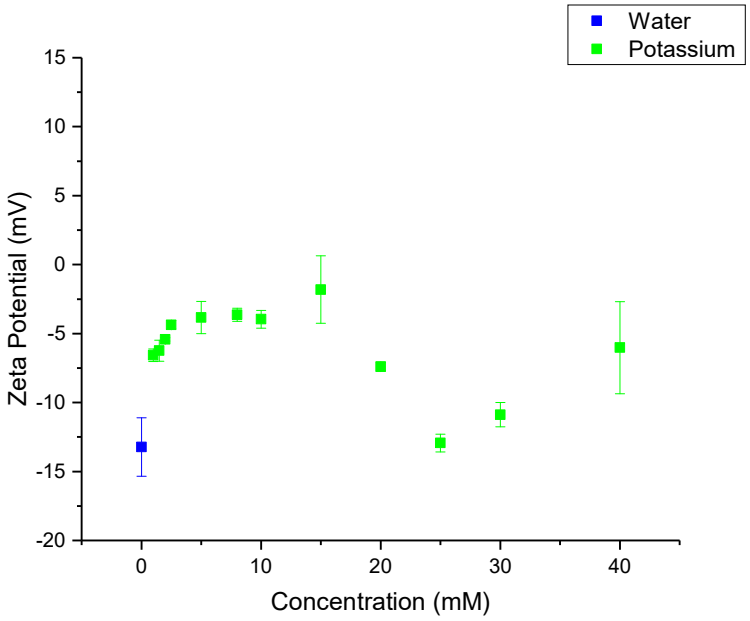

Figure 28: The effect of K^+ cations on the zeta potential of DOPC liposomes at 25˚C.

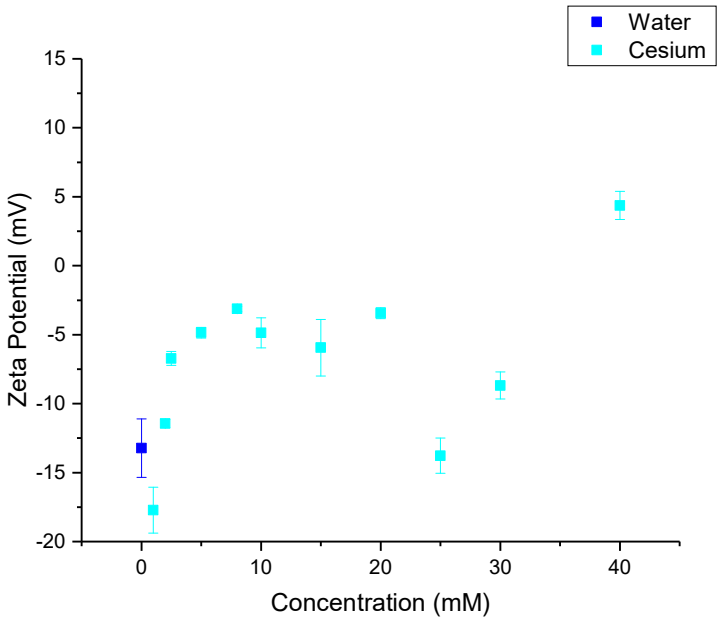

Figure 29: The effect of Cs^+ cations on the zeta potential of DOPC liposomes at 25˚C.

For comparison, the zeta potential results from all the monovalent ions are collated in Appendix C. Figures 26-29 show on increasing the concentration of all four cations, the value of the zeta potential becomes steadily more positive. In all four cases, once a certain concentration of cation is attained (~20 mM) there is a decrease in the zeta potential of the liposomes, which is followed by a slight increase again as the concentration of the cations is further increased. It is clear from Figures 26- 29 **that** the general trend for the change in zeta potential of DOPC liposomes in the presence of monovalent cations is similar for all the cations studied in this work. It can therefore be hypothesised that the interactions between phospholipids and ions are similar for all of the alkali metal cations examined in this work.

One explanation for this similarity could be found in considering the charge density of the monovalent cations and the hydration of the ions. The bare ion radii of Li^+, Na^+, K^+ and Cs^+ are 0.068 nm, 0.095 nm, 0.133 nm and 0.169 nm respectively[153]. Therefore moving down the series from Li^+ to Cs^+, the charge density becomes smaller, resulting in a decrease in hydration and hydration number. Li^+ has a hydration number of 5, Na^+ is hydrated by 4 water molecules, K^+ is hydrated by 3 water molecules and Cs^+ has a hydration number of 1[153]. Owing to the varying hydration of these cations, the resulting hydrated radii of the cations is fairly similar, and can explain why the cation interactions with the liposomes are comparable and the zeta potential results are similar for all four monovalent ions. The hydrated radii of Li^+, Na^+, K^+ and Cs^+ are 0.38 nm, 0.36 nm, 0.33 nm and 0.33 nm respectively[153]. As the hydrated radii of these ions vary by only 0.05 nm they have very similar sizes and therefore the same access to the head groups of the phospholipids and consequently compensate for the negatively charged phosphate group by the same amount, resulting in similar trends for the zeta potential values.

At low concentrations of cations (~2 – ~15 mM), for all four monovalent cations studied, an increase in the zeta potential of the DOPC liposomes is observed on increasing cation concentration, as can be seen from Figures 26-29. For all four cations, the zeta potential increases to a maximum and then as the concentration of the cations is increased further, there appears to be a small plateau observed and then the zeta potential begins to decrease (become more negative). The maximum zeta potential of the liposomes recorded is 4.80 mV in the presence of 20 mM Li^+ ions, 1.01 mV in the presence of 20 mM Na^+ ions and -1.81 mV and 4.37mV in the presence of 15 mM K^+ and 40 mM Cs^+ ions respectively. It is interesting to observe that the maximum zeta potential recorded in the presence of Na^+ and K^+ is ≈ 0 mV, and this is obtained at moderate ion concentrations, however for the Li^+ ions a more positive value for the zeta potential is recorded at these moderate concentrations. For the Cs^+ ion, the maximum zeta potential reached at the initial peak, at moderate concentration, is -3.13 mV which is in line with the trend for the Na^+, and K^+ ions. Interestingly, the Cs^+ induces the largest increase in the zeta potential of the liposomes at high concentrations.

This increase in zeta potential of the liposomes in the presence of cations has been observed widely in the literature previously. Sabín *et al.*[112] studied the effect of varying concentrations of Na^+ and K^+ on the zeta potential of egg yolk phosphatidylcholine (EYPC) liposomes. A fast increase of the initial, negative zeta potential was observed, attributed to the absorption of Na^+ and K^+ ions to the liposome surface. It is thought that cations associate with the surface of the polar head group of the phospholipid molecule, penetrating into the interfacial region of the bilayer and forming complexes with the lipids by binding to their phosphate and carbonyl groups[151, 154-156]. The association of the cations with the phospholipid is also entropically driven. As the ions bind to the lipid, the head group of the lipid is dehydrated and the cations shed the water molecules that make up their hydration layer. This liberates water molecules into the bulk solution and leads to a favourable gain in entropy[120, 157].

Extensive molecular dynamics (MD) simulations support the idea that cations associate with the hydrophilic head group of phospholipids. Sachs *et al.*[151] and López Cascales *et al.*[158] have used MD simulations to study the effect of monovalent salts on the POPC bilayer, and the effect of Li^+ and Na^+ ions on a charged membrane of dipalmitoylphosphatidylserine respectively. Both MD simulations produced results which supported the notion that cations are able to penetrate deep into the head group of the phospholipid owing to their high affinity for the head group. The positively charged cations are drawn to the negatively charged phosphate group of the phospholipid bilayer by the electrostatic attraction which exists between the two. The positive charge of the cation is then able to compensate for the negatively charged phosphate region of the lipid and hence the zeta potential becomes more positive. As the concentration of the cations is then increased, more cations adsorb to the liposome surface and therefore the zeta potential continues to become more positive.

As the concentration of the cations is increased further, for all four monovalent cations, there is a slight decrease in the value of the zeta potential of the liposomes followed by a small increase at high salt concentrations. In order to find an explanation for these changes in the zeta potential of the liposomes, it is vital to consider in more depth, the interactions between the cations and the phospholipid head groups.

It is widely acknowledged in the literature that the association of the cations with the head groups of the phospholipids causes a change in the conformation of the head group itself. As already outlined previously, the negatively charged phosphatidyl groups point towards the outside of the liposome, giving rise to the slight negative zeta potential in water. On the addition of cations, however, the head group conformation is affected and the direction in which the head group points is altered. Sachs *et al.*[151] studied the effect of monovalent cations on the head group tilt of phospholipids. In this work, they defined the head group tilt as the angle made by the phosphorus-nitrogen (PN) dipole with the bilayer normal. Head groups of lipids closely associated with cations were found to experience a

significantly increased tilt relative to the bilayer average and the ions were found to 'push the head group down' towards the bilayer plane. This effect was though to arise owing to the electrostatic repulsion between the choline group and the monovalent cation. This result is shown diagrammatically in Figure 30[151] which is adapted from the paper discussed previously.

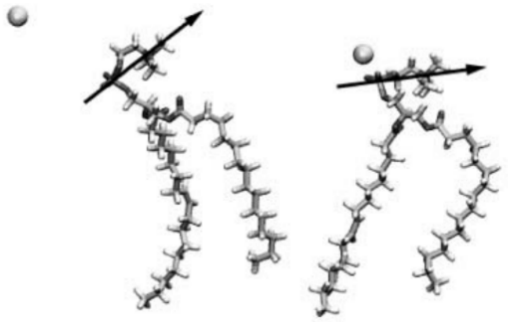

Figure 30: The effect of Na+ approach on the head group tilt of a POPC phospholipid, taken 250 ps apart from the 1 M NaCl simulation. The grey sphere represents the Na+ ion.[151] Taken from Reference 152.

These results are supported strongly by earlier work carried out in 1991 by Makino *et al.*[150]. In this work, the ionic strength-induced conformational changes in the lipid head group region of DPPC, DMPC and DSPC liposomes were examined using zeta potential data. The zeta potential of the liposomes in low ionic strength solutions was found to be negative and decreased in magnitude as the ionic strength was increased. It was hypothesised that as ionic strength increases, the head groups of the lipids could pack more closely together, because the electrostatic repulsion between the similarly charged groups is screened by an increase in the counter ion concentration around the charged groups. The lipids pass through a conformation where the head group is parallel to the liposome surface and continue to pack more closely on increasing ionic strength, resulting in an overall change in the direction of the head group of the lipid compared to in the absence of cations. Figure 30 shows the change in direction of the head group of the phospholipid as ionic strength is increased[150].

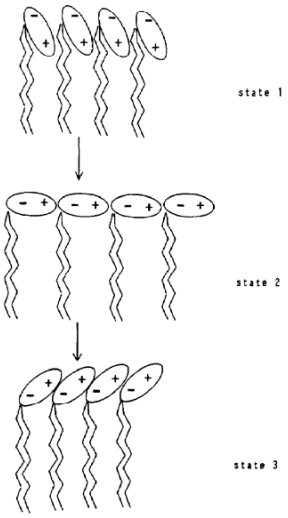

Figure 31: Change in conformation of the lipid head groups at stage 1) low ionic strength solution, stage 2) medium ionic strength solution and stage 3) high ionic strength solution. The (-) sign represents the phosphate group and the (+) sign represents the choline group. Reprinted from reference 151, Copyright © 1991, with permission from Elsevier

In this project, the fluctuations observed in the zeta potential measurements in the presence of monovalent cations at concentrations > 15 mM could be rationalised in terms of alterations in lipid head group conformation. At medium ionic strength a decrease in the zeta potential could arise from the reorientation of the head group, in the same way as shown in Figure 31, and consequently the adsorption of some of the Cl^- ions in the solution. It could be hypothesised that the Cl^- ions would begin to associate with the increasingly more positive head group of the phospholipid and therefore, cause the value of the zeta potential to become slightly more negative. When studying the effect of salts on the phospholipid bilayer, research tends to focus strongly on the interactions of the cations with the bilayer, and therefore the role of the Cl^- counter ion remains to be fully understood. The idea that Cl^- ions do not penetrate deep into the membrane, as cations do, but instead reside mostly in the water phase near the membrane surface, as well as the notion that cations preferentially associate with the phospholipid bilayer over anions (Cl^- ion in particular) is widely supported in the literature[109, 114, 118]. It is, however, also acknowledged that in some cases that the Cl^- ion, although not preferentially, will associate with the head group of the phospholipid. Redondo-Morata *et al.*[154] produced MD simulations which illustrated that the adsorption of Cl^- ions occurred at the choline region of the head of the phospholipid and similar research conducted by Pandit *et al.*[155] proved similar results. These results showed that, although the anion was less strongly bound than the cation, the Cl^- exhibited slight coordination with the choline (more specifically, the $^+N(CH_3)_3$ group) of the head group of the lipid[155].

Following the slight decrease in the zeta potential of the liposomes, for all four monovalent cations as the concentration is increased further up to 40 mM, the zeta potential becomes increasingly more positive. This increase in zeta potential can be attributed to the total reorientation of the lipid head groups as the cations continue to adsorb to the phosphate group of the head of the lipid. As the cation-lipid complexes form there is a change in the direction of the head group, as shown in Figure 31, and as high ion concentrations are reached, the positively charged choline group points out, towards the outside of the liposome, resulting in an increase in the zeta potential.

Finally, it is possible that the orientation of the head groups of the phospholipids could also account for the fluctuations in the zeta potentials of the liposomes at very low cation concentrations (~1 – ~2 mM). On initial addition of the cations, in the case of Li^+, Na^+ and Cs^+, there is a decrease in the zeta potential of the liposomes by 1.08 mV, 2.53 mV and 4.50 mV, respectively (Figures 26, 27 and 29). This is an interesting and perhaps unexpected observation, as, intuitively, the addition of a positive ion with an affinity to the head group should cause the zeta potential to become more positive. This decrease in zeta potential at low concentrations is, therefore, ion specific, as it was not observed in the case of the K^+ cation.

The decrease in the zeta potential of the liposomes is most pronounced in the case of the Cs^+ ion, followed by the Na^+ ion, and Li^+ shows the smallest effect. Considering the hydrated ionic radii of these cations could help to explain the strength of this effect. Cs^+ has a slightly smaller hydrated ionic radii (0.33 nm[153]) than Na^+ (0.36 nm[153]), which has a slightly smaller radii than Li^+ (0.38 nm[153]). Accordingly, it could be theorised that the Cs^+ ion can slightly more easily access the head groups of the phospholipids than the larger hydrated Na^+ and Li^+ ions and as a consequence, it has the greatest effect on the head group of the lipids at these low concentrations. As the concentrations of the cations are increased, the differences in the hydrated ionic radii become less profound as there are overall, more ions competing for association with the heads of the phospholipids in all cases.

This recorded initial decrease in the zeta potential of the liposomes at very low concentrations still remains a slight grey area. Previous literature falls short of providing an explanation as the focus of most research into specific ion effects on liposomes does not tend to be carried out at such low concentrations as these.

4.1.2 Effect of divalent cations: Ca^{2+} and Mg^{2+}

The effect of divalent cations on the electrophoretic mobility and the zeta potential of DOPC liposomes was also studied in this work. The impact of $CaCl_2$ and $MgCl_2$, at varying concentrations up to 40 mM, on DOPC liposomes at 25 ˚C was examined. Figure 32 and 33 show the change in the zeta potential of the liposomes in the presence of $CaCl_2$ and $MgCl_2$ respectively. For completeness, Appendix D shows the electrophoretic mobility as a function of Mg^{2+} concentration, as well as Ca^{2+} concentration. For comparison, the zeta potential results from all the divalent ions are collated in Appendix E.

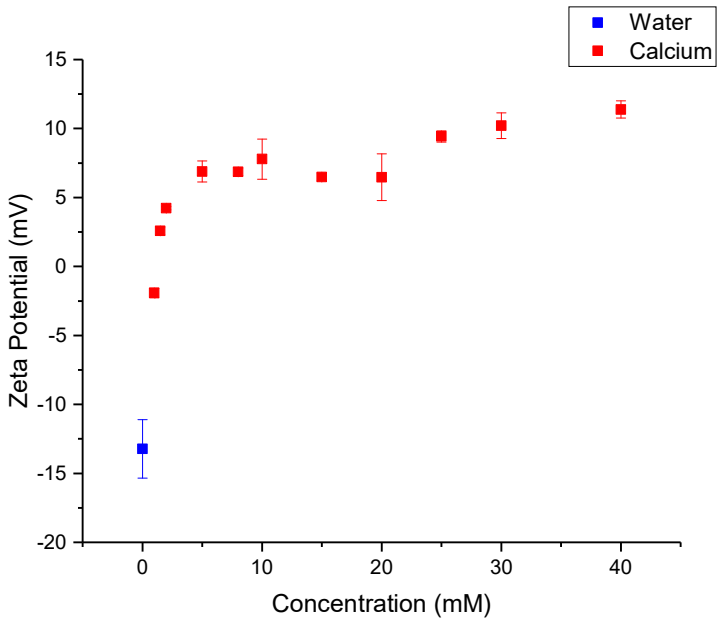

Figure 32: The effect of Ca^{2+} cations on the zeta potential of DOPC liposomes at 25˚C.

Figure 32 shows the zeta potential of the DOPC liposomes as a function of $CaCl_2$ concentration. On the initial addition of 1 mM $CaCl_2$, there is a large increase in the zeta potential of 11.31 mV, from -13.23 mV (DOPC liposomes in water, [$CaCl_2$] = 0 mM) to -1.92 mV. As the concentration of the $CaCl_2$ increases up to 5 mM, the zeta potential of the liposomes also increases sharply, with the value of the zeta potential already positive (2.57 mV) at [$CaCl_2$] = 1.5 mM. At 5 mM, the zeta potential of the liposomes has increased up to 6.88 mV. Following the initial increase of the zeta potential of the liposomes up to 5 mM, the zeta potential appears to plateau slightly from 5 mM to 8 mM, with only a change of 0.021 mV being recorded. At [$CaCl_2$] =15 mM and 20 mM, there appears to be a slight decrease in the zeta potential of the liposomes before a slight increase as the concentration of $CaCl_2$ is increased up to the maximum of 40 mM.

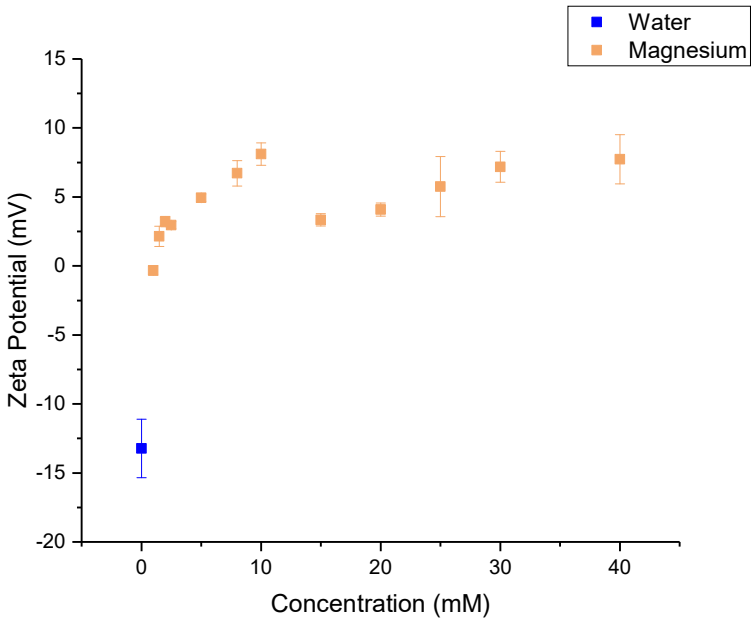

Figure 33: The effect of Mg^{2+} cations on the zeta potential of DOPC liposomes at 25˚C.

For completeness and comparison, Figure 34 shows the effect of the divalent cations on the zeta potential as a function of ionic strength (*I*). The ionic strength was calculated from the equation[141]:

$$I = \frac{1}{2}\sum z^2{}_i \, C_i \qquad (20)$$

where C_i is the ion concentration and z_i is the ion valency.

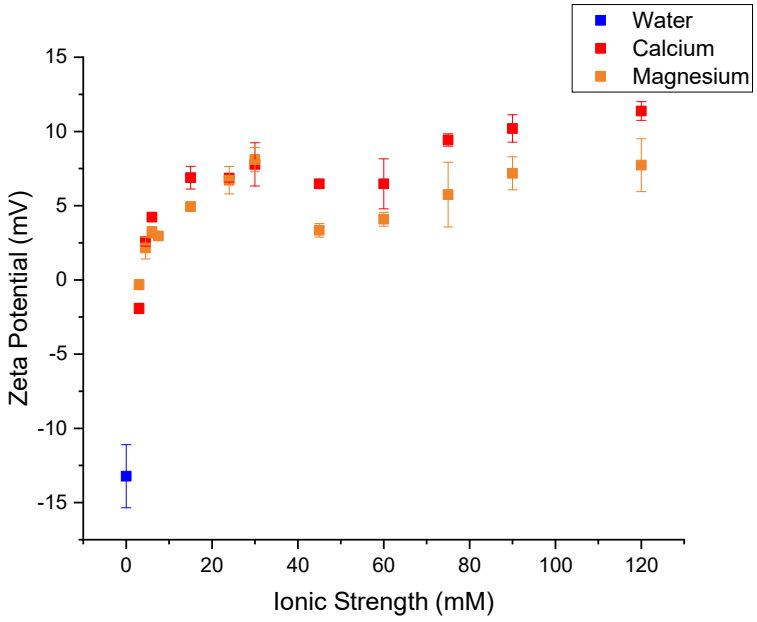

Figure 34: The effect of divalent cations on the zeta potential of DOPC liposomes at 25˚C as a function of ionic strength.

The zeta potential of the DOPC liposomes as a function of $MgCl_2$ concentration is shown in Figure 33**.** The trend observed for the zeta potential of the liposomes in the presence of $MgCl_2$ closely resembles the trend described above for the liposomes in the presence of $CaCl_2$. In 1 mM $MgCl_2$, there is a very sharp increase in the zeta potential up to -0.32 mM, which, even at this very low salt concentration, has already nearly compensated for the slight negative zeta potential of DOPC liposomes in water. As the concentration of $MgCl_2$ is then increased up to 10 mM, the zeta potential continues to increase gradually. At [$MgCl_2$] = 15 mM, the zeta potential then decreases by 4.77 mV to 3.34 mV, before gradually increasing as the $MgCl_2$ concentration is increased up to its maximum.

The trend in the zeta potential variation of the DOPC liposomes with respect to the ion concentration is similar for both the divalent cations studied in this work (as demonstrated in Figure 34) and hence, it can be concluded that the interactions between these two ions and the liposomes are similar. At low divalent cation concentrations, the zeta potential of the liposomes increases sharply, reflecting the strong attraction of the divalent cations to the phospholipid head group. The cation is thought to penetrate between the lipid head groups and form coordination complexes with one or more lipid phosphate groups[157]. The Ca^{2+} and Mg^{2+} ions adsorb strongly to the negatively charged phosphate group in the hydrophilic head of the lipid and therefore compensate for the negatively charged group and even reverse the sign of the zeta potential as the concentration continues to be increased[159, 160]. Sinn *et al.*[161] showed that the binding of the divalent ions to the lipid bilayer was an endothermic process and therefore, must be entropically driven. The gain in entropy is thought to arise from the release of water molecules from the hydration shell of the ion as well as the dehydration of the lipid bilayer.

The two cations interact with the liposomes in similar ways to one another as they have similar hydrated radii. Ca^{2+} has a hydrated radius of 0.41 nm[153], Mg^{2+} has a hydrated radius of 0.43 nm[153] and both ions have a hydration number of 6 (±1)[153]. Radii differing by only 0.02 nm means that these two ions have the comparable access to the head groups of the lipids and can therefore associate with the phosphate group to a similar extent.

In the case of both Ca^{2+} and Mg^{2+}, as the concentration is increased above 10 mM, there are no drastically large changes in the value of the zeta potentials observed. This is especially clear when examining the zeta potential of the liposomes in the presence of 25- 40 mM Ca^{2+} or Mg^{2+}. For Ca^{2+} in this concentration range, there is only a 21 % increase in the zeta potential and the value measured remains around $\xi \sim 10$ mV. Similarly, for Mg^{2+} ions, at high concentrations, the zeta potential only shows an 8 % change, plateauing at $\xi \sim 7.5$ mV. This plateau has been widely reported in the literature and is thought to occur due to saturation of the head groups of the phospholipids with cations[162, 163]. When the saturation of the head groups occurs, the zeta potential does not change dramatically as

the divalent cation concentration increases. It is interesting to also note that, unlike the rest of the monovalent cations studied in this work, the Na^+ ion appears to also induce a plateau in the zeta potential of the liposomes (Figure 27), suggesting that this ion behaves in a more similar manner to the divalent cations than the monovalent cations.

In order to gain more information on the effect of divalent cations on the zeta potential of DOPC liposomes, the data was analysed further. Melcrova *et al.*[163] studied the effect of calcium ions on the zeta potential of 1-palmitoyl-2-oleoyl-sn-glycero-3-phosphocholine (POPC) liposomes and mixed, 1-palmitoyl-2-oleoyl-sn-glycero-3-phosphocholine/ 1-palmitoyl-2-oleoyl-sn-glycero-3-phospho-L-serine (POPC/POPS) liposomes. The zeta potential of the liposomes was measured in the presence of $CaCl_2$, at a range of concentrations, up to 200 mM. The data obtained in the work was successfully fitted using the Langmuir-Freundlich (LF) adsorption model as can be seen from Figure 35[163]. However, they did not report the maximum zeta potential as we report here.

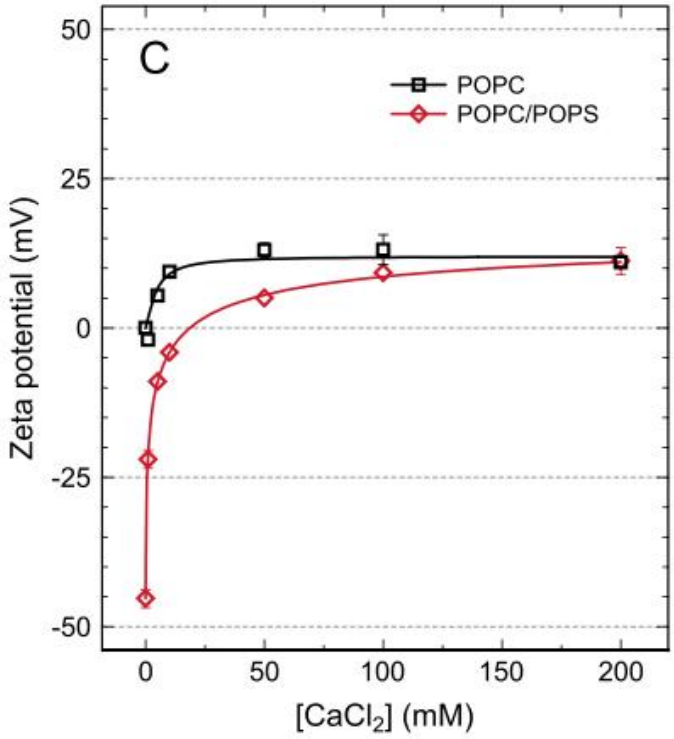

Figure 35: Graph plotted from data obtained by Melcrova et al[163]. Zeta potential of POPC and POPC/POPS liposomes measured as a function of $CaCl_2$ concentration. Data fitted with the Langmuir-Freundlich model. Taken from Reference 164.

From the data collected in this project, the change in the zeta potential of the liposomes in the presence of $CaCl_2$ and $MgCl_2$ showed a very similar trend to the trend shown in Figure 35**.**

Therefore, the data collected in this work was fitted using Igor Pro software package with the Langmuir-Freundlich equation of the following form [164, 165] :

$$\mu_{e,(LF)} = \mu_{e,0} + \frac{M(K[XCl_2])^n}{(K[XCl_2])^n+1} \quad (21)$$

where, in this case, *X* is Mg or Ca, *M* is the maximum value of electrophoretic mobility for excess $CaCl_2$ or $MgCl_2$, *K* is the equilibrium constant associated with the cation adsorption, $\mu_{e,0}$ is the electrophoretic mobility at $[XCl_2] = 0$, and *n* is an empirical constant. Graphs showing the data relating electrophoretic mobility of the liposomes to the $CaCl_2$ or $MgCl_2$ concentration fitted with Langmuir-Freundlich equation are shown in Figure 36**.** Additionally, the values of *M, K,* $\mu_{e,0}$ and *n* used to fit the data are shown in Table 5.

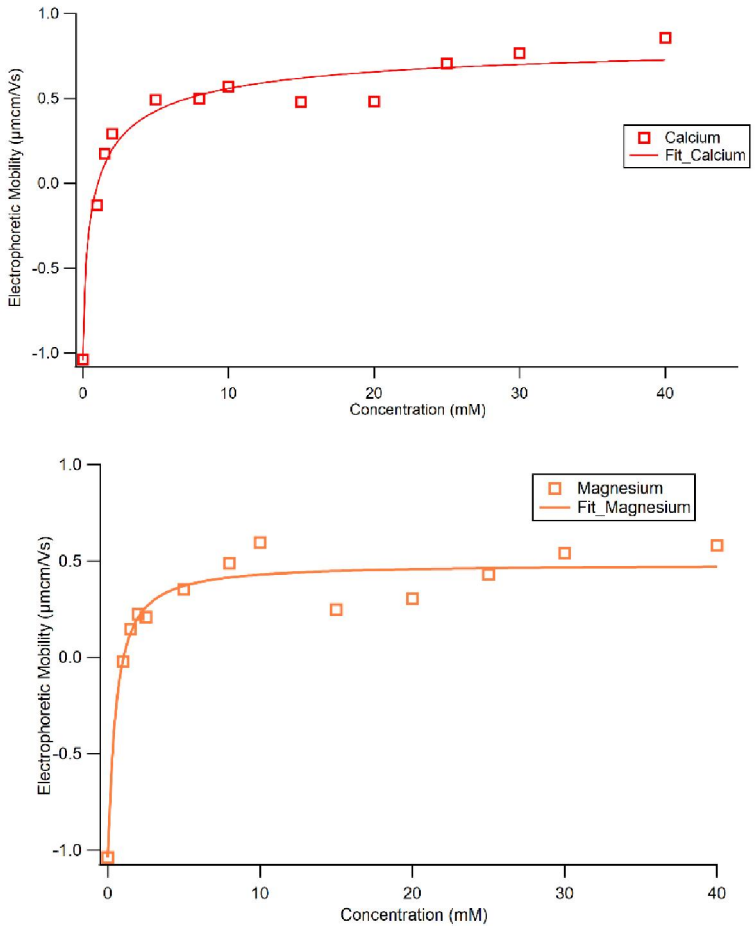

Figure 36: Measured electrophoretic mobility of DOPC liposomes as a function of a) $CaCl_2$ and b) $MgCl_2$ concentration. The solid red and orange lines represent the fits using the Langmuir-Freundlich adsorption model for calcium ions and magnesium ion respectively. Plotted using IGOR Pro.

Table 5: Fitting parameters obtained using Langmuir-Freundlich fits for data showing electrophoretic mobility as a function of divalent cation concentration (mM)

Cation	**Magnesium**	**Calcium**
M ($m^2V^{-1}s^{-1}$ x10^{-8})	1.52	1.91
K (mM^{-1})	1.90	1.30
***n* (n.a.)**	1.13	0.64
$\mu e_{,o}$ ($m^2V^{-1}s^{-1}$ x10^{-8})	-1.04	-1.04

In order to obtain more information regarding how the divalent cations affect the zeta potential of the DOPC liposomes, the fitting parameters were used to calculate the maximum zeta potential of the liposomes as the concentration of the cations tends to infinity. The maximum, saturation zeta potential can be found by calculating the sum of $\mu_{e,0}$ and $M_{,}$ and then converting the resulting electrophoretic mobility into zeta potential using the Henry equation (Equation 17). It is important to note here that when converting *M* to the zeta potential *f(ka)* was assumed to be 1.5. This is because the cation concentration tends to infinity and κ^{-1} tends 0. The saturation zeta potential was found to be 11.2 mV for liposomes in the presence of $CaCl_2$ and 6.17 mV for liposomes in the presence of $MgCl_2$.

An interesting observation obtained in this work, is the vast difference between the effects of monovalent and divalent cations on the zeta potentials of DOPC liposomes. The divalent cations cause the zeta potential of the liposomes to increase far more quickly than the monovalent cations, and this can be attributed to the stronger electrostatic attraction between the phosphate group of the lipid and the higher charge and charge density of the divalent ion. These results agree closely with those obtained by Mozuraityte *et al.*[166], who also found that higher valency ions resulted in more positive values of the zeta potential of liposomes. At moderate concentrations of the ions, the decrease in the zeta potential of the liposomes discussed for monovalent cations if far less pronounced in the case of the divalent cations. It is likely that this is because the head group of the phospholipid quickly becomes saturated with the divalent cations, and therefore there is less scope for vast changes in the conformation and the direction of the lipid head, as is hypothesised to occur in the case of monovalent ions.

4.1.3 Effect of trivalent cation: La^{3+}

For the final part of the investigation into the effect of inorganic cations on the zeta potential of DOPC liposomes, the effect of $LaCl_3$ was examined.

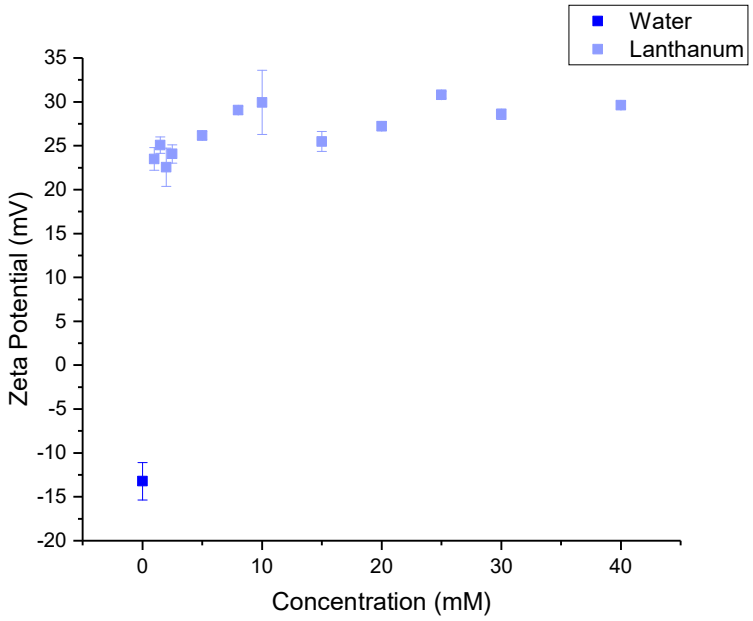

Figure 37: The effect of La^{3+} cations on the zeta potential of DOPC liposomes at 25˚C

From Figure 37 it is clear to see that even in the presence of very low concentrations (1 mM) of La^{3+} there is a remarkably large increase of 36.7 mV in the zeta potential of the liposomes up to 23.5 mV. As the concentration of La^{3+} is increased further, the zeta potential continues to increase slowly up to 29.9 mV at [La^{3+} = 10 mM]. At [La^{3+} = 15 mM] there is a 15 % decrease in the zeta potential of the liposomes, and then in the same way as seen with the divalent cations, the zeta potential begins to increase slowly until 30.8 mV, where it appears to plateau.

The trend in the zeta potential of the liposomes as a function of La^{3+} concentration bears close resemblance to the trend observed for the zeta potentials of the liposomes in the presence of the divalent cations, Ca^{2+} and Mg^{2+} (Figure 38). The main difference being that for the trivalent cation, the values of the zeta potential obtained are a lot more positive overall and the plateau occurs at much more positive zeta potential. These differences can be attributed to the 3+ valency of the La^{3+} ion. This higher valency means that the electrostatic attraction to the negatively charged phosphate group is stronger and therefore the La^{3+} ion has a higher affinity for the head of the phospholipid. It is able to compensate for the negatively charged phosphate group more effectively and therefore increase the

value of the zeta potential by a greater amount than the monovalent and divalent cations. The hydration number of La^{3+} is reported to be 9[167], meaning that the cation is surrounded by an average of 9 water molecules in aqueous solution. There is consequently a large entopic gain when the La^{3+} ion binds to the liposome and the 9 water molecules are liberated back into the bulk solution. This entropic effect will be stronger for the trivalent cations than for the monovalent and divalent cations because the La^{3+} ions are more strongly hydrated and therefore liberate more water molecules when they form complexes with the lipid head groups. For completeness, Figure 38 shows the effect of divalent and trivalent cations on the zeta potential of the DOPC liposomes as a function of ionic strength.

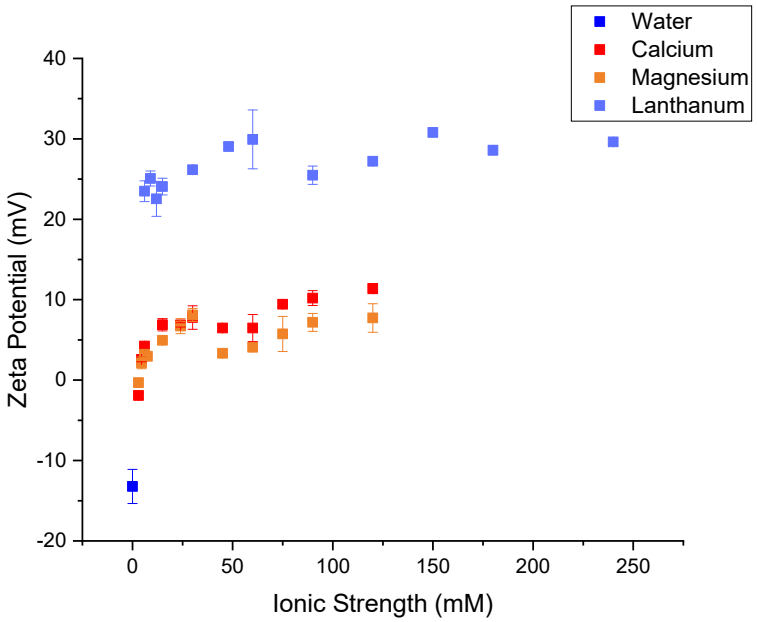

Figure 38: The effect of divalent and trivalent cations on the zeta potential of DOPC liposomes at 25˚C as a function of ionic strength.

These results are well aligned with findings in the literature. Lehrmann *et al.* confirmed that the binding of La^{3+} to POPC phospholipid vesicles is endothermic ($\Delta H \approx 1.8$ kcal/mol [168]), and therefore the adsorption of the metal ions to the membrane surface is driven predominately by entropy[168]. It is also worthwhile to point out that as the concentration of La^{3+} ions increases, the gradual accumulation of cations bound to the surface creates an increasingly more positive charge on the membrane surface. This makes further binding of the La^{3+} ion more and more difficult and is why there is a more profound increase in the zeta potential of the liposomes at lower cation concentrations.

The effect of metal cations on the zeta potential of the DOPC liposomes provides interesting results which are strongly supported by the literature and previous findings on specific ion effects. The results allow insight into the mechanism by which the ions associate with the head group of the lipids and also the interactions which allow these associations.

4.1.4 Effect of inorganic cations on the effective charge (Q_{eff}) of the DOPC liposomes

As well as insight into the zeta potential of the liposomes, the electrophoretic mobility (μ_e) measurements, obtained using DLS, also allow the effective charge associated with each liposome (Q_{eff}) to be calculated. Q_{eff} can be calculated using Equation 22[118, 169]:

$$Q_{eff} = 6\pi\eta r_{eff}\mu_e \quad (22)$$

where η is the solvent viscosity, in this case water, and r_{eff} is the effective radius of the liposome including the Stern layer. In this equation, the effective radius, r_{eff}, can be substituted for the hydrodynamic radius, *r,* as measured by DLS. This substitution can be made as the Stern layer and the shear plane are located only a few water layers apart, which is comparatively, a very small distance compared with the overall diameter of the vesicle (> 100 nm)[118].

In addition, the surface charge density (σ) can also calculated from Equation 23[169]:

$$\sigma = \frac{Q_{eff}}{4\pi r^2} \quad (23)$$

which can be simplified to:

$$\sigma = \frac{3\eta\mu_e}{d_h} \quad (24)$$

where d_h is the diameter of the liposomes, as measured by DLS.

The effective charge (Q_{eff}) of the liposomes in the aqueous salt solutions are shown below. Table 6 shows the effective charge of the liposomes in the presence of water and monovalent cations, Table 7 in the presence of divalent cations, and finally, Table 8 in the presence of trivalent cations.

Table 6: Effective charge (Q_{eff}) of liposomes in the presence of varying concentrations of monovalent cations at 25 ˚C

Ion concentration (mM)	Effective charge (Q_{eff}) of liposomes [number of electronic charges]			
	NaCl	LiCl	KCl	CsCl
0.0	-71.29 (in water)			
1.0	-45.45	-64.37	-28.37	-76.29
1.5	-77.38	-50.86	-26.97	-
2.0	-50.02	-53.09	-26.35	-52.97
2.5	-27.27	-36.10	-20.49	-31.64
5.0	-31.27	-23.42	-19.47	-23.59
8.0	-37.43	1.16	-20.63	-16.19
10.0	-15.39	-8.40	-22.08	-29.19
15.0	-18.70	-1.74	-9.16	-31.08
20.0	5.22	29.39	-39.34	-19.21
25.0	-28.02	0.07	-68.44	-80.41
30.0	-4.87	-51.14	-62.32	-51.08
40.0	-0.28	-19.80	-30.13	21.44

Table 7: Effective charge (Qeff) of liposomes in the presence of varying concentrations of divalent cations at 25 ˚C

Ion concentration (mM)	Effective charge (Qeff) of liposomes [number of electronic charges]	
	$CaCl_2$	$MgCl_2$
1.0	-9.39	-1.82
1.5	12.22	11.17
2.0	20.24	16.85
2.5		17.30
5.0	33.03	23.57
8.0	33.59	32.54
10.0	39.64	45.21
15.0	32.12	18.18
20.0	31.99	20.46
25.0	47.67	30.87
30.0	53.72	39.46
40.0	59.77	40.88

Table 8: Effective charge (Qeff) of liposomes in the presence of varying concentrations of trivalent cations at 25 ˚C

Ion concentration (mM)	(Qeff) of liposomes in $LaCl_3$ [number of electronic charges]
1.0	105.53
1.5	117.69
2.0	110.78
2.5	119.07
5.0	150.71
8.0	141.97
10.0	186.97
15.0	124.20
20.0	135.64
25.0	156.60
30.0	151.13
40.0	150.85

As can be seen in Tables 6, 7 and 8, the effective charges of the DOPC liposomes show a general increase as the concentration of monovalent ions increases. The effective charge of the liposomes show the same general trend as the zeta potential of the liposomes and therefore, can be rationalised in the same way. It is clear when studying these tables that the cations have an increasing impact on the effective charge of the liposomes of the order: monovalent cations < divalent cations < trivalent cations. The trivalent cation, La^{3+}, evidently causes liposomes to have the largest effective charges. Table 8 shows that in the presence of La^{3+}, even at very low concentrations, all liposomes have effective charges of > 100. As with the zeta potential results, the divalent cations have the second strongest impact of the liposomes. Table 7 shows that the divalent cations cause the liposomes have positive effective charges at all concentrations studied, except at very low concentrations of 1 mM. The monovalent ions cause the most fluctuating trend in the effective charge of the liposomes.

The surface charge densities (σ) of the liposomes in the presence of monovalent, divalent and trivalent cations are shown in Figure 39.

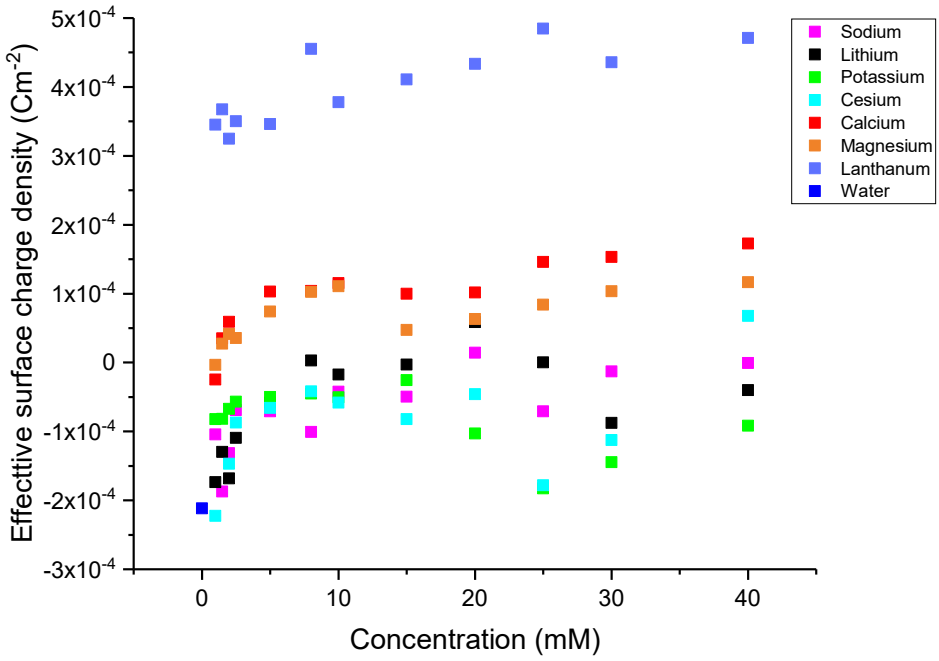

Figure 39: The effect of inorganic cations on the effective surface charge densities of DOPC liposomes at 25˚C

The surface charge densities of the liposomes increased on the addition of cations, as can be seen from Figure 39**.** The strength of the effect of the cations on the surface charge densities of the liposomes is of the order monovalent < divalent < trivalent. Additionally, and especially clear in the case of the divalent and trivalent cations, at higher ion concentrations, the surface charge density was less sensitive to cation concentration. The increasing surface charge densities support the notion that cations bind to the head groups of the lipids and, in the case of the higher valency ions, the plateau in the surface charge densities at high ion concentrations supports the size and zeta potential measurements, indicating saturation of the lipids with the cations.

4.2 Effect of inorganic cations on the size of DOPC liposomes

Dynamic light scattering was used to characterize the size (diameter, *d*) of the DOPC liposomes in the presence of various inorganic cations. Figures 40 - 43 show the size of the liposomes as a function of LiCl, NaCl, KCl and CsCl concentration respectively. The average size of the DOPC liposomes in water was found to be 131.0 nm, as measured by DLS.

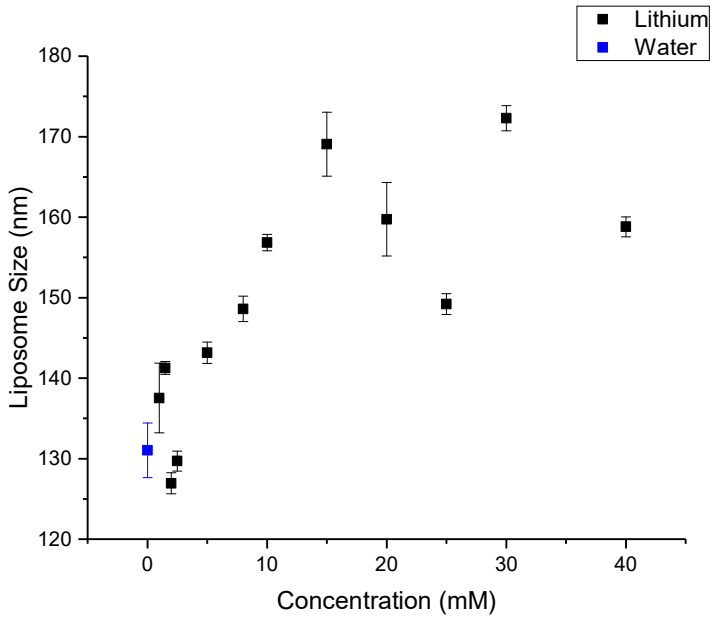

Figure 40: The change in DOPC liposome size as a function of lithium cation concentration, at 25 ˚C, as measured by DLS.

It is evident to see that the presence of cations causes notable changes in the size of the liposomes. Figure 40 shows the change in the size of the DOPC liposomes as a function of LiCl concentration. At 1 mM and 1.5 mM there is a slight increase in the size of the liposomes to 137.5 nm and 141.3 nm respectively. Following this small increase, there is then a shrink in the size of the liposomes by 10 % to 126.9 nm at [LiCl] = 2 mM. Then, as the concentration of LiCl is then increased up to 15 mM, the liposomes increase in size up to 169.1 nm, which is 38.1 nm greater than the DOPC liposomes in the absence of ions. As the concentration is then increased up to 40 mM, the liposomes show a general decrease in size, aside from an unexpected result at [LiCl]= 30 mM where the liposomes are much larger than expected at 172.3 nm.

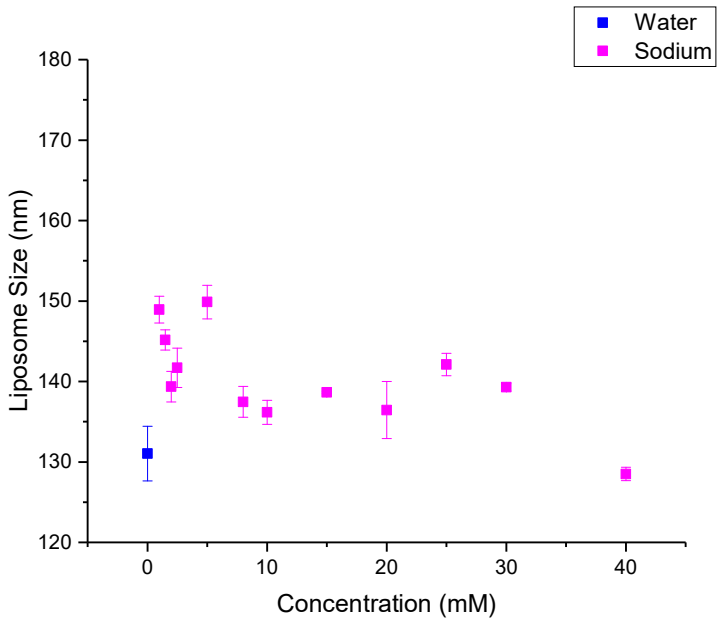

Figure 41: The change in DOPC liposome size as a function of sodium cation concentration, at 25 ˚C, as measured by DLS.

The effect of NaCl on the size of the liposomes is significantly different from the effect of LiCl. Figure 41 shows the change in the size of the liposomes at varying NaCl concentrations. At low NaCl concentrations, the liposomes increase in size, relative to water, and also tend to exhibit small fluctuations. At [NaCl] = 1 and 1.5 mM, the size of the liposomes increase to 148.9 nm and 145.2 nm respectively. As the concentration is increased further to 2 mM there is a decrease in the size of the liposomes by 4 % to 139.4 nm and then the liposomes increase in size up to [NaCl]= 5 mM, where the liposomes are a maximum size of 149.9 nm. As the concentration is increased further the liposomes decrease in size and then remain approximately the same size (d ~ 138 nm), demonstrating a small decrease to 128.5 nm at high concentrations ([NaCl] = 40 mM). It is important to note the plateau in the size of the liposomes which occurs at moderate Na^+ concentrations, as it appears to be a unique effect of sodium and not observed as profoundly in the cases of the other monovalent cations.

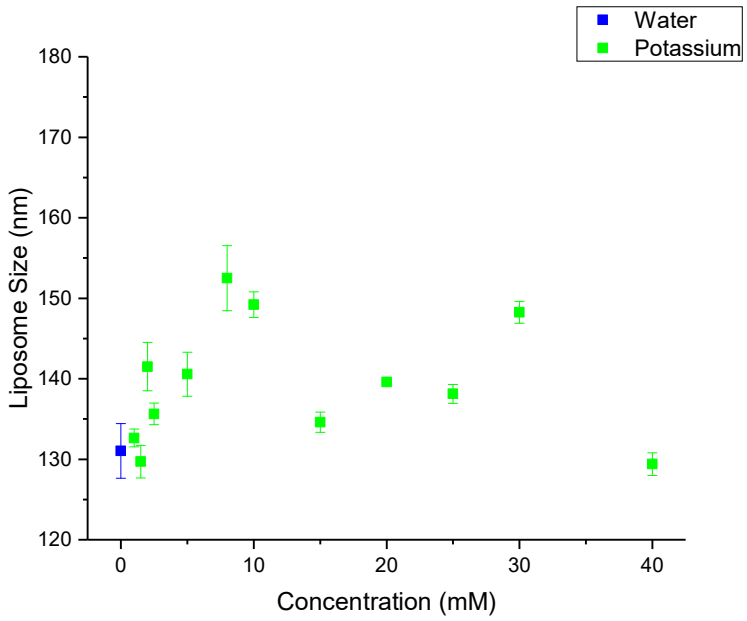

Figure 42: The change in DOPC liposome size as a function of potassium cation concentration, at 25 ˚C, as measured by DLS.

The effect of KCl on the size of DOPC liposomes is slightly more straightforward to describe. As the concentration of KCl is increased up to 8 mM, the liposomes gradually increase in size until a maximum size of 152.5 nm is reached. Following this maximum, the liposomes then show a general decrease in size, with the decrease becoming less and less large as the concentration is increased. At [KCl] = 30 mM, the liposomes increase in size from 138.1 nm at [KCl] =25 mM, to 148.3 nm. The liposomes then decrease in size at [KCl] = 40 mM by 13 % to 129.4 nm. The increase in the size of the liposomes at [KCl] =30 mM does not fit with the general decrease in size as the concentration is increased from 10 mM to 40 mM. Therefore, it is important to consider the possibility that this measurement may be anomalous.

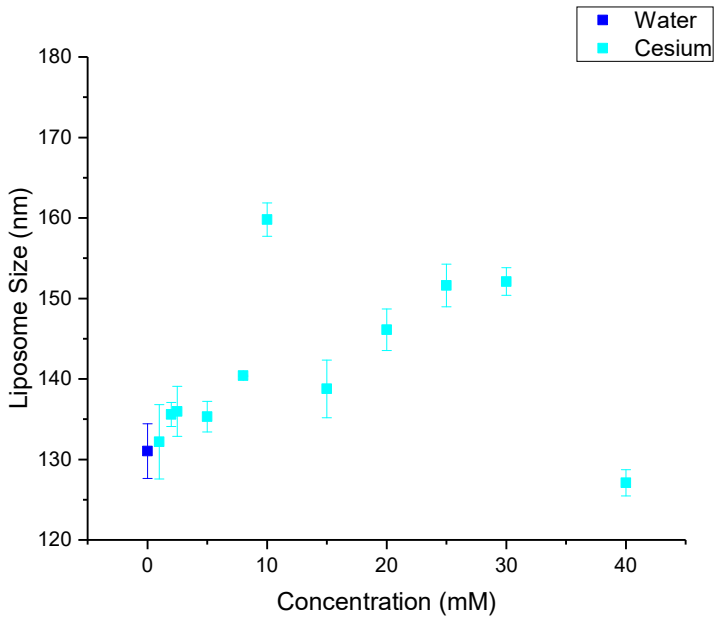

Figure 43: The change in DOPC liposome size as a function of cesium cation concentration, at 25 ˚C, as measured by DLS.

Finally, Figure 43 shows the change in the size of DOPC liposomes as a function of CsCl concentration. It is clear from Figure 43 that as the concentration of Cs^+ increases up to 30 mM, the size of the liposomes gradually increases as well. The liposomes are at a maximum size of 152.1 nm at [CsCl] = 30 mM. Interestingly, at [CsCl]= 40 mM the liposomes were found to be 127.1 nm, indicating a 16% decrease in size by increasing the Cs^+ concentration from 30 mM to 40 mM. The size of the liposomes had also decreased by such an amount at [CsCl] = 40 mM, that they have shrunk to be slightly smaller than the liposomes formed in water. There also appears to be a point on Figure 43 that does not fit the general trend observed in the graph. At [CsCl] = 10 mM, the average liposome size is much larger than expected (159.8 nm). Additionally, as will be discussed later in the following section, the polydispersity index is higher than expected, indicating that this system may have been contaminated and this measurement could be an anomaly.

As described above, at low concentrations of all monovalent cations studied in this project, the DOPC liposomes show a general increase in their size. As discussed in the previous section of this chapter and confirmed by the zeta potential measurements obtained, the cations adsorb to the head group regions of the phospholipid molecules in the liposomes. This is an important point to consider when rationalising the change in the size of the liposomes in the presence of the cations. The observed increase in the size of the liposomes could be attributed to two factors. The first factor is that as the cations bind to the phospholipids there is decreased electrostatic repulsion between the neighbouring lipid molecules in the liposome. As a consequence, the lipid molecules can pack more closely and the

bilayer of the liposome is more rigid. The increased rigidity of the bilayer causes an increase in the energetic cost of bending the membrane into the spherical liposome, which causes an increased tendency for lower curvature in the liposome bilayer and hence, a larger liposome size. The second factor which could cause an increase in the size of the liposomes is cross-linking of the phospholipid molecules. The cations can associate with the head groups of more than one phospholipid molecule in the liposome, and this can also lead to rigidification of the bilayer and hence for the same reasons as outlined above, larger liposomes. This effect will become more pronounced as the cation concentration increases. For these reasons, the increasing size of the liposomes in the presence and increasing concentration of monovalent cations can be understood. At very low cation concentrations (up to 2.5 mM), the size of the liposomes tends to fluctuate, and this is especially clear in the case of the Li^+ and Na^+ cations (Figures 40 and 41). These fluctuations in liposome size could be attributed to the reorientation of the head groups of the phospholipids. As discussed in the previous section, cation adsorption to phospholipids causes change in the conformation and direction of the head groups of the lipids. As the phospholipid heads change direction on adsorption of cations, their ability to pack together is altered and therefore the rigidity and curvature of the bilayer is also affected, hence the size of the liposomes change.

At low concentrations of 2 and 2.5 mM NaCl, LiCl or KCl and 5 mM CsCl, the size of the liposomes decreases. This decrease in the liposome size could also be attributed to the change in orientation of the lipid head groups. As the cation concentration increases, the lipid head group conformations are altered. The head groups of the phospholipid in the liposome become parallel to the liposome surface (depicted diagrammatically in Figure 31) which means they cannot pack as closely together and the bilayer becomes more fluid, causing the energetic cost of bending the bilayer to decrease and hence allowing the liposomes to constrict in size. As the cation concentration is increased higher than the aforementioned concentrations, and more cations associate with the head group of the phospholipid, the lipid head group conformations are altered further, resulting in the choline group pointing out and the phosphate group pointing towards the inside of the liposome (Figure 31). With the head groups in this conformation, the strong electrostatic attraction between the head groups will then cause the lipids to pack more closely and will therefore rigidify the bilayer, causing the liposomes to swell and increase their size. The extent to which the monovalent cations studied in this project affect the size of the liposomes at low ion concentrations seems to differ for each cation, therefore the changes in size are said to be a cause of *ion-specific* effects.

For liposomes in the presence of all the cations studied, the increase in the size of liposomes is followed by a decrease, in line with the expectation that at high ionic strength the liposomes would shrink in size. At high ionic strength the concentration of ions in the aqueous environment is higher,

therefore the ions are able to 'shield' the charged surface of the liposome more effectively and as a consequence there will be a decrease in Debye length and a contraction of the double layer thickness. As a result, this would increase the diffusion coefficient of the liposomes resulting in a smaller apparent diameter of the liposomes (see Stokes Einstein equation, Equation 16). The decrease in the size of the liposomes at high ionic strength of monovalent cations is therefore consistent with a non-specific *bulk* effect[138]. In addition to this effect, osmotic effects are also hypothesised to play a role in the decrease of liposomes at higher ionic concentrations. Sabin *et al.*[112] hypothesised that as the concentration of the salt is increased, the concentration gradient at both sides of the membrane generates an osmotic force. At high salt concentrations, when the gradient of concentration of the cations through the bilayer is too large, an osmotic force is generated and as a consequence, the liposomes eject water from their centre to compensate for the excess cations outside the liposome. This ejection of water causes a decrease in the diameter and the size of the liposome until the maximum compaction of the bilayer is obtained. It is important to note, however, that osmotic factors are likely to have a relatively small effect, as these factors dominate after the liposomes have been formed. Factors which influence the formation of the liposomes themselves are likely to be more profound in governing the size of the vesicles. The results obtained in this work coincide well with the literature as other authors have also observed a decrease in the size of the liposomes at high ion concentrations[121, 122].

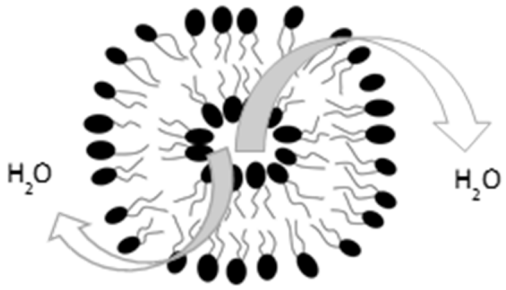

Figure 44: Schematic illustration of the osmotic effect induced by cations on DOPC liposomes.

The decrease in the size of the liposomes occurs at [LiCl] = 20 mM, [NaCl] = 8 mM, [KCl] = 10 mM and [CsCl] = 30 mM, in line with charge density, therefore the ions can be ordered $Na^+ > K^+ > Cs^+$ with the Li^+ ion appearing to behave anomalously. From Figure 40**,** which shows the change in the size of the liposomes as a function of Li^+ concentration there is a very large increase in the liposome size as the concentration is increased up to [LiCl]= 15 mM. As previously mentioned, it appears that the Li^+ cation has a slightly greater effect on the DOPC liposomes than the other monovalent cations. This idea is illustrated by the marginally higher value of the maximum zeta potential of the liposomes in the presence of the Li^+ ion as well as the large increase in the size of the liposomes. One explanation of this result could be that the lithium ion has a higher affinity for the DOPC head group than the other monovalent ions. This hypothesis has also been supported in the literature where similar results have been observed. Very recently in 2016, Kotyńska *et al.*[170] studied the association of alkali metal cations with the PC liposomal membrane surface. Li^+ was found to have the highest affinity to the PC head group and it was attributed to the fact the cation is the most charge dense out of the alkali metal ions and therefore forms the strongest electrostatic interactions with the membrane and ion pairs with the lipid head groups. Kruczek *et al.*[126] used molecular dynamics simulations to show that Li^+ is found to associate overwhelmingly with the highly electronegative oxygen atoms in the PO_4 group of the lipid head, and is able to penetrate deeper than the other monovalent ions owing to its much smaller size. In similar work, Klasczyk *et al.*[118] studied the interactions of alkali metal chlorides with palmitoyloleoylphosphatidylcholine (POPC) vesicles. Electrophoretic mobility and zeta potential measurements, also carried out by DLS, supported the notion that Li^+ had the greatest affinity for lipid head groups, showing the largest increase in the zeta potential of the liposomes, a result which closely agrees with that observed in this work. Isothermal titration calorimetry (ITC) measurements also showed that Li^+ was the only ion to bind exothermically to the POPC vesicle, causing the largest decrease in area per lipid of all the cations studied. These results strongly support the results obtained in this work, as the largest decrease in the area per lipid would cause the closest packing of lipid molecules, and hence, the largest increase in the size of the liposomes, which is what is observed here.

The effect of divalent cations on the size of DOPC liposomes was also examined in this work. The impact of $CaCl_2$ and $MgCl_2$, at varying concentrations up to 40 mM, on the size of the DOPC liposomes at 25 ˚C was studied. Figure 45 and 46 show the change in the size of the liposomes in the presence of $CaCl_2$ and $MgCl_2$ respectively.

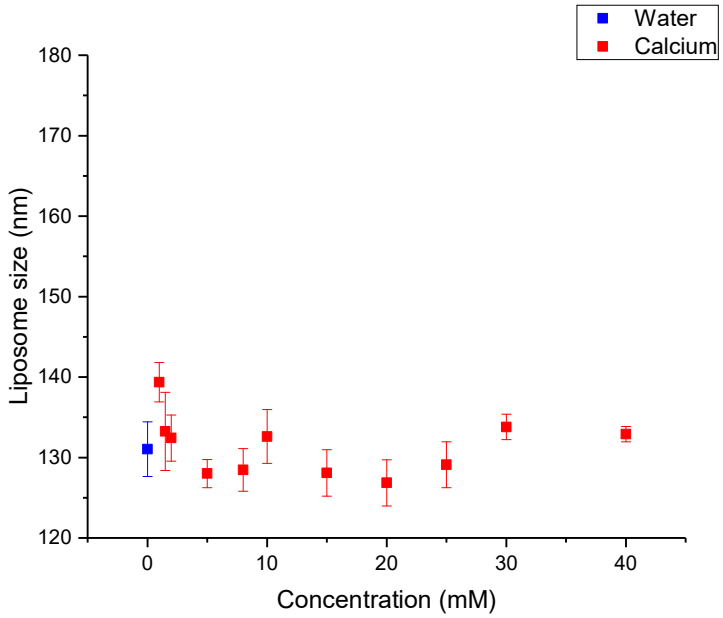

Figure 45: The change in DOPC liposome size as a function of calcium cation concentration, at 25 ˚C, as measured by DLS.

Figure 45 shows the change in DOPC liposome size as a function on $CaCl_2$ concentration. At [$CaCl_2$] = 1 mM there is an 8.4 nm, 6.4%, increase in the size of the liposomes. As the $CaCl_2$ concentration is then increased further, the liposomes show a gradual decrease in size down to 128.0 nm at [$CaCl_2$] = 5 mM and 128.5 nm [$CaCl_2$] = 8 mM. At 10 mM, the liposomes show a small increase up to 132.6 nm. Then, at $CaCl_2$ concentrations up to 25 mM, the liposomes show a plateau in their size, remaining fairly constant at d ≈128 nm. At higher $CaCl_2$ concentrations, ([$CaCl_2$] ≥ 30 mM), the liposomes increase in size by a small amount up to 133.8 nm and then decrease slightly to 132.9 nm at the highest concentration of [$CaCl_2$] = 40 mM.

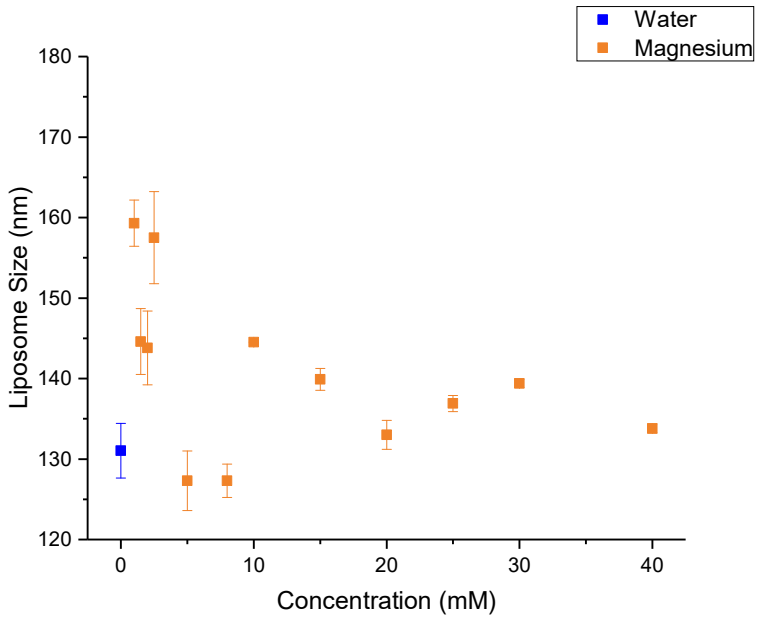

Figure 46: The change in DOPC liposome size as a function of magnesium cation concentration, at 25 ˚C, as measured by DLS.

The change in the size of the liposomes as a function of $MgCl_2$ concentration is shown in Figure 46. As can be seen on comparison of Figure 45 and 46, there are vast differences in the effect of the two divalent cations on the size of the liposomes. Figure 46 shows that on initial addition of 1 mM $MgCl_2$ there is a 28.3 nm increase in the size of the liposomes compared with the liposomes in salt free systems. This 21.6% increase in the size of the liposomes is then followed by a gradual decrease in size as the concentration is increased up to [$MgCl_2$] = 8 mM. In the same way as observed with the Ca^{2+} ions, the size of the liposomes at [$MgCl_2$] = 5 mM and [$MgCl_2$] = 8 mM shrink to $d \approx 127$ nm, which is smaller than the liposomes in pure water. At [$MgCl_2$] = 10 mM, the liposomes increase in size up to 144.5 nm, which is a 13.5% increase compared with the size of the liposomes at [$MgCl_2$] = 8 mM. As the concentration is then increased further up to higher ionic concentrations ([$MgCl_2$] = 20 mM), the liposomes show a gentle decrease in size, followed by a very small increase in-between [$MgCl_2$] = 20 mM and [$MgCl_2$] = 30 mM and then a small decrease of 5.6 nm at the highest $MgCl_2$ concentration of 40 mM. It is clear to see from Figure 46 that $MgCl_2$ has a far more profound effect on the size of the liposomes at low concentrations (≤ 10 mM) than $CaCl_2$. There are very large changes in the liposome sizes at low concentrations. However, at moderate to high concentrations, there are far fewer drastic changes. This is illustrated by the fact that from [$MgCl_2$]= 10 mM to [$MgCl_2$]= 40 mM there is an overall decrease in the size of the liposomes, but through this concentration range there is only a 7.4% decrease which is small compared to the changes which occur at lower salt concentrations.

It is very interesting to compare the effect of Ca^{2+} and Mg^{2+} on the size of the liposomes, as although these ions have the same valency and show very similar trends for the zeta potential, their effect on the size of the liposomes shows profound differences. The general trend for the changes in the size of the liposomes under the influence of the two ions is similar, however in the case of the Mg^{2+} ion, the general trend seems to be much more exaggerated.

For both cations, in the presence of 1 mM salt, the liposomes show an increase in size. As discussed previously, the cations associate with the head group of the phospholipid and therefore reduce repulsion between neighbouring lipids, allowing closer packing of the lipids and therefore increase the bending energy of the lipid bilayer, resulting in larger liposomes. At 1 mM, the Mg^{2+} ions cause a much larger increase in the size of the liposomes, and this is in line with the slightly more positive value of the zeta potential observed for Mg^{2+} than Ca^{2+}, which was measured as -0.32 mV and -1.92 mV respectively. At this concentration therefore, it can be concluded that the Mg^{2+} ion has a very slightly higher affinity for the DOPC head group than the Ca^{2+} ion, and therefore it is able to compensate for the slightly negative zeta potential of liposomes in water more effectively, and therefore increase the size of the liposomes by a greater amount. This slightly higher affinity could be attributed to the slightly smaller bare ion radius of Mg^{2+} than Ca^{2+}. Mg^{2+} has an ion radius of 0.065 nm[153], whilst Ca^{2+} has an ion radius of 0.099 nm[153]. The smaller bare radius of Mg^{2+} means that once the cation has shed its hydration sheath and associated with the lipid head group, other cations can more easily access the head group and associate with the lipid. The liposomes in the presence of 1 mM divalent salt also cause larger increases in the size of the liposomes than in 1 mM monovalent salts. This is as expected, because the higher valency of the divalent salts would be more strongly attracted to the head group of the lipid and reduce the repulsion between lipid molecules more effectively resulting in liposomes with larger diameters.

Following the initial increase in the size of the liposomes, the liposomes then show a gradual decrease as the concentration of $CaCl_2$ and $MgCl_2$ is increased. In the same way as with the monovalent cations, this decrease can potentially be attributed to a combination of changes in direction of the lipid head group and also potential osmotic effects. As can be seen from Figure 46, the decrease in the size of the liposomes in increasing concentrations of $MgCl_2$ is rather large (From [$MgCl_2$] = 2.5 mM to [$MgCl_2$] = 5 mM the size of the liposomes decrease by 30.2 nm) and therefore it is very unlikely this is due to the changes in lipid head group direction. More likely, is that the decrease is due to osmotic effects. The divalent cations will cause a concentration gradient at a lower salt concentration than the monovalent ions and therefore, it is likely that the osmotic effects would occur at lower concentrations of $CaCl_2$ and $MgCl_2$ than LiCl, NaCl, KCl and CsCl.

At moderate to high concentrations of both divalent ions, the size of the liposomes do not alter by large amounts, as can be seen in Figures 45 and 46. The 'plateau' in the size of the liposomes is most likely a result of the saturation of the head group of the phospholipids with cations. If the head group of the lipid if saturated with cations, then additional cations in the system will not have access to the head groups and therefore not have a profound effect on the size of the liposomes. This hypothesis agrees strongly with the zeta potential results obtained, which clearly demonstrate that in the case of both Ca^{2+} and Mg^{2+}, saturation of the head group occurs within this concentration range. An interesting point to note here is the similarity in the trend observed for the size of the liposomes in increasing concentrations of Na^{+}, Ca^{2+} and Mg^{2+}. As can be seen from Figures 41, 45 and 46, the shape of the size graph for Na^{+} resembles the shape of the size graphs for Ca^{2+} and Mg^{2+} much more closely that the graphs of the other monovalent ions. Additionally, from Figures 27, 32 and 33, it is clear to see that the shape of the graph of the change in the zeta potential of the liposomes in the presence of NaCl resembles the graphs showing the change in the zeta potential of the liposomes in the presence of divalent cations more closely. It appears from the zeta potential graph (Figure 27) that there is a plateau in the data, suggesting that the Na^{+} ion may cause saturation of the DOPC head group of the lipid, much like Ca^{2+} and Mg^{2+}. In a similar thread, there also appears to be a plateau in the graph showing the change in the size of liposomes as a function of NaCl concentration, supporting the idea that saturation has occurred. Sabin *et al.*[112] studied the effect of Na^{+} on the diameter of EYPC liposomes and found very similar results to those obtained in this work. The results showed a plateau at moderate concentrations and then a slight decrease in the size of liposomes as the concentration was increased further. It could be hypothesised therefore, that the Na^{+} ion tends to behave more like a divalent cation than a monovalent cation.

In previous work on divalent cations and their interactions with PC liposomes, there is much more focus on the Ca^{2+} ion due to its biological relevance. Melcrova *et al.*[163] studied exclusively calcium interactions with phospholipid bilayers. Using a near identical experimental method to that used in this work, 100 nm, unilamellar DOPC liposomes were prepared and the effect of $CaCl_2$ on their size distribution was examined. The results obtained by Malcrova *et al.* agree closely with ours, demonstrating that at concentrations even up to 200 mM, $CaCl_2$ does not induce very large changes in the size of the liposomes.

Martín-Molina *et al.*[171] helped to shed light on the differences between the interactions of Ca^{2+} and Mg^{2+} by carrying out work on the effects of these ions on phosphatidylserine membranes. Electrokinetic measurements confirmed that the two ions had similar affinity for the PS^{-} liposomes. This strongly supports the results obtained in this work, as the similar zeta potential curves demonstrate that the ions have very similar affinities to the DOPC liposomes. Martín-Molina *et al.*

found additionally that, interestingly, Ca^{2+} and Mg^{2+} induce very different aggregation behaviour for PS^- liposomes despite the fact they have very similar affinity for the lipids. From these results it was suggested that the two cations induce substantial structural differences in the lipid bilayers and therefore the cations have strong *ion-specific* effects on the structure of the PS^- membrane. It was also found in that work that the two cations have different binding sites and configurations in the membrane, as well as causing varying membrane hydration. Simulations carried out showed that the hydration of the lipids in the PS membrane was 7.5 and 9 water molecules per lipid[171], for Ca^{2+} and Mg^{2+} respectively. These conclusions can help to understand the differences in the effects of Ca^{2+} and Mg^{2+} on the size of the DOPC liposomes, and it can be concluded with confidence that the divalent cations demonstrate *ion-specific* effects. Although the reasons behind the differences in divalent cation interactions with DOPC liposomes are still not entirely clear, it is likely that the subtle differences in the way Ca^{2+} and Mg^{2+} ions interact with the bilayer at the molecular level play an important role.

Finally, the effect of $LaCl_3$ on the size of DOPC liposomes was examined. DLS was used to measure the size of the liposomes at concentrations of $LaCl_3$ up to 40 mM. Figure 47 shows the change in the size of the liposomes in the presence of $LaCl_3$.

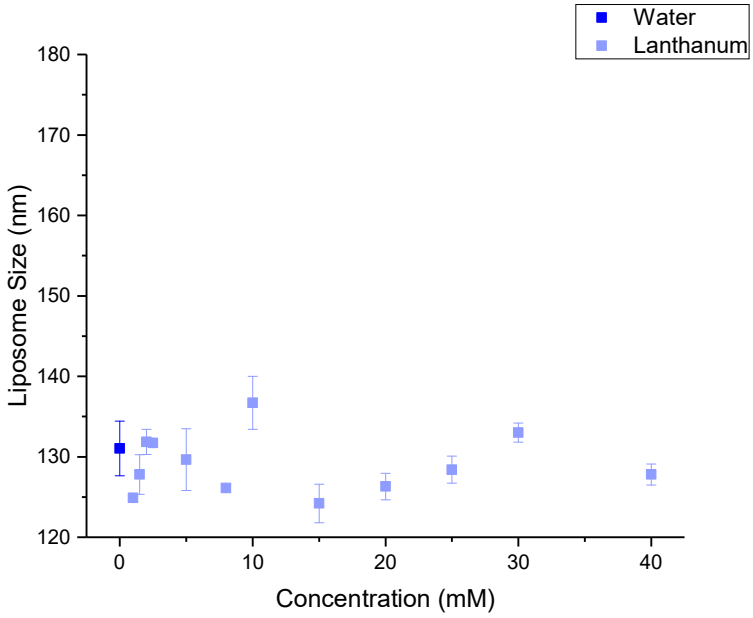

Figure 47: The change in DOPC liposome size as a function of lanthanum cation concentration, at 25 ˚C, as measured by DLS.

At low concentrations of $LaCl_3$ (1-5 mM) the size of the DOPC liposomes is not greatly altered by the presence of the La^{3+}. From [$LaCl_3$] = 5mM to [$LaCl_3$] =15 mM there is an overall decrease in the size of the liposomes of 5.45 nm. However, the size of the liposomes at [$LaCl_3$] =10 mM is larger than expected, with an average of 136.7 nm. As the concentration of $LaCl_3$ is increased from 15 mM to 30 mM, there is a very gradual increase in the size of the liposomes and then at [$LaCl_3$] = 40 mM, the size of the liposomes show a slight shrink.

Overall, from the data shown in Figure 47, it is clear that the La^{3+} ions have a relatively small effect on the size of the DOPC liposomes, compared with the effects of the monovalent cations. The effect of La^{3+} ion on the size of the liposomes is most comparable to the effects shown in Figure 45, of the Ca^{2+} ions. For completeness, Appendix G shows the shows the liposome size as a function of ionic strength for all the ions studied in this work.

It is likely that the small fluctuations in liposome size at low concentrations, is a result of a change in the lipid head group direction. As demonstrated by the zeta potential data, the La^{3+} ions have an exceptionally high affinity for the DOPC lipid head group and therefore it is probable that at low cation

concentrations they have a large effect on the head group position. As the concentration is increased from [$LaCl_3$] = 2.5 mM to [$LaCl_3$] = 15 mM, the overall decrease in liposome size can be attributed to osmotic effects. At concentrations higher than 15 mM, there are only very subtle changes in the size of the liposomes and this is likely to be due to lipid head group saturation with the cations. The zeta potential measurements discussed in Section 4.1 confirm that at concentrations <15 mM, the lipid head group is saturated with cations and therefore the size of the liposomes observed at these concentrations is fairly constant.

Interestingly, La^{3+} has been widely observed in the literature to induce the fusion or aggregation of liposomes[113]. From the results shown in Figure 47**,** it is clear that at the concentrations studied in this work, La^{3+} does not induce aggregation of vesicles, as there are no drastic changes observed in the Z-average size of the liposomes.

4.3 Effect of inorganic cations on the polydispersity index of the liposome systems

The polydispersity index of the liposome suspensions in the presence of the inorganic cations was measured using DLS. The polydispersity index is a very useful number, providing information about the uniformity of the size of the liposomes in a given suspension. The PdI of the liposomes in pure water was found to be 0.098.

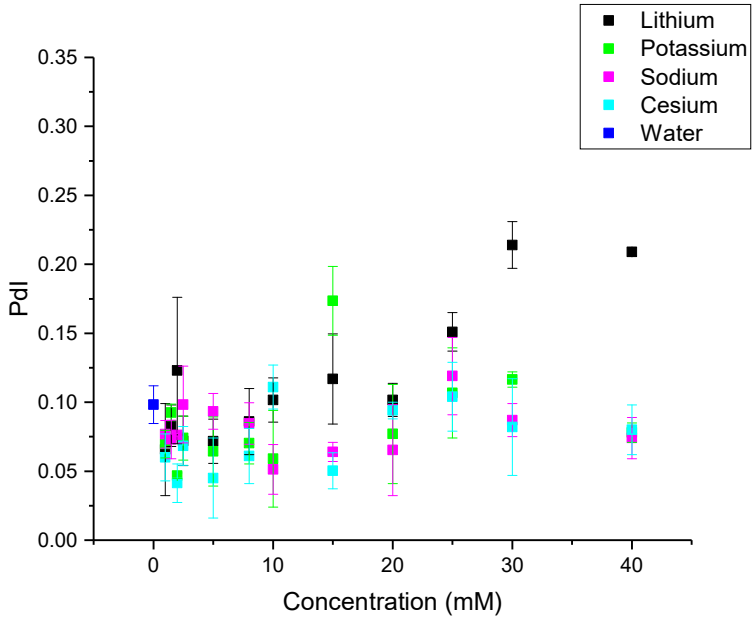

Figure 48: The change in the PdI of DOPC liposome suspensions in the presence of monovalent cations at 25˚C, as measured by DLS.

As previously mentioned, a PdI value of < 0.2 is indicative of a uniform, monodisperse system. Figure 48 shows the PdI values for the inorganic monovalent cations at varying concentrations. As can be seen from Figure 48**,** all of the liposomes have a PdI of ≤ ≈0.2. The average PdI values of the liposomes in the presence of LiCl, NaCl, KCl and CsCl are 0.0981, 0.0802, 0.0858 and 0.0724 respectively, indicating that the liposomes are monodisperse and uniform in size. It was also found that in general, the addition of the ions to the liposomes in pure water at most low to moderate concentrations (up to 20 mM) causes a decrease in the PdI, indicating that the ions cause a structure stabilising effect by reducing the repulsion between neighbouring lipids. At [LiCl] = 25 mM, there is a slight increase in the PdI of liposomes. At [LiCl]= 30 and 40 mM the PdI is the highest value observed for the liposomes in the presence of monovalent cations (0.21 for both concentrations), highlighting again, the somewhat anomalous behaviour of the Li^+ cation. The Na^+ cation, in particular, has exceptionally low values for

the PdI (nearly all < 0.1) at the concentrations observed. The K^+ and Cs^+ ions have more fluctuating PdI values, and as mentioned in the previous section, the PdI at [CsCl] = 10 mM is somewhat higher than expected. It is important to note here that the experimental procedure for the preparation of liposomes, although well defined, is not identical each time it is carried out. Slight variations in the sonication time, or the number of extrusions can have an effect on the PdI of the liposome systems and although every attempt was made to keep the preparation of each sample exactly the same, some variations could have occurred. It is for these reasons that slight fluctuations in the PdI are normal to observe in systems such as these.

Comparable work carried out previously supports the results obtained in this project. Sabín *et al.*[112] showed that the PdI of egg yolk phosphatidylcholine (EYPC) liposomes in the presence of Na^+ and K^+ ions remains ≤ 0.2 even up to cation concentrations of 100 mM. From these results, it can therefore be concluded with confidence that there is no aggregation of the vesicles in the presence of monovalent cations at the concentrations studied in this project.

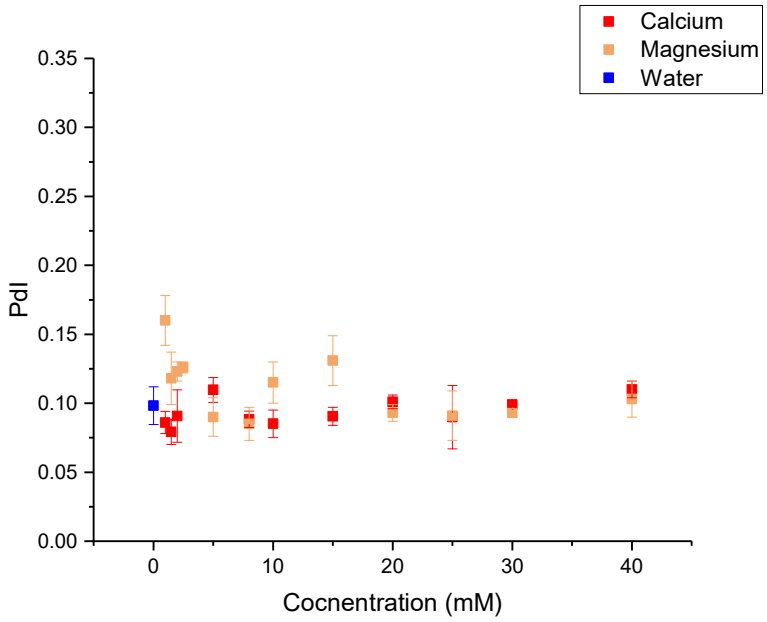

Figure 49: The change in the PdI of DOPC liposome suspensions in the presence of divalent cations at 25˚C, as measured by DLS.

Figure 49 shows the change in the polydispersity index for the liposomes in the presence of divalent cations, Ca^{2+} and Mg^{2+}. As with the monovalent cations, the PdI of the liposomes in all of the ion concentrations studied is < 0.2, showing that within this concentration range there is no aggregation of clustering of the vesicles. The PdI of the liposomes in the presence of Ca^{2+} ions is exceptionally low, with an average value of 0.094, indicating that the liposomes are of very uniform size. The PdI of the liposomes in the presence of Mg^{2+} ions is slightly higher at concentrations up to 5 mM, potentially owing to the very large liposomes formed at these low concentrations, and at higher concentrations, the PdI of the liposomes remains very low, indicating a uniform, monodisperse system. This result suggests that once saturation of the head group of the lipid has occurred, the liposomes remain the same size and have the same very narrow size distribution as the concentration of Ca^{2+}/Mg^{2+} is increased up to 40 mM. Owing to this, we can conclude that following saturation of the lipid by the cations, the liposome systems are stable. The PdI in the presence of divalent cations is generally lower than the PdI of liposomes in water, in the absence of added electrolyte (0.115) and in the presence of monovalent cations. It can therefore be concluded that the divalent cations have a stronger structure stabilizing effect than the monovalent cations.

Finally, Figure 50 shows the polydispersity index of the liposomes as a function of $LaCl_3$ concentration.

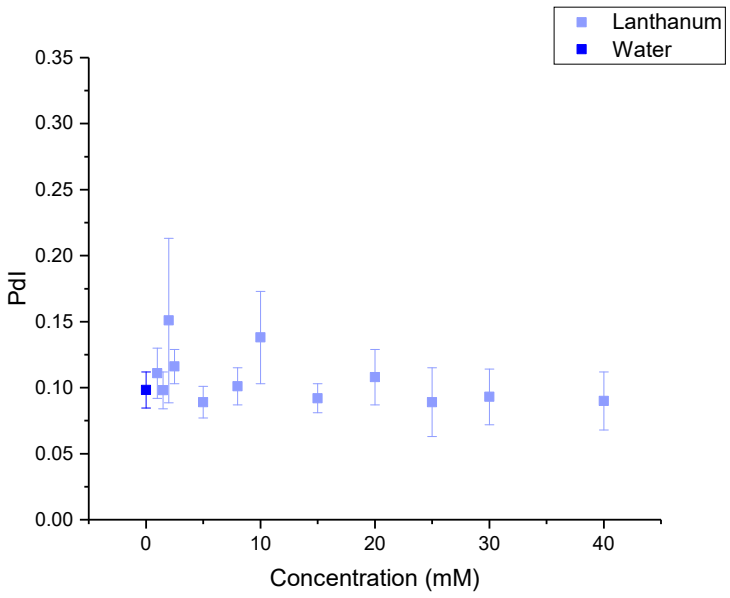

Figure 50: The change in the PdI of DOPC liposome suspensions in the presence of trivalent cations at 25˚C, as measured by DLS.

The PdI values of the liposomes in the presence of La^{3+} closely resemble the values obtained for the divalent cations. At low La^{3+} concentrations, the PdI is ≤ 0.15, demonstrating small fluctuations, then as the concentration is increased to > 5 mM, the PdI values are all exceptionally low (≈0.1). These results prove that the La^{3+} ions also have a strong structure stabilising effect. The stabilising effect can be ordered in terms of strongest to weakest: $La^{3+} > Ca^{2+} > Mg^{2+} > Na^{+} > K^{+} \approx Cs^{+} > Li^{+}$, or more generally trivalent cations > divalent cations > monovalent cations, in line with the Hofmeister series[51, 138, 172].

Interestingly, in previous literature, the Ca^{2+} and the La^{3+} ions have been widely found to induce the fusion or aggregation of vesicles. Sabín *et al.*[113] used polydispersity measurements and transmission electron microscopy (TEM) to successfully prove that La^{3+} induces the aggregation of EYPC vesicles. They observed a sharp increase in the size and polydispersity of the vesicles at 0.3 M La^{3+} and the resulting aggregates were > 500 nm. Toimil *et al.*[173] also calculated the critical aggregation concentration (c.a.c.) of DPPC liposomes in the presence of La^{3+} to be 0.12 M and at $[La^{3+}] > 0.12$ M, the PdI of the system increased drastically to ≈ 0.8. Lastly, in the case of Ca^{2+}, Melcrova *et al.*[163] observed DOPC liposome aggregation which was induced at $[CaCl_2] = 1$ M. It can, therefore, be concluded with confidence that at the cation concentrations studied in this work, there is no aggregation of liposomes and all the systems are monodisperse, containing liposomes of uniform size.

Chapter 5: The effect of organic hydrophobic ions on the DOPC liposomes

5.1 Effect of hydrophobic ions on the electrophoretic mobility and zeta potential of DOPC liposomes

In this chapter, the effect of two organic hydrophobic ions on the size (d) and zeta potential (ξ) of the DOPC liposomes was studied. The two ions chosen were tetraphenylphosphonium chloride (Figure 22) and sodium tetraphenylborate (Figure 23), reproduced below. Figure 51 shows the variation in the zeta potential of the DOPC liposomes as a function of tetraphenylphosphonium chloride (TPP^+) concentration.

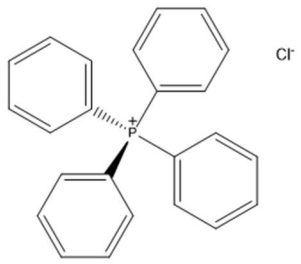

Figure 22: The structure of tetraphenylphosphonium chloride

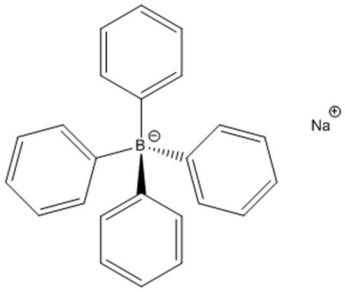

Figure 23: The structure of sodium tetraphenylborate

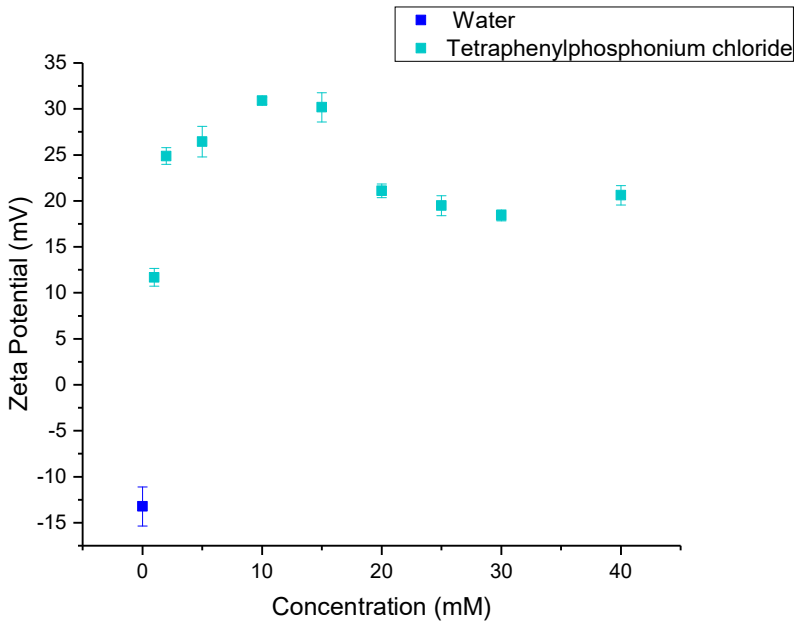

Figure 51: The change in the zeta potential of DOPC liposomes as a function of TPP^+ concentration at 25˚C, as measured by DLS.

It is clear from the results in Figure 51 that the TPP^+ ions have a very large effect on the zeta potential of the DOPC liposomes. In the presence of only 1 mM TPP^+, the zeta potential of the liposomes increases by 24.9 mV to 11.7 mV compared to the zeta potential of the liposomes in pure water (-13.2 mV). Already at this very low TPP^+ concentration, the sign of the zeta potential is reversed and the slight negative value of the zeta potential of the liposomes in water has already been more than compensated for. As the concentration of TPP^+ is increased to 2 mM, there is another large increase in the zeta potential of the liposomes of 13.2 mV, up to 24.9 mV, showing that the zeta potential has increased by 288% compared with the value obtained in water. As the TPP^+ concentration is then increased further up to 10 mM, the zeta potential of the liposomes continues to increase but at a much slower rate, reaching a maximum of 30.9 mV. As the [TPP^+] is increased up to 40 mM, the liposomes show a gradual decrease in the zeta potential, with the decrease becoming more gradual as the concentration is increased. The graph appears to plateau at TPP^+ concentration of 20 mM to 40 mM, with only maximum change in the zeta potential of 2.7 mV.

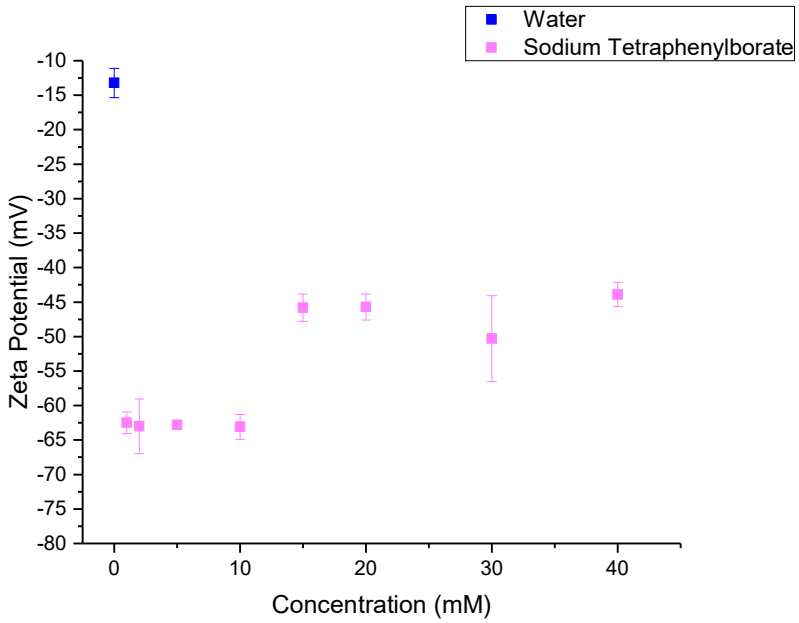

Figure 52: The change in the zeta potential of DOPC liposomes as a function of TPB- concentration at 25˚C, as measured by DLS.

Figure 52 shows the change in the zeta potential of the liposomes as a function of sodium tetraphenylborate (TPB^-) concentration, as measured by DLS.

As can be seen in Figure 52, TPB^- ions also have a profound effect on the zeta potential of the DOPC liposomes. On initial addition of 1 mM of the TPB^- anions the zeta potential of the DOPC liposomes becomes much more negative (-62.5 mV) and then as the concentration is increased up to 10 mM the zeta potential remains largely the same at $\xi \approx$ -63 mV. The zeta potential of the liposomes then becomes more positive at [TPB^-] = 15 mM, increasing up to $\xi =$ -45 mV. As the TPP^- concentration is then increased up to 40 mM, the zeta potential appears to plateau again at $\xi \approx$ -46 mV.

There is an increasing amount of interest and research into the effect of hydrophobic ions on lipid bilayers and liposomes as they have been found to be unique and effective probes of the electronic structure of biological membranes. Interestingly, antimicrobial properties of some quaternary phosphonium salts have also been reported[174] and arylphosphonium salts are of particular interest as they have been found to preferentially accumulate in cancerous tumour cells and are therefore being studied as tumour imaging agents[175]. Hydrophobic ions are known to be poorly soluble in water, in the case of the ions studied in this project, this is due to the large surrounding phenyl rings. As a result of this poor hydration, the ions are easily expelled from water and 'stick' to hydrophobic surfaces. There is a gain in entropy when the hydrophobic ions associate with the membrane and this is part of the driving force that causes the ion-membrane interaction. The vast changes in the zeta potential values of the liposomes in the presence of hydrophobic ions can be attributed to the ion association with both the hydrophilic head group of the lipid, and the hydrophobic tail. The large decrease in the zeta potential of the liposomes in the presence of TPB^- can be partially attributed to the association with the head group of the lipid. Leontidis *et al.*[127] found that TPB^- interacted via the electrostatic interaction with the ammonium groups in the head group of phospholipids. In this way, the negatively charged ions can compensate for the positive charge of the choline group and therefore cause the zeta potential to become more negative. ^{1}H Nuclear Overhauser Effect Spectroscopy carried out by Ellena *et al.*[176] confirmed the complexation of TPB^- with the choline group of the lipid and also showed that TPP^+ associates with the hydrophilic lipid head. TPP^+ was found to be approximately 4 Å from the carbonyl group of the *sn-1* (palmitoyl) chain as can be seen in Figure 53[176].

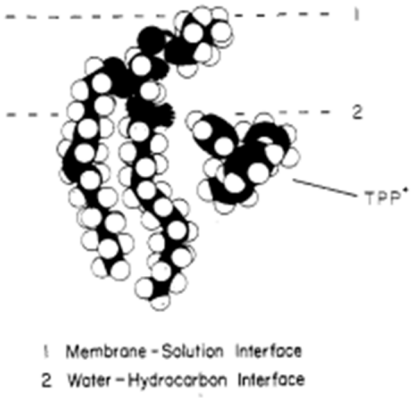

Figure 53: Schematic to show the average placement of the hydrophobic ion TPP^+ with respect to phospholipid, POPC in the bilayer. Reprinted with permission from reference 176. Copyright © 1987, American Chemical Society.

It can be concluded, therefore, that TPP^+ associates with the phosphate group in the head of the lipid and is able to compensate for the negatively charged group, causing the zeta potential of the liposomes to become more positive. Given the hydrophobic nature of the TPB^- and TPP^+ ions, it is widely acknowledged that these ions also associate strongly with the hydrophobic tails of the lipids as well as the heads[176, 177] and the ions are largely found to be located at the aqueous membrane interfacial regions of lipid bilayers[176-178]. Leontidis *et al.*[127] proposed that the hydrophobic ions would 'push' the surface molecules in the bilayer aside as the organic ions compete for interfacial sites in the membrane. Hydrophobic ions are thought to adsorb at the surface of the lipid-water domains and at the same time, the ions force the lipids apart which can, at high concentrations, cause the bilayers to become charged[127].

As an increasing amount of work has been carried out on the interactions of hydrophobic ions with lipid membranes, the attention of researchers has been drawn to the TPP^+ and TPB^- ions, as, despite their structural similarities, they have been found to interact with lipid bilayers very differently[176, 177]. It has been consistently observed in the literature that hydrophobic anions bind more strongly to and move more quickly across bilayers than structurally similar cations[176, 177, 179]. As can be seen from Figures 22 and 23, the structures of TPP^+ and TPB^- ions are very similar. Both ions are singly charged and have an ionic radius of 0.42 Å[40] as well as the same hydration enthalpies, as suggested by the well-known TATB hypothesis[180]. Given the extensive similarities as outlined, the differing behaviour of the ions was a puzzling concept.

In 1969, Liberman *et al.*[181] observed a higher permeability of the membrane for TPB^- compared with TPP^+ and hypothesised that the interior of the membrane must possess a slight positive charge. Haydon and coworkers[182] later recognised that the positive charge within the membrane was most

likely to arise from orientated molecular dipoles in the membrane surface and subsequently devised the term 'di-pole potential', presumably responsible for the observed difference between the cation and anion interactions.

In more recent work carried out by Schamberger and coworkers[183] however, it was suggested that in fact the TPB^- anion was more strongly hydrated that the TPP^+ cation analogue. Theoretical calculations carried out in that work showed that this was due to the charge distribution in the ions. It was found that, for TPP^+, the charge is more positively localised on the central P atom, whereas in the case of TPB^- the negative charge is delocalized over the carbon atoms of the phenyl rings. Therefore, the charge of TPP^+ would be more sterically hindered by the surrounding phenyl rings and as a consequence the interaction with the surrounding solvent molecules would be much weaker. The delocalized charge of TPB^- onto the phenyl rings would allow closer contact between the surrounding water molecules and the charge, as well as polarization of the surrounding solvent molecules and therefore the anion would be more strongly hydrated. This could be used to rationalise the stronger binding of TPB^- to the membrane, as if these hydrophobic ions are more strongly hydrated, then there is a larger entropic gain when the water molecules in the ion hydration sheath are released back into the bulk on binding.

Flewelling *et al.*[177] found that the differences between anion and cation binding could be attributed to their enthalpies. The enthalpy for TPP^+ binding is endothermic (repulsive), *i.e.* ΔH =+3.5 kcal/mol whilst the enthalpy for TPB^- binding is ΔH= -1.8 kcal/mol, which is exothermic (attractive)[177]. This observation established a fundamental difference between the anion and cation electrostatic interactions with membranes, most likely with the membrane dipole potential or with the lipid head groups. It is possible that the stronger anionic associations to the membrane are due to a combination of these factors.

Despite this previous work, there is a lack of research on the effect of these organic hydrophobic ions on DOPC liposomes. The effect of these ions of the zeta potential of liposomes has been reported, however, until now, the effect on the size and PdI of the liposomes has not been described. The novelty of the work presented in this chapter lies in the range of effects studied and the use of DOPC liposomes which possess higher membrane fluidity compared with those comprised of DPPC and DMPC.

In the present work, in the case of the TPP^+ cation, the change in the zeta potential of the liposomes at low concentrations is more gradual than that for TPB^-, evident from Figures 51 and 52**.** From these results, it can be inferred that at low concentrations the TPB^- ions show stronger interactions with the DOPC liposomes than the TPP^+ ions, in line with the literature discussed previously. For both

hydrophobic ions studied, there appears to be a plateau in the zeta potential of the liposomes at ~20 mM. As was discussed in the case of the inorganic cations, this is likely to be the consequence of saturation of the liposomes with ions. It is interesting to note that the saturation of liposomes in the presence of hydrophobic monovalent ions occurs at much lower concentrations than the inorganic monovalent cations and this is probably due to sterics, as the organic ions are much larger and bulkier and therefore will occupy a much larger proportion of the membrane on binding than the inorganic ions.

The results of the effect of hydrophobic ions on the zeta potential of DOPC liposomes correlate closely with results obtained in previous literature. Smejitek and co-workers[184] studied the electrophoretic mobility of DPPC vesicles in the presence of tetraphenylborate at 25 ˚C. The electrophoretic mobility was converted to the zeta potential using the Helmholtz equation. At low concentrations, Smejitek *et al.* found very similar values for the zeta potential of the liposomes as those observed in this project. The zeta potential of the liposomes decreased to $\xi \approx 60$ mV[184] and then showed a small plateau, which is the same trend as observed with the DOPC liposomes.

The vast changes in the zeta potential of the DOPC liposomes in the presence of these hydrophobic, organic ions shows that the ions have a large impact on the liposomes, penetrating into the bilayer and interacting with both the heads and tails of the phospholipid molecules. The tetraphenylborate anions show a slightly higher affinity for the PC bilayer than the tetraphenylphosphonium cations, and this is supported by previous findings in the literature and can be largely attributed to charge distribution and electrostatic interactions with the dipole potential.

5.2 Effect of hydrophobic ions on the size and polydispersity index potential of DOPC liposomes

The effect of tetraphenylphosphonium chloride (TPP^+) and sodium tetraphenylborate (TPB^-) on the size and PdI of DOPC liposomes was studied. Figures 54 and 55 shows the changes in the size and PdI of liposomes as a function of TPP^+ concentration respectively.

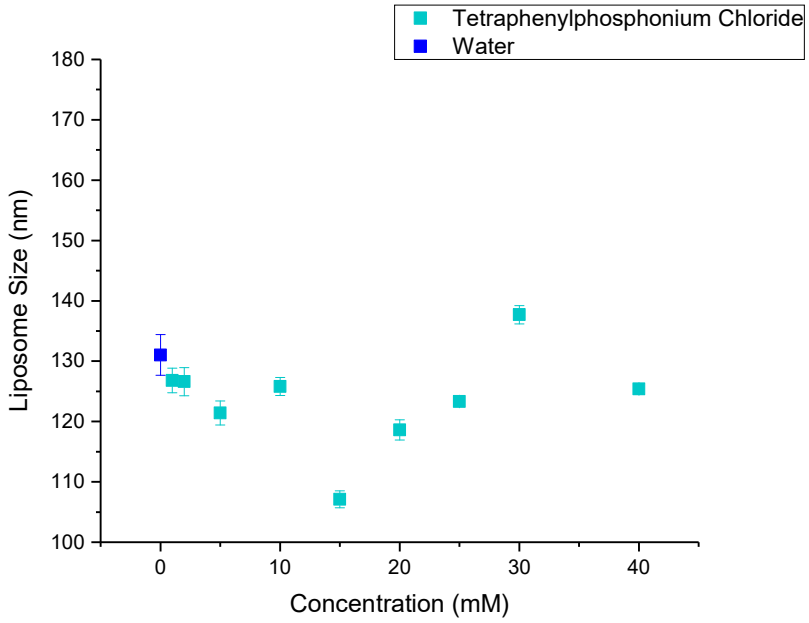

Figure 54: The change in the size of DOPC liposomes in the presence of hydrophobic ions, TPP^+ at 25˚C, as measured by DLS.

As can be seen from Figure 54, on the initial addition of TPP^+ cations, there is a small shrink in the size of the liposomes. As the concentration of TPP^+ is increased up to 15 mM, there is an overall decrease in the size of the liposomes, and at [TPP^+] = 15 mM the liposomes show a minimum size of d = 107.1 nm, which is 23.9 nm decrease compared to the liposomes in the absence of salt. Following this minima, the liposomes begin to increase in size gradually as the TPP^+ concentration is increased to 30 mM. At [TPP^+] = 30 mM, the liposomes are d = 137.7 nm and at [TPP^+] = 40 mM, the liposomes shrink slightly by 12.3 nm to d = 125.4nm.

Figure 55 shows the PdI of the liposomes in the presence of TPP^+ at varying concentrations. The PdI of the liposome systems remains between ~0.1 and ~0.15 in the presence of all concentrations of TPP^+ except at [TPP^+]= 15 mM, where the PdI is slightly higher at 0.19. Despite the fluctuations, the PdI does not exceed 0.2 for any of the TPP^+ concentrations used in this work therefore, as was the case for a number of the inorganic ions, it can be concluded that the liposomes are a fairly uniform in size and exist in a largely monodisperse systems.

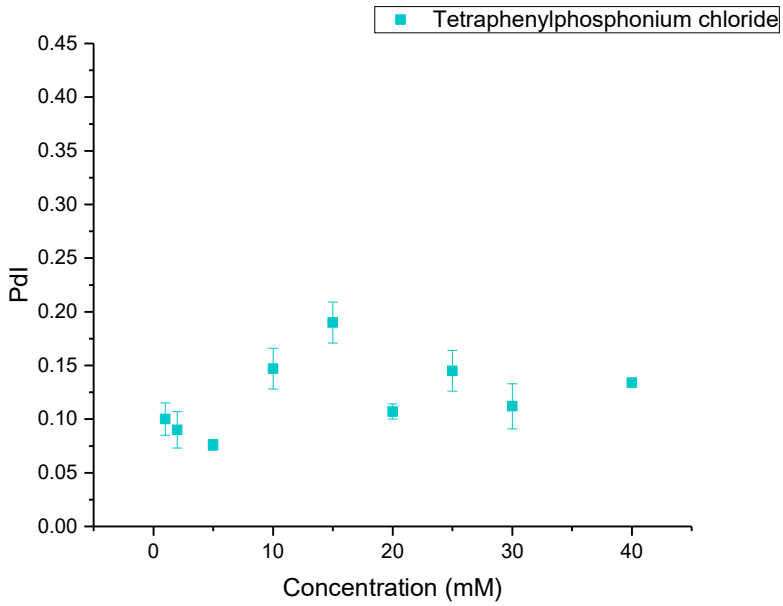

Figure 55: The PdI of DOPC liposome suspensions in the presence of hydrophobic ions, TPP+ at 25˚C, as measured by DLS

Figures 56 and 57 show the size and the PdI of DOPC liposomes as a function of TPB^- concentration respectively. Interestingly, the size and PdI results obtained differ substantially compared with those obtained for the TPP^+ cations.

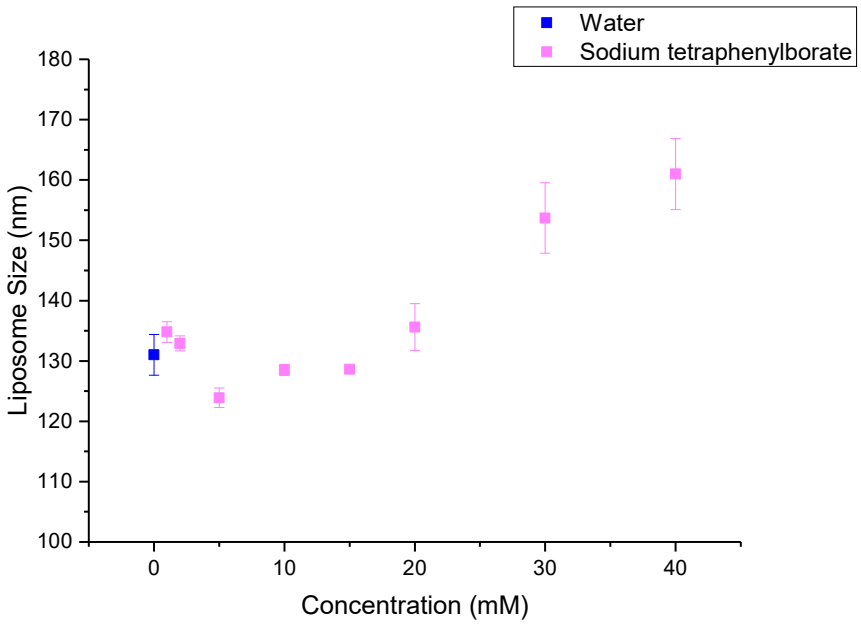

Figure 56: The change in the size of DOPC liposomes in the presence of hydrophobic ions, TPB- at 25˚C, as measured by DLS.

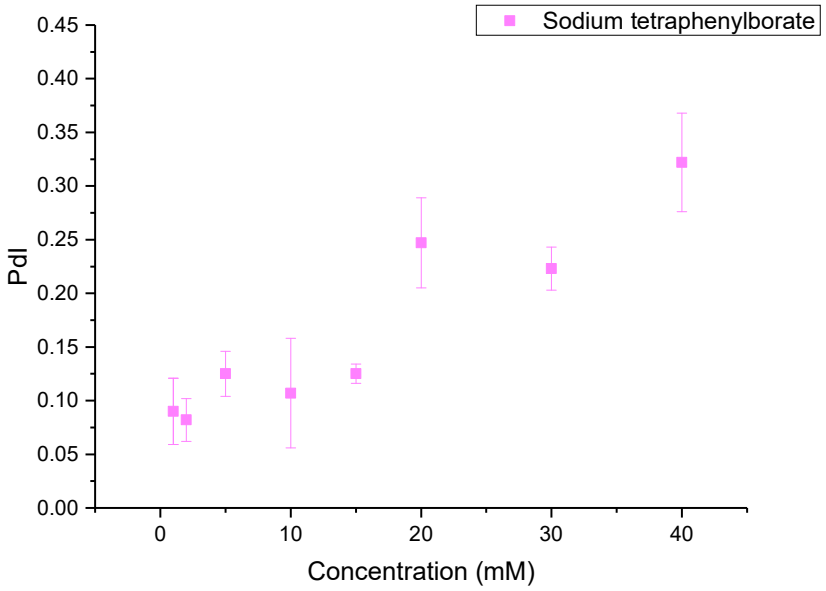

Figure 57: The PdI of DOPC liposome suspensions in the presence of hydrophobic ions, TPB- at 25˚C, as measured by DLS

At low anion concentrations (1-2 mM) there is not a substantial change in the size of the DOPC liposomes, at [TPB^-]= 1 mM, *d* = 134.8 nm and at [TPB^-]= 2 mM, *d* = 132.9 nm. As the concentration is increased to 5 mM, the liposomes shrink in size to *d*= 123.9 nm and then remain at *d* ~ 128 nm at [TPB^-] = 10 and 15 mM. As the TPB^- concentration is then increased up to 40 mM, there is a gradual increase in the size of the liposomes up to *d* = 161.0 nm. Interestingly, the change in the PdI as a function of TPB^- concentration shows a very similar trend. Up to [TPB^-] = 15 mM, the PdI of the DOPC liposome systems remains fairly constant at ~ 0.1 with only small fluctuations being observed. However, as the concentration is increased further from 20 mM to 40 mM, there is a sharp increase in the values of the PdI. At [TPB^-] = 20 mM, the PdI shows a sharp increase to 0.25 and at [TPB^-] = 40 mM the PdI has increased even further up to 0.32. There does not appear to be a plateau in the size or the PdI of liposomes in the presence of TPB^- and additionally, the size and PdI trends differ considerably from those observed with the TPP^+ cations highlighting the differences, already outlined from the zeta potential data, in the interactions between the two organic ions with the liposomes.

In the case of tetraphenylphosphonium ion, at concentrations up to 15 mM, there is a decrease in the size of the liposomes. This decrease in size can be explained by the association of the TPP^+ cation with the DOPC lipids. As already discussed above, as the ions adsorb to the surface of the lipid-water domains, they push apart the lipids and interact with both the tails and the heads of the phospholipids. As the concentration increases up to 15 mM the bilayers become more charged, as supported by the zeta potential data, and the apparent area per lipid increases[127]. As the area per lipids increases, the bilayers of the liposomes become less rigid and more flexible. The bending energy decreases and

therefore the liposomes shrink in size. As the concentration of TPP^+ is increased further (>15mM), the size of the liposomes gradually increases (Figure 54) and the zeta potential also decreases (Figure 51). These two effects could be attributed to the adsorption of some of the chloride counter ions to the head groups of the phospholipids. The smaller, more charge dense Cl^- ions (0.181 nm[153]) have an electrostatic attraction to the choline groups of the lipid, and owing to their small radii, they can more easily access the head groups of the lipids than the bulky organic ions. The chloride ions would reduce repulsion between the neighbouring lipids by screening the charges and therefore allowing the lipids to pack together more closely, resulting in the liposomes increasing in size. Additionally, and as was the case with the inorganic ions studied, the orientation of the head groups of the lipids may also contribute to the changes in liposome size.

As already outlined, the effect of the TPB^- anions on the size of the DOPC liposomes shows fairly different results compared with the TPP^+ cations. At low concentrations, however, a similar trend is observed. The slight decrease in the size of the liposomes at low TPB^- concentrations can be attributed to the increase in the area per lipid on the adsorption of the anions to the lipids. As explained above, this increase in area would result in a lower bending energy and also a decrease in the size of the liposomes. At high enough ion concentrations, the bilayers become highly charged and as the area per lipid continues to increase, the packing parameter decreases, resulting in the lamellae transforming into other structures, such as micelles[127] (spherical or cylindrical). These vast changes in the phospholipid structure could be responsible for the increase in the PdI at moderate and high TPB^- concentrations. Additionally, TPB^- has also been observed to induce fusion in small sonicated egg phosphatidylcholine vesicles[176] and in aqueous solutions TPB^- has been found to form a precipitate with the choline[176]. In our case, it is very likely that the TPB^- induces the fusion of DOPC liposomes as both the size and the PdI of the liposomes increase at ~ 15 mM, as shown in Figures 56 and 57. In order to investigate the potential fusion of the liposomes further, the intensity (percent) vs. size (d) graphs obtained by DLS were examined (Appendix I). The Figures show that in the presence of 1-10 mM TPB^-, there is only one peak with 100% intensity at ~ 140 nm confirming that the system is monodisperse. At $[TPB^-]$ = 20 mM, there is a small peak with intensity of 1.2% at d ~ 5000 nm, and at $[TPB^-]$ = 30 mM, the small peak is still present and larger than at the lower 20 mM. As the concentration of TPB^- is increased to 40 mM, the peak becomes even more pronounced, and is shown as 6.1% intensity at d ~ 4688 nm. This evidence strongly suggests that there are larger fused liposomes forming as the TPB^- concentration is increased higher than 15 mM and the aggregates are likely to be d ~ 5 µm. The combination of the change of lipid structure and the fusion of vesicles is likely to be responsible for the vast increase in size and polydispersities of the liposomes at high TPB^- concentrations.

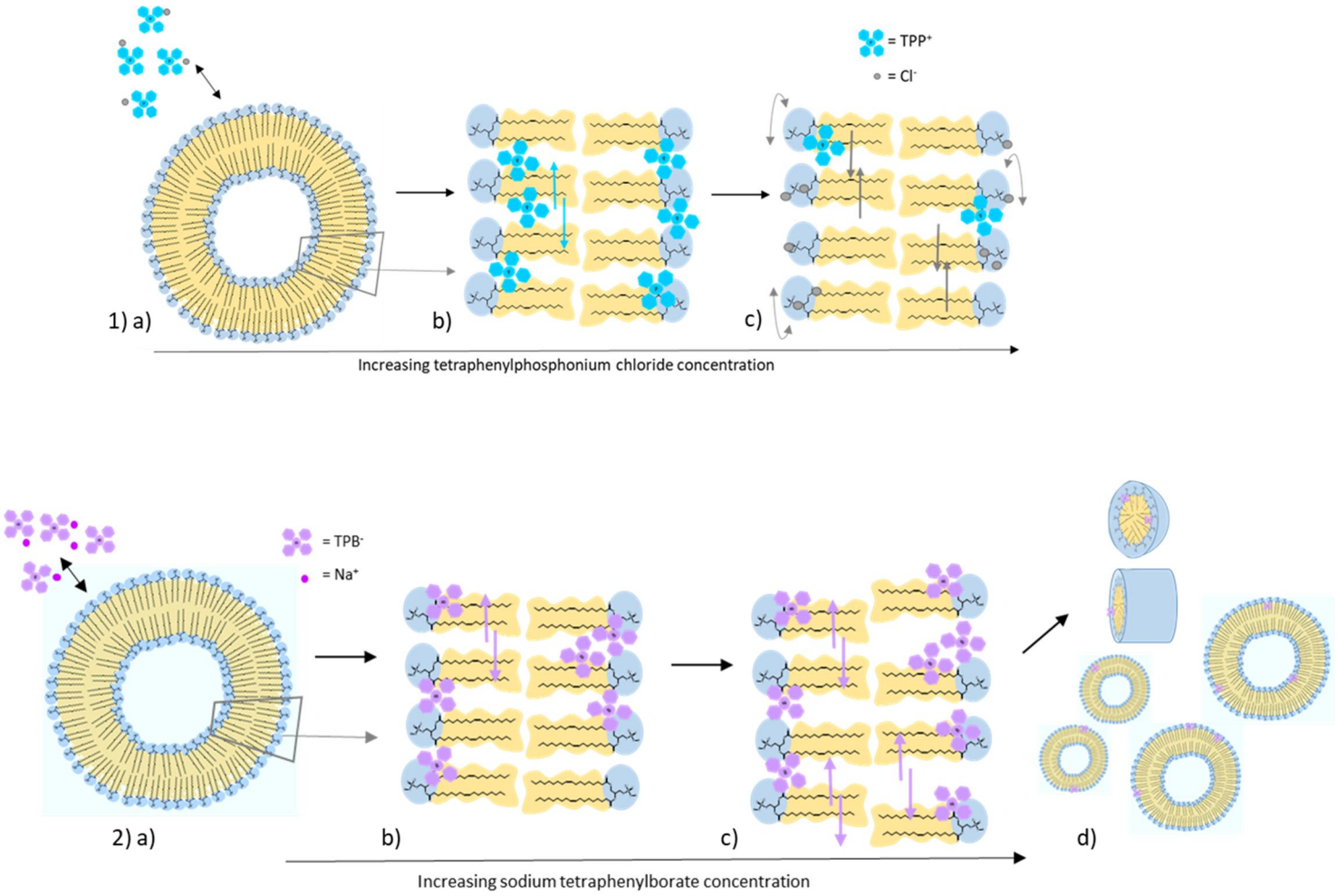

Figure 58: Schematic 1 shows the effect of TPP^+ on DOPC liposomes; 1a) initial addition of TPP^+, 1b) association of the TPP^+ cations and 1c) association of the Cl^- ions. Schematic 2 shows the effect of TPB^- ions on DOPC liposomes; 2a) initial addition of TPB^-, 2b) association of TPB^- ions, 2c) increase in area per lipid at high TPB^- concentrations and 2d) fusion of DOPC liposomes and the other lipid structures formed.

The differences between the effects of the TPP^+ and TPB^- ions on liposomes are clearly highlighted from the results obtained in this work. Previous work carried out on these ions strongly supports the results observed here and confirms that the effects of large, organic, hydrophobic ions on soft matter structures are a hugely interesting and growing area of research in colloid science.

Chapter 6: The effect of temperature and trivalent cations on DOPC and DPPC liposomes

6.1. Effect of temperature on the size of DOPC and DPPC liposomes

Temperature is one of the most important physical parameters in chemistry and it measures the average rate of random motions of atoms and molecules. The higher the temperature, the faster the motion[185]. As well as being a critical factor in all biological processes, temperature is also known to affect the ordering of ions in the Hofmeister series[186] as well as the structure of water[187] and the hydration of ions[188, 189]. As a consequence, understanding the effect of temperature on specific ion effects is vitally important when studying the Hofmeister series. Thus, the effect of temperature on DOPC and DPPC liposomes was studied. The liposomes were prepared in a selection of pure water, mono-, di- and trivalent salt solutions and two different lipids were chosen in order to take into account the effect of the transition temperature of the lipids on the size of the liposomes. As can be seen from Table 4**,** the transition temperature of DOPC and DPPC are -17 ˚C and 41 ˚C respectively. The temperature range was chosen to be 25 ˚C to 60 ˚C to allow the effect of temperature to be examined far above the transition temperature, in the case of DOPC, and also through the transition temperature, in the case of the DPPC liposomes. In order to draw comparisons between the mono-, di-, and trivalent cations, liposomes were prepared in NaCl, $CaCl_2$ or $LaCl_3$ aqueous solutions of equal ionic strength (I = 5 mM). At this point, it is important to acknowledge that DOPC produces more stable liposome suspensions than DPPC at the temperatures studied in this work, as a result of its far lower transition temperature.

The results obtained from DLS for the effect of temperature on the size of DOPC liposomes showed that as the temperature was increased from 25 ˚C to 40 ˚C there was no effect on the size of the liposomes in any of the aqueous solutions studied (Appendix J). These results are expected as the transition temperature of the lipid has been widely acknowledged in the literature to be responsible for the changes in lipid structures which occur at varying temperatures[150, 190] and therefore by examining the impact of temperature on liposomes far above the transition temperature, one would not expect vast changes in the sizes of the liposomes.

In order to study the effect of heating below and above the DPPC transition temperature, DPPC liposomes were heated from 25 ˚C to 60 ˚C, at 2.5 ˚C intervals. Figure 59 shows the change in the DPPC liposome size as a function of temperature in water, as measured by DLS.

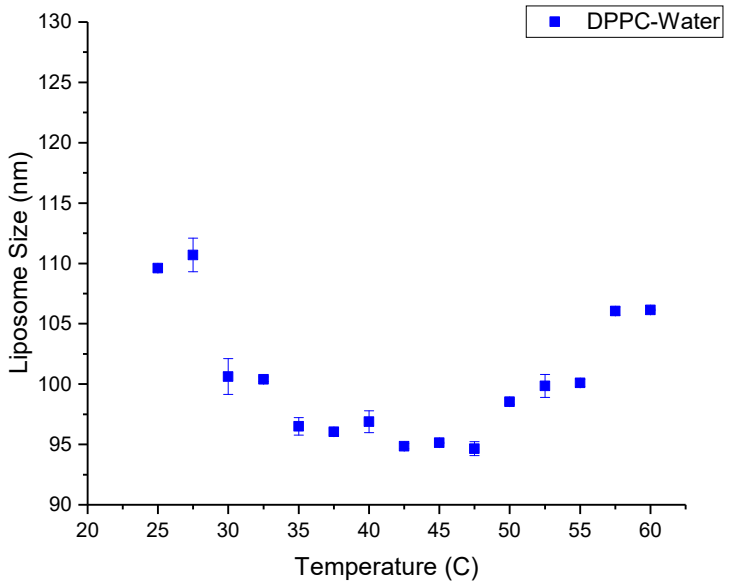

Figure 59: The effect of temperature on the size of DPPC liposomes in water as measured by DLS. The temperature range used was 25˚C to 60˚C.

As can be seen in Figure 59, at 25 ˚C the DPPC liposomes in pure water are 109.6 nm. On increasing the temperature, there is a steady decrease in the size of the liposomes and the smallest size is *d* = 94.8 nm at 42.5 ˚C. The decrease in the size of the liposomes is most profound up to 35 ˚C and from 35 ˚C to 47.5 ˚C the size of the liposomes does not alter vastly. Following the decrease in liposome size, the liposomes begin to increase gradually in size as the temperature continues to rise from 42.5 ˚C to 60 ˚C, and at the maximum temperature the liposome size is *d* = 106.2 nm.

It is clear from Figure 59 that the DPPC liposomes exhibit a size constriction around ~ 41 ˚C, which corresponds to the chain melting temperature of the lipids in the liposome bilayer. At this temperature, a change in the lipid physical state from the gel phase (ordered) to the liquid crystalline phase (disordered) will occur[191]. In the gel phase, the lipids are closely packed together and the hydrocarbon tails are fully extended, whilst in the liquid crystalline phase, the hydrocarbon tails are much more fluid and randomly orientated, making it possible to interpenetrate.

Roy *et al.*[192] also used DLS to examine the size of DPPC liposomes at varying temperatures and observed the same trend of a decrease in liposome size around the transition temperature of 41 ˚C.

This decrease in liposome size as the temperature approaches the transition temperature can be attributed to an increase in membrane fluidity. As the lipids change into the liquid crystalline phase, they become more fluid and more disordered, the lipids do not pack as closely and hence they occupy a larger area. This decreases the rigidity of the bilayer and therefore it is more energetically favourable for the liposomes to decrease in size. The notion that phospholipid bilayer fluidity increases as the temperature increases is supported by Sulkowki *et al.*[193] who found that the *S* order parameter, which is characteristic for liposome structural changes, decreased with temperature. The *S* order parameter is equal to zero when a membrane is in total disorder and equal to one when the membrane has a crystal structure[194, 195].

As already mentioned, the liposome size seems to plateau in-between 35 ˚C and 47.5 ˚C. In some literature, a 'pretransition' has been observed in the case of DPPC unilamellar vesicles[191, 196] and is thought to occur at 35 ˚C[196]. In this work therefore, it is likely that both the 'pretransition' and the 'main' transition occur in the plateau shown in Figure 59. Roy and his co-workers[192] also observed the same increase in liposome size above the transition temperature as can be seen in Figure 59. The increases in size was found to be mostly irreversible and occurred because of the increase in liposome volume, which is common for dispersions at high temperatures[197]. Additionally, Zook *et al.*[190] hypothesised that around the transition temperature, the increase in liposome size may occur due to the decreased stability of mixed gel and liquid phase liposomes. This decreased stability may cause liposome fusion or Oswald ripening[190] (the insertion of free phospholipid molecules into the bilayer on formation of the liposomes) which could result in larger vesicles. Finally, Datta[198] attributed the enlargement of PC and cholesterol liposomes at high temperatures to aggregation. It was hypothesised that at 50 ˚C the Brownian motion of the liposomes would increase and lead to aggregation and coalescence resulting in larger clusters of liposomes. It is difficult to define which of these factors may be responsible for the increase in the size of the liposomes, but due to the system, it is likely that Oswald ripening factors could play an important role.

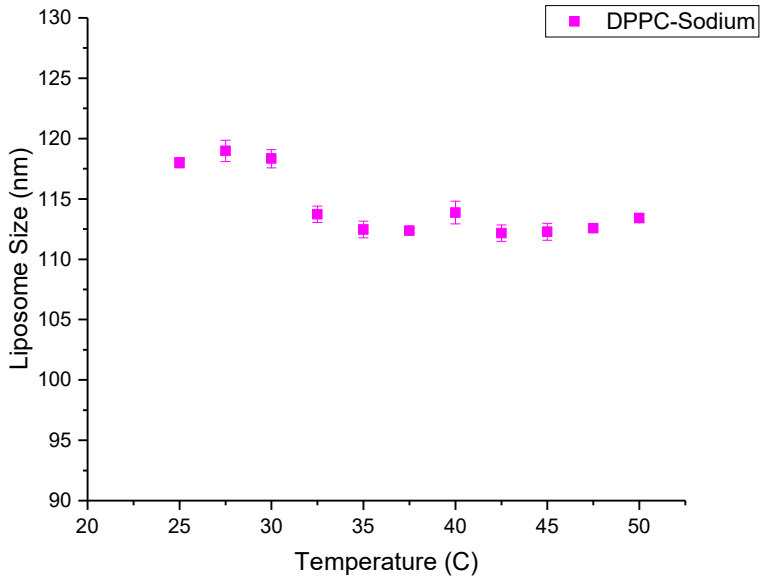

Figure 60: The effect of temperature on the size of DPPC liposomes in NaCl (aq) as measured by DLS. The temperature range used was 25˚C to 50˚C.

Figure 60 shows the change in DPPC liposome size as a function of temperature in the presence of NaCl (*I* = 5 mM) at 2.5 ˚C intervals. As can be seen from the graph, up to 30 ˚C, the DPPC liposomes remain at a constant size of *d* = 118 nm. As the temperature reaches 32.5 ˚C, there is a reduction in the size of the vesicles to *d* = 113.7 nm and as the temperature is then increased further up to 50 ˚C, the liposomes remain at *d* = 112 nm.

Figure 61 shows the impact of temperature increase on DPPC liposome size in the presence of $CaCl_2$ (*I* = 5 mM). As with Figures 56 and 57, the temperature was increased in 2.5 ˚C increments.

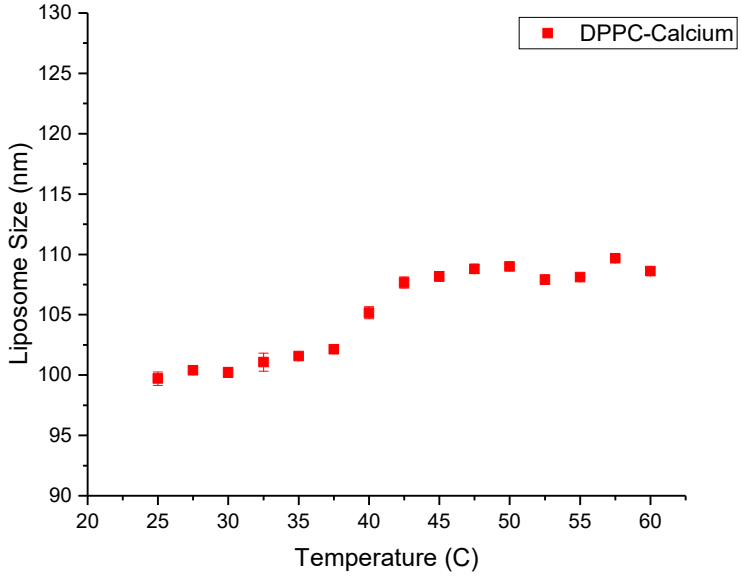

Figure 61: The effect of temperature on the size of DPPC liposomes in $CaCl_2$ (aq) as measured by DLS. The temperature range used was 25˚C to 60˚C.

Figure 61 shows that as the temperature is increased from 25 ˚C to 37.5 ˚C the liposomes do not drastically change in size with *d* ~ 100 nm. At 40 ˚C there is a small increase in the size of the liposomes to *d* ~ 105.2 nm, and at 42.5 ˚C there is another small increase to *d* ~ 107.7 nm. As the temperature is then heated to 60 ˚C the DPPC liposomes remain at *d* ~ 108 nm in size.

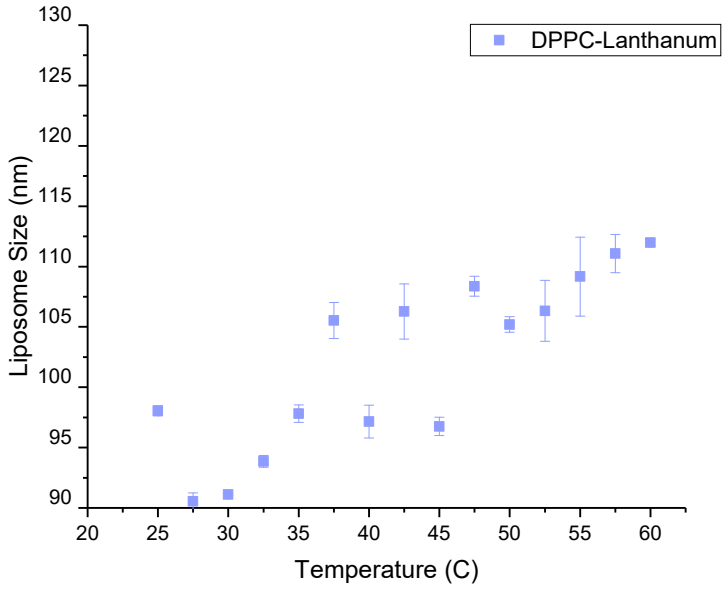

Figure 62: The effect of temperature on the size of DPPC liposomes in $LaCl_3$ (aq) as measured by DLS. The temperature range used was 25˚C to 60˚C.

Finally, the effect of temperature on the size of DPPC liposomes in the presence of $LaCl_3$ (*I* = 5 mM) was studied and the results are displayed in Figure 62. Overall as the temperature is increased from 25 ˚C to 60 ˚C the size of the DPPC liposomes increases and the general trend is that the higher the temperature, the larger the liposome size. However, there are some interesting fluctuations observed in the graph in Figure 61. On initial heating of the DPPC liposome suspension to 27.5 ˚C there is a decrease in the size of the liposomes by 2.5 nm from *d* ~ 98.0 nm to *d* ~ 95.5 nm. As the temperature is then increased up to 37.5 ˚C there is a smooth increase in the size of the liposomes up to *d* ~ 105.5 nm and as the temperature is increased further, the liposomes show an overall increase in size up to *d* ~ 109 nm. However, at 40 ˚C and 45 ˚C, interestingly, the liposomes are smaller than expected at *d* ~ 97.2 nm and 96.8 nm respectively.

In order to understand and explain the data described above, it is important to note that there are two different types of results observed when studying how the size of the DPPC vesicles varies with temperature in the presence of inorganic ions. The first, is that on an increase in temperature the DPPC vesicles show an overall decrease in size and the second is that on an increase in temperature the DPPC liposomes are found to increase in size. From the results shown in Figures 58, 59 and 60**,** it is clear to see that the first type of result is obtained when examining DPPC-NaCl suspensions, and the

second type of result is obtained when studying DPPC-$CaCl_2$ and DPPC-$LaCl_3$ systems. Furthermore, however, the $LaCl_3$ system appears to have a much larger effect on liposome size than the $CaCl_2$ system. The NaCl and $CaCl_2$ seem to show comparable effects as they cause an overall change in the liposome size of ~6%, whilst $LaCl_3$ causes the liposome to show an overall increase in size of 18%.

In the case of the DPPC-NaCl liposome suspension, the decrease in liposome size can be partly attributed to the transition of the lipid in the liposomes from a gel like state to a more fluid state at the transition temperature. As discussed previously, around the transition temperature of DPPC, the lipid will become more fluid and therefore reduce the rigidity of the bilayer, decreasing the bending energy of the bilayer and allowing the formation of smaller liposomes. From Figures 59 and 60, it is clear to see that the decrease in liposome size is more profound for the DPPC vesicles prepared in water compared with those prepared in NaCl. This is an expected result as salts are known to increase the rigidity of the bilayer[110] by associating with the head groups of the phospholipids and screening the repulsion between neighbouring lipid molecules. Therefore, in the presence of NaCl, the effect of the increased fluidity of the bilayer at elevated temperatures will be reduced and therefore the liposomes will not decrease in size as much as in the pure water systems.

In the presence of Na^+, the liposomes shrink at ~ 32.5 ˚C, which is slightly lower than the aforementioned 'pretransition' temperature of DPPC of 35 ˚C. This could be the consequence of a salt induced depression of the transition temperature. Previous literature has shown that anions and cations can have an effect on the transition temperature of phospholipids[199] and specific work on monovalent cations has shown that they cause the lipid bilayers transition temperatures to decrease[200, 201]. Additionally, as previously mentioned, an increase in temperature causes an increase in the mobility of water molecules. It follows that, the water molecules begin to expand away from the ions and the lipid head groups, partially dehydrating them. Owing to the single, monovalent charge of the Na^+ cation, the ion is not able to sufficiently stabilise the liposomes and therefore the only way the system can gain stability is by forming smaller liposomes[117]. It is for these two reasons that on increasing the temperature of DPPC-NaCl suspensions, there is an overall decrease in the size of the liposomes.

In the case of the DPPC-$CaCl_2$ and DPPC-$LaCl_3$ liposome suspensions, the size of the liposomes increases on increasing temperature. In the same way as previously mentioned, the increased mobility of water molecules at increased temperatures causes the Ca^{2+} and La^{3+} ions to be stripped of some water molecules from their hydrations sheaths. The result is that the cations occupy a smaller volume and can more easily access the head groups of the phospholipids. The higher charge densities of the Ca^{2+} and La^{3+} ions means they are more strongly attracted to the lipid phosphate groups and therefore can stabilise the liposomes effectively, allowing them to increase in size.

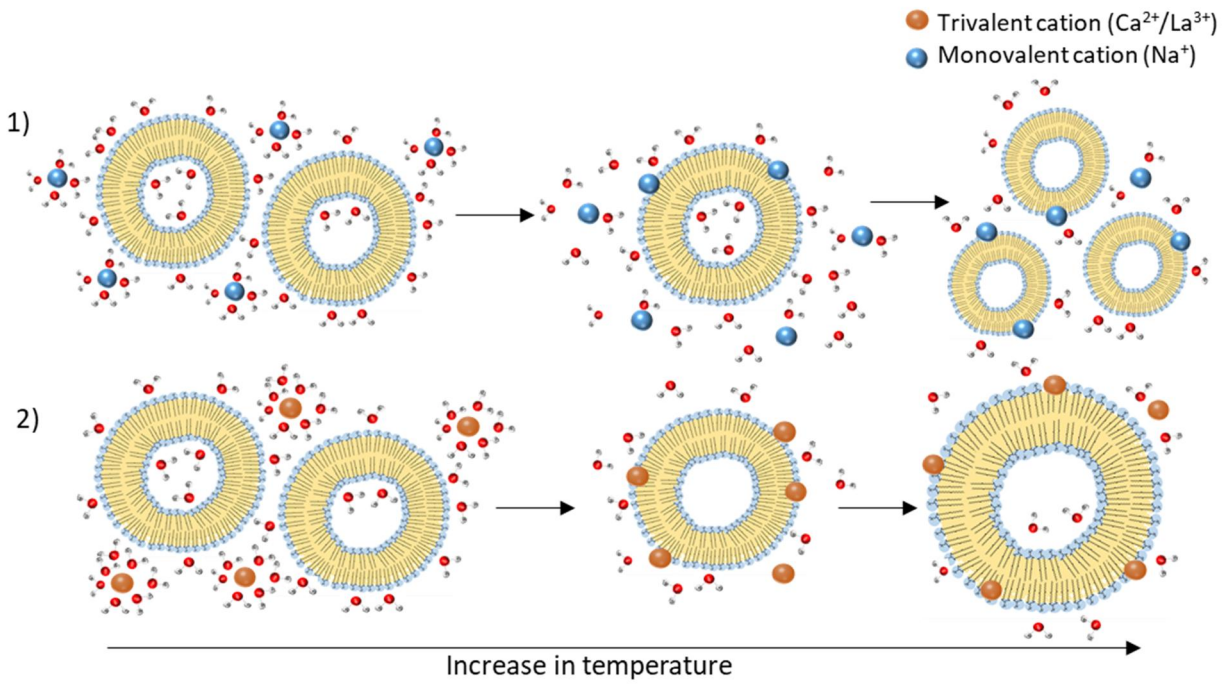

Figure 63: The effect of increasing temperature on the DOPC liposomes in the presence of inorganic cations. 1) Shows the mechanism for the decrease in liposome size in the presence of Na^{+} cations, 2) shows the mechanism for the increase in size of the liposomes in the presence of Ca^{2+} or La^{3+}.

For the $CaCl_2$ system, the jump in size of the liposomes occurs between 40 ˚C and 42.5 ˚C, indicating that the Ca^{2+} cation does not have a large effect on the transition temperature of DPPC. In previous studies, divalent cations (Mg^{2+} and Ca^{2+}) have been found to increase and broaden the transition temperature of phospholipids[200]. The ions associating with the head groups of the lipids contribute directly to interlipid cohesion and help to increase the stability of the ordered lipid phases thereby increasing the chain melting temperature[202]. It is possible that the concentration of Ca^{2+} examined here is not high enough in order to invoke this effect as the ionic strength of the systems was only 5 mM.

For the $LaCl_3$ system, the graph obtained of liposome size against temperature is not as smooth. Around the transition temperature of DPPC, there are large fluctuations in the size of the liposomes. Additionally, the fluctuations in liposome size occur over quite a large temperature range (~ 37.5 ˚C – 47.5 ˚C) which could indicate that the trivalent cation causes a broadening of the chain melting temperature of the lipid. The observation is supported by previous studies on the effect of La^{3+} cations on DPPC bilayers carried out by Chowdhry *et al.*[203] who found that the gel to liquid crystalline transitions were broadened, and the T_m increased by a maximum of 5 ˚C. The fluctuations observed in this work could perhaps be attributed to the changes in the interactions in the non-polar part of the bilayer resulting from the association of the La^{3+} cations with the phospholipid head groups. Chowdhry and co-workers[203] also found that changes in the interactions in the non-polar parts of the bilayer could result in changes in thermodynamics of the $P_\beta \rightarrow L_\alpha$ transition (Figure 64).

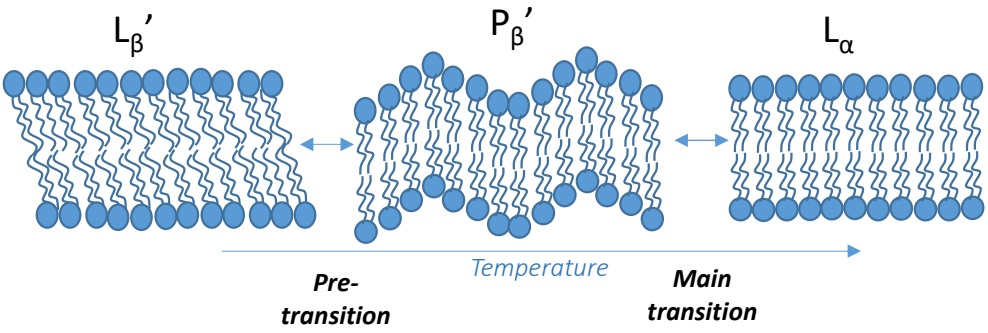

Figure 64: Phase transition in lipid bilayer. From left to right there is an increase in temperature, as the lipid passes through the pre-transition and the main transition. Image adapted from Avanti Polar Lipids, Inc.

Owing to the broadening of the main transition of DPPC in the presence of La^{3+} cations, the phases in the phase transition of the lipid are less defined. In this way, it could be possible that the changes in hydrocarbon tilt angle in the liposome have a profound effect on the size of the vesicle and hence the fluctuations are observed. In contrast, in the case of the mono-, and divalent cations studied in this work, the phase transition is not as broad and hence the fluctuations do not occur as the changes are much more defined at specific temperatures. As confirmed in the previous section by the zeta potential measurements, the La^{3+} ions also have the highest affinity for the PC head groups, especially at low concentrations. It is therefore likely, that these trivalent ions have the most profound effect on the head group tilt of the phospholipid and as a consequence, the largest effect on hydrocarbon tilt.

The effect of temperature on the size of the DPPC liposomes in the presence of mono-, di- and trivalent cations reveals interesting results. Despite the importance of temperature in colloid chemistry, however, there is a distinct lack of research carried out in this area. Broadly, for the ions examined in this section, Na^+ was found to have the least stabalizing effect, causing a slight depression in the transition temperature of DPPC, attributed to its low charge density. Ca^{2+} was found to stabalize the vesicles as the temperature was increased, yet the divalent cation appeared to have no impact on the T_m of the lipid. Finally, La^{3+} caused an overall increase in liposome size as the temperature was increased attributed to its strong stabalisng effect at low concentrations. La^{3+} was also found to substantially broaden the transition temperature of DPPC, in agreement with past results. Consequently, at increasing temperatures the stabalising effect of the cations studied is of the order $Na^+ < Ca^{2+} < La^{3+}$ in line with the ions of the Hofmeister series and increasing charge density.

6.2. Effect of trivalent cations on the electrophoretic mobility of DPPC liposomes

In order to examine in more detail the effect of trivalent cations on PC liposomes, the effects of La^{3+}, chromium (Cr^{3+}) and iron (Fe^{3+}) cations on DPPC liposomes were studied. As illustrated in section 4.1**,** trivalent cations are known to have a strong affinity to PC membranes and therefore the interactions between the ions and bilayers are very interesting. Iron is the most abundant trace element in the world and partakes in important roles in biology including oxygen transport and DNA synthesis[204]. Incorporating iron into colloids has become increasingly widespread in recent years. For instance, in 2015 Yuan *et al.*[204] found that iron liposomes could be used in treating iron deficiency diseases, in particular anaemia of inflammation. Iron has also been used increasingly in the synthesis of magnetic liposomes, which can be used as drug carriers[205] and for tumour targeting[206]. On the other hand, in the case of the chromium ion, there is significantly less research that has been carried out on interactions with phospholipid structures.

Figure 65 shows the electrophoretic mobility of DPPC liposomes as a function of trivalent cation concentration at 25 ˚C. electrophoretic mobility of the DPPC liposomes in pure water was found to be -1.04 µmcm/Vs.

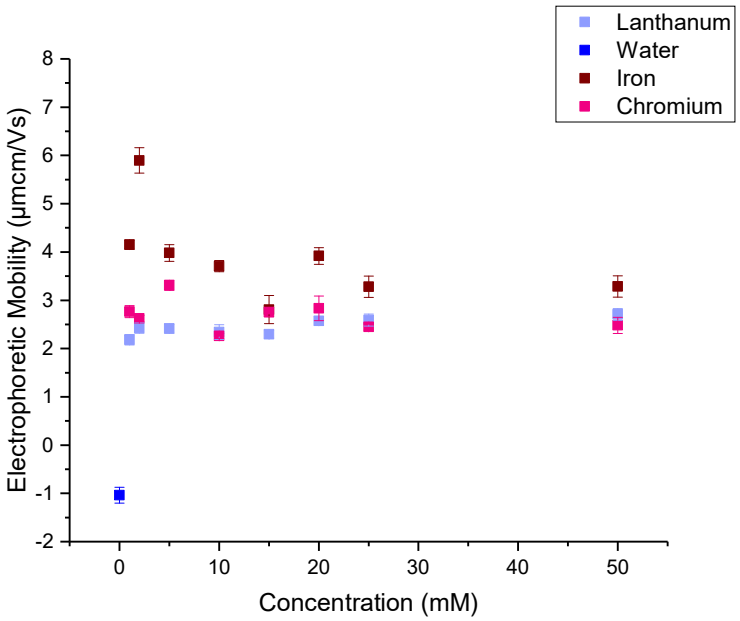

Figure 65: The change in electrophoretic mobility of DPPC liposomes as a function of trivalent cation concentration at 25˚C.

As can be seen in Figure 65, in the presence of all three cations there is an initial large increase in the electrophoretic mobility of the DPPC liposomes. In the presence of 1mM La^{3+}, the electrophoretic mobility of the liposomes increases up to μ = 2.18 µmcm/Vs, which is 3.22 µmcm/Vs greater than the electrophoretic mobility of liposomes in the absence of salt. The electrophoretic mobility of the liposomes then remains fairly constant, at μ ~ 2.4 µmcm/Vs as the concentration of $LaCl_3$ is increased up to 50 mM.

In the case of the Cr^{3+} ion, in the presence of 1 mM $CrCl_3$, the electrophoretic mobility of the liposomes increases to μ = 2.77 µmcm/Vs, which is 3.81 µmcm/Vs higher than the DPPC liposomes in 1 mM La^{3+}. On increasing Cr^{3+} concentration, there are slight fluctuations in the electrophoretic mobility up to [$CrCl_3$] =5 mM and at high ion concentrations the electrophoretic mobility remains fairly constant at μ ~ 2.6 µmcm/Vs.

The electrophoretic mobility of DPPC liposomes in the presence of Fe^{3+} shows a slightly different trend. As can be seen from Figure 65**,** in the presence of 1 mM Fe^{3+}, the electrophoretic mobility of the liposomes increases to μ = 4.15 µmcm/Vs and as the Fe^{3+} concentration is increased to 2 mM, the electrophoretic mobility increases even further by 42 % to μ = 5.90 µmcm/Vs. As the $FeCl_3$ concentration is increased further to 15 mM, there is a gradual decrease in the electrophoretic mobility followed by a plateau in the data when the electrophoretic mobility is μ ~ 3.5 µmcm/Vs.

From the results described above, it is clear that the La^{3+} and Cr^{3+} exhibit similar behaviour in their interactions with DPPC liposomes. In the same way as discussed in section 4.1, the sizable increase in the electrophoretic mobility of the liposomes at low ion concentrations is due to the strong electrostatic attractions between the cations and the phosphate groups of the phospholipids. The plateau in the electrophoretic mobility as the concentration is increased further is indicative of saturation of the head groups of the phospholipids with cations. The initial increase and the plateau in the electrophoretic mobility of the liposomes is slightly higher in the presence of Cr^{3+} compared with La^{3+} which could signify that Cr^{3+} has a slightly higher affinity for the DPPC membrane. Although the trend observed for the electrophoretic mobility in the presence of Fe^{3+} is substantially different, the increase in the electrophoretic mobility of the liposomes at low Fe^{3+} concentrations is likely to be due to the same interactions as outlined previously. Overall, the electrophoretic mobility values obtained in the presence of Fe^{3+} are much higher than for the other two cations studied. Thus, it can be hypothesised that the Fe^{3+} cations have the strongest associations with the DPPC liposomes. In order to investigate this hypothesis further, it is constructive to consider the surface charge densities of the liposomes.

Table 9: The surface charge densities of DPPC liposomes in the presence of Fe^{3+}, Cr^{3+} and La^{3+}cations at varying concentrations.

Ion concentration (mM)	Ionic Strength (mM)	σ ($LaCl_3$) (C m^{-2})	σ ($CrCl_3$) (C m^{-2})	σ ($FeCl_3$) (C m^{-2})
1.0	6.0	6.02E-04	7.83E-04	2.92E-03
2.0	12.0	5.74E-04	6.17E-04	2.81E-03
5.0	30.0	6.39E-04	8.09E-04	1.61E-03
10.0	60.0	6.66E-04	6.23E-04	1.17E-03
15.0	90.0	5.84E-04	6.18E-04	8.43E-04
20.0	120.0	6.61E-04	7.10E-04	1.10E-03
25.0	150.0	5.87E-04	5.50E-04	8.51E-04
50.0	300.0	6.52E-04	4.98E-04	8.13E-04

As can be seen in Table 9, the surface charge densities of DPPC liposomes in the presence of Fe^{3+} are higher than in the presence of Cr^{3+} and La^{3+} cations at all concentrations examined. These results help support the hypothesis that the Fe^{3+} ions have a greater affinity to the DPPC head groups of the lipids and we can conclude that the Fe^{3+} cations are able to fix on the liposome surface more effectively than the other two cations examined in this work, hence producing the highest values of the electrophoretic mobility. The similarities in the behaviour of the La^{3+} and Cr^{3+} is also highlighted in Table 9. The surface charge densities of the DPPC liposomes are similar in the presence La^{3+} and Cr^{3+} at moderate concentrations. At low concentrations the surface charge densities are slightly higher in the presence of Cr^{3+}, supporting the notion that this ion has a very slightly higher affinity for the PC membrane than the La^{3+} ion.

Given the vast difference in the results produced by the DPPC-$FeCl_3$ system, it is likely that an *ion-specific* effect is occurring in this suspension. In order to further investigate this idea, the effect of the trivalent cations on the size and PdI of the liposomes was examined.

6.3. Effect of trivalent cations on the size and polydispersity index of DPPC liposomes

In order to better understand the effects of La^{3+}, Cr^{3+} and Fe^{3+} cations on DPPC liposomes, the change in the size of the liposomes as a function of trivalent cation concentration at 25 ˚C was studied. Figure 66 shows how the trivalent cations influence the size of the liposomes, as measured by DLS. The size of the DPPC liposomes in pure water was found to be *d* = 110.5 nm.

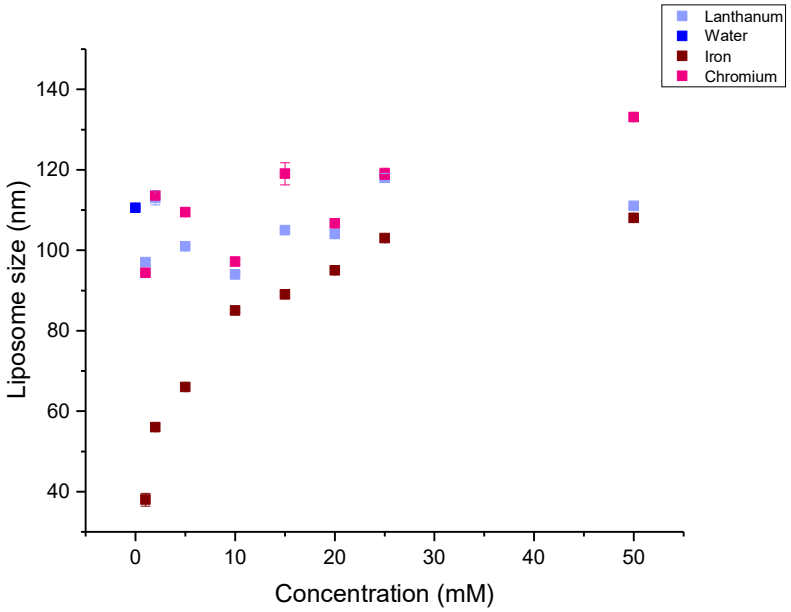

Figure 66: The effect of trivalent cations on the size of DPPC liposomes, at 25˚C, as measured by DLS.

As can be seen from Figure 66, it is clear that the trivalent cations have a profound effect on the size of the DPPC liposomes. In the case of the La^{3+} ions, the size of the liposomes were found to decrease at low $LaCl_3$ concentrations (up to 10 mM) and a minimum liposome size was observed at *d* = 94.0 nm. As the concentration was then increased up to 25 mM, there is a gradual increase in the size of the liposomes up to *d* = 118.0 nm. At the maximum concentration of [$LaCl_3$] = 50 mM, the liposomes shrink slightly to *d* = 111.0 nm. A very similar trend is observed for the influence on Cr^{3+} on the size of the DPPC liposomes. As the concentration is increased to 10 mM, there is a decrease in the size of the liposomes. Following this initial decrease in size, as the $CrCl_3$ concentration is increased up to 50 mM, the liposomes gradually grow in size, and the largest liposomes are observed at [$CrCl_3$]= 50 mM and

were found to be d = 133.1 nm. As with the DPPC-La^{3+} system, the increase in the size of the liposomes becomes less profound as the concentration is increased, and as with the electrophoretic mobility data, the influence of Fe^{3+} on the size of the liposomes appears to be strikingly different from the other cations examined. In the presence of 1 mM $FeCl_3$, there is a drastic decrease in the size of the liposomes to d = 38.0 nm, which is a 66% decrease compared with the liposomes prepared in the absence of salt. As the concentration of $FeCl_3$ is then increased further up to 25 mM, the size of the liposomes gradually increases until a size of d = 103.0 nm is reached. At [$FeCl_3$] = 50 mM the size of the liposomes is 108 nm, indicating that there is a plateau in the data and that the increase in the size of the liposomes is greatest at lower cation concentrations.

Figure 67 shows the change in the polydispersity index of the liposome-cations systems, as a function of ion concentration, as measured by DLS. The PdI of the liposomes in the absence of salt was found to be 0.051.

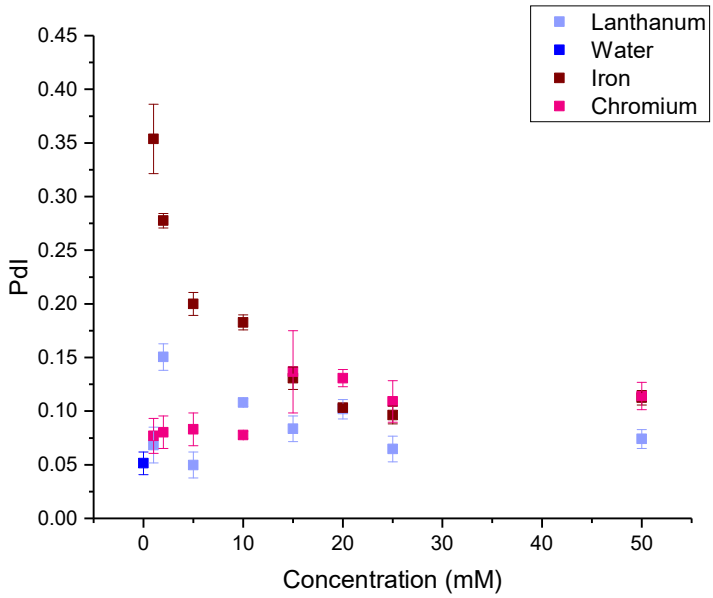

Figure 67: The change in the PdI of DPPC liposome suspensions in the presence of trivalent cations, at a range of concentrations, at 25˚C. Data measured by DLS.

Figure 67 shows that for all concentrations of $LaCl_3$ studied in this work, the PdI of the systems remains below 0.2, indicating that liposomes are uniform in size and can be considered as monodisperse suspensions. The PdI of the liposomes in the presence of 2 mM $LaCl_3$ is slightly higher than expected, however does not exceed 0.2. As mentioned in section 4.3, this slightly higher than expected result is most likely to be due to variations in the experimental preparation procedure. The PdI of the liposomes in the presence of $CrCl_3$ is also always below 0.2. It can therefore be concluded with confidence that the liposomes are all uniform in size, and the Cr^{3+} ion does not cause the liposomes to aggregate. For the DPPC-$FeCl_3$ systems, the PdI of the liposomes presents a very different trend. In the presence of 1 mM $FeCl_3$, the PdI increased to 0.35 indicating that the structures in the system had a wide range of sizes. As the concentration of $FeCl_3$ was increased further the PdI of the liposomes showed a gradual decrease. At [$FeCl_3$] = 2 mM and 5 mM the PdI of the liposomes was measured to be 0.28 and 0.20 respectively. This indicates that, although as the Fe^{3+} concentration is increased the PdI is decreasing, both these systems are still polydisperse. As the concentration of $FeCl_3$ is increased to > 10 mM, the PdI of the liposomes is found to fall below 0.2 for all the Fe^{3+} concentrations examined. It can be concluded therefore, that at low Fe^{3+} concentrations the liposome suspensions are polydisperse, at moderate Fe^{3+} concentrations the liposome suspensions become more monodisperse and then at high ion concentrations the vesicles become more uniform in size.

From the results described in this section, it is clear that the Fe^{3+} cation produces a very different effect on the DPPC liposomes compared with the La^{3+} and Cr^{3+} cations. The La^{3+} and Cr^{3+} cations have very similar, comparable effects on the DPPC liposomes, therefore it is likely that they are interacting in very similar manners. With regard to the changes in liposome size, it is likely that the decrease in the size of the liposomes in the presence of low concentrations of La^{3+} and Cr^{3+} is due to osmotic effects and reorientation of the DPPC head groups. As described in section 4.2, the increase in cation concentration outside the liposomes will cause a concentration gradient to be created between the inside and the outside of the lipid bilayer. As a consequence, in order to compensate for the increase in ion concentration outside the bilayer, the liposomes eject water from their aqueous core and, as a result, shrink in size. In addition, as the cations form complexes with the head groups of the phospholipids, they cause a change in the lipid head group direction, causing an increase in area per lipid and bilayer fluidity and consequently a decrease in the vesicle size. At moderate La^{3+} and Cr^{3+} concentrations, the liposomes do not increase dramatically in size, but the small size increases can be attributed to closer packing of the lipids in the vesicle following the association of the cations with the head groups (As confirmed by the electrophoretic mobility measurements (Figure 65)). As the lipids pack more closely, they cause the bilayer of the liposome to become more rigid, and therefore there

is an increase in the bending energy required to form a vesicle, resulting in the formation of larger liposomes.

On closer inspection of the effect of Cr^{3+} and La^{3+} on the DPPC liposomes it was found that the Cr^{3+} ions have a slightly greater effect than the La^{3+} ions, as illustrated by the changes in the size and electrophoretic mobility of the liposomes in the presence of the two cations. In order to interpret this result, it is interesting to further consider the properties of the two cations[207].

Table 10 Properties of Cr^{3+} and La^{3+} cations [207]. From left to right the table shows the bare ion radius, the hydrated ion radius, the hydration number, the Gibbs free energy, enthalpy and entropy of hydration of the cations.

Ion	Bare ion radius (nm)	Hydrated ion radius (nm)	Hydration number	$\Delta_{hyd}G$ ($kJmol^{-1}$)	$\Delta_{hyd}H$ ($kJmol^{-1}$)	$\Delta_{hyd}S$ ($JK^{-1}mol^{-1)}$
Cr^{3+}	0.062	358	17.4	-4010	-4670	-533
La^{3+}	0.105	307	10.3	-3145	-3310	-474

Table 10 shows that the Cr^{3+} ions are smaller than La^{3+} ions by 0.043 nm, which means that they possess a higher charge density and therefore more strongly hydrated, clearly illustrated by the higher hydration number. The entropic gain from the liberation of bound water molecules on binding of the ions to the lipid head will therefore be greater in the case of the Cr^{3+} ions as more water molecules will be released back into the bulk. It is likely that the slightly higher affinity of the Cr^{3+} cations to the membrane compared with La^{3+} ions is due to this increased entropic gain. Additionally, since the bare ion radii of the Cr^{3+} ions are slightly smaller than La^{3+}, after shedding their hydration sheath, more Cr^{3+} cations are able to associate with the head group of the lipids. Therefore, the Cr^{3+} cations are able to produce a somewhat larger effect on the DPPC liposomes than the La^{3+} ions, as demonstrated by the larger liposomes produced at high Cr^{3+} concentrations, and the higher electrophoretic mobility values found at low Cr^{3+} concentrations.

From the results displayed in Figures 63, 64 and 65**,** it is clear that the Fe^{3+} ions have a unique effect on the DPPC liposomes. Since there is a distinct lack of work regarding the effect of iron compounds on PC liposomes, the interactions at play here are difficult to define. The vast decrease in the size of the vesicles and the increase in the PdI of the system on the initial addition of Fe^{3+} indicates that it is likely there are a number of different structures, with varying sizes, being formed. In order to try to explain these changes, it is helpful to consider the behaviour of $FeCl_3$ in aqueous solution. Iron has a very strong tendency to hydrolyse and form complexes when in an aqueous environment, resulting in soluble mononuclear hydrolysis products, multinuclear clusters, as well as precipitates[208]. When $FeCl_3$

is added to water, the compound dissolves and hydrated iron (III) complexes form ($[Fe(H_2O)_6]^{3+}$). As the Fe^{3+} cation is very charge dense, the O-H bonds are considerably weakened and hydrolysis can occur forming complexes such as $[Fe(H_2O)_5(OH)]^{2+}$ and also H_3O^+ which causes the solution to become slightly acidic[208]. Interestingly, Fe^{2+} complexes have been reported in the literature, to cause oxidation of phospholipid molecules[209-211]. It could therefore be possible that, in the presence of Fe^{3+}, structural changes to the DPPC membrane in the liposomes are induced, which causes the liposomes to become less stable and therefore shrink in size. The large shrinking in liposome size and the large increase in PdI in the presence of low concentrations of $FeCl_3$ indicate that there are a range of liposomes with varying sizes present in the suspension. It is likely that the complexes formed interact in very different and multifaceted ways with the DPPC liposomes and therefore are not as easy to define as in the case with other inorganic cations. As previously mentioned, the alteration of the pH of the system in the presence of $FeCl_3$ may also have an affect on the suspension. The pH of a solution is known to have a large effect on PC liposomes, and changes in pH have been reported to alter the fluidity, stability and structure of DPPC liposomes[192, 193, 212]. It is possible that the increase in the size of the liposomes as the concentration of $FeCl_3$ is increased is due to greater rigidity of the DPPC bilayers as a consequence of increased hydrogen bonding. At lower pH, the phosphate groups of the lipids become protonated and as a consequence, form hydrogen bonds with neighbouring phospholipid molecules[194]. These hydrogen bonds increase the rigidity of the bilayer and therefore allow larger liposomes to form. Since the concentration of $FeCl_3$ used in this work is low and the increase in concentration is gradual, the effect of increasing bilayer rigidity can also be assumed to be gradual and smooth, which helps to explain the shape of the Fe^{3+} graph shown in Figure 66. At moderate Fe^{3+} concentrations, it is also possible that the extent of hydration of the lipid decreases, as a result of the decreased hydrophilicity of the head groups of the lipids, as more groups become protonated. This decreased hydrophilicity could result in a slight instability of the liposomes which may induce liposome fusion or Oswald ripening (insertion of free phospholipid molecules into the bilayer) which could also promote the formation of larger liposomes.

As illustrated by the PdI values, the stability of the $FeCl_3$-DPPC system seems to increase and the suspensions become more monodisperse as the concentration of $FeCl_3$ is increased. The increase in the size of the liposomes slows and the electrophoretic mobility of the liposomes plateaus at high concentrations (<20 mM). It can therefore be concluded that at Fe^{3+} concentrations greater than 20 mM, the liposomes are stable and uniform in size and the system has reached an apparent '*equilibrium*' which no longer alters dramatically as the Fe^{3+} concentration is increased further.

This section presents some especially thought-provoking results on the effect of trivalent cations on DPPC liposomes. This section is particularly interesting as it contains novel results, gained from

systems that have not been examined previously. The La^{3+} and Cr^{3+} were found to have very similar effects to one another and also to the divalent and trivalent cations examined in Section 4. The La^{3+} and Cr^{3+} ions interact strongly with the head groups of the phospholipids invoking osmotic effects and changes in the lipid head group direction. The electrophoretic mobility measurements indicate that the head groups of the lipid are likely to become saturated with the trivalent cations at low concentrations. The Fe^{3+} cations produce vastly different effects on the DPPC liposomes, which is expected to be a consequence of their unique behaviour in water, and their tendency to form a variety of complexes. The partial acidification of the aqueous solution is also hypothesised to play a role. At low concentrations the Fe^{3+} ions produce a vastly different *ion-specific* effect to La^{3+} and Cr^{3+} (the effect of trivalent cations on DPPC liposomes is of the order $Fe^{3+} > La^{3+} \approx Cr^{3+}$). However, at higher concentrations all three ions produce comparable ion-DPPC liposome systems ($Fe^{3+} \approx La^{3+} \approx Cr^{3+}$).

Chapter 7: TEM images

7.1. TEM images of DOPC liposomes

In order to examine the morphology and shape of the DOPC liposomes more closely, TEM was used. DLS falls short in providing direct structural information about the liposomes and therefore TEM was a very valuable technique to be employed in this project. Four different suspensions were prepared for analysis by TEM, DOPC liposomes in pure water and DOPC liposomes in salt solutions of NaCl, $CaCl_2$ and $LaCl_3$ respectively. All the salt solutions were prepared at equal ionic strength (I = 5 mM) in order to allow comparison of the effects of mono-, di-, and trivalent cations on the liposome size, shape and lamellarity. In the figures in this chapter, the yellow arrows represent unilamellar liposomes, the blue arrows denote multilamellar vesicles and the red arrows signify multivesicular liposomes. Black arrows are used to identify other structures of interest.

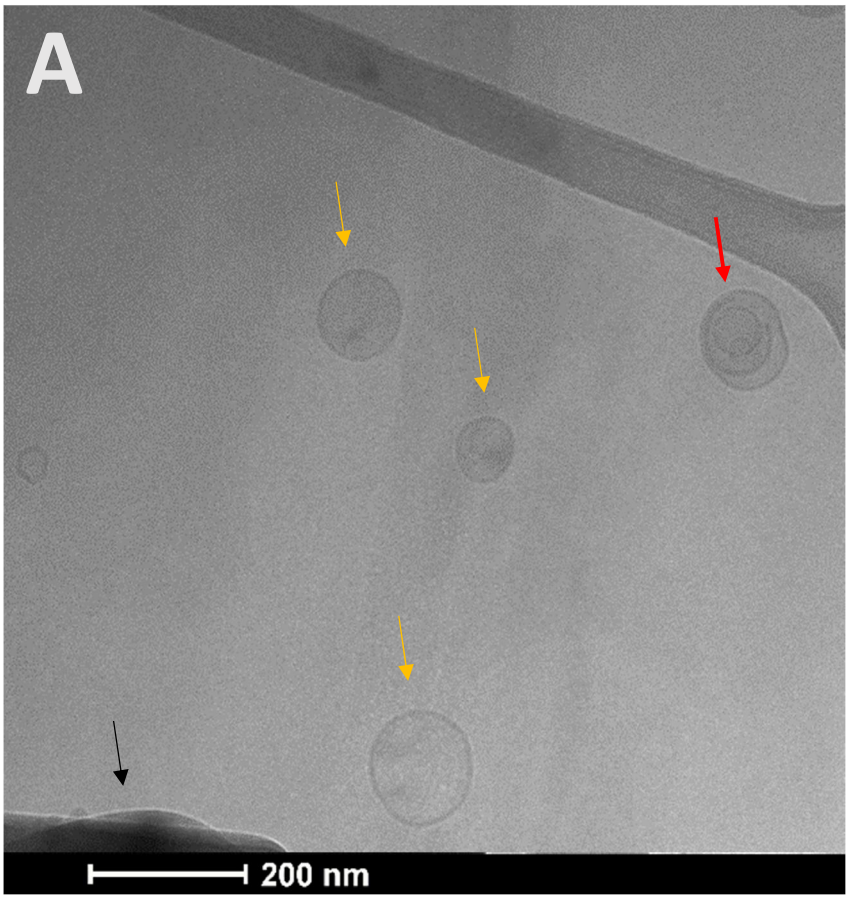

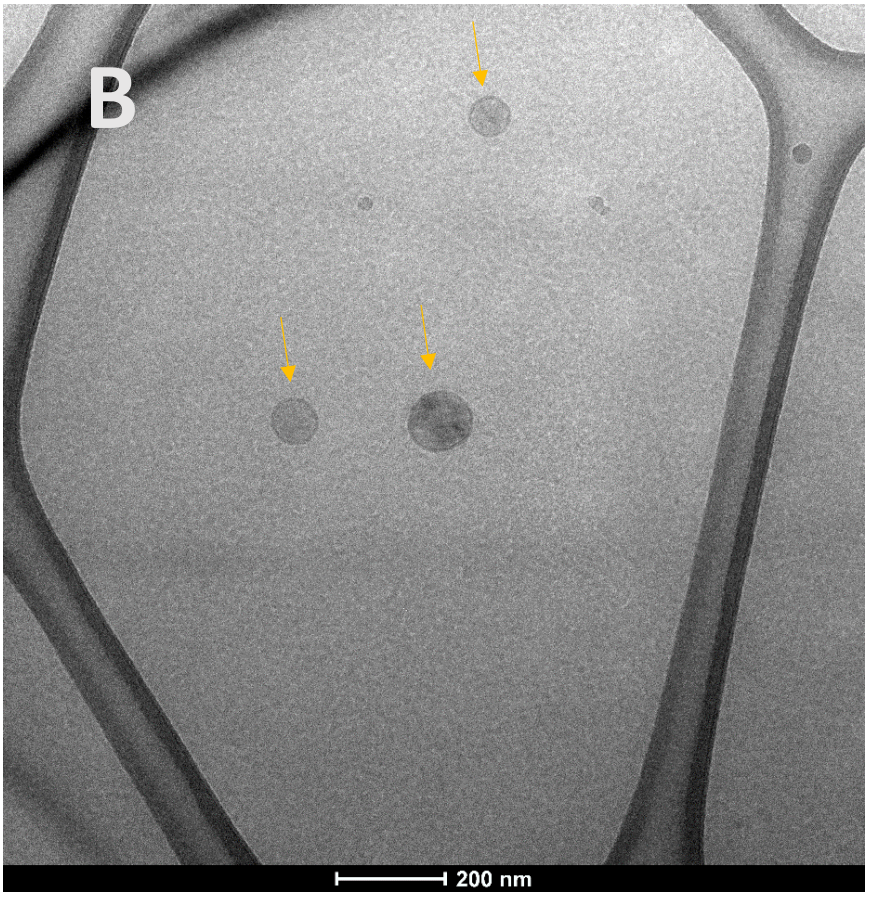

Figure 68: Cryo-TEM images of sonicated and extruded DOPC liposomes in water. The scale bar shown is 200 nm. Images A and B are taken from different areas of the TEM grid.

Figure 68 shows the cryo-TEM images of DOPC liposomes prepared in water. The DLS measurements carried out on the sample found the Z-average size *d* = 130.7 nm and PdI = 0.028. Images A and B are taken from different areas of the same TEM grid and are an appropriate representation of the whole grid. In Figure 68 (A), a number of unilamellar liposomes can be clearly seen (yellow arrows) and one multivesicular liposome is also observed (red arrow). In addition, Figure 68 (B) shows unilamellar liposomes formed (yellow arrows), most of which appear to be of the expected size, predicted from DLS data. It is important to note that in Figure 68 (A) at the bottom left hand side of the image, a dark area is clearly observed (black arrow). This is an area of crystalline ice, most likely formed during the sample freezing process.

From the images shown in Figure 68, it can be concluded that in water monodisperse, spherical, unilamellar DOPC liposomes are formed, supporting the DLS data obtained on the sample. Owing to the zwitterionic nature of the DOPC lipids, on liposome formation, there is sufficient repulsion between neighbouring lipid bilayers to promote the formation of predominately unilamellar vesicles, hence there is a distinct lack of multilamellar vesicles observed in this sample.

It can also be concluded that the liposome preparation process is successful in promoting the formation of a monodisperse and unilamellar liposome suspension. Sonication and extrusion encourage the effective sizing of liposomes, allowing unilamellar liposomes to be created in a system which has an exceptionally low PdI.

The conclusions drawn from the cryo-TEM data in this work are supported by previous literature. In 2013, Huy *et al.*[213] used cryo-TEM to obtain images of DOPC liposomes prepared in water, in order to study lipid membrane mediated Hemozoin formation. In this work, majority of the DOPC liposomes observed were spherical and had a smooth, curved bilayer membrane. A very small number of multilamellar vesicles were also observed in the images obtained in this work.

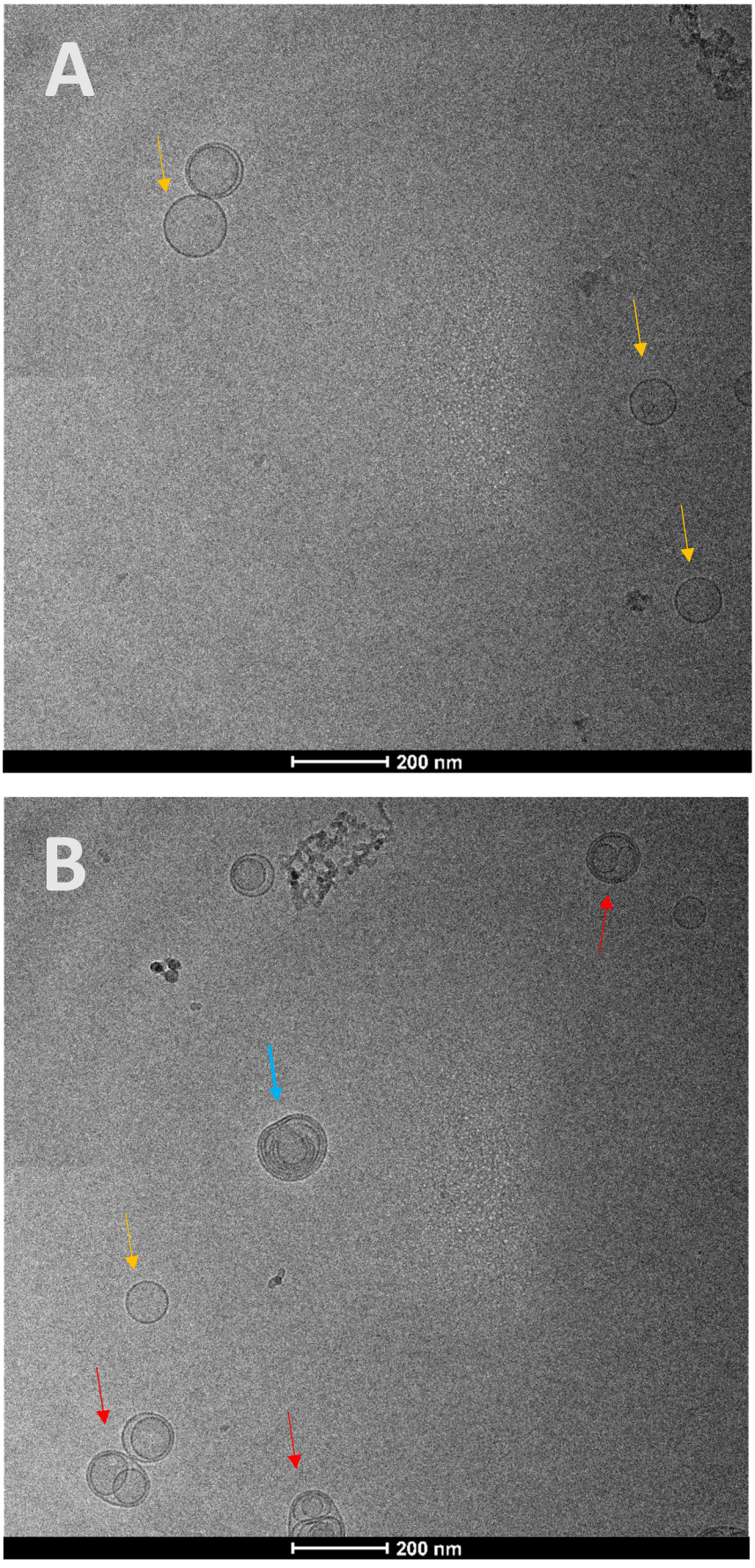

Figure 69 Cryo-TEM images of sonicated and extruded DOPC liposomes in the presence of NaCl (I = 5 mM) The scale bar shown is 200 nm. Images A and B are taken from different areas of the TEM grid.

Figure 69 shows the TEM images of DOPC liposomes in NaCl, images A and B are taken from different areas of the TEM grid and these images were selected as they are most representative of the entire grid. For completeness, Appendix K shows additional TEM images of DOPC liposomes in NaCl. In order to ensure that the samples were suitable for TEM, DLS measurements were taken beforehand. The DLS measurements show that the liposomes in the presence of NaCl have a Z-average size d = 127.6 nm and PdI = 0.06. The liposomes shown in Figure 69 (A) are mostly uni-lamellar (yellow arrows) although one bi-lamellar liposome can also be clearly seen. In Figure 69 (B) the liposomes appear to be more varied. There are unilamellar and bilamellar liposomes, but interestingly, there are also multilamellar (blue arrow) and multivesicular liposomes (red arrows). As can be seen, the organisation of the lamellae in the vesicles can be complex. However, in most cases there appears to be two or three lamellae present, usually one or two smaller structures contained inside a larger unilamellar vesicle. The TEM images support the DLS data obtained for this system, in both images, the unilamellar and bilamellar liposomes size are d ~ 125 nm, and the multivesicular and multilamellar liposomes appear to be slightly larger. Furthermore, from the images, it is clear to see that the suspension is largely monodisperse, in close agreement with the very low value of the PdI obtained, as measured by DLS. It can also be concluded from TEM that the liposomes are predominantly spherical in shape in the presence of NaCl, although undergo slight shape modifications on the formation of multivesicular liposomes.

A vast amount of cryo-TEM has been reported in the literature on liposomes and other phospholipid structures; however, there is a lack of images collected which show the effect of salts on the morphology of liposomes comprised of a single lipid. Zidovska et al. [214] studied the effect of NaCl on block liposomes made of cationic lipid MVLBG2 and DOPC in aqueous systems using cryo TEM. It was found that in the low-salt regime, NaCl promoted the formation of primarily bilamellar vesicles. The outer bilayer was observed to wrap around the inner vesicle at a constant intralamellar distance. Although the vesicles observed in this work do not appear to possess constant intralamellar distances, it is encouraging that the results obtained in this work are similar to those observed by Zidovska *et al*. which support the notion that salt promotes the formation of multilamellar and multivesicular liposomes.

In order to understand this effect more fully it is important to consider the interactions between the cations and the phospholipids. The zeta potential measurements discussed in Section 4.1 confirm that the cations associate with the head groups of the phospholipids and screen the electrostatic charges between neighbouring lipid molecules. It is also likely therefore, that the presence of salt screens the electrostatic interactions between the lipid bilayers, and therefore reduces the repulsion between bilayers and as a consequence, allowing the formation of an increased number of multilamellar and

multivesicular liposomes[214]. Whilst this effect is observed in the presence NaCl, it is possible that as the cations are only singly charged they can only screen the repulsion between bilayers a sufficient amount in order to form bilamellar liposomes as opposed to multilamellar vesicles. This is supported by the zeta potential data, as at this low NaCl concentration (*I*= 5 mM), the liposomes still have a fairly negative value of the zeta potential (ξ ~ -9 mV) and therefore there is still substantial repulsion between the lipid bilayers. It is for these reasons that there are still a large number of unilamellar liposomes in the system.

Figure 70 shows TEM images of DOPC liposomes prepared in the presence of $CaCl_2$ (*I*=5 mM). Images A, B and C are taken from different areas of the TEM grid and these images were selected as they are most representative of the entire grid. The liposomes in the presence of $CaCl_2$ had a Z-average size of 134.4 nm and PdI of 0.189, as measured by DLS.

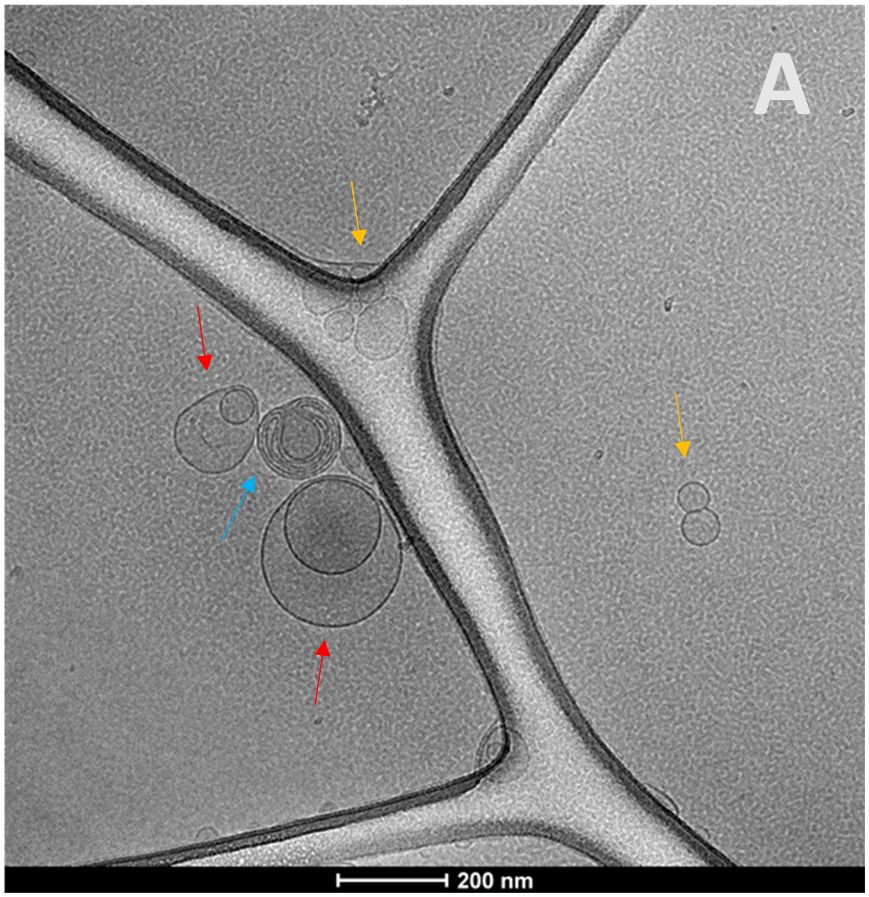

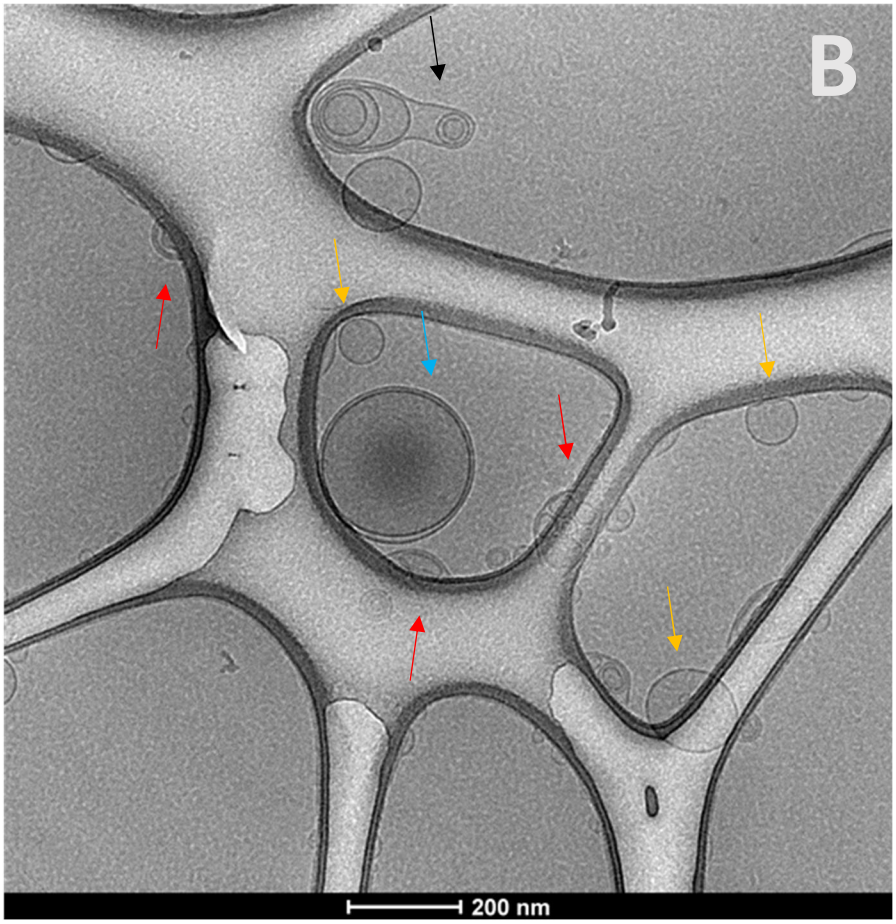

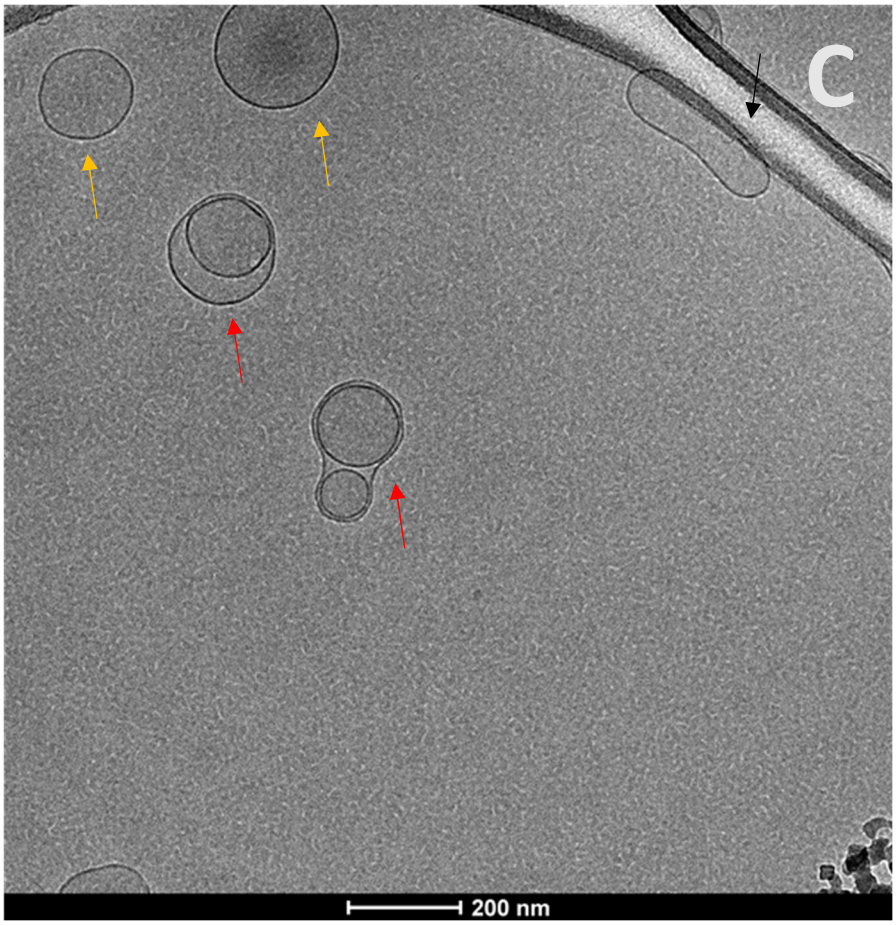

Figure 70: Cryo-TEM images of sonicated and extruded DOPC liposomes in the presence of $CaCl_2$ (I = 5 mM). The scale bar shown is 200 nm. Images A, B and C are taken from different areas of the TEM grid.

Figure 70 (A) shows that in the presence of $CaCl_2$, the liposomes formed possess a fairly wide range of sizes and lamellarities. A number of smaller, unilamellar liposomes can be seen, which have sizes of between 50 nm and 150 nm (yellow arrows). In addition, two larger multivesicular liposomes can also be seen clearly (red arrows) as well as a multi-lamellar liposome (blue arrow) which appears to have lamellae wrapped around an aqueous core, enclosed by a single lamellar. Interestingly, the inner lamellae have not joined together with one another at their ends and therefore appear as a multi-lamellar 'worm like' structure which curves into a spherical shape. Figure 70 (B) shows another area of the TEM grid in the DOPC-$CaCl_2$ system. In this image, a wide range of liposomes are observed, supporting the DLS data which found that the Ca^{2+} ions cause the liposome suspension to become slightly polydisperse (PdI = 0.189). There are a number of smaller unilamellar vesicles (yellow arrows) and an abundance of multivesicular liposomes (red arrows), which have varying sizes, in addition to a large bilamellar liposome which can be seen clearly in the centre of the image (blue arrow). The uni- and bilamellar liposomes observed are spherical whilst the multivesicular liposomes tend to vary more in their shape, appearing fairly spherical, however also forming cylindrical shaped structures on occasion (black arrows). These cylindrical shaped structures are also unmistakably observed in Figure 70 (C), which also shows unilamellar and multivesicular liposomes.

It is clear from the TEM images observed that the presence of $CaCl_2$ causes the liposomes to form more polydisperse suspensions than in the presence of NaCl or in pure water, which is consistent with the DLS data recorded for these systems. Additionally, it is apparent that a larger number of multivesicular liposomes are formed, as well as cylindrical shaped liposomes. It can be hypothesised that the formation of a higher number of these types of structures is due to the reduced repulsion between the lamellae, as a consequence of cation association with the head group of the phospholipids in the liposomes. As a result of its divalent charge, Ca^{2+} can more effectively reduce the repulsion between lamellae than Na^+ and therefore the lamellae are more likely to pack more closely together and form multivesicular structures. This effect also explains the formation of larger liposomes and the higher polydispersity of this system, compared with the DOPC-water and DOPC-NaCl systems, as the closer packing of lipids will cause an increase in bending energy during the formation of the liposomes which will result in more larger liposomes being formed. The zeta potential data discussed in Section 4.1**,** also supports this hypothesis as the zeta potential of the liposomes in the presence of $CaCl_2$ (I =5 mM) was found to be ξ ~ 2.5 mV. This zeta potential value is less positive than the zeta potential for DOPC liposomes in NaCl is negative, and therefore it is for this reason that the number of unilamellar liposomes formed is greater in the presence of NaCl than $CaCl_2$.

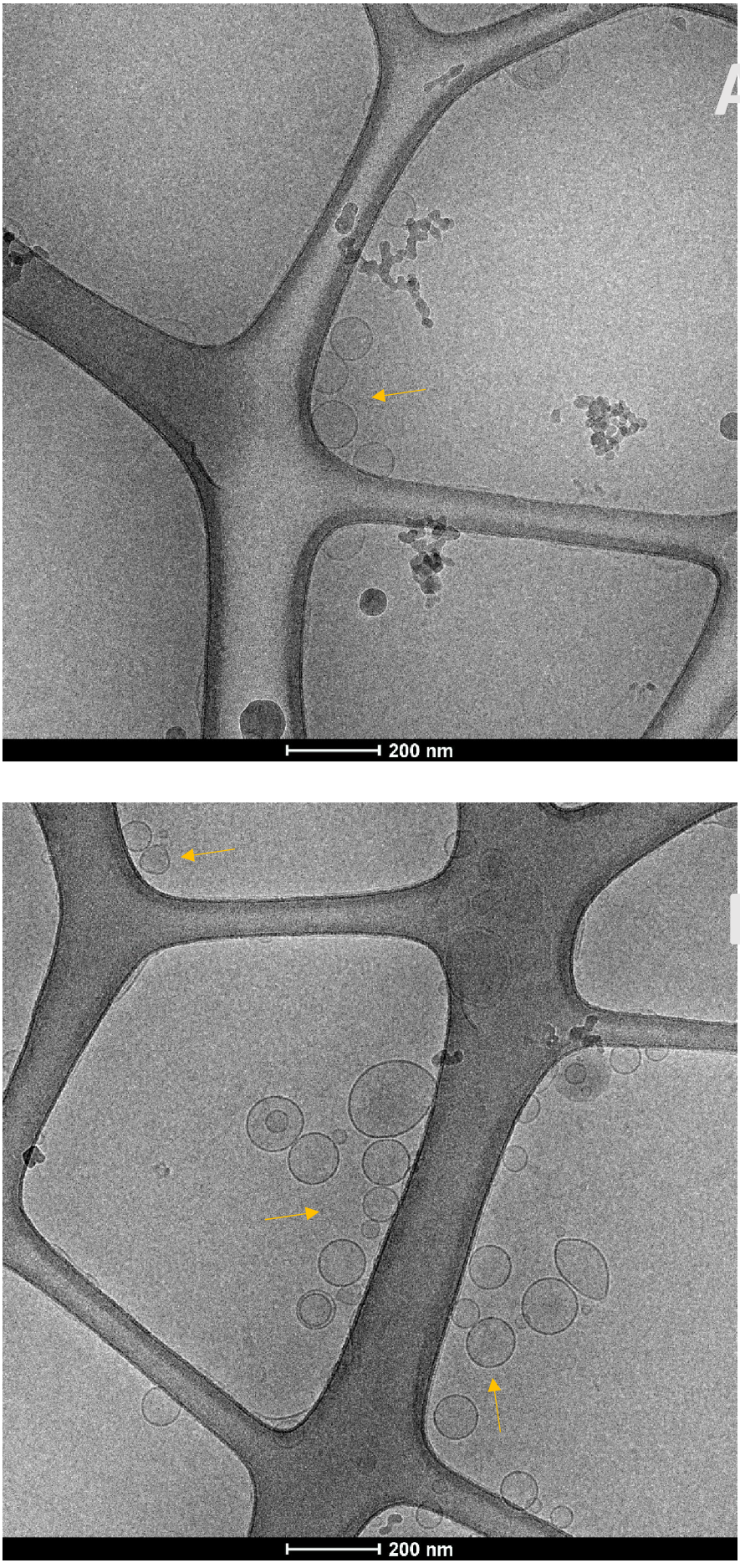

Figure 71: Cryo-TEM images of sonicated and extruded DOPC liposomes in the presence of $LaCl_3$ (I = 5 mM). The scale bar shown is 200 nm. Images A and B are taken from different areas of the same TEM grid.

Figure 71 shows Cryo-TEM images of DOPC liposomes in the presence of $LaCl_3$ (I = 5 mM). From the images in Figure 71 it can be concluded that the DOPC liposomes formed in the presence of La^{3+} are mostly unilamellar and spherical in shape (yellow arrows). The liposomes appear to possess a wide range of sizes, which is in agreement with the DLS measurement of PdI = 0.229 obtained for this suspension. In order to explain the effect of La^{3+} on the formation of DOPC liposomes, as with the previous two images, it is important to consider the zeta potential of the liposomes in this system. The zeta potential of the DOPC liposomes at La^{3+} (I=5 mM) is ξ ~ 23 mV which is a far higher value than the values for the zeta potential of the liposomes observed in the presence of NaCl and $CaCl_2$ respectively. The large, positive zeta potential value is a consequence of association of the trivalent cations with the head groups of the phospholipids on formation of the liposome. As a result of this strong affinity of the ion to the lipid head, the lipid bilayers formed become highly charged and therefore repel each other to a greater degree than in the presence of Na^+ and Ca^{2+}, hence, more unilamellar liposomes are formed than multilamellar or multivesicular. Comparing all of the TEM images obtained it is also evident that the liposomes in the presence of $CaCl_2$ and $LaCl_3$ seem to be found close to the lacey carbon instead of in ice in the centre of the grid. Since the lacey carbon has a slight negative charge, the liposomes in the presence of higher valency cations are attracted to it and therefore are found in higher densities surrounding it.

From the TEM images obtained in this project, it can be concluded that the presence of cations has a profound effect on the lamellarity and polydispersity of the DOPC liposomes. DOPC liposomes formed in pure water are unilamellar and spherical and the presence of Na^+ causes a small number of multilamellar and multivesicular liposomes to be formed. Liposomes formed in the presence of La^{3+} are also spherical and mainly unilamellar, owing to the increased electrostatic repulsion between lamellae and vesicles. Ca^{2+} promoted the formation of a large number of multilamellar and multivesicular liposomes and also a small number of cylindrical structures. It is likely that the close zero value of the zeta potential causes the least repulsion between lamellae and therefore allows the formation of more complex phospholipid vesicular structures. The images obtained for the DOPC liposomes in water are consistent with the literature and the liposome-salt suspensions allow us to collect novel cryo-TEM images and obtain additional morphological information about the liposomes which has not been reported previously. Overall we can conclude with confidence that DOPC liposomes formed in the presence of all three salts were largely spherical and therefore strongly support the DLS data obtained in this project. Without TEM, significantly less information on the morphology of the liposomes would have been obtained and therefore it was an exceptionally beneficial technique and extremely valuable to this project.

Chapter 8: Conclusions and future works

8.1. Conclusion

Specific ion effects are universal in many branches of science and understanding how ions interact with other molecules is vital to helping comprehend numerous biological and chemical processes. Since Franz Hofmeister began studying the effects of anions and cations on proteins in aqueous solutions in 1888, specific ion effects have been a prominent, and growing, area of research in physical and colloid chemistry. The Hofmeister (or lyotropic) series of simple inorganic cations or anions is the most common established, qualitative scale of specific ion effects, which holds true (in its forward or reversed form) for an exceptionally broad range of phenomena at interfaces, in the bulk, and in biological systems.

Since this fascinating series was first proposed, attempts have been made to help explain the positioning of ions within the sequence and the interactions at play. Presented initially by Hofmeister himself, the rationalization of specific ion effects on 'general' solutes, in terms of the interactions of the salts with water and the classification of ions as either 'kosmotropes' or 'chaotropes', falls short in providing an explanation for the ordering of the ions in the series. Although the simplicity of this explanation is appealing, the importance of considering more complex interactions is vital in order to rationalise the Hofmeister series. In particular, there are many questions raised in the literature regarding the role of water molecules when studying specific ion effects in aqueous systems, the hydration of ions, dispersion forces, ion pairing and hydrophobicity.

That being said, ideas have emerged which have influenced and progressed the way scientists think about specific ion effects. One of the most profound examples was the ion-pairing hypothesis presented by Collins in 1997, known as the 'Law of matching water affinities'. The hypothesis evolved from electrolyte hydration enthalpies, and considers the hydration sheaths around ions and the ease at which ions shed the water molecules from their hydration shells in order to form contact ion pairs in bulk electrolytes. This hypothesis was then later elaborated for interfacial systems containing molecules with charged head groups and is now a very valuable tool to explain experimental results in systems influenced largely by ion hydration and ion pair formation where ionic interactions dominate. Nevertheless, despite growing interest in specific ion effects, the mechanism for the Hofmeister series remains to be fully understood. Scientists are yet to be able to unravel the complex interactions which exist when studying specific ion effects and hence, the Hofmeister series remains a largely unknown entity.

This project was carried out in order to begin to understand the ordering of ions in the Hofmeister series more comprehensively, and highlight which interactions are important in understanding specific ion effects. In this project we hoped that progress would be made through the design and execution of simple experiments on model systems which would provide useful information allowing us to investigate a small number of interactions occurring in soft matter systems at one time. In particular, the aim of this work was to shed light on if, and how, hydration influences specific ion effects and the ordering of ions in the Hofmeister series. In this project, lipids were used as probe systems. Liposomes made of zwitterionic lipids, DOPC or DPPC, were prepared and the effects of inorganic and organic salts on the zeta potential, size and polydispersity of the liposomes were studied using two main techniques, dynamic light scattering and cryo-transmission electron microscopy. In addition, the effect of temperature was considered. The aim of this work was to observe, understand and explain the molecular interactions which occur between ions and liposomes and shed light on specific ion effects and the ordering of ions in the Hofmeister series.

From the study of the effect of inorganic cations on DOPC liposomes, TEM images confirm that liposomes are formed in the presence of the salts and the DLS results indicate that all of the cations associate with the head groups of the phospholipids via electrostatic interactions. The positively charged cations are attracted to the negatively charged phosphate groups of the DOPC lipids, as demonstrated by the increase in the zeta potential in the presence of cations. The electrostatic attraction between the cations and the lipid head groups increases according to the series $Li^+ < Cs^+ \approx K^+ < Na^+ < Mg^{2+} < Ca^{2+} < La^{3+}$ (i.e. monovalent < divalent < trivalent), in line with increasing charge and charge density of the cations. From the size and zeta potential results it can be concluded that saturation of the lipid head group occurs in the presence of di- and trivalent cations but not in the presence of any of the monovalent cations studied in this work. It is likely that entropic factors contribute to the association of the ions with the head groups of the phospholipids, as water molecules in the hydration sheath of the lipid and ion are liberated into the bulk on association.

Additionally, as a result of the adsorption of the cations to the head group of the lipids, it is likely there is a change in the orientation of the lipid head groups as well as reduced repulsion between neighbouring lipid molecules which affects the bending energy of the lipid bilayer during the formation of the liposomes, as a consequence, the size of the liposomes themselves. The size of the liposomes is also affected by non-specific bulk effects and possible osmotic effects at high ion concentrations, evident from the TEM images obtained.

From the results obtained in this work on the effect of inorganic cations on DOPC liposomes, information can be attained regarding specific ion effects and the Hofmeister series. The cations with higher valencies which are strongly hydrated were found to exhibit stronger interactions with the

DOPC liposomes and saturate the head groups of the phospholipids within the liposomes more quickly (such as La^{3+}, Ca^{2+} and Mg^{2+}, which have decreasing charge density: $La^{3+} > Ca^{2+} > Mg^{2+}$). Although care must be taken when classifying ions according to such simple theories, it is interesting to consider the classifications proposed by Hofmeister himself. From the results obtained in this work, La^{3+}, Ca^{2+} and Mg^{2+} can be known as 'kosmotropes' or 'hard' cations.

This conclusion agrees closely with the aforementioned Collins' law of matching water affinities, which classifies the phosphate group of the DOPC lipid as a 'hard' group and therefore would predict interactions of this kind to be likely. On the other hand, cations with a lower valency and charge density which are more weakly hydrated (Such as Li^+, Cs^+, K^+ and Na^+) were found to demonstrate weaker interactions with the DOPC liposomes. These cations can be referred to as 'soft' or 'chaotropic' in the context of this project.

From the results obtained in Chapter 4, on the effects of inorganic cations on DOPC liposomes, it can be hypothesised that entropic effects play a significant role in the ordering of ions in the Hofmeister series. As the cations associate with the lipids, the favourable interactions formed between liberated water molecules in the bulk is likely to be a significant contributing factor to the aforementioned association. The results obtained in Chapter 5 on the effects of organic, hydrophobic ions (TPB- and TPP+) on DOPC liposomes appear to support this hypothesis, highlighting the importance of the hydrophobic effect in specific ion effects. The vast change in the zeta potential of the DOPC liposomes, even at very low hydrophobic ion concentration, is likely to be driven by electrostatic interaction between the central atom and the lipid head group, the entropic effect of liberating water molecules into the bulk, and the binding of the lipid tails to the hydrophobic phenyl groups of the ions. From these results it can be concluded that the organic, hydrophobic ions have a greater effect on the DOPC liposomes than the inorganic cations (organic ions > inorganic cations) and additionally, that the role of water is vital in specific ion effects and the ordering of ions in the Hofmeister series.

In Chapter 6 further investigation was carried out into the effect of trivalent cations on liposomes, in order to more closely examine the effects of cations, with high valencies, which are more strongly hydrated. This work presents some interesting and unique results indicating potential hydrolysis of hydrated iron complexes to form slightly acidic solutions which induce exceptionally high zeta potential and PdI values of the liposomes. Additionally, it was hypothesised that potential oxidation of phospholipid molecules could have caused structural changes in the liposomes in the presence of Fe^{3+}. These results were very interesting as little work has been carried out which focuses specifically on the effects of trivalent cations. From this chapter, the results indicate that it is vital to consider the behaviour of the ions themselves in water, as unique ion behaviour can result in more complex and varied interactions. Overall, the trivalent cations were found to affect the DPPC liposomes in an

increasing fashion according to the series La^{3+} < Cr^{3+}< Fe^{3+}. Again, these results highlight the importance of considering the role of water as a solvent when examining the effects of cations on liposomes and can also validate that the role of water is important when describing and explaining specific ion effects.

The final part of this work involved investigation into how changes in temperature affect the size and PdI of DOPC and DPPC liposomes in pure water, and in the presence of mono-, di- and trivalent cations. The results of this chapter indicate that the most important effect induced by cations on the DPPC liposomes is the effect on the transition temperature of the lipids. As the valency of the ion increases, the ions were found to more effectively stabilize the liposomes when the system was exposed to vast changes in temperature. The transition temperatures themselves and the breadth of the transition temperatures were affected by the ions in all three cases. It can be concluded, therefore, that the stabilising effect of the cations against changes in temperature, is of the order Na^{+} <Ca^{2+} < La^{3+}. This series is in line with the Hofmeister series and agrees closely with the results from other similar work conducted on these effects.

To summarize, our results have provided molecular insight into the interactions between ions and liposomes, and an investigation into the mechanism of the Hofmeister series has been carried out. This work has allowed us to observe, understand and explain the molecular interactions which occur between ions and liposomes. The information provided by these studies will help improve our understanding of specific ion effects, in particular the effects of ions on biological molecules, and pave the way for future research of this kind. This work also helps to shed light on the mechanism of the Hofmeister series, a complex and thus far unexplained phenomena at the heart of colloid chemistry.

8.2. Future work

The experimental methods in this work have employed dynamic light scattering and cryo-transmission electron microscopy, and the studies have focused the molecular interactions between ions and liposomes. It would be interesting and useful to use other complementary techniques to confirm the results we have obtained so far and add further insights to our interpretations. Additionally, it would also be valuable to use other experimental systems, in order to gain more information and insight into the Hofmeister series.

Firstly, it would be beneficial to confirm the hypothesis that entropic factors are significant in driving the association of the ions with the lipid head groups of the liposomes. The binding affinity and thermodynamics of the biomolecular interactions can be quantitatively examined using isothermal titration calorimetry (ITC). ITC works by directly determining the heat that is absorbed or released during the binding of the ion to the liposome. ITC would be suitable for our experimental setup as it can determine the binding parameters through a single experiment with little modification to the sample. Measuring the transfer of heat during the binding of ions to liposomes would allow the binding constant (K_D), the reaction enthalpy (ΔH) and entropy (ΔS) to be accurately determined, providing a thermodynamic outline of the molecular interaction occurring. It is a technique widely used to investigate the thermodynamics of binding kinetics[169, 215] and therefore would be very appropriate to use ITC in future work related to this study in order to clarify more about the mechanisms underlying the specific ion effects.

It would also be beneficial to take further advantage of cryo-transmission electron microscopy, as only a limited number of images were obtained in this project. In particular, it would be exceptionally interesting to obtain cryo-TEM images of DOPC liposomes in the presence of the organic ions in order to confirm the structural changes that occur in the bilayer induced by hydrophobic ions as well as gain further insight into the exact binding location of the ions.

Secondly, modifications could be made to the systems studied in this work, which would allow a more extensive understanding of the effects of ions on liposomes. In this project, exceptionally low ion concentrations were used; it would be interesting to examine how higher concentrations of ions affect the liposomes. By studying higher concentrations of salts and the effect that they have on liposomes, it would also be possible to draw more comparisons with studies carried out in the literature, as many of these focus on salt concentrations up to and including 1 M. Additionally, in order to obtain more biologically relevant results, intracellular or extracellular ion concentrations could be examined. Not only would this be exceptionally interesting, using modified liposomes (for example, incorporating

cholesterol into the bilayer) would allow the work to reveal information about specific ion effects in the cell membrane.

Zwitterionic lipids were chosen in this work as they offer the important benefit that the ion-lipid coulombic interaction is strongly reduced and therefore the secondary interactions are made more visible. It would be interesting to study the effects of ions on liposomes comprised of phospholipids which possess similar types of lipid chain structure but have different head groups, for example, liposomes comprised of phosphatidylethanolamines or negatively charged phosphatidylserines. This type of work would allow closer investigation into the subtle ion lipid head group interactions, which have been found to be vital in the association of the ions with the liposomes in this work.

This further work would facilitate greater insight into the effect of ions on liposomes, allow a deeper understanding the Hofmeister series, and be useful for fundamental research into specific ion effects and biophysical interactions.

8.3. References

[1] Theophanides, T. (1984) Metal ions in biological system, *International Journal of Quantum Chemistry 26*, 933-941.

[2] Szent-Györgyi, A. G. (1975) Calcium regulation of muscle contraction, *Biophysical Journal 15*, 707-723.

[3] Rhoades, R., and Bell, D. R. (2009) *Medical Physiology: Principles for Clinical Medicine*, Lippincott Williams & Wilkins.

[4] Solomon, E. P. (2015) *Introduction to Human Anatomy and Physiology*, Elsevier - Health Sciences Division.

[5] Sizer, F., and Whitney, E. (2007) *Nutrition: Concepts and Controversies*, Cengage Learning.

[6] Lack, A. J., and Evans, D. E. (2005) *Plant Biology*, Taylor & Francis.

[7] Kunz, W., Henle, J., and Ninham, B. W. (2004) 'Zur Lehre von der Wirkung der Salze' (about the science of the effect of salts): Franz Hofmeister's historical papers, *Current Opinion in Colloid & Interface Science 9*, 19-37.

[8] Xie, W., Liu, C., Yang, L., and Gao, Y. (2014) On the molecular mechanism of ion specific Hofmeister series, *Science China Chemistry 57*, 36-47.

[9] Xie, W. J., and Gao, Y. Q. (2013) A Simple Theory for the Hofmeister Series, *Journal of Physical Chemistry Letters 4*, 4247-4252.

[10] Leontidis, E. (2016) Chaotropic salts interacting with soft matter: Beyond the lyotropic series, *Current Opinion in Colloid & Interface Science 23*, 100-109.

[11] Pinna, M. C., Salis, A., Monduzzi, M., and Ninham, B. W. (2005) Hofmeister Series: The Hydrolytic Activity of Aspergillus niger Lipase Depends on Specific Anion Effects, *The Journal of Physical Chemistry B 109*, 5406-5408.

[12] Breschi, G. L., Cametti, M., Mastropietro, A., Librizzi, L., Baselli, G., Resnati, G., Metrangolo, P., and de Curtis, M. (2013) Different Permeability of Potassium Salts across the Blood-Brain Barrier Follows the Hofmeister Series, *PLOS ONE 8*, e78553.

[13] Li, R., Jiang, Z., Chen, F., Yang, H., and Guan, Y. (2004) Hydrogen bonded structure of water and aqueous solutions of sodium halides: a Raman spectroscopic study, *Journal of Molecular Structure 707*, 83-88.

[14] Rashin, A. A., and Honig, B. (1985) Reevaluation of the Born model of ion hydration, *The Journal of Physical Chemistry 89*, 5588-5593.

[15] Roux, B., Yu, H. A., and Karplus, M. (1990) Molecular basis for the Born model of ion solvation, *The Journal of Physical Chemistry 94*, 4683-4688.

[16] Lo Nostro, P., and Ninham, B. W. (2012) Hofmeister Phenomena: An Update on Ion Specificity in Biology, *Chemical Reviews 112*, 2286-2322.

[17] Atkins, P., and de Paula, J. (2010) *Atkins' Physical Chemistry*, OUP Oxford.

[18] Bockris, J. (2012) *Modern Electrochemistry: An Introduction to an Interdisciplinary Area*, Springer US.

[19] Chang, R. (2005) *Physical Chemistry for the Biosciences*, University Science Books.

[20] Tyagi, P. (2006) *Electrochemistry*, Discovery Publishing House.

[21] Salis, A., and Ninham, B. W. (2014) Models and mechanisms of Hofmeister effects in electrolyte solutions, and colloid and protein systems revisited, *Chem Soc Rev 43*, 7358-7377.

[22] Outhwaite, C. W. (1969) Extension of the Debye–Hückel Theory of Electrolyte Solutions, *The Journal of Chemical Physics 50*, 2277-2288.

[23] Abbas, Z., Gunnarsson, M., Ahlberg, E., and Nordholm, S. (2002) Corrected Debye−Hückel Theory of Salt Solutions: Size Asymmetry and Effective Diameters, *The Journal of Physical Chemistry B 106*, 1403-1420.

[24] Cosgrove, T. (2010) *Colloid Science: Principles, Methods and Applications*, John Wiley & Sons.

[25] Lo Nostro, P., and Ninham, B. W. (2016) Editorial: Electrolytes and specific ion effects. New and old horizons, *Current Opinion in Colloid & Interface Science 23*, A1-A5.
[26] Ninham, B. W. (1999) On progress in forces since the DLVO theory, *Advances in Colloid and Interface Science 83*, 1-17.
[27] Kunz, W. (2010) Specific ion effects in colloidal and biological systems, *Current Opinion in Colloid & Interface Science 15*, 34-39.
[28] Cao, G. (2004) *Nanostructures & Nanomaterials: Synthesis, Properties & Applications*, Imperial College Press.
[29] Boström, M., Williams, D. R. M., and Ninham, B. W. (2001) Specific Ion Effects: Why DLVO Theory Fails for Biology and Colloid Systems, *Physical Review Letters 87*, 168103.
[30] Collins, K. D. (1995) Sticky ions in biological systems, *Proceedings of the National Academy of Sciences of the United States of America 92*, 5553-5557.
[31] Collins, K. D. (2004) Ions from the Hofmeister series and osmolytes: effects on proteins in solution and in the crystallization process, *Methods 34*, 300-311.
[32] Collins, K. D. (1997) Charge density-dependent strength of hydration and biological structure, *Biophysical Journal 72*, 65-76.
[33] Lund, M., Vrbka, L., and Jungwirth, P. (2008) Specific Ion Binding to Nonpolar Surface Patches of Proteins, *Journal of the American Chemical Society 130*, 11582-11583.
[34] Patil, R. S., Shaikh, V. R., Patil, P. D., Borse, A. U., and Patil, K. J. (2014) The viscosity B and D coefficient (Jones–Dole equation) studies in aqueous solutions of alkyltrimethylammonium bromides at 298.15 K, *Journal of Molecular Liquids 200, Part B*, 416-424.
[35] Jenkins, H. D. B., and Marcus, Y. (1995) Viscosity B-Coefficients of Ions in Solution, *Chemical Reviews 95*, 2695-2724.
[36] Baldwin, R. L. (1996) How Hofmeister ion interactions affect protein stability, *Biophysical Journal 71*, 2056-2063.
[37] He, L., Cai, S., Wu, B., Mu, C., Zhang, G., and Lin, W. (2012) Trivalent chromium and aluminum affect the thermostability and conformation of collagen very differently, *Journal of Inorganic Biochemistry 117*, 124-130.
[38] Von Hippel, P. H., and Schleich, T. (1969) Ion effects on the solution structure of biological macromolecules, *Accounts of Chemical Research 2*, 257-265.
[39] Ni, N., and Yalkowsky, S. H. (2003) Prediction of Setschenow constants, *International Journal of Pharmaceutics 254*, 167-172.
[40] Marcus, Y. (2015) *Ions in Solution and Their Solvation*, Wiley.
[41] Lee, J. D. (1991) *Concise Inorganic Chemistry*, Springer US.
[42] Clugston, M., and Flemming, R. (2000) *Advanced Chemistry*, OUP Oxford.
[43] Weller, M., Overton, T., Rourke, J., and Armstrong, F. (2014) *Inorganic Chemistry*, OUP Oxford.
[44] Vlachy, N., Jagoda-Cwiklik, B., Vácha, R., Touraud, D., Jungwirth, P., and Kunz, W. (2009) Hofmeister series and specific interactions of charged headgroups with aqueous ions, *Advances in Colloid and Interface Science 146*, 42-47.
[45] Kramer, Ryan M., Shende, Varad R., Motl, N., Pace, C N., and Scholtz, J M. (2012) Toward a Molecular Understanding of Protein Solubility: Increased Negative Surface Charge Correlates with Increased Solubility, *Biophysical Journal 102*, 1907-1915.
[46] Zhang, Y., and Cremer, P. S. (2006) Interactions between macromolecules and ions: the Hofmeister series, *Current Opinion in Chemical Biology 10*, 658-663.
[47] Omta, A. W., Kropman, M. F., Woutersen, S., and Bakker, H. J. (2003) Negligible Effect of Ions on the Hydrogen-Bond Structure in Liquid Water, *Science 301*, 347-349.
[48] Paterová, J., Rembert, K. B., Heyda, J., Kurra, Y., Okur, H. I., Liu, W. R., Hilty, C., Cremer, P. S., and Jungwirth, P. (2013) Reversal of the Hofmeister Series: Specific Ion Effects on Peptides, *The Journal of Physical Chemistry B 117*, 8150-8158.

[49] Boström, M., Parsons, D. F., Salis, A., Ninham, B. W., and Monduzzi, M. (2011) Possible Origin of the Inverse and Direct Hofmeister Series for Lysozyme at Low and High Salt Concentrations, *Langmuir 27*, 9504-9511.
[50] Zhang, Y., and Cremer, P. S. (2009) The inverse and direct Hofmeister series for lysozyme, *Proceedings of the National Academy of Sciences 106*, 15249-15253.
[51] Schwierz, N., Horinek, D., and Netz, R. R. (2013) Anionic and Cationic Hofmeister Effects on Hydrophobic and Hydrophilic Surfaces, *Langmuir 29*, 2602-2614.
[52] Bilaničová, D., Salis, A., Ninham, B. W., and Monduzzi, M. (2008) Specific Anion Effects on Enzymatic Activity in Nonaqueous Media, *The Journal of Physical Chemistry B 112*, 12066-12072.
[53] Peruzzi, N., Ninham, B. W., Lo Nostro, P., and Baglioni, P. (2012) Hofmeister Phenomena in Nonaqueous Media: The Solubility of Electrolytes in Ethylene Carbonate, *The Journal of Physical Chemistry B 116*, 14398-14405.
[54] Mazzini, V., and Craig, V. S. J. (2016) Specific-ion effects in non-aqueous systems, *Current Opinion in Colloid & Interface Science 23*, 82-93.
[55] Whitesides, G. M., Mathias, J. P., and Seto, C. T. (1991) Molecular self-assembly and nanochemistry: a chemical strategy for the synthesis of nanostructures, *Science 254*, 1312.
[56] Buehler, L. (2015) *Cell Membranes*, Taylor & Francis Group.
[57] Bilalov, A., Olsson, U., and Lindman, B. (2012) Complexation between DNA and surfactants and lipids: phase behavior and molecular organization, *Soft Matter 8*, 11022-11033.
[58] Whitesides, G. M., and Boncheva, M. (2002) Beyond molecules: Self-assembly of mesoscopic and macroscopic components, *Proceedings of the National Academy of Sciences 99*, 4769-4774.
[59] Boundless (2016) *Boundless Biology*.
[60] Li, J., Wang, X., Zhang, T., Wang, C., Huang, Z., Luo, X., and Deng, Y. (2015) A review on phospholipids and their main applications in drug delivery systems, *Asian Journal of Pharmaceutical Sciences 10*, 81-98.
[61] Aroti, A., Leontidis, E., Dubois, M., Zemb, T., and Brezesinski, G. (2007) Monolayers, bilayers and micelles of zwitterionic lipids as model systems for the study of specific anion effects, *Colloids and Surfaces A: Physicochemical and Engineering Aspects 303*, 144-158.
[62] Huque, E. M. (1989) The hydrophobic effect, *Journal of Chemical Education 66*, 581.
[63] Lazaridis, T. (2001) Hydrophobic Effect, In *eLS*, John Wiley & Sons, Ltd.
[64] Schneck, E., Sedlmeier, F., and Netz, R. R. (2012) Hydration repulsion between biomembranes results from an interplay of dehydration and depolarization, *Proceedings of the National Academy of Sciences of the United States of America 109*, 14405-14409.
[65] Paunov, V. N., Dimova, R. I., Kralchevsky, P. A., Broze, G., and Mehreteab, A. (1996) The Hydration Repulsion between Charged Surfaces as an Interplay of Volume Exclusion and Dielectric Saturation Effects, *Journal of Colloid and Interface Science 182*, 239-248.
[66] Guida, V. (2010) Thermodynamics and kinetics of vesicles formation processes, *Advances in Colloid and Interface Science 161*, 77-88.
[67] Sironi, B. (2016) Lipid Adsorption at Interfaces: A Synchrotron X-Ray Reflectivity Study, p 210, University of Bristol, Faculty of Science, School of Chemistry.
[68] Israelachvili, J. N., Mitchell, D. J., and Ninham, B. W. (1977) Theory of self-assembly of lipid bilayers and vesicles, *Biochimica et Biophysica Acta (BBA) - Biomembranes 470*, 185-201.
[69] Israelachvili, J. N., Mitchell, D. J., and Ninham, B. W. (1976) Theory of self-assembly of hydrocarbon amphiphiles into micelles and bilayers, *Journal of the Chemical Society, Faraday Transactions 2: Molecular and Chemical Physics 72*, 1525-1568.
[70] Balazs, D. A., and Godbey, W. (2011) Liposomes for Use in Gene Delivery, *Journal of Drug Delivery 2011*.
[71] Antonietti, M., and Förster, S. (2003) Vesicles and Liposomes: A Self-Assembly Principle Beyond Lipids, *Advanced Materials 15*, 1323-1333.

[72] Zhang, J., Li, X., and Li, X. (2012) Stimuli-triggered structural engineering of synthetic and biological polymeric assemblies, *Progress in Polymer Science 37*, 1130-1176.
[73] Šegota, S., and Težak, D. u. i. (2006) Spontaneous formation of vesicles, *Advances in Colloid and Interface Science 121*, 51-75.
[74] Akbarzadeh, A., Rezaei-Sadabady, R., Davaran, S., Joo, S. W., Zarghami, N., Hanifehpour, Y., Samiei, M., Kouhi, M., and Nejati-Koshki, K. (2013) Liposome: classification, preparation, and applications, *Nanoscale Research Letters 8*, 9.
[75] Jesorka, A., and Orwar, O. (2008) Liposomes: technologies and analytical applications, *Annu Rev Anal Chem (Palo Alto Calif) 1*, 801-832.
[76] Gregoriadis, G., Leathwood, P. D., and Ryman, B. E. (1971) Enzyme entrapment in liposomes, *FEBS Letters 14*, 95-99.
[77] Keller, B. C. (2001) Liposomes in nutrition, *Trends in Food Science & Technology 12*, 25-31.
[78] Faure, C., Meyre, M.-E., Trépout, S., Lambert, O., and Lebraud, E. (2009) Magnetic Multilamellar Liposomes Produced by In Situ Synthesis of Iron Oxide Nanoparticles: “Magnetonions”, *The Journal of Physical Chemistry B 113*, 8552-8559.
[79] Massing, U., and Fuxius, S. (2000) Liposomal formulations of anticancer drugs: selectivity and effectiveness, *Drug Resistance Updates 3*, 171-177.
[80] Andresen, T. L., Jensen, S. S., and Jørgensen, K. (2005) Advanced strategies in liposomal cancer therapy: Problems and prospects of active and tumor specific drug release, *Progress in Lipid Research 44*, 68-97.
[81] Seltzer, S. E. (1989) The role of liposomes in diagnostic imaging, *Radiology 171*, 19-21.
[82] Schwendener, R. A. Liposomes as vaccine delivery systems: a review of the recent advances.
[83] Lasic, D. D. (1998) Novel applications of liposomes, *Trends in Biotechnology 16*, 307-321.
[84] Moussaoui, N., Cansell, M., and Denizot, A. (2002) Marinosomes®, marine lipid-based liposomes: physical characterization and potential application in cosmetics, *International Journal of Pharmaceutics 242*, 361-365.
[85] Schreier, H., and Bouwstra, J. (1994) Liposomes and niosomes as topical drug carriers: dermal and transdermal drug delivery, *Journal of Controlled Release 30*, 1-15.
[86] Marsanasco, M., Márquez, A. L., Wagner, J. R., del V. Alonso, S., and Chiaramoni, N. S. (2011) Liposomes as vehicles for vitamins E and C: An alternative to fortify orange juice and offer vitamin C protection after heat treatment, *Food Research International 44*, 3039-3046.
[87] Karp, G. (2009) *Cell and Molecular Biology: Concepts and Experiments*, John Wiley & Sons.
[88] Cooper, G. M. (2000) *The Cell: A Molecular Approach*, ASM Press.
[89] Bangham, A. D. (1972) LIPID BILAYERS AND BIOMEMBRANES, *Annual Review of Biochemistry 41*, 753-&.
[90] Peetla, C., Stine, A., and Labhasetwar, V. (2009) Biophysical interactions with model lipid membranes: applications in drug discovery and drug delivery, *Molecular pharmaceutics 6*, 1264-1276.
[91] Maheswari, K. U. (2001) Lipid bilayer-methotrexate interactions: A basis for methotrexate neurotoxicity, *Current Science 81*, 571-573.
[92] Alberts, B., Johnson, A., Lewis, J., Raff, M., Roberts, K., and Walter, P. (2002) *Molecular Biology of the Cell*, Garland Science, New York.
[93] Lapinski, M. M., Castro-Forero, A., Greiner, A. J., Ofoli, R. Y., and Blanchard, G. J. (2007) Comparison of Liposomes Formed by Sonication and Extrusion: Rotational and Translational Diffusion of an Embedded Chromophore, *Langmuir 23*, 11677-11683.
[94] Olson, F., Hunt, C. A., Szoka, F. C., Vail, W. J., and Papahadjopoulos, D. (1979) Preparation of liposomes of defined size distribution by extrusion through polycarbonate membranes, *Biochimica et Biophysica Acta (BBA) - Biomembranes 557*, 9-23.
[95] Gregoriadis, G. (2016) *Liposome Technology: Liposome Preparation and Related Techniques*, CRC Press.
[96] Torchilin, V., and Weissig, V. (2003) *Liposomes: A Practical Approach*, OUP Oxford.

[97] Szoka, F., and Papahadjopoulos, D. (1980) Comparative Properties and Methods of Preparation of Lipid Vesicles (Liposomes), *Annual Review of Biophysics and Bioengineering 9*, 467-508.
[98] Helenius, A., and Simons, K. (1975) Solubilization of membranes by detergents, *Biochimica et Biophysica Acta (BBA) - Reviews on Biomembranes 415*, 29-79.
[99] Schubert, R. (2003) Liposome Preparation by Detergent Removal, In *Methods in Enzymology*, pp 46-70, Academic Press.
[100] Zumbuehl, O., and Weder, H. G. (1981) Liposomes of controllable size in the range of 40 to 180 nm by defined dialysis of lipid/detergent mixed micelles, *Biochimica et Biophysica Acta (BBA) - Biomembranes 640*, 252-262.
[101] Jiskoot, W., Teerlink, T., Beuvery, E. C., and Crommelin, D. J. A. (1986) Preparation of liposomes via detergent removal from mixed micelles by dilution, *Pharmaceutisch Weekblad 8*, 259-265.
[102] Batzri, S., and Korn, E. D. (1973) Single bilayer liposomes prepared without sonication, *Biochimica et Biophysica Acta (BBA) - Biomembranes 298*, 1015-1019.
[103] Pons, M., Foradada, M., and Estelrich, J. (1993) Liposomes obtained by the ethanol injection method, *International Journal of Pharmaceutics 95*, 51-56.
[104] Fan, M., Xu, S., Xia, S., and Zhang, X. (2008) Preparation of salidroside nano-liposomes by ethanol injection method and in vitro release study, *European Food Research and Technology 227*, 167-174.
[105] Christoforou, M., Leontidis, E., and Brezesinski, G. (2012) Effects of sodium salts of lyotropic anions on low-temperature, ordered lipid monolayers, *The Journal of Physical Chemistry B 116*, 14602-14612.
[106] Rojas, E., and Tobias, J. M. (1965) Membrane model: Association of inorganic cations with phospholipid monolayers, *Biochimica et Biophysica Acta (BBA) - Biophysics including Photosynthesis 94*, 394-404.
[107] Leontidis, E., Aroti, A., and Belloni, L. (2009) Liquid Expanded Monolayers of Lipids As Model Systems to Understand the Anionic Hofmeister Series: 1. A Tale of Models, *The Journal of Physical Chemistry B 113*, 1447-1459.
[108] Aroti, A., Leontidis, E., Dubois, M., and Zemb, T. (2007) Effects of Monovalent Anions of the Hofmeister Series on DPPC Lipid Bilayers Part I: Swelling and In-Plane Equations of State, *Biophysical Journal 93*, 1580-1590.
[109] Valley, C. C., Perlmutter, J. D., Braun, A. R., and Sachs, J. N. (2011) NaCl interactions with phosphatidylcholine bilayers do not alter membrane structure but induce long-range ordering of ions and water, *J Membr Biol 244*, 35-42.
[110] Pabst, G., Hodzic, A., Štrancar, J., Danner, S., Rappolt, M., and Laggner, P. (2007) Rigidification of Neutral Lipid Bilayers in the Presence of Salts, *Biophysical Journal 93*, 2688-2696.
[111] Ruso, J. M., Besada, L., Martínez-Landeira, P., Seoane, L., Prieto, G., and Sarmiento, F. (2003) Interactions Between Liposomes and Cations in Aqueous Solution, *Journal of Liposome Research 13*, 131-145.
[112] Sabin, J., Prieto, G., Ruso, J. M., Hidalgo-Alvarez, R., and Sarmiento, F. (2006) Size and stability of liposomes: a possible role of hydration and osmotic forces, *Eur Phys J E Soft Matter 20*, 401-408.
[113] Sabín, J., Prieto, G., Messina, P. V., Ruso, J. M., Hidalgo-Alvarez, R., and Sarmiento, F. (2005) On the Effect of Ca2+ and La3+ on the Colloidal Stability of Liposomes, *Langmuir 21*, 10968-10975.
[114] Gurtovenko, A. A., and Vattulainen, I. (2008) Effect of NaCl and KCl on Phosphatidylcholine and Phosphatidylethanolamine Lipid Membranes: Insight from Atomic-Scale Simulations for Understanding Salt-Induced Effects in the Plasma Membrane, *The Journal of Physical Chemistry B 112*, 1953-1962.

[115] Cordomí, A., Edholm, O., and Perez, J. J. (2008) Effect of Ions on a Dipalmitoyl Phosphatidylcholine Bilayer. A Molecular Dynamics Simulation Study, *The Journal of Physical Chemistry B 112*, 1397-1408.
[116] Ferber, U. M., Kaggwa, G., and Jarvis, S. P. (2011) Direct imaging of salt effects on lipid bilayer ordering at sub-molecular resolution, *European Biophysics Journal 40*, 329-338.
[117] Martin, P. (2015) Effect of cations on dipalmitoylphosphatidylcholine liposomes, University of Bristol.
[118] Klasczyk, B., Knecht, V., Lipowsky, R., and Dimova, R. (2010) Interactions of Alkali Metal Chlorides with Phosphatidylcholine Vesicles, *Langmuir 26*, 18951-18958.
[119] Bentz, J., and Duezguenes, N. (1985) Fusogenic capacities of divalent cations and effect of liposome size, *Biochemistry 24*, 5436-5443.
[120] Binder, H., and Zschörnig, O. (2002) The effect of metal cations on the phase behavior and hydration characteristics of phospholipid membranes, *Chemistry and Physics of Lipids 115*, 39-61.
[121] Claessens, M. M. A. E., van Oort, B. F., Leermakers, F. A. M., Hoekstra, F. A., and Cohen Stuart, M. A. (2004) Charged Lipid Vesicles: Effects of Salts on Bending Rigidity, Stability, and Size, *Biophysical Journal 87*, 3882-3893.
[122] Pencer, J., White, G. F., and Hallett, F. R. (2001) Osmotically induced shape changes of large unilamellar vesicles measured by dynamic light scattering, *Biophysical Journal 81*, 2716-2728.
[123] Philippot, J. R., and Schuber, F. (1994) *Liposomes as Tools in Basic Research and Industry*, Taylor & Francis.
[124] Silvius, and R., J. (1982) Thermotropic Phase Transitions of Pure Lipids in Model Membranes and Their Modifications by Membrane Proteins, In *Lipid-Protein Interactions*, John Wiley & Sons, Inc, New York.
[125] Thomas, A. S., and Elcock, A. H. (2007) Molecular Dynamics Simulations of Hydrophobic Associations in Aqueous Salt Solutions Indicate a Connection between Water Hydrogen Bonding and the Hofmeister Effect, *Journal of the American Chemical Society 129*, 14887-14898.
[126] Kruczek, J., Chiu, S.-W., Jakobsson, E., and Pandit, S. A. (2017) Effects of Lithium and Other Monovalent Ions on Palmitoyl Oleoyl Phosphatidylcholine Bilayer, *Langmuir 33*, 1105-1115.
[127] Leontidis, E. (2016) Chaotropic salts interacting with soft matter: Beyond the lyotropic series, *Current Opinion in Colloid & Interface Science 23*, 100-109.
[128] Instruments, M., and Limited. (2017) Measuring the zeta potential of High

Conductivity Samples using the Zetasizer

Nano.
[129] Instruments, M. (2004) Zetasizer Nano Series

User Manual, Malvern Instruments Ltd., United Kingdom.
[130] Meurant, G. (2012) *Introduction to Dynamic Light Scattering by Macromolecules*, Elsevier Science.
[131] Pecora, R. Dynamic Light Scattering Measurement of Nanometer Particles in Liquids, *Journal of Nanoparticle Research 2*, 123-131.
[132] Elmore, W. C., and Heald, M. A. (1969) *Physics of Waves*, Dover Publications.
[133] Clogston, J. D., and Patri, A. K. (2011) Zeta Potential Measurement, In *Characterization of Nanoparticles Intended for Drug Delivery* (McNeil, E. S., Ed.), pp 63-70, Humana Press, Totowa, NJ.
[134] Ohshima, H. (2006) *Theory of Colloid and Interfacial Electric Phenomena*, Elsevier Science.
[135] Bhattacharjee, S. (2016) DLS and zeta potential – What they are and what they are not?, *Journal of Controlled Release 235*, 337-351.

[136] Somasundaran, P. (2006) *Encyclopedia of Surface and Colloid Science, Second Edition - Eight-Volume Set (Print)*, Taylor & Francis.
[137] Delgado, A. V., González-Caballero, F., Hunter, R. J., Koopal, L. K., and Lyklema, J. (2007) Measurement and interpretation of electrokinetic phenomena, *Journal of Colloid and Interface Science 309*, 194-224.
[138] Redeker, C. (2017) Lipopolysaccharides in solution and at the solid-liquid interface: Structure and interactions, p 267.
[139] Kohonen, M. M., Karaman, M. E., and Pashley, R. M. (2000) Debye Length in Multivalent Electrolyte Solutions, *Langmuir 16*, 5749-5753.
[140] Nishi, Y., and Doering, R. (2007) *Handbook of Semiconductor Manufacturing Technology, Second Edition*, CRC Press.
[141] Salgın, S., Salgın, U., and Bahadır, S. (2012) Zeta potentials and isoelectric points of biomolecules: the effects of ion types and ionic strengths, *Int. J. Electrochem. Sci 7*, 12404-12414.
[142] Prakash, S., Mishra, R., Malviya, R., and Sharma, P. K. Measurement Techniques and Pharmaceutical Applications of Zeta Potential: A Review, *Journal of Chronotherapy and Drug Delivery 5*, 2.
[143] Somasundaran, P. (2006) *Encyclopedia of Surface and Colloid Science*, Taylor & Francis.
[144] Koning, R., and Koster, A. (2013) *Cellular Nanoimaging by Cryo Electron Tomography*, Vol. 950.
[145] Bozzola, J. J. (2001) Electron Microscopy, In *eLS*, John Wiley & Sons, Ltd.
[146] Dubochet, J., Adrian, M., Chang, J.-J., Homo, J.-C., Lepault, J., McDowall, A. W., and Schultz, P. (1988) Cryo-electron microscopy of vitrified specimens, *Quarterly Reviews of Biophysics 21*, 129-228.
[147] Thompson, R. F., Walker, M., Siebert, C. A., Muench, S. P., and Ranson, N. A. (2016) An introduction to sample preparation and imaging by cryo-electron microscopy for structural biology, *Methods 100*, 3-15.
[148] Hunter, R. J., Ottewill, R. H., and Rowell, R. L. (2013) *Zeta Potential in Colloid Science: Principles and Applications*, Elsevier Science.
[149] Chibowski, E., and Szcześ, A. (2016) Zeta potential and surface charge of DPPC and DOPC liposomes in the presence of PLC enzyme, *Adsorption 22*, 755-765.
[150] Makino, K., Yamada, T., Kimura, M., Oka, T., Ohshima, H., and Kondo, T. (1991) Temperature- and ionic strength-induced conformational changes in the lipid head group region of liposomes as suggested by zeta potential data, *Biophysical Chemistry 41*, 175-183.
[151] Sachs, J. N., Nanda, H., Petrache, H. I., and Woolf, T. B. (2004) Changes in Phosphatidylcholine Headgroup Tilt and Water Order Induced by Monovalent Salts: Molecular Dynamics Simulations, *Biophysical Journal 86*, 3772-3782.
[152] Egawa, H., and Furusawa, K. (1999) Liposome Adhesion on Mica Surface Studied by Atomic Force Microscopy, *Langmuir 15*, 1660-1666.
[153] Israelachvili, J. N. (2011) 4 - Interactions Involving Polar Molecules, In *Intermolecular and Surface Forces (Third Edition)*, pp 71-90, Academic Press, San Diego.
[154] Redondo-Morata, L., Oncins, G., and Sanz, F. (2012) Force Spectroscopy Reveals the Effect of Different Ions in the Nanomechanical Behavior of Phospholipid Model Membranes: The Case of Potassium Cation, *Biophysical Journal 102*, 66-74.
[155] Pandit, S. A., Bostick, D., and Berkowitz, M. L. (2003) Molecular Dynamics Simulation of a Dipalmitoylphosphatidylcholine Bilayer with NaCl, *Biophysical Journal 84*, 3743-3750.
[156] Clarke, R. J., and Lüpfert, C. (1999) Influence of Anions and Cations on the Dipole Potential of Phosphatidylcholine Vesicles: A Basis for the Hofmeister Effect, *Biophysical Journal 76*, 2614-2624.
[157] Garidel, P., and Blume, A. (1999) Interaction of Alkaline Earth Cations with the Negatively Charged Phospholipid 1,2-Dimyristoyl-sn-glycero-3-phosphoglycerol: A Differential Scanning and Isothermal Titration Calorimetric Study, *Langmuir 15*, 5526-5534.

[158] López Cascales, J. J., and Garcia de la Torre, J. (1997) Effect of lithium and sodium ions on a charged membrane of dipalmitoylphosphatidylserine: A study by molecular dynamics simulation, *Biochimica et Biophysica Acta (BBA) - Biomembranes 1330*, 145-156.
[159] Akashi, K.-i., Miyata, H., Itoh, H., and Kinosita Jr, K. (1998) Formation of Giant Liposomes Promoted by Divalent Cations: Critical Role of Electrostatic Repulsion, *Biophysical Journal 74*, 2973-2982.
[160] Tatulian, S. A., Gordeliy, V. I., Sokolova, A. E., and Syrykh, A. G. (1991) A neutron diffraction study of the influence of ions on phospholipid membrane interactions, *Biochimica et biophysica acta 1070*, 143-151.
[161] Sinn, C. G., Antonietti, M., and Dimova, R. (2006) Binding of calcium to phosphatidylcholine–phosphatidylserine membranes, *Colloids and Surfaces A: Physicochemical and Engineering Aspects 282-283*, 410-419.
[162] Szcześ, A. (2013) Effects of DPPC/Cholesterol liposomes on the properties of freshly precipitated calcium carbonate, *Colloids and Surfaces B: Biointerfaces 101*, 44-48.
[163] Melcrová, A., Pokorna, S., Pullanchery, S., Kohagen, M., Jurkiewicz, P., Hof, M., Jungwirth, P., Cremer, P. S., and Cwiklik, L. (2016) The complex nature of calcium cation interactions with phospholipid bilayers, *Scientific reports 6*, 38035.
[164] Dhaouadi, H., and M'Henni, F. (2009) Vat dye sorption onto crude dehydrated sewage sludge, *Journal of Hazardous Materials 164*, 448-458.
[165] Jeppu, G. P., and Clement, T. P. (2012) A modified Langmuir-Freundlich isotherm model for simulating pH-dependent adsorption effects, *Journal of Contaminant Hydrology 129*, 46-53.
[166] Mozuraityte, R., Rustad, T., and Storr⍁, I. (2006) Oxidation of cod phospholipids in liposomes: Effects of salts, pH and zeta potential, *European Journal of Lipid Science and Technology 108*, 944-950.
[167] Clavaguéra, C., Pollet, R., Soudan, J. M., Brenner, V., and Dognon, J. P. (2005) Molecular Dynamics Study of the Hydration of Lanthanum(III) and Europium(III) Including Many-Body Effects, *The Journal of Physical Chemistry B 109*, 7614-7616.
[168] Lehrmann, R., and Seelig, J. (1994) Adsorption of Ca2+ and La3+ to bilayer membranes: Measurement of the adsorption enthalpy and binding constant with titration calorimetry, *Biochimica et Biophysica Acta (BBA) - Biomembranes 1189*, 89-95.
[169] Maity, P., Saha, B., Kumar, G. S., and Karmakar, S. (2016) Binding of monovalent alkali metal ions with negatively charged phospholipid membranes, *Biochimica et Biophysica Acta (BBA) - Biomembranes 1858*, 706-714.
[170] Kotyńska, J., Dobrzyńska, I., and Figaszewski, Z. A. (2016) Association of alkali metal cations with phosphatidylcholine liposomal membrane surface, *European Biophysics Journal*, 1-7.
[171] Martín-Molina, A., Rodríguez-Beas, C., and Faraudo, J. (2012) Effect of Calcium and Magnesium on Phosphatidylserine Membranes: Experiments and All-Atomic Simulations, *Biophysical Journal 102*, 2095-2103.
[172] Poovaiah, B. W., and Leopold, A. C. (1976) Effects of Inorganic Solutes on the Binding of Auxin, *Plant Physiology 58*, 783-785.
[173] Toimil, P., Daviña, R., Sabín, J., Prieto, G., and Sarmiento, F. (2012) Influence of temperature on the colloidal stability of the F-DPPC and DPPC liposomes induced by lanthanum ions, *Journal of Colloid and Interface Science 367*, 193-198.
[174] Pugachev, M. V., Shtyrlin, N. V., Sysoeva, L. P., Nikitina, E. V., Abdullin, T. I., Iksanova, A. G., Ilaeva, A. A., Musin, R. Z., Berdnikov, E. A., and Shtyrlin, Y. G. (2013) Synthesis and antibacterial activity of novel phosphonium salts on the basis of pyridoxine, *Bioorganic & Medicinal Chemistry 21*, 4388-4395.
[175] Bergeron, K. L., Murphy, E. L., Majofodun, O., Muñoz, L. D., Williams, J. C., and Almeida, K. H. (2009) Arylphosphonium salts interact with DNA to modulate cytotoxicity, *Mutation Research/Genetic Toxicology and Environmental Mutagenesis 673*, 141-148.

[176] Ellena, J. F., Dominey, R. N., Archer, S. J., Xu, Z. C., and Cafiso, D. S. (1987) Localization of hydrophobic ions in phospholipid bilayers using proton nuclear Overhauser effect spectroscopy, *Biochemistry 26*, 4584-4592.
[177] Flewelling, R. F., and Hubbell, W. L. (1986) Hydrophobic ion interactions with membranes. Thermodynamic analysis of tetraphenylphosphonium binding to vesicles, *Biophysical Journal 49*, 531-540.
[178] Andersen, O. S., Feldberg, S., Nakadomari, H., Levy, S., and McLaughlin, S. (1978) Electrostatic interactions among hydrophobic ions in lipid bilayer membranes, *Biophysical Journal 21*, 35-70.
[179] Pickar, A. D., and Benz, R. (1978) Transport of oppositely charged lipophilic probe ions in lipid bilayer membranes having various structures, *The Journal of Membrane Biology 44*, 353-376.
[180] Schurhammer, R., and Wipff, G. (1999) About the TATB hypothesis: solvation of the As[small phi]4+ and B[small phi]4- ions and their tetrahedral and spherical analogues in aqueous/nonaqueous solvents and at a water-chloroform interface, *New Journal of Chemistry 23*, 381-392.
[181] Liberman, E. A., and Topaly, V. P. (1969) [Permeability of bimolecular phospholipid membranes for fat-soluble ions], *Biofizika 14*, 452-461.
[182] Haydon, D. A., and Myers, V. B. (1973) Surface charge, surface dipoles and membrane conductance, *Biochimica et Biophysica Acta (BBA) - Biomembranes 307*, 429-443.
[183] Schamberger, J., and Clarke, R. J. (2002) Hydrophobic ion hydration and the magnitude of the dipole potential, *Biophysical journal 82*, 3081-3088.
[184] Smejtek, P., and Wang, S. R. (1990) Adsorption to dipalmitoylphosphatidylcholine membranes in gel and fluid state: pentachlorophenolate, dipicrylamine, and tetraphenylborate, *Biophysical Journal 58*, 1285-1294.
[185] Reynolds, W. W., and Casterlin, M. E. (1980) The Role of Temperature in the Environmental Physiology of Fishes, In *Environmental Physiology of Fishes* (Ali, M. A., Ed.), pp 497-518, Springer US, Boston, MA.
[186] Senske, M., Constantinescu-Aruxandei, D., Havenith, M., Herrmann, C., Weingartner, H., and Ebbinghaus, S. (2016) The temperature dependence of the Hofmeister series: thermodynamic fingerprints of cosolute-protein interactions, *Physical Chemistry Chemical Physics 18*, 29698-29708.
[187] Walrafen, G. E. (1967) Raman Spectral Studies of the Effects of Temperature on Water Structure, *The Journal of Chemical Physics 47*, 114-126.
[188] Zavitsas, A. A. (2005) Aqueous Solutions of Calcium Ions: Hydration Numbers and the Effect of Temperature, *The Journal of Physical Chemistry B 109*, 20636-20640.
[189] Kurisaki, T., Yamaguchi, T., and Wakita, H. (1993) Effect of temperature on the structure of hydrated lanthanide(III) ions in crystals and in solution, *Journal of Alloys and Compounds 192*, 293-295.
[190] Zook, J. M., and Vreeland, W. N. (2010) Effects of temperature, acyl chain length, and flow-rate ratio on liposome formation and size in a microfluidic hydrodynamic focusing device, *Soft Matter 6*, 1352-1360.
[191] Eze, M. O. (1991) Phase transitions in phospholipid bilayers: Lateral phase separations play vital roles in biomembranes, *Biochemical Education 19*, 204-208.
[192] Roy, B., Guha P Fau - Bhattarai, R., Bhattarai R Fau - Nahak, P., Nahak P Fau - Karmakar, G., Karmakar G Fau - Chettri, P., Chettri P Fau - Panda, A. K., and Panda, A. K. Influence of Lipid Composition, pH, and Temperature on Physicochemical Properties of Liposomes with Curcumin as Model Drug.
[193] Sułkowski, W. W., Pentak, D., Nowak, K., and Sułkowska, A. (2005) The influence of temperature, cholesterol content and pH on liposome stability, *Journal of Molecular Structure 744-747*, 737-747.

[194] Sułkowski, W. W., Pentak, D., Nowak, K., and Sułkowska, A. (2005) The influence of temperature, cholesterol content and pH on liposome stability, *Journal of Molecular Structure 744*, 737-747.
[195] Sauerheber, R. D., and Gordon, L. M. (1975) Spin Label Studies on Rat Liver Plasma Membrane: Calcium Effects on Membrane Fluidity, *Proceedings of the Society for Experimental Biology and Medicine 150*, 28-31.
[196] Andersson, M., Hammarstroem, L., and Edwards, K. (1995) Effect of Bilayer Phase Transitions on Vesicle Structure, and its Influence on the Kinetics of Viologen Reduction, *The Journal of Physical Chemistry 99*, 14531-14538.
[197] Moulik, S. P., De, G. C., Bhowmik, B. B., and Panda, A. K. (1999) Physicochemical Studies on Microemulsions. 6. Phase Behavior, Dynamics of Percolation, and Energetics of Droplet Clustering in Water/AOT/n-Heptane System Influenced by Additives (Sodium Cholate and Sodium Salicylate), *The Journal of Physical Chemistry B 103*, 7122-7129.
[198] Maurya Sheo, D. (2013) Effects of Ph, Salt, Temperature on Conventional Liposomes Size Enlargement Analyzed by Optical Microscope, *International Journal of Drug Regulatory Affairs 1*, 10-15.
[199] Epand, R. M., and Bryszewska, M. (1988) Modulation of the bilayer to hexagonal phase transition and solvation of phosphatidylethanolamines in aqueous salt solutions, *Biochemistry 27*, 8776-8779.
[200] Träuble, H., and Eibl, H. (1974) Electrostatic Effects on Lipid Phase Transitions: Membrane Structure and Ionic Environment, *Proceedings of the National Academy of Sciences of the United States of America 71*, 214-219.
[201] Perkins, W. R., Li, X., Slater, J. L., Harmon, P. A., Ahl, P. L., Minchey, S. R., Gruner, S. M., and Janoff, A. S. (1997) Solute-induced shift of phase transition temperature in Di-saturated PC liposomes: adoption of ripple phase creates osmotic stress, *Biochimica et Biophysica Acta (BBA) - Biomembranes 1327*, 41-51.
[202] Cevc, G. (1991) Isothermal lipid phase transitions, *Chemistry and Physics of Lipids 57*, 293-307.
[203] Chowdhry, B. Z., Lipka, G., Dalziel, A. W., and Sturtevant, J. M. (1984) Effect of lanthanum ions on the phase transitions of lecithin bilayers, *Biophys J 45*, 633-635.
[204] Yuan, L., Geng, L., Ge, L., Yu, P., Duan, X., Chen, J., and Chang, Y. (2013) Effect of iron liposomes on anemia of inflammation, *International Journal of Pharmaceutics 454*, 82-89.
[205] Shi, D. r. n. M. G. r. n. W. T. Magnetic ferri-liposomes for triggered drug release across the blood- brain barrier, *Frontiers in Bioengineering and Biotechnology*.
[206] Pradhan, P., Banerjee, R., Bahadur, D., Koch, C., Mykhaylyk, O., and Plank, C. (2017) Targeted Magnetic Liposomes Loaded with Doxorubicin, *Methods Mol Biol 1522*, 257-272.
[207] Marcus, Y. (1994) A simple empirical model describing the thermodynamics of hydration of ions of widely varying charges, sizes, and shapes, *Biophysical Chemistry 51*, 111-127.
[208] Hellman, H., Laitinen, R. S., Kaila, L., Jalonen, J., Hietapelto, V., Jokela, J., Sarpola, A., and Rämö, J. (2006) Identification of hydrolysis products of FeCl3 · 6H2O by ESI-MS, *Journal of Mass Spectrometry 41*, 1421-1429.
[209] Reis, A., and Spickett, C. M. (2012) Chemistry of phospholipid oxidation, *Biochimica et Biophysica Acta (BBA) - Biomembranes 1818*, 2374-2387.
[210] Oborina, E. M., and Yappert, M. C. (2003) Effect of sphingomyelin versus dipalmitoylphosphatidylcholine on the extent of lipid oxidation, *Chemistry and Physics of Lipids 123*, 223-232.
[211] Carlsen, C. U., Møller, J. K. S., and Skibsted, L. H. (2005) Heme-iron in lipid oxidation, *Coordination Chemistry Reviews 249*, 485-498.
[212] Kato, N., Ishijima, A., Inaba, T., Nomura, F., Takeda, S., and Takiguchi, K. (2015) Effects of Lipid Composition and Solution Conditions on the Mechanical Properties of Membrane Vesicles, *Membranes 5*, 22-47.

[213] Huy, N. T., Shima, Y., Maeda, A., Men, T. T., Hirayama, K., Hirase, A., Miyazawa, A., and Kamei, K. (2013) Phospholipid membrane-mediated hemozoin formation: the effects of physical properties and evidence of membrane surrounding hemozoin, *PloS one 8*, e70025.
[214] Zidovska, A., Ewert, K. K., Quispe, J., Carragher, B., Potter, C. S., and Safinya, C. R. (2009) The effect of salt and pH on block liposomes studied by cryogenic transmission electron microscopy, *Biochimica et Biophysica Acta (BBA) - Biomembranes 1788*, 1869-1876.
[215] Knecht, V., and Klasczyk, B. (2013) Specific Binding of Chloride Ions to Lipid Vesicles and Implications at Molecular Scale, *Biophysical Journal 104*, 818-824.

Appendix A

Debye length and Henry's function

Table A1: Calculated Debye length (κ^{-1}) and f(κa) values, as given by the Ohshima equation, for DOPC liposomes in various salt concentrations for all monovalent ions studied.

[LiCl] Concentration (mM)	Debye length (κ^{-1}) (nm)	$f(\kappa\alpha)$ (a.u.)
1	9.608	1.204
1.5	7.845	1.240
2	6.794	1.246
2.5	6.077	1.266
5	4.297	1.329
8	3.397	1.361
10	3.038	1.379
15	2.481	1.404
20	2.148	1.411
25	1.922	1.415
30	1.754	1.431
40	1.519	1.435

[NaCl] Concentration (mM)	Debye length (κ^{-1}) (nm)	$f(\kappa\alpha)$ (a.u.)
1	9.608	1.216
1.5	7.845	1.244
2	6.794	1.260
2.5	6.077	1.279
5	4.297	1.335
8	3.397	1.353
10	3.038	1.364
15	2.481	1.387
20	2.148	1.398
25	1.922	1.411
30	1.754	1.416
40	1.519	1.421

[KCl] Concentration (mM)	Debye length (κ^{-1}) (nm)	$f(\kappa\alpha)$ (a.u.)
1	9.608	1.198
1.5	7.845	1.226
2	6.794	1.262
2.5	6.077	1.273
5	4.297	1.326
8	3.397	1.364
10	3.038	1.374
15	2.481	1.384
20	2.148	1.400
25	1.922	1.409
30	1.754	1.421
40	1.519	1.421

[CsCl] Concentration (mM)	Debye length (κ^{-1}) (nm)	$f(\kappa\alpha)$ (a.u.)
1	9.608	1.198
1.5	7.845	-
2	6.794	1.256
2.5	6.077	1.273
5	4.297	1.321
8	3.397	1.355
10	3.038	1.381
15	2.481	1.387
20	2.148	1.404
25	1.922	1.416
30	1.754	1.423
40	1.519	1.420

Divalent ions Table A2: Calculated Debye length (κ^{-1}) and f(κa) values, as given by the Ohshima equation, for DOPC liposomes in various salt concentrations for all divalent ions studied.

[$MgCl_2$] Concentration (mM)	Debye length (κ^{-1}) (nm)	$f(\kappa\alpha)$ (a.u.)
1	5.547	1.309
1.5	4.529	1.323
2	3.922	1.341
2.5	3.508	1.364
5	2.481	1.378
8	1.961	1.400
10	1.754	1.419
15	1.432	1.430
20	1.240	1.434
25	1.109	1.444
30	1.013	1.449
40	0.877	1.454

[$CaCl_2$] Concentration (mM)	Debye length (κ^{-1}) (nm)	$f(\kappa\alpha)$ (a.u.)
1	5.547	1.290
1.5	4.529	1.312
2	3.922	1.330
2.5	3.508	-
5	2.481	1.379
8	1.961	1.401
10	1.754	1.413
15	1.432	1.425
20	1.240	1.433
25	1.109	1.441
30	1.013	1.447
40	0.877	1.454

Trivalent ions

Table A3: Calculated Debye length (κ^{-1}) and f(κa) values, as given by the Ohshima equation, for liposomes in various salt concentrations for all trivalent ions studied.

[$CrCl_3$] Concentration (mM)	Debye length (κ^{-1}) (nm)	*f*(κα) (a.u.)
1	3.922	1.284
2	3.203	1.337
5	2.774	1.350
10	2.481	1.349
15	1.754	1.404
20	1.387	1.414
25	1.240	1.429
50	1.013	1.447

[$LaCl_3$] Concentration (mM)	Debye length (κ^{-1}) (nm)	*f*(κα) (a.u.)
1	3.922	1.323
1.5	3.203	1.351
2	2.774	1.370
2.5	2.481	1.382
5	1.754	1.421
8	1.387	1.426
10	1.240	1.446
15	1.013	1.444
20	0.877	1.451
25	0.784	1.457
30	0.716	1.462
40	0.620	1.465

[$FeCl_3$] Concentration (mM)	Debye length (κ^{-1}) (nm)	*f*(κα) (a.u.)
1	3.922	1.146
2	3.203	1.235
5	2.774	1.282
10	2.481	1.332
15	1.754	1.377
20	1.387	1.405
25	1.240	1.420
50	1.013	1.436

Appendix B

The electrophoretic mobilities of DOPC liposomes as a function of monovalent cation concentration

Figures B1- B4: Electrophoretic mobilities of the DOPC liposomes as a function of monovalent cation concentration, as recorded by DLS. The electrophoretic mobility values were used to calculate the zeta potential values discussed in this work.

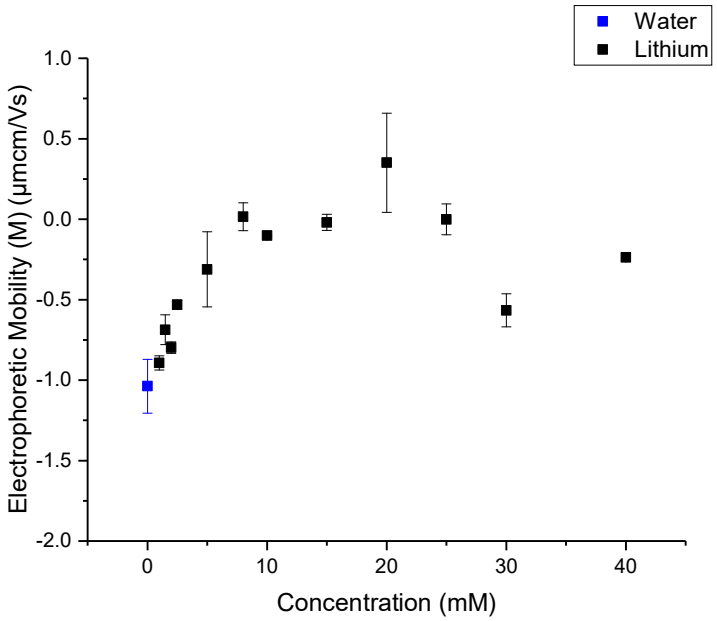

Figure B 1: The electrophoretic mobility of DOPC liposomes as a function of Li^+ concentration at 25˚C, as measured by DLS.

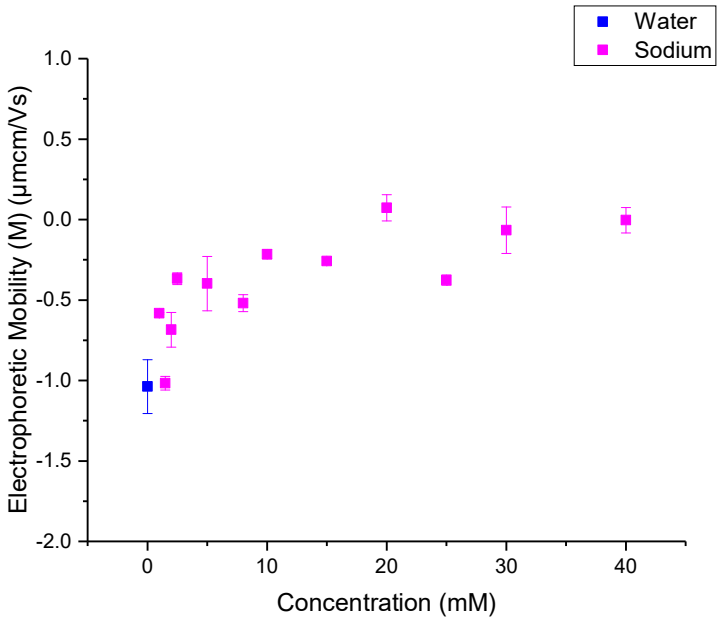

Figure B 2: The electrophoretic mobility of DOPC liposomes as a function of Na^+ concentration at 25˚C, as measured by DLS

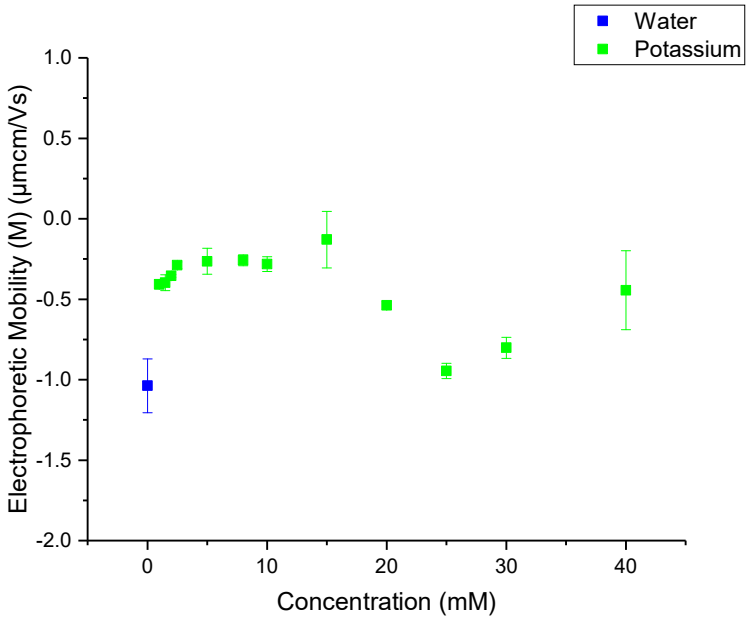

Figure B 3: The electrophoretic mobility of DOPC liposomes as a function of K^+ concentration at 25˚C, as measured by DLS

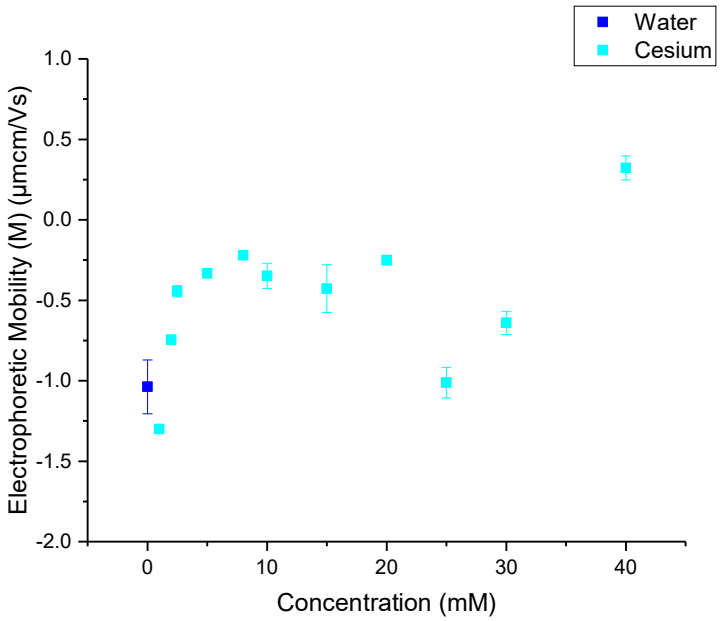

Figure B 4: The electrophoretic mobility of DOPC liposomes as a function of Cs^+ concentration at 25˚C, as measured by DLS

Appendix C

The zeta potential of DOPC liposomes as a function of monovalent cation concentration

Figure C1: The zeta potential of the DOPC liposomes as a function of monovalent cation concentration. The graph shows the zeta potential results for all monovalent cations studied in this work.

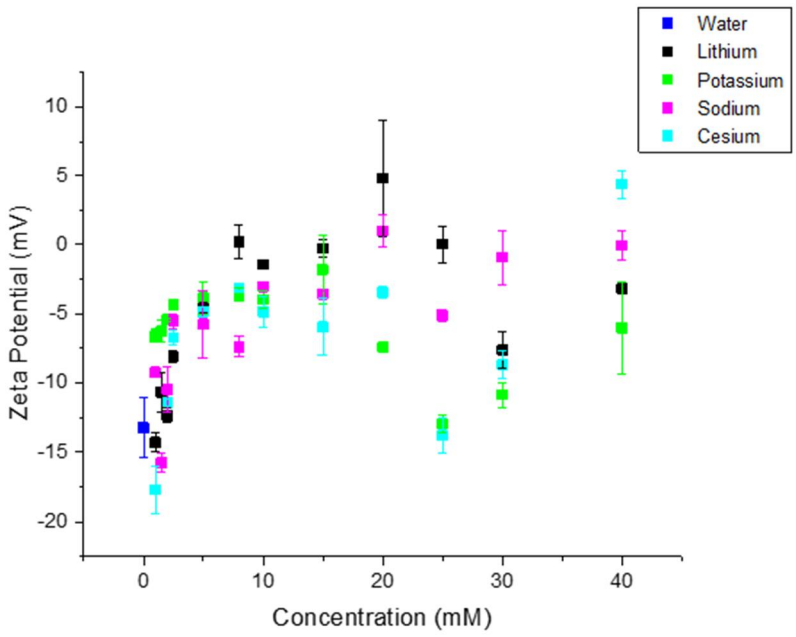

Figure C 1: The zeta potential of DOPC liposomes as a function of monovalent cation concentration at 25˚C.

Appendix D

The electrophoretic mobilities of DOPC liposomes as a function of divalent cation concentration

Figures D1 & D2: Electrophoretic mobilities of the DOPC liposomes as a function of divalent cation concentration, as recorded by DLS. The electrophoretic mobility values were used to calculate the zeta potential values discussed in this work. Figure D1 shows the change in the electrophoretic mobility of the liposomes as a function of $CaCl_2$ concentration and Figure D2 shows the change in the electrophoretic mobility of the liposomes as a function of $MgCl_2$ concentration.

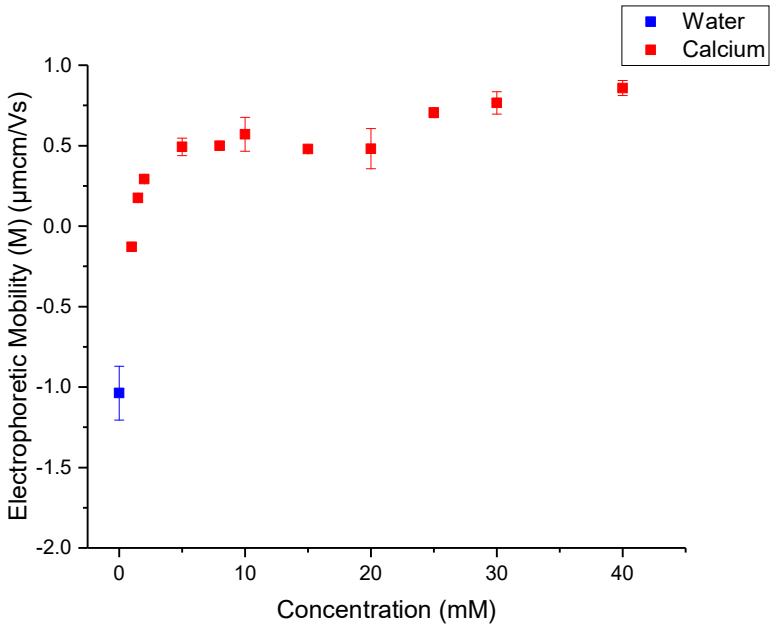

Figure D 1: The electrophoretic mobility of DOPC liposomes as a function of Ca^{2+} concentration at 25˚C, as measured by DLS

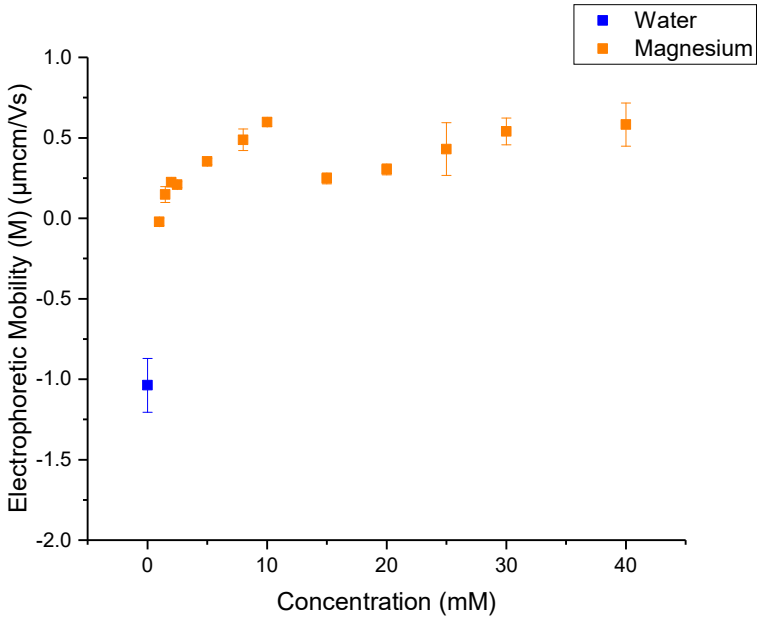

Figure D 2: The electrophoretic mobility of DOPC liposomes as a function of Mg^{2+} concentration at 25˚C, as measured by DLS

Appendix E

The zeta potential of DOPC liposomes as a function of divalent cation concentration

Figure E1: The zeta potential of the DOPC liposomes as a function of monovalent cation concentration. The graph shows the zeta potential results for all divalent cations studied in this work.

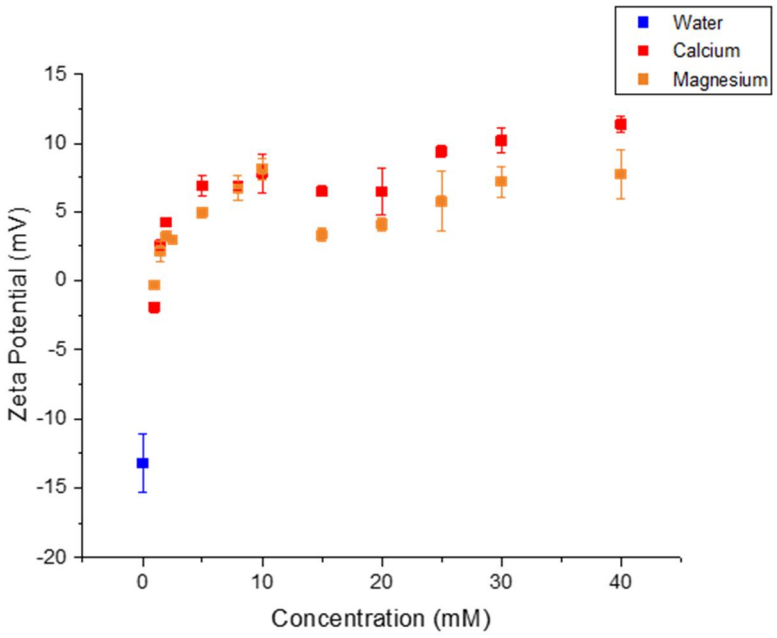

Figure E 1: The zeta potential of DOPC liposomes as a function of divalent cation concentration at 25˚C.

Appendix F

The electrophoretic mobilities of DOPC liposomes as a function of trivalent cation concentration

Figure F1: Electrophoretic mobilities of the DOPC liposomes as a function of trivalent cation concentration, as recorded by DLS. The electrophoretic mobility values were used to calculate the zeta potential values discussed in this work. Figure F1 shows the change in the electrophoretic mobility of the liposomes as a function of $LaCl_3$ concentration

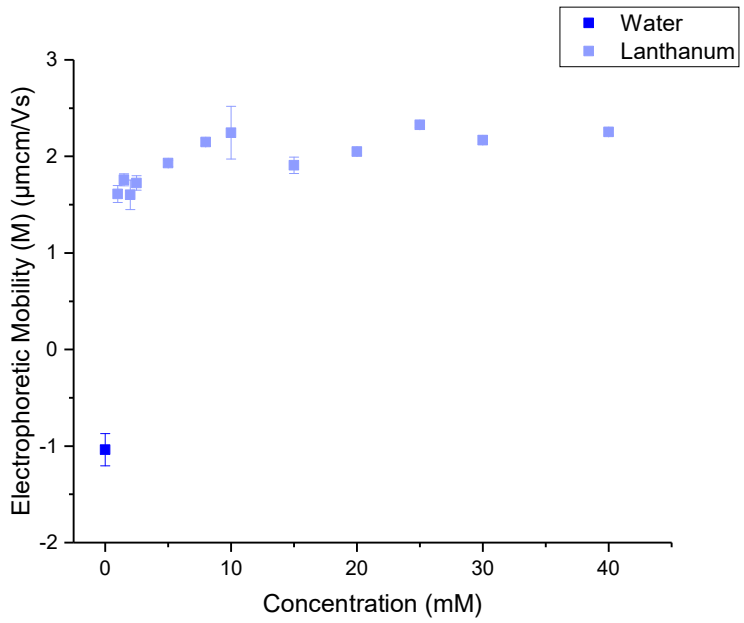

Figure F 1: The electrophoretic mobility of DOPC liposomes as a function of La^{3+} concentration at 25˚C, as measured by DLS

Appendix G

The size of DOPC liposomes as a function of ionic strength

Figure G1: The size of DOPC liposomes as a function of ionic strength. The maximum ionic strength shown is 60 mM (A) and 240 mM (B).

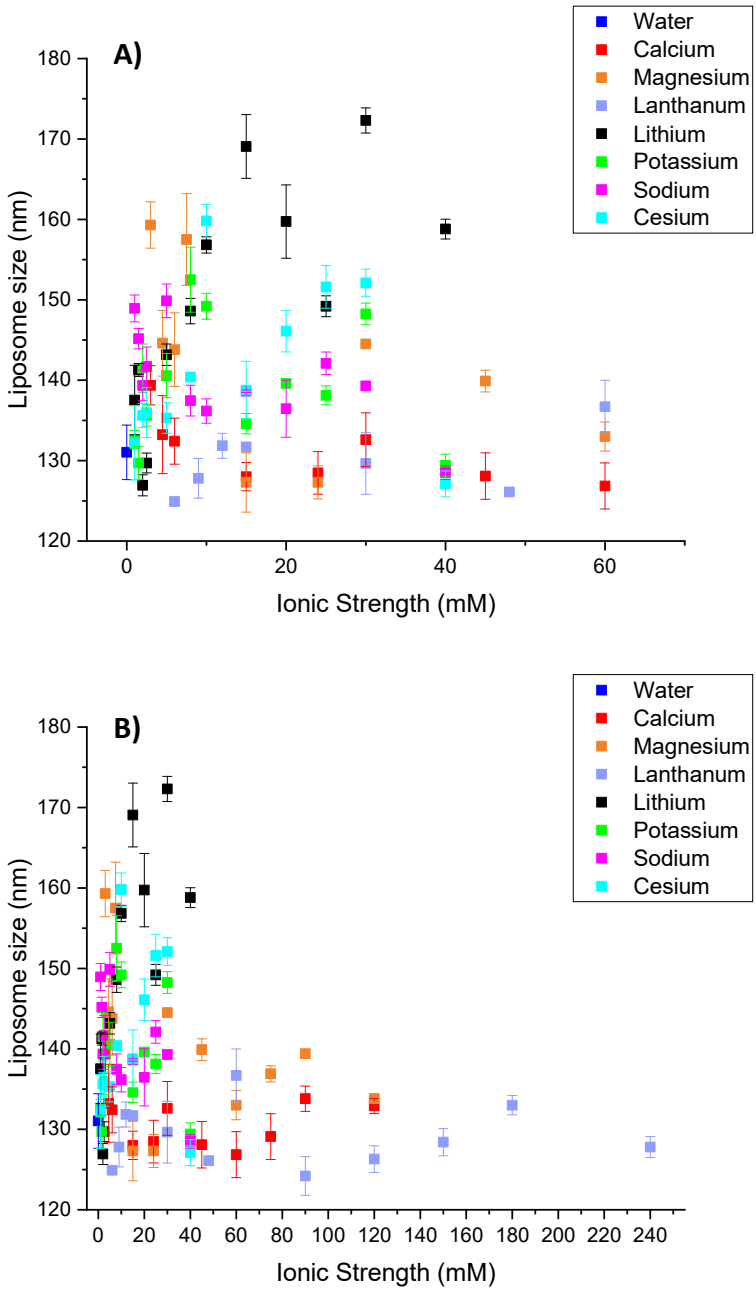

Figure G 2: The size of DOPC liposomes as a function of ionic strength.

Appendix H

The electrophoretic mobilities of DOPC liposomes as a function of organic, hydrophobic ion concentration

Figures H1 & H2: Electrophoretic mobilities of the DOPC liposomes as a function of hydrophobic cation concentration. Figure H1 shows the change in the electrophoretic mobility of the liposomes as a function of tetraphenylphosphonium chloride concentration and Figure H2 shows the change in the electrophoretic mobility of the liposomes as a function of sodium tetraphenylborate concentration.

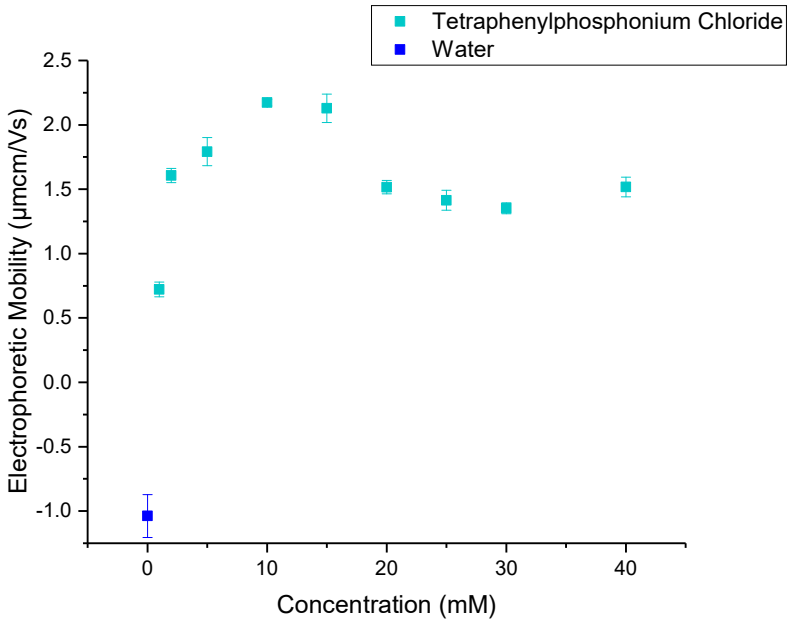

Figure H 1: The electrophoretic mobility of DOPC liposomes as a function of hydrophobic TPP+ concentration at 25˚C, as measured by DLS.

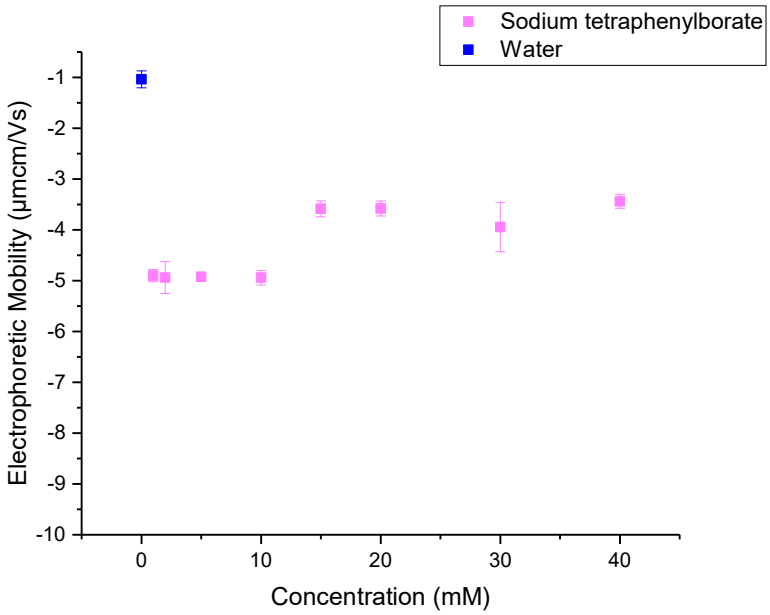

Figure H 2: The electrophoretic mobility of DOPC liposomes as a function of hydrophobic TPP+ concentration at 25˚C, as measured by DLS.

Appendix I

Size distribution by intensity graphs in the presence of varying concentrations of tetraphenylborate

Figures I1, I2, I3 and I4: The size distribution of the DOPC liposomes in 1-10 mM, 20 mM, 30 mM and 40 mM sodium tetraphenylborate respectively. As is described in Section 5.2, as the concentration of TPB^- increases the graphs confirm that fusion and aggregation of the liposomes is occurring due to the presence of a peak at 5000 nm which increases in size, in line with concentration.

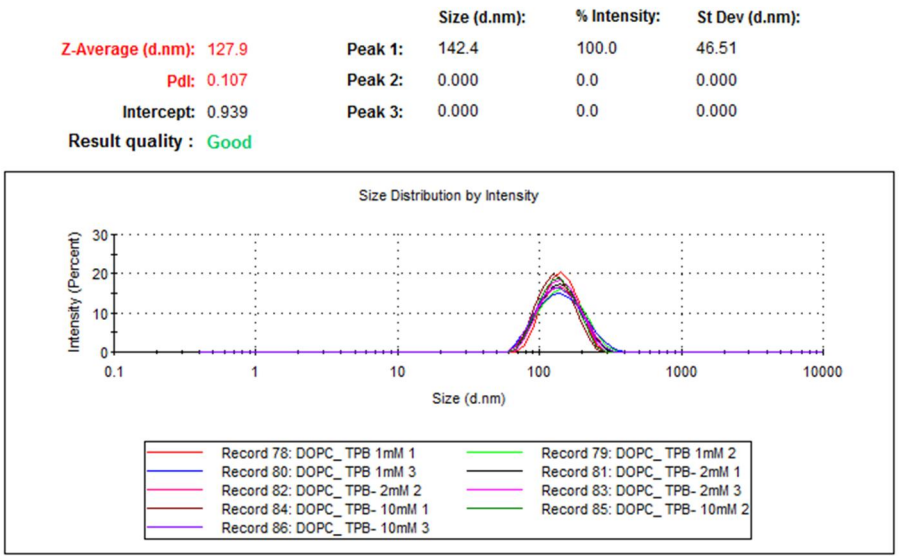

Figure I 1: The size distribution of DOPC liposome suspensions in the presence of 1-10 mM TPB-. Measured by DLS at 25˚C.

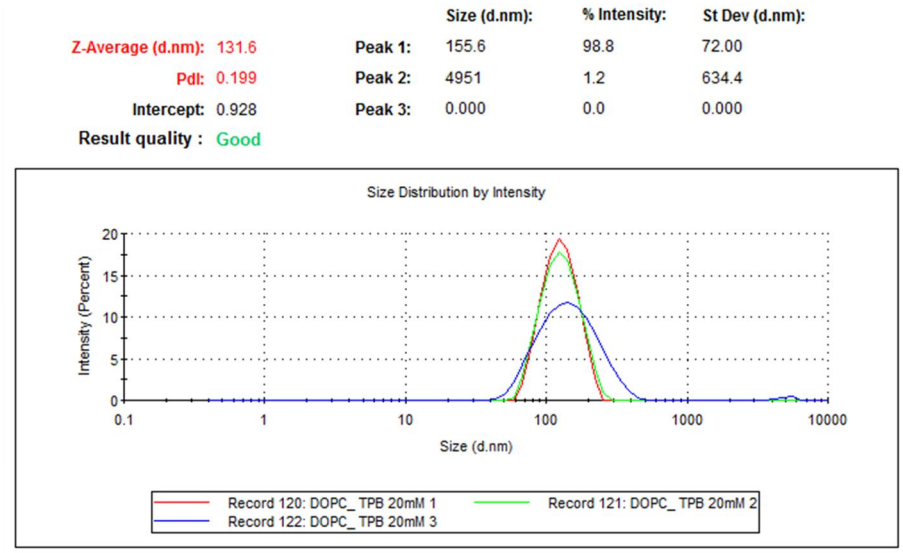

Figure I 2: The size distribution of DOPC liposome suspensions in the presence of 20 mM TPB-. Measured by DLS at 25˚C.

		Size (d.nm):	% Intensity:	St Dev (d.nm):
Z-Average (d.nm): 158.8	Peak 1:	162.4	100.0	46.64
PdI: 0.204	Peak 2:	0.000	0.0	0.000
Intercept: 0.942	Peak 3:	0.000	0.0	0.000
Result quality : Good				

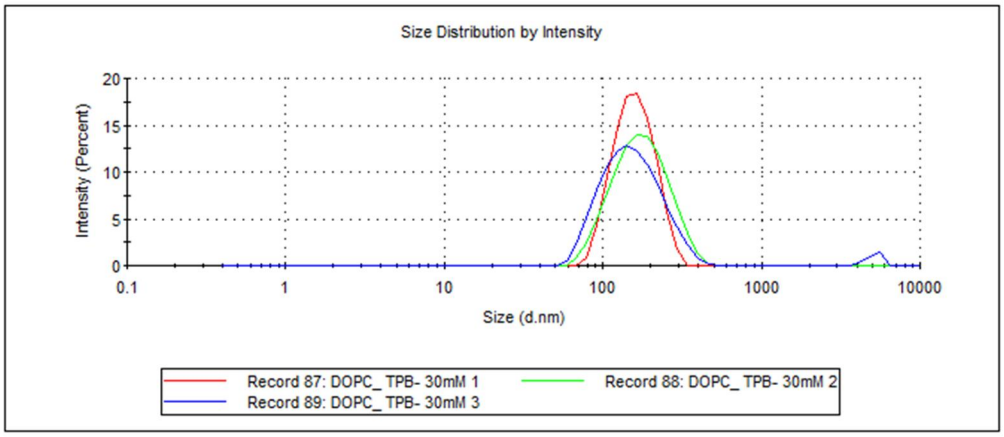

Figure I 3: The size distribution of DOPC liposome suspensions in the presence of 30 mM TPB-. Measured by DLS at 25˚C.

		Size (d.nm):	% Intensity:	St Dev (d.nm):
Z-Average (d.nm): 137.2	Peak 1:	159.0	93.9	88.79
PdI: 0.349	Peak 2:	4688	6.1	797.6
Intercept: 0.948	Peak 3:	0.000	0.0	0.000
Result quality : Good				

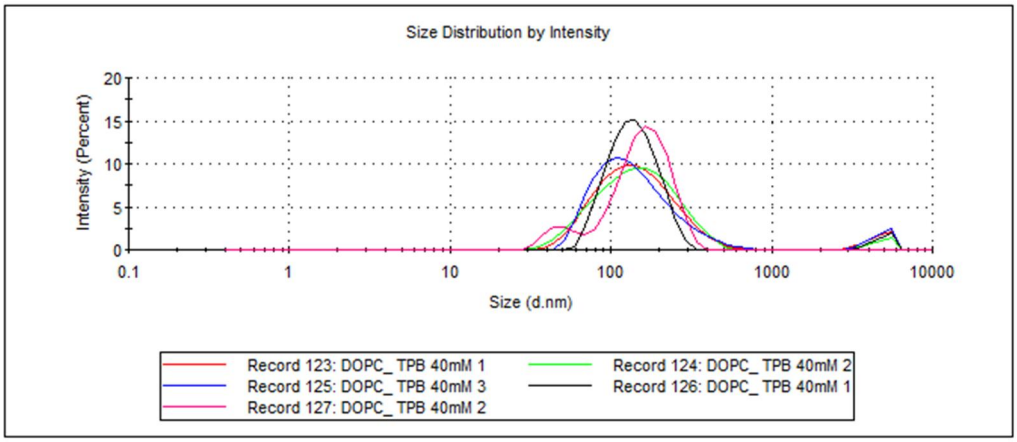

Figure I 4: The size distribution of DOPC liposome suspensions in the presence of 40 mM TPB-. Measured by DLS at 25˚C.

Appendix J

The effect of temperature on the size and PdI of DOPC liposomes

Figures J1, J2 and J3: The change in the size of DOPC liposomes in the presence of water, NaCl (*I* =5 mM), and $CaCl_2$ (*I* =5 mM) respectively. It is clear from the Figures that the change in temperature from 25 ˚C to 50 ˚C does not affect the size of the liposomes.

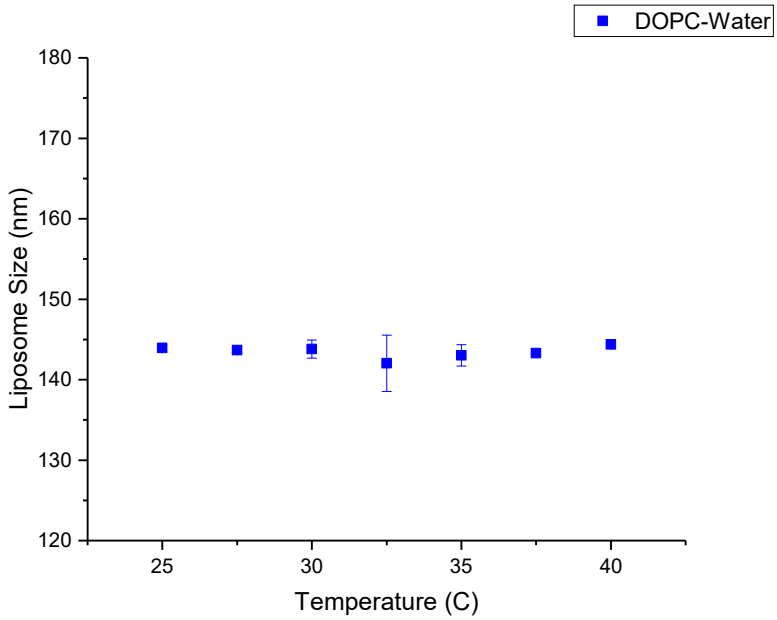

Figure J 1: The effect of temperature on the size of DOPC liposomes in water. The data was collected using DLS and the temperature range used was 25-40 ˚C.

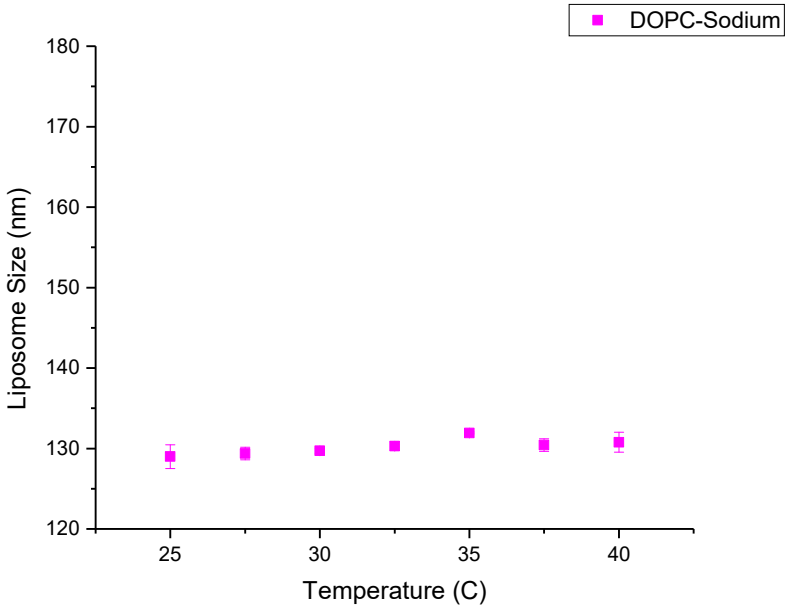

Figure J 2: The effect of temperature on the size of DOPC liposomes in NaCl (aq). The data was collected using DLS and the temperature range used was 25-40 ˚C.

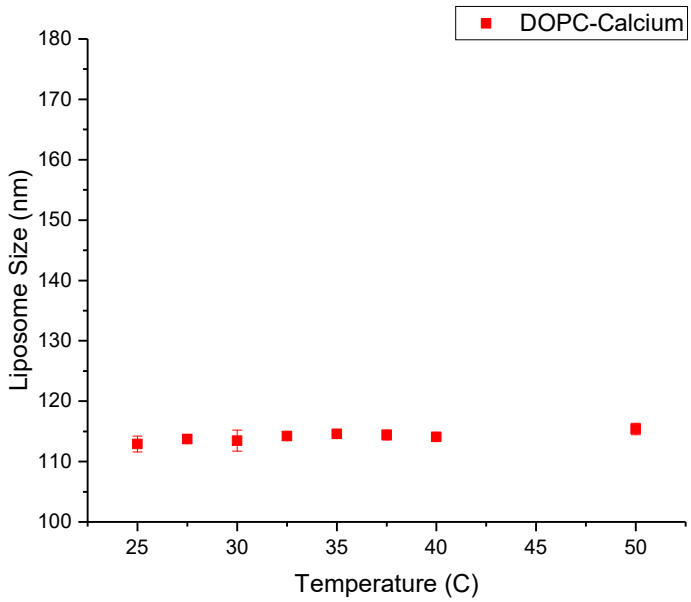

Figure J 3: The effect of temperature on the size of DOPC liposomes in $CaCl_2$ (aq). The data was collected using DLS and the temperature range used was 25-40 ˚C.

Figures J4, J5 and J6 show the change in the polydispersities of the DOPC liposomes in the presence of water, NaCl (*I* =5 mM), and $CaCl_2$ (*I* =5 mM) respectively. It is clear from the Figures that the change in temperature from 25 ˚C to 50 ˚C does not affect the PdI of the liposome suspensions.

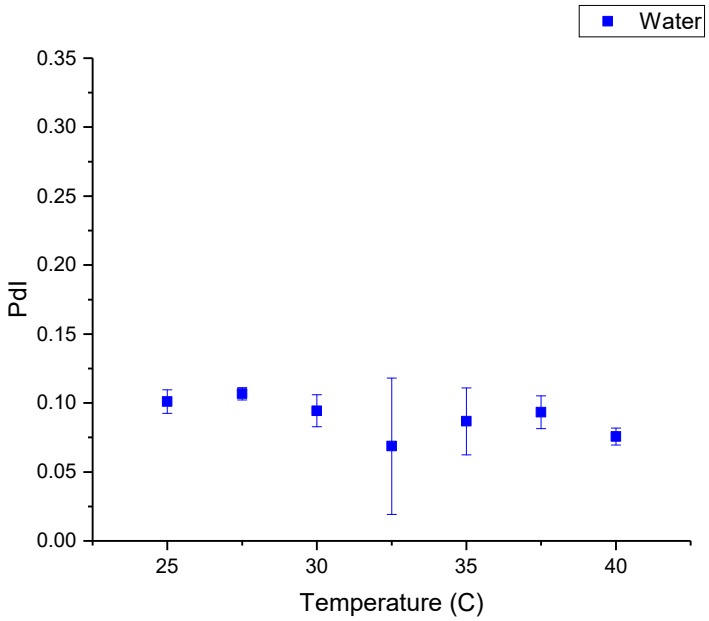

Figure J 4: The effect of temperature on the PdI of DOPC liposome suspensions in water. The data was collected using DLS and the temperature range used was 25-40 ˚C.

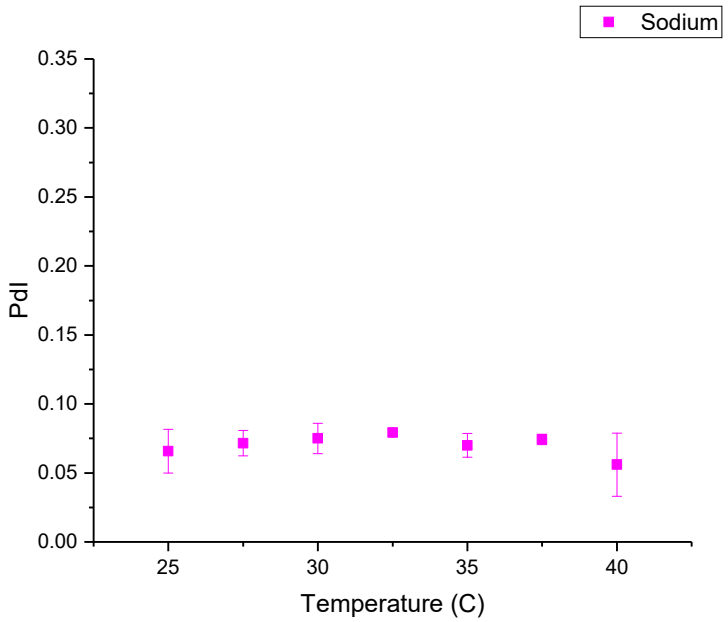

Figure J 5: The effect of temperature on the PdI of DOPC liposome suspensions in NaCl (aq). The data was collected using DLS and the temperature range used was 25-40 ˚C.

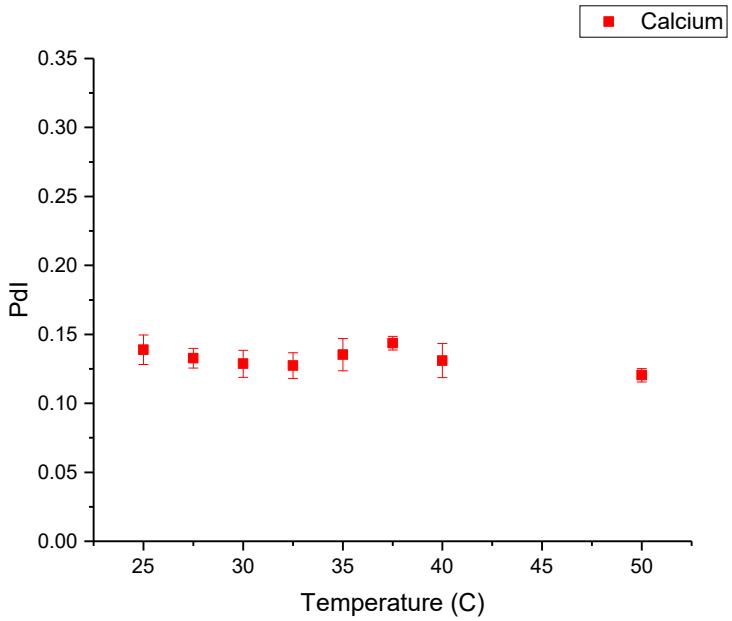

Figure J 6: The effect of temperature on the PdI of DOPC liposome suspensions in $CaCl_2$ (aq). The data was collected using DLS and the temperature range used was 25-50 ˚C.

Appendix K

Additional TEM images of DOPC liposomes

Figures K1, (A, B and C) show cryo-TEM images of DOPC liposomes in the presence of NaCl (*I*=5 mM). The images are from different regions of the TEM grid. Yellow arrows highlight unilamellar liposomes, blue arrows show the multilamellar vesicles and red arrows denote the multivesicular liposomes. In Figure K1 a number of multilamellar and multivesicular liposomes can be seen.

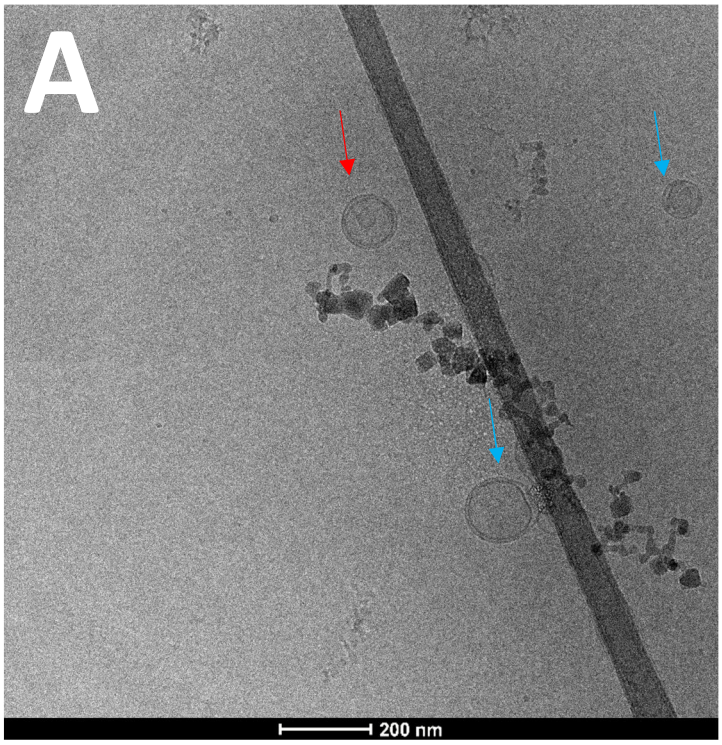

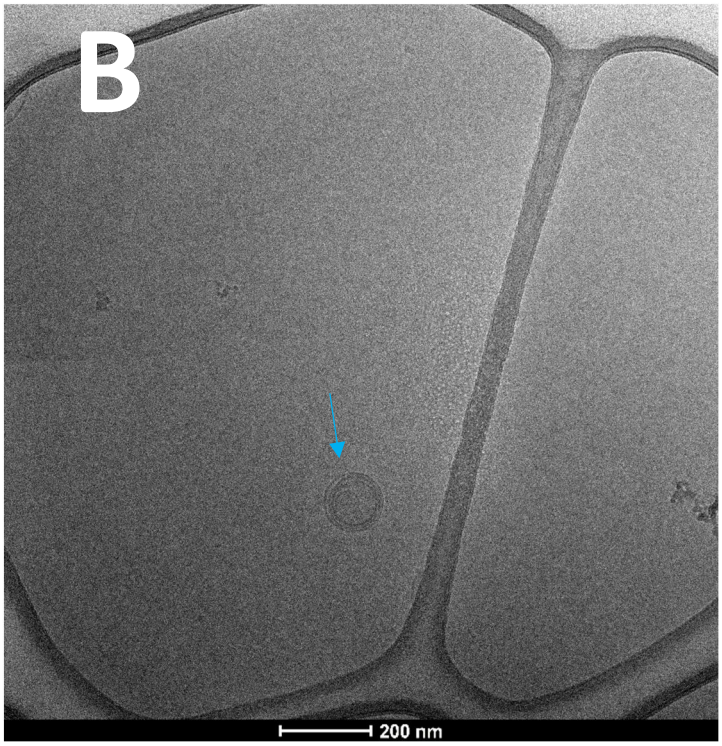

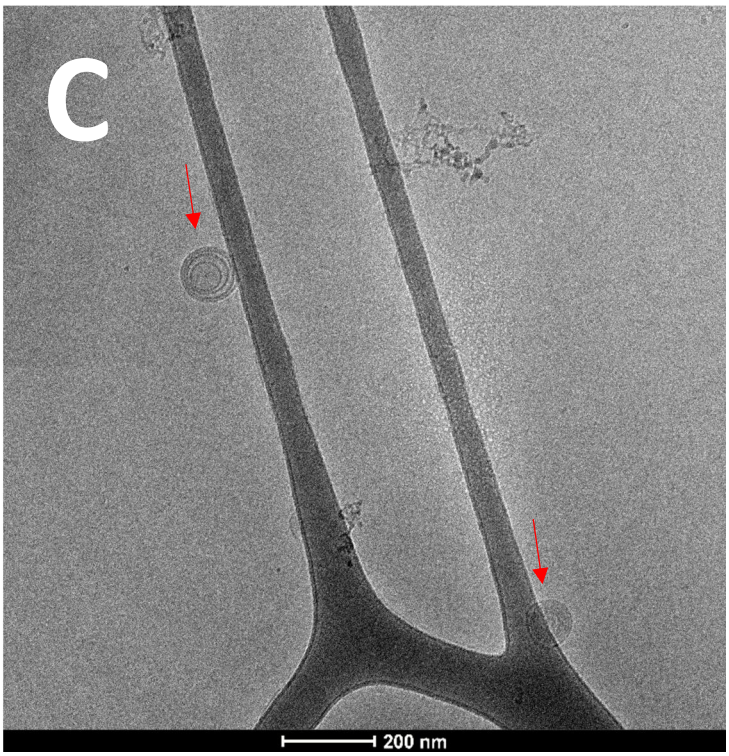

Figure K 1: Additional cryo-TEM images of DOPC liposomes in the presence of NaCl (I=5 mM).

Figures K2 (A, B and C) show cryo-TEM images of DOPC liposomes in the presence of $CaCl_2$ (*I*=5 mM). The images are from different regions of the TEM grid. In Figures K2 (A, B and C) a range of structures are observed. Cylindrical phospholipid structures (black arrows), unilamellar (yellow arrows), bilamellar (blue arrows) and multivesicular liposomes (red arrows) can be seen.

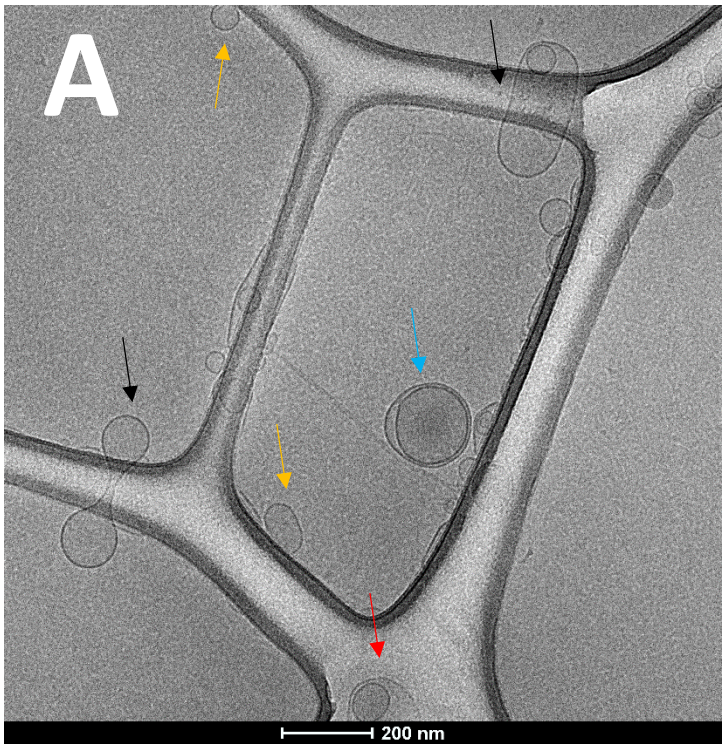

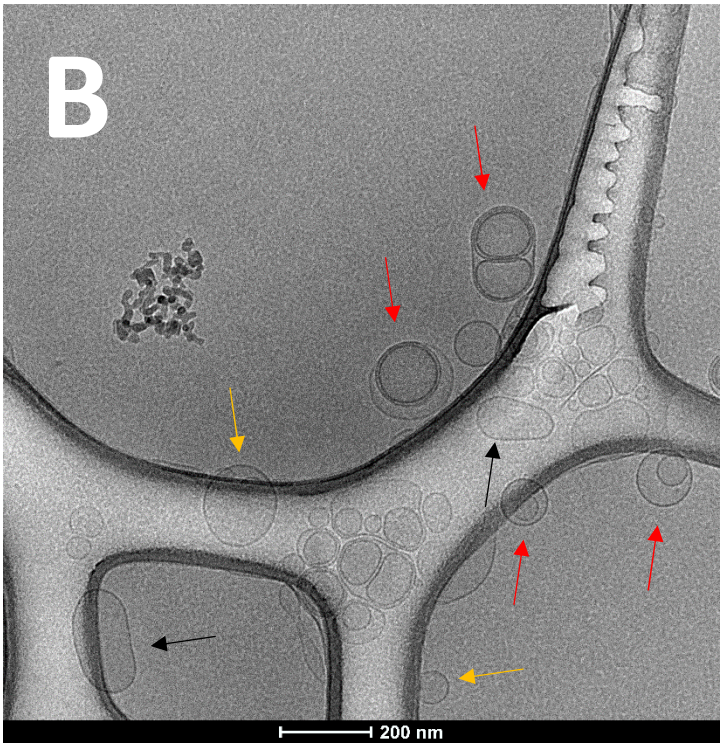

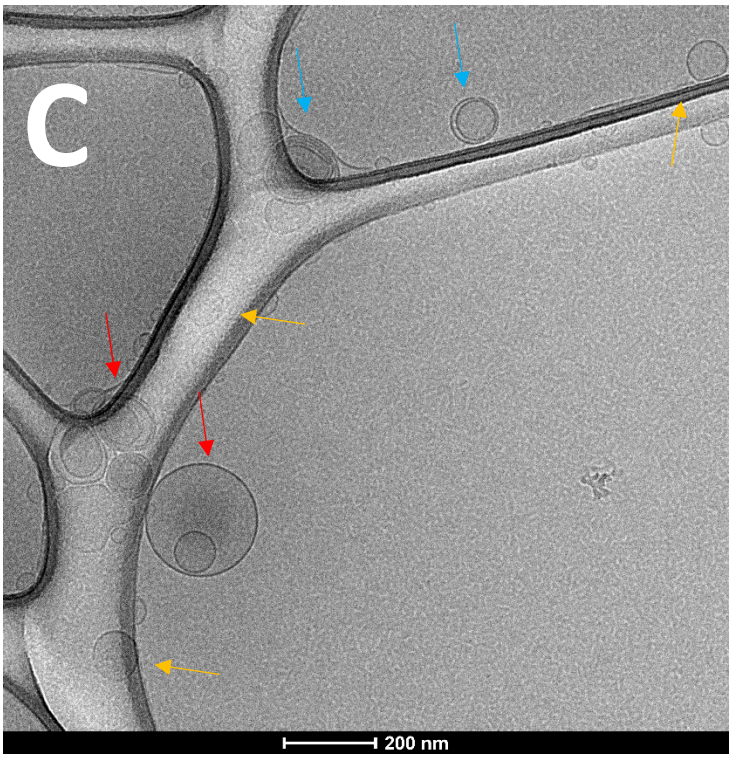

Figure K 2: Additional cryo-TEM images of DOPC liposomes in the presence of $CaCl_2$ (I=5 mM).

Figures K3 (A and B) show cryo-TEM images of DOPC liposomes in the presence of $LaCl_3$ (*I*=5 mM). The images are from different regions of the TEM grid. In Figures K3 (A and B) a large number of unilamellar liposomes (yellow arrows) can be seen, as well as a small number of multivesicular liposomes (red arrows).

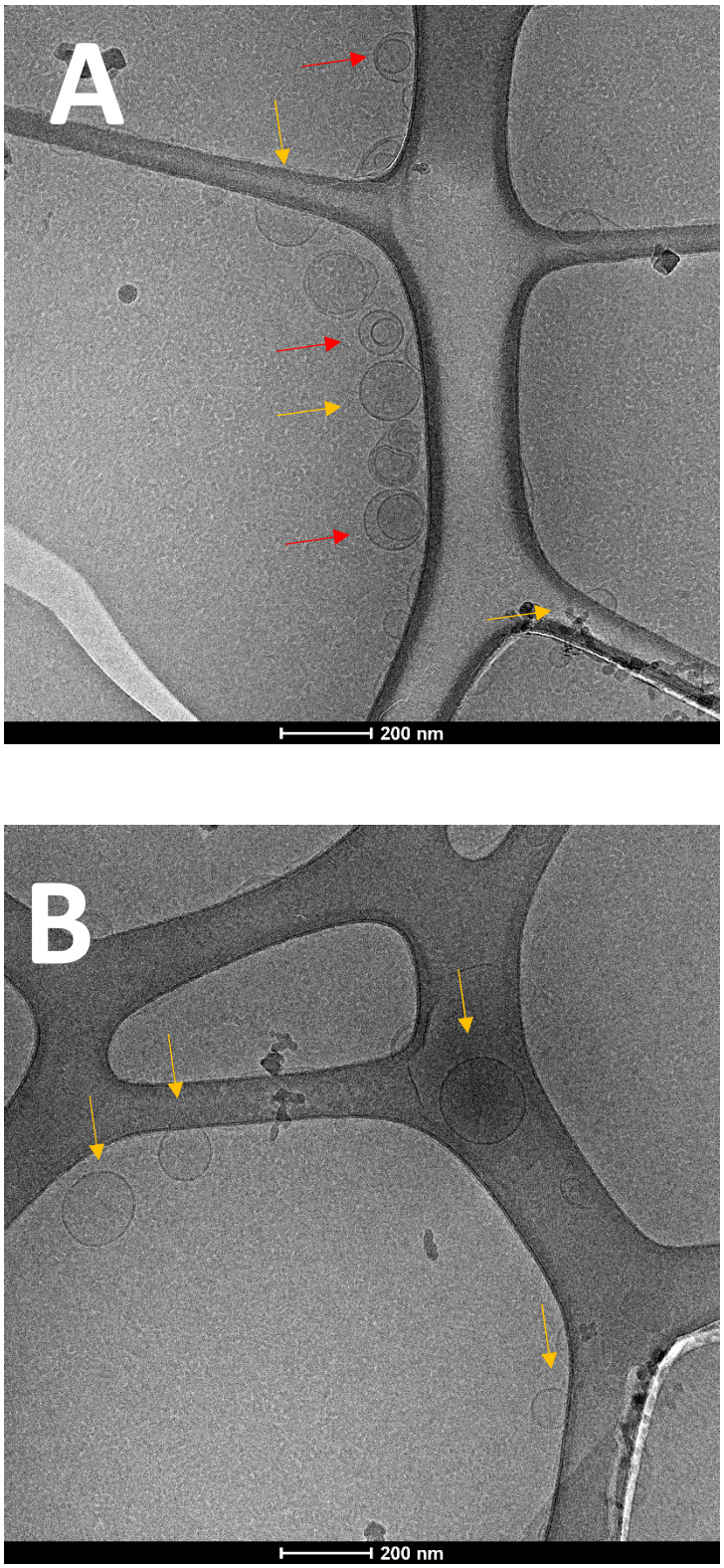

Figure K 3: Additional cryo-TEM images of DOPC liposomes in the presence of LaCl3 (I=5 mM).